LONGITUDINAL DISPERSION IN LABORATORY AND NATURAL STREAMS

by

Hugo B. Fischer

W. M. Keck Laboratory of Hydraulics and Water Resources
Division of Engineering and Applied Science
CALIFORNIA INSTITUTE OF TECHNOLOGY
Pasadena, California

Report No. KH-R-12 June 1966

LONGITUDINAL DISPERSION IN LABORATORY AND NATURAL STREAMS

by

Hugo B. Fischer

Project Supervisor:

Norman H. Brooks
Professor of Civil Engineering

Supported in part by the
Water Resources Division
United States Geological Survey
Department of the Interior

and by fellowships under the
National Defense Education Act
and from the
Fannie and John Hertz Foundation

W. M. Keck Laboratory of Hydraulics and Water Resources
Division of Engineering and Applied Science
California Institute of Technology
Pasadena, California

Report No. KH-R-12

June 1966

ACKNOWLEDGEMENTS

To Dr. Norman H. Brooks, who suggested this project and was throughout a source of constant and kind advice, assistance, and encouragement, the writer expresses his deepest gratitude.

The writer also wishes to thank Dr. Vito A. Vanoni and Dr. Fredric Raichlen for their continuous advice and assistance.

For his assistance and patient instruction in building the experimental set up, the writer is deeply indebted to Mr. Elton F. Daly, supervisor of the shop and laboratory. Appreciation is also due Mr. Robert L. Greenway, who assisted with construction of the apparatus; Mr. Leonard A. Fisher, who assisted in performing the experiments and analyzed much of the data; Mr. Ronald Handy, who prepared the drawings; Mrs. Patricia A. Rankin, who typed the manuscript; Mr. Frederick A. Wild, who constructed the conductivity probes; and Mr. Carl T. Eastvedt, who took all of the laboratory photographs.

The field experiments were carried out by the U. S. Geological Survey in cooperation with the Municipality of Metropolitan Seattle, as part of a project of the Washington District of the Water Resources Division under Mr. L. B. Laird, District Chief and Mr. J. F. Santos, Project Chief. The writer expresses his appreciation to the many members of the district staff who participated with him in data collection and analysis. Most of the drawings and photographs in Chapter VI were kindly supplied by the Washington District office.

The writer's study was supported by fellowships received under the National Defense Education Act (1962-65), and from the Fannie and John Hertz Foundation (1965-66).

The writer wishes to thank the U. S. Geological Survey for payment of laboratory research expenses under terms of Memorandum of Agreement No. 14-08-0001-10059 between the Geological Survey and the California Institute of Technology, under which the writer was a Research Participant. Except for the field studies, the research was performed in the W. M. Keck Laboratory of Hydraulics and Water Resources at the California Institute of Technology.

This report is a minor revision of a thesis of the same title submitted by the writer in May 1966, to the California Institute of Technology in partial fulfillment of the requirements for the degree of Doctor of Philosophy in Civil Engineering.

ABSTRACT

This study concerns the longitudinal dispersion of fluid particles which are initially distributed uniformly over one cross section of a uniform, steady, turbulent open channel flow. The primary focus is on developing a method to predict the rate of dispersion in a natural stream.

Taylor's method of determining a dispersion coefficient, previously applied to flow in pipes and two-dimensional open channels, is extended to a class of three-dimensional flows which have large width-to-depth ratios, and in which the velocity varies continuously with lateral cross-sectional position. Most natural streams are included. The dispersion coefficient for a natural stream may be predicted from measurements of the channel cross-sectional geometry, the cross-sectional distribution of velocity, and the overall channel shear velocity. Tracer experiments are not required.

Large values of the dimensionless dispersion coefficient D/rU^* are explained by lateral variations in downstream velocity. In effect, the characteristic length of the cross section is shown to be proportional to the width, rather than the hydraulic radius. The dimensionless dispersion coefficient depends approximately on the square of the width to depth ratio.

A numerical program is given which is capable of generating the entire dispersion pattern downstream from an instantaneous point or plane source of pollutant. The program is verified by the theory for two-dimensional flow, and gives results in good agreement with laboratory and field experiments.

Both laboratory and field experiments are described. Twenty-one laboratory experiments were conducted: thirteen in two-dimensional flows, over both smooth and roughened bottoms; and eight in three-dimensional flows, formed by adding extreme side roughness to produce lateral velocity variations. Four field experiments were conducted in the Green-Duwamish River, Washington.

Both laboratory and flume experiments prove that in three-dimensional flow the dominant mechanism for dispersion is lateral velocity variation. For instance, in one laboratory experiment the dimensionless dispersion coefficient D/rU^* (where r is the hydraulic radius and U^* the shear velocity) was increased by a factor of ten by roughening the channel banks. In three-dimensional laboratory flow, D/rU^* varied from 190 to 640, a typical range for natural streams. For each experiment, the measured dispersion coefficient agreed with that predicted by the extension of Taylor's analysis within a maximum error of 15%. For the Green-Duwamish River, the average experimentally measured dispersion coefficient was within 5% of the prediction.

CONTENTS

CONTENTS (cont.)

CONTENTS (cont.)

CONTENTS (cont.)

LIST OF FIGURES

LIST OF FIGURES (cont.)

LIST OF FIGURES (cont.)

LIST OF FIGURES (cont.)

LIST OF FIGURES (cont.)

LIST OF TABLES

CHAPTER I

INTRODUCTION

This study seeks an understanding of the mechanics of longitudinal dispersion in flow conditions similar to those found in natural streams. Longitudinal dispersion is the action by which a flowing stream spreads out and dilutes a mass of pollutant. Rather than moving downstream as a slug, such a mass will be distributed along the length of the stream, some parts traveling faster and some slower than the mean flow velocity. The rate at which the cloud spreads out, the decrease in peak concentration, and the resulting concentration pattern along the stream are of great importance in pollution control. The dispersion characteristics of natural streams have been observed to vary greatly from stream to stream; preparation of a rational pollution control program for a particular stream requires knowledge of the stream's individual dispersion characteristics.

Accelerated programs to end pollution of individual streams are being proposed by President Lyndon Johnson and members of Congress. Impressive economics are involved; Fortune magazine (1) has proposed a three billion dollar per year program of pollution control, and the State of New York has passed a $100 million bond issue to clean up the Hudson River. Thus considerable practical importance attends estimation of rates of dispersion. In this study, a method has been sought to link the dispersion characteristics of any channel to other flow parameters, such as the width, depth, and distribution of flow velocity.

The first important study of dispersion in turbulent shear flow was published by G. I. Taylor (2) in 1954. Taylor asserted, for reasons given in the next chapter, that although the primary mechanism for dispersion in shear flow is the variation in convective velocity within the cross section, the entire process could be described by a one-dimensional Fickian diffusion equation, written in the direction of flow. Taylor restricted his analysis to a long, straight circular pipe, and found that the coefficient in the diffusion equation would be,

$$D = 10.1\, a\, U^* \tag{1}$$

in which a is the pipe radius, and U* is the shear velocity ($\sqrt{\frac{\tau_o}{\rho}}$, where τ_o is the wall shear and ρ is the density). D is called the dispersion coefficient, to distinguish from classical diffusion. Using the same reasoning, Elder (3) found for an infinitely wide open channel,

$$D = 5.9\, d\, U^* \tag{2}$$

in which d is the depth of flow. Since the geometric radius of a pipe is twice its hydraulic radius, and since natural streams are geometrically some cross between an infinitely wide channel and a pipe, these two equations seemed to many workers to define the entire range of dispersion coefficients.

Both Taylor and Elder verified their results experimentally for the conditions under which they were derived, Taylor using a 3/8-inch diameter pipe and Elder a flow 1 cm. deep down a wide water table. Experimental results in natural streams, however, have not been within the expected range; dispersion coefficients have varied from 50 to 700 r U* (see Section II-E), where r is the hydraulic radius.

Nor have previous investigators been able to obtain any correlation between the dispersion coefficient and any group of bulk channel parameters. Moreover, the shape of experimental curves measured in natural rivers has been distinctly non-Gaussian, implying that the whole concept of Fickian diffusion might be in error.

The next chapter gives first the basic equation for convective turbulent diffusion. Attempts at solution by various workers are explained, the most important of which is Taylor's concept of one-dimensional dispersion. The results of previous experiments on longitudinal dispersion are summarized, and turbulent diffusion coefficients for transverse mixing are discussed.

In Chapter III a qualitative explanation is given for the appearance of non-Gaussian concentration distributions in natural rivers. Fickian diffusion is shown to be a correct description of dispersion only after an initial convective period, whose length may be estimated from a dimensionless parameter. Finally, a method is given for predicting dispersion coefficients in natural rivers, which satisfactorily explains the large measured values of the dispersion coefficient in rivers, and the reason why they do not fall in the range of equations 1 and 2.

Chapter IV describes a typical experiment on longitudinal dispersion, and details how a dispersion coefficient is calculated from experimental data. Chapter V presents laboratory experiments, both for conditions under which Elder's analysis should apply and conditions resembling natural streams. Chapter VI describes a series of experiments in a natural stream. In Chapter VII the hydraulic conditions of

some of the experiments described in Chapters V and VI are used in conjunction with a numerical program developed in Chapter III, and the numerical and experimental results are compared. Chapter VIII discusses the results and summarizes the experimental conclusions.

Chapter IX is a self-contained unit recapitulating what is known about dispersion in natural streams, what has been contributed by this study, and what requires further research. The reader wishing a brief summation may turn first to Chapter IX.

CHAPTER II

PREVIOUS STUDIES

This chapter gives the results of previous studies of dispersion in turbulent shear flow. Analytical studies of the basic differential equation are described, followed by experimental results reported in the literature.

II-A The Conservation of Mass Equation

The motion of a solute in a turbulent flow is described by an equation for the conservation of mass, which may be derived from the instantaneous conservation of mass equation by a procedure given by Holley and Harleman (4). In this procedure, the instantaneous equation is averaged over a time period long enough to average short-time turbulent fluctuations, but short enough so that one may speak of long-term changes in the time-averaged values. Two types of mass transport result: convection by the time-averaged velocities, and diffusion by turbulent fluctuations (by use of the Boussinesq assumption as discussed below). The resulting equation is:

$$\frac{\partial c}{\partial t} + u\frac{\partial c}{\partial x} + v\frac{\partial c}{\partial y} + w\frac{\partial c}{\partial z} = \frac{\partial}{\partial x}\left(\epsilon_x \frac{\partial c}{\partial x}\right) + \frac{\partial}{\partial y}\left(\epsilon_y \frac{\partial c}{\partial y}\right) + \frac{\partial}{\partial z}\left(\epsilon_z \frac{\partial c}{\partial z}\right) \quad (3)$$

In this equation:

c = time-averaged value of concentration;

t = time;

x, y, z = cartesian coordinates;

u, v, w = time-averaged velocities in the x, y, and z directions, respectively; and

ϵ_x, ϵ_y, ϵ_z = turbulent mixing coefficients in the x, y, and z directions, respectively.

The left hand side of equation 3 describes convection along a streamline, and the right hand side diffusion between streamlines. Molecular diffusion has been neglected, its effect being much less than that of the turbulent motion. Turbulent transport has been assumed to be proportional to the gradient of mean concentration, a suggestion made by Boussinesq (5) for momentum transport and applied to mass transport according to the Reynolds analogy (6). The mass transport coefficient should actually be written as a two-dimensional tensor,

$$-\epsilon_{ij} \frac{\partial c}{\partial x_j} = \frac{1}{T^*} \int_0^{T^*} u''_i \, c'' \, dt, \qquad (4)$$

in which c'' and u'' are instantaneous values of concentration and velocity, the subscripts i and j refer to the coordinate axes in usual tensor notation, and T* is the period required for time averaging. If the principal axes of the tensor are assumed to be the coordinate axes the non-diagonal terms are zero, i.e. $\epsilon_{ij} = 0$ for $i \neq j$, and the notation may be abbreviated to ϵ_i. This assumption is untrue if there is a preferred direction of motion diagonal to the coordinate axes, as in the vicinity of a sloping wall, but it is usual for convenience.

Equation 3, a linear partial differential equation with Neumann boundary conditions, is the basic description of convective turbulent diffusion on which the remainder of this study is based. Solution is difficult only because of its variable coefficients. In channel flow the coefficients v and w are often zero, and the mixing coefficients ϵ_i may

be assumed constant without introducing much error, but the variation of u is of paramount importance. Some workers have tried to avoid the problem by substituting for u the mean flow velocity $\bar{u}$; however, as will be seen in the next section, the cross-sectional variation of u is the primary mechanism for longitudinal dispersion, and must not be neglected. Because of this, no complete solution to equation 3 at present exists; various workers have devised approximate or asymptotic solutions, which will be examined next.

II-B Taylor's Concept of One-Dimensional Dispersion

An important approximate solution of equation 3 has been given by G. I. Taylor (2), who studied the case of uniform flow in a long, straight pipe. Adopting his theory of diffusion by continuous movements (7), he reasoned that in a coordinate system moving with the mean velocity of the flow the spread of the cross-sectional mean value of concentration must follow a Fickian diffusion equation:

$$\frac{\partial \bar{c}}{\partial t} = D \frac{\partial^2 \bar{c}}{\partial \xi^2} \tag{5}$$

in which $\xi = x - \bar{u}t$,

x = direction of the mean flow,

$\bar{u}$ = cross-sectional mean velocity of flow,

$\bar{c} = \frac{1}{A} \iint_A c \, dA$, and

A = area of flow cross section.

Here, and in all that follows, an overbar indicates a cross-sectional average as shown, rather than a temporal average. It must be

emphasized that all of the temporal averaging normally connected with turbulence analysis has been carried out in the derivation of equation 3.

Taylor obtained the coefficient, D, in equation 5 by making certain simplifications in equation 3. Let

$$c = \bar{c} + c' \tag{6}$$

and

$$u = \bar{u} + u' \tag{7}$$

define the spatial variations of concentration, c', and velocity, u', from the cross-sectional mean values. Taylor's assumptions were:

(1) $c' = c'(y, z)$;

(2) the term, $\frac{\partial}{\partial x}\left(\epsilon_x \frac{\partial c}{\partial x}\right)$, the longitudinal transport due to turbulence, may be neglected;

(3) the term $\frac{Dc}{Dt} = \frac{\partial c}{\partial t} + \bar{u}\frac{\partial c}{\partial x}$, which is the time rate of change of concentration at a point moving at the mean velocity, may also be neglected; and

(4) $v = w = 0$.

Equation 3 becomes:

$$u' \frac{\partial \bar{c}}{\partial \xi} = \frac{\partial}{\partial y}\left(\epsilon_y \frac{\partial c'}{\partial y}\right) + \frac{\partial}{\partial z}\left(\epsilon_z \frac{\partial c'}{\partial z}\right), \tag{8}$$

with the condition that the normal derivative of c' vanishes on the boundary. This is a linear, second-order, inhomogeneous Neumann problem for c'; it has the general solution,

$$c' = f(P) \frac{\partial \bar{c}}{\partial \xi} , \tag{9}$$

in which f is a function depending only on the flow parameters and shape of the cross section, and P is any point on the cross section. The coefficient in a diffusion equation is a measure of the local mass transport, $\dot{M}$, defined by:

$$\dot{M} = \int_A u'c' \, dA = -A \, D \frac{\partial \bar{c}}{\partial \xi} \tag{10}$$

Substituting the value for c' given by equation 9 into equation 10 gives:

$$D = - \overline{u'f} \ . \tag{11}$$

To obtain values of f, Taylor used the universal velocity distribution for pipes given by Nikuradse, and assumed the Reynolds analogy (discussed in section F). Since only radial variations need to be considered, equation 8 can be written in radial coordinates in terms of radial distance only, and a solution obtained by integration. Taylor's result, given as equation 1 in Chapter I, was

$$D = 10.1 \, a \, U^* .$$

II-C Applications of Taylor's Concept

The first use of Taylor's concept in other than pipe flows was presented by I. E. Thomas (8) as a Ph. D. dissertation at Northwestern

University in 1958. Thomas considered unidirectional flow in an infinitely wide open channel, in which variations are in the vertical (y) direction only. He assumed a power law velocity distribution.

$$u = \left(\frac{y}{d}\right)^n, \tag{12}$$

and obtained ε_y from the Reynolds analogy. Equations 8 and 11 combine to give:

$$D = -d^2 \int_o^1 u' dy' \int_o^{y'} \frac{1}{\varepsilon_y} dy' \int_o^{y'} u' dy', \tag{13}$$

in which $y' = y/d$. The integration gives a complicated function of n, which for smooth channels can be plotted as a function of Reynolds number, as shown on page 232 (Appendix II).

Elder (3), a year later, presented a study identical except in assuming a logarithmic velocity profile,

$$u' = \frac{U^*}{\varkappa} (1 + \log_e y'), \tag{14}$$

in which $\varkappa$ is the von Karman constant. Equation 13 was integrated to yield:

$$D = \frac{0.404}{\varkappa^3} d U^*. \tag{15}$$

The effect of turbulent diffusion was assumed to be additive, and equal to the cross-sectional average of ϵ_y,

$$\overline{\epsilon_y} = \frac{\kappa}{6} d U^* . \tag{16}$$

Assuming that $\kappa = 0.41$, Elder presented the result given in chapter I:

$$D = 5.93 \, d U^* \tag{17}$$

The figure on page 232 shows that Thomas's and Elder's results are quite similar. Elder's has been used more frequently, partly because it is simpler and has no Reynolds number or friction factor dependence, and partly because it is the only one published.

II-D Other Solutions of the Basic Equation

Aris (9) considered uniform flow in a long straight tube of arbitrary cross section and velocity distribution, and obtained a solution of equation 3 which does not neglect any of the terms except those containing secondary mean velocities (i.e. $v = w = 0$). By taking moments in the direction of flow (x), he obtained sets of equations for the pth moment,

$$c_p(y, z) = \int_{-\infty}^{\infty} c(x, y, z) x^p \, dx , \tag{18}$$

and its cross-sectional average, $\overline{c_p}$, which could be solved to any desired value of p. In practice, only the first three moments are required, since for a finite source the distribution can be shown to tend to normality. Aris's solution can be applied to the flows considered by Taylor and Elder, and yields identical results in both cases.

Saffman (10), in extending Aris's method to include flow between parallel planes, noted that Taylor's approach yields only an asymptotic solution, which should not be expected to apply for short times. Aris's equation for the zeroth moment is the diffusion equation in the cross section:

$$\frac{\partial c_o}{\partial t} = \nabla\cdot(\epsilon \nabla c_o) , \qquad (19)$$

in which ϵ is an isotropic turbulent diffusion coefficient. Saffman reasoned that the characteristic times for diffusion within the cross section and application of Taylor's solution would be the same; hence he limits Taylor's solution to times much greater than $\ell^2/2\epsilon$, where ℓ is a characteristic length and ϵ a characteristic mixing coefficient for the cross section.

A more conventional approach to equation 3 has been given by Farrell and Leonard (11), who investigated convective diffusion of a point source on the centerline of laminar flow in a pipe. They were able to solve the Laplace transform of the equation with initial and boundary conditions, but experienced difficulty in inverting the transformed results. Their work is difficult to extend to more complicated initial, boundary, or flow conditions.

Yotsukura and Fiering (12) have given a numerical solution to equation 3, valid for the same flow conditions as studied by Thomas and Elder. In a published discussion (13, Appendix II) the writer has pointed out that, although their solution seemed to represent the dispersion process correctly, the asymptotic dispersion coefficient obtained was not in agreement with the work of Thomas, Elder, or Aris. In their closing discussion (14), Yotsukura and Fiering report discovery of their error, and claim to have a workable solution. Their method requires 1.75 hours of computation by an IBM 7090 computer to reach a value of 15 on a dimensionless time scale(to be defined in chapter III).

Bugliarello and Jackson (15), also using a high-speed computer, have presented a random walk solution. A large number of individual particles originate motion from one point in the flow. During each time increment, there are two steps: first, in the plane of the cross section a step of given length but random direction; secondly, in the direction of mean flow, a step of length corresponding to the velocity at that cross-sectional point at which it is located after the first step. An experiment was conducted simulating laminar flow in a straight pipe, using 3000 particles. After a certain period, the longitudinal variance was observed to grow linearly at approximately the rate predicted by Taylor's analysis for laminar flow (16).

One other suggestion must be included for completeness. Patterson and Gloyna (17), basing their work on experiments by Yotsukura (18) and Godfrey and Frederick (19), proposed an experimental formula,

$$D = k_1 \left[\frac{\bar{u}}{\ell n \left(\frac{b}{d} \right)} \right]^{k_2} \qquad (20)$$

in which: b = width of channel;

k_1 = 0.258 (laboratory flumes), or 229 (natural streams);and

k_2 = 0.830 (laboratory flumes), or 0.269 (natural streams).

The suggestion is not dimensionally homogeneous, is not claimed to apply equally to laboratory and field conditions, and is even a poor fit to the data on which it is based.

II-E Longitudinal Dispersion Experiments

Table 1 summarizes a literature search for experimental values of the longitudinal dispersion coefficient. As much descriptive information is included as possible; blanks indicate that the data were not available. The dimensionless time span, $t' = t/T$, where T is a time scale for the channel as defined in chapter III, is for the passage of the mean from the first to the last measuring station; in most cases, intermediate measurements were also taken.

Experiments are listed in order of ascending dimensionless dispersion coefficient, D/r U*. The hydraulic radius is used in comparing results, since for most channels it equals approximately the mean depth, and is the more consistently reported parameter. The depths listed are believed to be the maximum depth of the channel except where noted.

Table 1. Previous Measurements of Longitudinal Dispersion.

Source	Channel	Tracer	Depth d (cm.)	Width b (m.)	Hyd. Rad. r (cm.)	Mean Velocity $\bar{u}$ (cm./sec.)	Shear Velocity U* (cm./sec.)	Dimensionless Time Span t'	Dispersion Coefficient D (cm^2/sec.)	Dimensionless Dispersion Coefficient D/rU*
Elder (3)[1]	Laboratory Flume	Dye	1.27	∞	1.27	1.27	1.6	2-10	14	6.8
Schuster (20)[2]	Yuma Mesa A Canal	Gold 198	345		181	68.1	3.45		7,600	12
Glover (21)[3]	Laboratory Flume, Rough Bottom	Salt	15.0	2.42	13.4	62.5	6.9	4.5-13.5	1,170	13
"	Triangular Flume	Salt	44.8	0.896	15.9	70.1	2.75	2.0-10.0	766	18
"	Laboratory Flume, Smooth Bottom	Salt	16.6	2.42	14.6	42.5	1.83	1.6- 4.8	653	24
Thomas (8)[4]	Chicago Ship Canal	Tritium	807	48.8	615	27.2	1.91	3.9-15.1	30,000	24.9
Godfrey & Frederick (19)[5]	Clinch River (below gage)	Gold 198	213	59.4	210	93.8	10.4	0.6- 5.8	111,000	50.5
" "	" " " "	"	209	53.3	205	83.1	10.7	0.7- 9.4	112,000	57.5
Sacramento River Pollution Study (22)[6]	Sacramento River	Agricultural Drain water	400		380	53	5.1		150,000	77
Godfrey & Frederick	Clinch River (below gage)	Gold 198	104	47.2	103	31.5	6.86	0.8- 9.8	91,000	109
Owens, Edwards & Gibbs (23)[6]	River Derwent	Bromine 82	25			38	14		46,000	131
Godfrey & Frederick	Copper Creek (above gage)	Gold 198	39.4	17.1	38.5	15.8	11.9	1.4- 9.3	91,000	216
" "	Coachella Canal	"	156	24.4	149	70.9	4.08	0.6-36.0	177,000	278
" "	Copper Creek (below gage)	"	49.8	15.8	49.4	27.1	8.03	1.4-37.1	151,000	355
" "	" " " "	"	49.1	16.0	47.9	26.3	7.92	1.3-33.8	155,000	408
" "	" " " "	"	84.4	18.2	82.2	60.4	10.1	1.3-22.5	418,000	477
Glover	South Platte River	Potassium carbonate			46.3	65.8	6.90		162,000	510
Godfrey & Frederick	Clinch River above Clinchport	Gold 198	58.2	35.8	57.8	21.1	4.78	1.1-10.5	197,000	535
" "	Powell River	"	85.4	33.8	84.6	15.4	5.43	3.6-20.5	268,000	654

Notes:

1. Concentrations obtained from photographs of dye drops. Channel considered infinitely wide because edge of drops did not approach sides of channel.
2. Dispersion coefficient obtained by Sayre (24), using change of moment method (described in Chapter IV).
3. Method of obtaining dispersion coefficients not reported. Probably compared measured curves to Gaussian distribution, although due to low dimensionless times comparison was probably poor.
4. Dispersion coefficient calculated by author, using change of moment method. Methods used in source not correct.
5. Dispersion coefficients calculated by plotting moments, and also from decay of peak concentration. Moments obtained by comparing measured curves to Pearson Type III distribution; this may cause significant errors. Depths indicated are mean depths.
6. Dispersion coefficient calculated by author, using change of moment method. Depths and hydraulic radius are estimated average over reach. Width of River Derwent unknown, depth used to calculate dimensionless coefficient.

The table indicates that results in open channels cannot be correlated solely on the basis of hydraulic radius and shear velocity. In general, laboratory experiments have given smaller dimensionless coefficients than field experiments, which explains why some workers have suggested the need for a "scale factor". However, both the deepest and widest channels (the Chicago Ship Canal and the Clinch River) have relatively small dimensionless coefficients. The reason for the diversity of results is explained by an analysis in chapter III. In Table 31 (Chapter VIII) the list of previous results is repeated along with the results of present experiments. The dimensionless results of the present laboratory experiments will be seen to span entirely the range of previous studies.

II-F Turbulent Mixing Coefficients

In Section II-A the tensor of turbulent mass transport, ϵ_{ij}, was discussed and limited to a diagonal form containing only the terms ϵ_x, ϵ_y, and ϵ_z. The lateral and vertical coefficients, ϵ_y and ϵ_z, are of fundamental importance in the study of longitudinal dispersion, because of their appearance in equation 8, Taylor's simplified version of the basic conservation equation. Experimental data on these coefficients have been obtained only in rectangular flumes with smooth sides and either smooth or rough bottoms.

The coefficient for vertical transport of momentum, ϵ_y, may be obtained theoretically for turbulent flow in an infinitely wide open channel, since both the distribution of shear and velocity are known.

Using the logarithmic velocity profile, equation 14, and the linear shear distribution,

$$\frac{\tau^*}{\rho} = (d-y)\, g\, S = -\overline{u''v''} = \varepsilon_y \frac{\partial u}{\partial y}, \tag{21}$$

in which τ^* is the local shear stress, ρ the mass density, g the acceleration of gravity, d the depth, and S the slope, we obtain

$$\varepsilon_y = \kappa\, (1 - y/d)\, (y/d)\, d\, U^* \tag{22}$$

for the transport of momentum. Experimental evidence for Reynolds's analogy of mass transport has been obtained by Kalinske and Pien (25), Vanoni (26), and Al Saffar (27). Vanoni studied the distribution of concentration of small sediment particles with respect to depth; Al Saffar introduced neutrally buoyant salt solution at the surface and measured downstream concentration profiles. Both studies were extensive and detailed, and validated the Reynolds analogy over the entire depth within a maximum error of 10%. Kalinske and Pien obtained the same verification, but in less detail.

The coefficient of lateral mixing, ε_z, has received less attention. The only accurate experiment in which the tracer extended throughout the depth has been that of Elder, who, as part of his study of longitudinal dispersion, obtained a lateral diffusion coefficient,

$$\varepsilon_z = 0.23\, d\, U^*. \tag{23}$$

Orlob (28) studied lateral diffusion at the surface of a flow in a rectangular flume, in which increased turbulence was generated by roughening the bottom with expanded metal mesh. His analysis is based on an extension of the Kolmogoroff similarity hypothesis to turbulent mixing, although the connection is somewhat obscure. On the basis of a large number of experiments he proposed that

$$\epsilon_z = 0.0136\, E^{1/3} L_e^{4/3} \tag{24}$$

in which E is the rate of energy dissipation per unit mass, and L_e is the Lagrangian eddy size. In discussion, this was modified to include effects of the friction factor, which could not be proved by the experiments.

Orlob's arguments for the similarity hypothesis apply equally well if one considers vertical mixing, for which the dependence on d U* has been well established (equation 22). There is no reason to believe that lateral mixing, at least in an infinitely wide channel, should depend on any other parameters. Equation 24 can be made compatible with equation 23 if

$$L_e \alpha\, d\, f_*^{1/8} \tag{25}$$

in which f_* is the Darcy-Weisbach friction factor, but there is no direct evidence for this. Neverthless, a brief check of Orlob's data indicates no major disagreements with equation 23.

Sayre and Chamberlain (29) made a study similar to Orlob's, using a flow 18 cm. deep over sand dunes 0.9 cm. in height. They

obtained

$$\epsilon_z = 0.24\ d\ U^*. \tag{26}$$

Of the three experiments, Elder's is the most applicable to longitudinal dispersion, since it is the only one in which the tracer was distributed over the depth of flow. Neither Orlob's nor Sayre and Chamberlain's results being in conflict, Elder's result (equation 23) has been adopted for provisional use.

II-G Summary

This chapter has presented several approximate solutions to the equation for conservation of mass in a turbulent flow. Taylor's approach, applied to flow in an infinitely wide open channel, yields a result which is greatly different from measurements in natural streams. The essential difference and consequences thereof between an infinitely wide open channel and a natural stream, and the proper application of Taylor's approach to natural streams, will be discussed in the next chapter.

CHAPTER III

ANALYTICAL INVESTIGATIONS

This chapter discusses the assumptions involved in Taylor's concept of one-dimensional dispersion, and shows how the analysis may be applied to three-dimensional flows such as found in natural streams. First, however, a qualitative explanation will be given for the frequent observation of skewed concentration distributions.

III-A Explanation of Skewed Distributions

If the initial condition is a Dirac delta function distribution of concentration, the solution to the diffusion equation (equation 5) is the Gaussian distribution. Nevertheless, every experimenter has observed that, following introduction of a point or plane source of tracer (corresponding to a delta function in the direction of flow) into any channel flow, a longitudinal concentration distribution is produced which is markedly skewed. Concentration in the leading (downstream) limb of the cloud rises very steeply to the peak, while the concentration in the trailing (upstream) limb decreases slowly. This phenomenon has caused several speculations on the nature of dispersion. Elder (3) assumed that the material in the trailing part was caught in the laminar sub-layer, so should be subtracted from the overall concentration distribution in obtaining a dispersion coefficient. The pronounced skew observed in concentration curves from natural streams by Godfrey and Frederick (19) has been explained by Hays, Schnelle, and Krenkel (30) as resulting from dead zones along the stream banks, which

absorb and hold material from the leading limb for later release into the trailing limb.

A more reasonable explanation is that, as Taylor (16) originally noted, the one-dimensional diffusion equation represents only an asymptotic behavior of the tracer cloud some time after its insertion. Figures 1 through 3 show qualitatively the initial behavior of the tracer cloud originating from a plane source in an infinitely wide channel flow. The dominant initial motion is by convection; the ideal plane source quickly assumes a shape similar to that of the velocity profile. Induced vertical concentration gradients are then destroyed more slowly by vertical diffusion. If, shortly after insertion, a plot is made of cross-sectional mean concentration as a function of distance, the result (figure 3) is a sharply skewed curve.

In natural streams the same mechanism is present in more pronounced form. In general, any point or line source of tracer introduced into a flow will produce a highly skewed distribution during the convection-dominated period; this distribution may be taken as an initial condition when sufficient time has elapsed for Taylor's diffusion equation to apply. Thus dispersion from an instantaneous source of tracer may be divided into two periods: a convective period, which includes all time up to the point where Taylor's solution applies; and all subsequent time, which might be referred to as the "Taylor" period to indicate that the cloud follows Taylor's one-dimensional theory.

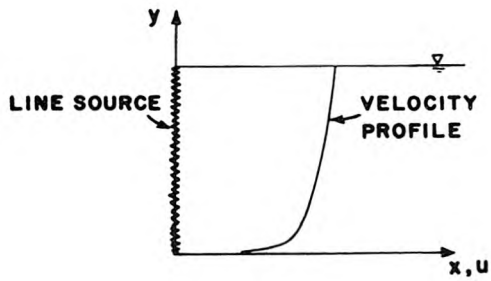

Fig. 1. Typical velocity profile and line source

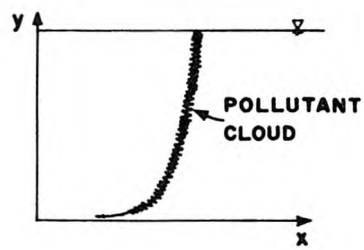

Fig. 2. Appearance of line source after initial convection

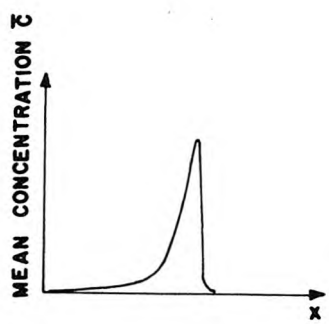

Fig. 3. Mean concentration distribution for cloud shown in Fig. 2

III-B A Time Scale for Dispersion

Saffman has suggested (Section II-D) that the period required before Taylor's solution would be valid should be proportional to that required for diffusion within the flow cross section. On dimensional grounds, a time scale for cross-sectional diffusion is,

$$T' = \frac{\ell^2}{\epsilon} \tag{27}$$

in which ℓ is a characteristic length and ϵ a characteristic diffusion coefficient for the cross section. T' may be referred to as the Eulerian time scale.

A Lagrangian time scale can be obtained by an application of Taylor's theory of diffusion by continuous movements, mentioned in Chapter II. Batchelor (31) has pointed out that because the motion of a particle constrained in uniform flow in a channel is a stationary random function, Taylor's original reasoning for homogeneous turbulence applies. Let a statistically large number of tracer particles be distributed uniformly over a cross section at $\xi = 0$ at time $t = 0$, where ξ is the longitudinal coordinate in a coordinate system moving at the mean flow velocity. Then for any later time t the position of each particle is

$$\xi(t) = \int_0^t u''(\tau)\, d\tau \ , \tag{28}$$

where u'' is the instantaneous particle velocity relative to the mean velocity of flow. Then

$$\xi^2(t) = \int_0^t \int_0^t u''(\tau_1)\, u''(\tau_2)\, d\tau_1\, d\tau_2 , \tag{29}$$

and

$$\overline{\xi^2(t)} = \int_0^t \int_0^t \overline{u''(\tau_1)\, u''(\tau_2)}\, d\tau_1\, d\tau_2 , \tag{30}$$

in which a wavy overbar denotes an ensemble average, and the interchangeability of integration and ensemble averaging has been assumed. Because u'' is a stationary random function, a correlation coefficient may be defined which depends only on the difference in times:

$$\psi(\tau_2 - \tau_1) = \frac{\overline{u''(\tau_1)\, u''(\tau_2)}}{\overline{u''^2}} \tag{31}$$

Since the particles must remain uniformly distributed with respect to cross-sectional position, and since variations in velocity due to turbulence are much smaller than those due to changes in cross-sectional position, a good approximation is:

$$\overline{u''^2} \cong \overline{u'^2} , \tag{32}$$

where the straight overbar implies average over the cross section, and u' is the time-averaged variation from the cross-sectional mean. An integral formula, which may be proved by 45° rotation of the coordinate axis, is:

$$\int_0^L \int_0^L g\,(x-y)\,dx\,dy = 2\int_0^L (L-s)\,g(s)\,ds. \tag{33}$$

Substituting equations 31 and 32 into 30, and making the transformation of equation 33, yields:

$$\widetilde{\xi^2}\,(t) = 2\,\overline{u'^2}\int_0^t (t-\tau)\,\psi\,(\tau)\,d\tau. \tag{34}$$

$\widetilde{\xi^2}$ is equivalent to the variance of the particle cloud, σ_ξ^2, defined by

$$\sigma_\xi^2 = \frac{\int_{-\infty}^{\infty} \overline{c}\,\xi^2\,d\xi}{\int_{-\infty}^{\infty} \overline{c}\,d\xi}\,. \tag{35}$$

If both sides of the diffusion equation (equation 5) are multiplied by ξ^2 and integrated between $\xi = \pm\,\infty$, the time derivative taken outside the integral, and the right hand side integrated by parts twice, there results:

$$\frac{\partial}{\partial t}\int_{-\infty}^{\infty} \overline{c}\,\xi^2 d\xi = 2D\int_{-\infty}^{\infty} \overline{c}\,d\xi\,, \tag{36}$$

or

$$D = \frac{1}{2}\,\frac{\partial}{\partial t}\,\sigma_\xi^2\,. \tag{37}$$

Differentiating equation 34 with respect to time yields,

$$D = \overline{u'^2} \int_0^t \psi(\tau)\, d\tau. \tag{38}$$

Assuming that $\psi(\tau)$ is sufficiently well behaved so that the integral converges as $\tau \to \infty$, the Lagrangian time scale may be defined as:

$$T = \int_0^\infty \psi(\tau)\, d\tau, \tag{39}$$

and

$$D = \overline{u'^2}\, T. \tag{40}$$

For the flow in an infinitely wide open channel, a relation may be obtained between the Eulerian and Lagrangian time scales. Elder's result (equation 15) was

$$D = \frac{0.404}{\kappa^3}\, d\, U^*.$$

Integrating the square of the velocity, using the logarithmic velocity profile (equation 14), gives

$$\overline{u'^2} = \left(\frac{U^*}{\kappa}\right)^2 . \tag{41}$$

Hence

$$T = \frac{0.404}{\kappa} \frac{d}{U*} \tag{42}$$

For the Eulerian time scale, T', the appropriate length and mixing coefficient are d and $\overline{\epsilon}_y$ (equation 16). Substituting these in the definition of the Eulerian scale (equation 27) gives

$$T' = \frac{6}{\kappa} \frac{d}{U*} . \tag{43}$$

Comparing equations 42 and 43 shows that

$$T' = 14.8\ T . \tag{44}$$

As will be shown in section F, reasonable grounds exist for estimating the Eulerian time scale in more complicated flows, although not the Lagrangian scale. If equation 44 is assumed to apply to these flows, equation 40 provides a rapid means of estimating the dispersion coefficient, as a value of $\overline{u'^2}$ can usually be obtained. The time scales also provide a rational basis for dimensionless time in classifying experimental results into the convective or diffusive periods.

III-C Discussion of Taylor's Analysis

Taylor's analysis contains the two assumptions that (a) in a coordinate system moving at the mean velocity the time derivative of concentration is zero, and (b) the concentration distribution may be divided into two additive portions, one varying only with cross-sectional position, and the other only with longitudinal distance. Assumption (b) is questionable; and (a) neglects the desired solution entirely. Both assumptions may be justified on the ground that they work, since Aris's method involves no assumptions whatsoever and yields an identical answer. Taylor's approach is superior to Aris's, however, because it exhibits the physical mechanism involved in dispersion; consequently it is important to understand why it works.

Returning to section II-B and maintaining the reasonable physical assumptions of no secondary mean flow and negligible contribution by longitudinal turbulence (assumptions (2) and (4) on page 8), but not the mathematical ones, given as (a) and (b) above, equation 3 takes the form:

$$\frac{\partial}{\partial t}(\overline{c} + c') + u' \frac{\partial}{\partial \xi}(\overline{c} + c') = \frac{\partial}{\partial y}\left(\epsilon_y \frac{\partial c'}{\partial y}\right) + \frac{\partial}{\partial z}\left(\epsilon_z \frac{\partial c'}{\partial z}\right) \qquad (45)$$

Averaging equation 45 across the cross section with the condition of no transport across the boundaries, yields:

$$\frac{\partial}{\partial t}\overline{c} + \frac{\partial}{\partial \xi}\overline{u'c'} = 0 \, . \qquad (46)$$

Substituting equation 46 into 45 yields:

$$\frac{\partial}{\partial t}c' + u'\frac{\partial \bar{c}}{\partial \xi} + \frac{\partial}{\partial \xi}(u'c' - \overline{u'c'}) = \frac{\partial}{\partial y}(\epsilon_y \frac{\partial c'}{\partial y}) + \frac{\partial}{\partial z}(\epsilon_z \frac{\partial c'}{\partial z}). \quad (47)$$

Both $\bar{c}$ and c' are time-averaged quantities, which may be expected to vary in an orderly fashion with x and t. Hence if c' is considerably smaller than $\bar{c}$, which will be the case if adequate time has elapsed for diffusion to take place within the cross section, it is likely that $\frac{\partial c'}{\partial \xi}$ will be negligible compared to $\frac{\partial \bar{c}}{\partial \xi}$. The third term in equation 47 may be written

$$u'\frac{\partial c'}{\partial \xi} - \overline{u'\frac{\partial c'}{\partial \xi}},$$

and, by the above argument, the first part, $u'\frac{\partial c'}{\partial \xi}$ is negligible compared to the second term in the equation, $u'\frac{\partial \bar{c}}{\partial \xi}$. The second part, $\overline{u'\frac{\partial c'}{\partial \xi}}$, being the cross-sectional average of the first part, must be of the same order of magnitude, so that the entire term may be neglected.

Equation 47 may now be written:

$$\left[\frac{\partial}{\partial t} - \frac{\partial}{\partial y}\epsilon_y\frac{\partial}{\partial y} - \frac{\partial}{\partial z}\epsilon_z\frac{\partial}{\partial z}\right]c' = -u'\frac{\partial \bar{c}}{\partial \xi}. \quad (48)$$

which is identical to equation 8, Taylor's simplification of the conservation equation, except in the transient term, $\frac{\partial c'}{\partial t}$. Equation 9,

$$c' = f(P)\frac{\partial \bar{c}}{\partial \xi}, \quad (9)$$

can be identified as the steady-state solution to equation 48, assuming that the right hand side is not time-dependent.

Obviously, if Taylor's solution yielding the classical one-dimensional diffusion equation (equation 5) is valid, the right hand side of equation 48 is indeed time dependent. The crux of the solution is that the rate of change of the right hand side, $-u' \frac{\partial}{\partial t} \frac{\partial \bar{c}}{\partial \xi}$, decreases with increasing time, whereas the time scale for decay of transients in the cross section, already identified as T', is constant. Hence the end of the convective period and beginning of Taylor diffusion may be identified as that point after which, for each cross section in the flow, there is sufficient time for cross-sectional diffusion to establish the concentration profile called for by equation 9, prior to a significant change in $\frac{\partial \bar{c}}{\partial \xi}$.

Equation 9 is henceforth referred to as the steady-state concentration profile, although in actual fact it is steady only so long as $\frac{\partial \bar{c}}{\partial \xi}$ remains constant. One of the aims of the experimental part of this study is to validate Taylor's method by demonstrating achievement of the concentration profile in various flow situations.

III-D The Two-Dimensional Steady-State Concentration Profile

As an example, and for comparison with experimental measurements, the steady state concentration profile will be computed for two-dimensional flow in an infinitely wide open channel. The logarithmic velocity profile (equation 14) and the mixing coefficient resulting from the Reynolds analogy (equation 22) are assumed. Since

there are no variations in the lateral direction, equation 8 may be integrated in the form:

$$f(y) = \frac{c'}{\frac{\partial \bar{c}}{\partial \xi}} = \int_o^y \frac{1}{\epsilon_y} dy \int_o^y u' dy$$

$$= \frac{1}{\kappa^2 d} \int_o^y \frac{1}{(1 - y/d)(y/d)} dy \int_o^y (1 + \ell n\, y/d)\, dy$$

$$= \frac{d}{\kappa^2} \left[\sum_{n=1}^{\infty} \frac{1}{n^2} \left(\frac{d-y}{d} \right)^n - 0.648 \right] \qquad (49)$$

in which the condition has been imposed that $\bar{f} = 0$.

A third integration with u' will yield Elder's result (equation 15), $D = 0.404\, d\, U^*/\kappa^3$. The experiments are compared with this equation in chapter V.

III-E Extension of Taylor's Analysis to Three-Dimensional Flows

Previous solutions using Taylor's approach have been limited to cross sections characterized by only one dimension. Extension to a two-dimensional cross section is conceptually simple; one need only specify the values of ϵ_y, ϵ_z, and u' as a function of cross-sectional position, and obtain the solution of Taylor's simplified equation (equation 8), subject to the condition of no transport across the boundaries. A solution for any reasonable specification could be easily obtained by finite difference techniques using modern high-speed computers. The only problem is that detailed information on the

variations of ϵ_y and ϵ_z is difficult to obtain.

Many flows which have variations in two cross-sectional dimensions, including most in natural channels, are much wider than they are deep, and have major lateral variations in velocity. For these flows, an hypothesis has been made which renders the cross-section one-dimensional and equation 8 again integrable. Consider equation 8, rewritten in the form,

$$\frac{\partial}{\partial y}\left(\epsilon_y \frac{\partial f}{\partial y}\right) + \frac{\partial}{\partial z}\left(\epsilon_z \frac{\partial f}{\partial z}\right) = u'(y, z) . \tag{50}$$

If f and u' were to vary in only one direction, ζ, which might be either y (vertical) or z (lateral), equation 50 could be integrated to give,

$$f(\zeta) = \int_o^{\zeta} \frac{1}{\epsilon_\zeta} d\zeta \int_o^{\zeta} u' d\zeta . \tag{51}$$

Since ϵ_ζ and u' are of the same order of magnitude in either direction, the value of the integral depends mainly on the square of the distance over which the integration is made, either the depth or the width. For a channel which is much wider than deep, one might therefore expect that f will vary considerably more in the lateral than the vertical direction. Recalling that the dispersion coefficient is the cross-sectional mean value of the product -u'f (equation 11), the hypothesis is made that only lateral variations of depth-averaged values of u' and f need be considered. The hypothesis may be expressed as:

$$D = -\frac{1}{A} \int_o^b d(z)\, u'(z)\, f(z)\, dz \qquad (52)$$

in which: A = area of channel;

b = width of channel;

$d(z)$ = depth of channel at point z;

$f(z)$ = position function derived below; and

$u'(z)$ = local depth averaged velocity deviation

$$= \frac{1}{d(z)} \int_o^{d(z)} u'dy \ .$$

The concentration function, $f(z)$, to be used in equation 52, may be obtained by assuming that ϵ_z and c' (or f) are not functions of y. Considering an element of depth $d(z)$ and width Δz, with boundary condition of zero flow through the upper and lower surface, the conservation equation analogous to equation 50 is:

$$\int_o^{d(z)} u'(y, z)dy = \frac{\partial}{\partial z}\ \epsilon_z d\ \frac{\partial f}{\partial z} \qquad (53)$$

Further integrations yield:

$$f(z) = \int_o^z \frac{1}{\epsilon_z d}\ dz \int_o^z \int_o^{d(z)} u'\, dy\, dz \qquad (54)$$

and, substituting in equation 52,

$$D = -\frac{1}{A} \int_o^b u'(z)\, d(z)\, dz \int_o^z \frac{1}{\epsilon_z d(z)}\ dz \int_o^z \int_o^{d(z)} u'\, dy\, dz \qquad (55)$$

The error involved in neglecting vertical variations may be estimated by calculating a dispersion coefficient according to equation 13, in which only vertical variations are included. For all of the three-dimensional experimental flows, coefficients calculated by equation 55 were far in excess of those by equation 13, indicating that vertical variations were probably not important.

III-F Time Scale in Three-Dimensional Flows

Since in three-dimensional flows lateral variations in velocity and concentration appear to dominate the dispersion mechanism, the appropriate length and mixing coefficient for the time scale are those applying to lateral motion. For symmetrical channels, the half-width is an appropriate characteristic length, but most channels are not symmetric. The important length is the maximum distance over which mixing must take place to establish a uniform distribution; accordingly the characteristic length for natural channels is defined to be the distance between the thread of maximum velocity and the furthest distant point within the flow cross section. A close approximation is that ℓ is the distance from the point of maximum surface velocity to the most distant bank.

In section II-F it was decided to adopt Elder's lateral mixing coefficient, $\epsilon_z = 0.23\ d\ U^*$. In natural channels the local depth must be replaced by a mean quantity, the most often reported being r, the hydraulic radius. On this basis, the Eulerian time scale is

$$T' = \frac{\ell^2}{0.23\ r\ U*} \tag{56}$$

and, assuming equation 44, the Lagrangian time scale is

$$T = 0.30\ \frac{\ell^2}{r\ U*} \tag{57}$$

In the experiments which follow, times have been made dimensionless by the Lagrangian scale, T, because of its more fundamental significance.

The argument above is an attempt to relate dispersion in complex channels to bulk characteristics of the channel. The relations which actually control dispersion, i.e. equation 3, make any such attempt clearly an approximation whose validity rests on the cross-sectional distribution of depth, velocity, and mixing coefficient. A correct time scale can always be obtained after an experiment by application of equation 40. Nevertheless it is important to formulate an expression (such as equation 57) whose value can be calculated in advance of an experiment, or for a channel in which an experiment is not possible.

III-G Length Scales

Time scales have been presented which, it is supposed, relate to the period required before Taylor's theory describes the dispersion process. An associated scale for required length of uniform channel is clearly,

$$L_1 = \bar{u}\, T \ , \tag{58}$$

so that the distance downstream from the source point may be made dimensionless by setting,

$$x^* = \frac{x}{\bar{u}\, T} \ . \tag{59}$$

However, a different length scale applies to spreading within the cloud itself; combining equations 37 and 40 gives,

$$\overline{u'^2}\ T = 1/2\ \frac{d}{dt}\ \sigma_\xi^{\,2} \ . \tag{60}$$

This equation may be made dimensionless by setting

$$\xi' = \frac{\xi}{\sqrt{\overline{u'^2}}\ T} \ , \tag{61}$$

and

$$t' = \frac{t}{T} \ . \tag{62}$$

Equation 60 becomes:

$$\frac{d}{dt'}\ \sigma_{\xi'}^{\,2} = 2 \ , \tag{63}$$

in which $\sigma_{\xi_1}^2$ is the variance based on the dimensionless variable ξ'. Thus an appropriate scale for distances within the cloud itself is

$$L_2 = \sqrt{\overline{u'^2}}\ T \ . \tag{64}$$

This scale will be used to compare experimental results in varying flow conditions.

III-H Numerical Analysis

A finite difference solution to equation 3, simplified to two dimensions, has been given by Yotsukura and Fiering (section II-D). Since their method appeared to yield an incorrect result, and as corrected requires a large amount of computer time, another method was sought. The solution given here is not a direct solution to the differential equation; rather, it is a step by step simulation of what is believed to be the physical process.

Consider the cross section shown in figure 4. The total flow is divided by vertical lines into n stream tubes, of area $A_1, \ldots, A_n$, where n is not greater than 10. Each stream tube is assigned a relative velocity, $u'_1, \ldots, u'_n$, based on actual velocity measurements, care being taken that

$$\sum_{i=1}^{n} u'_i A_i = 0 \ . \tag{65}$$

A 600 by 10 computer mesh for concentration values, c(I, J), is established, where I refers to longitudinal distance in a coordinate system moving at the mean flow velocity, and J to the jth stream tube. A time step, Δt, is selected, subject to conditions given below; the computer longitudinal distance step is taken as

$$\Delta x = u'_{i\ max}\ \Delta t\ , \tag{66}$$

i.e. the average flow in the stream tube of maximum relative velocity, $u'_{i\ max}$, is moving at plus or minus one computer mesh point per time step.

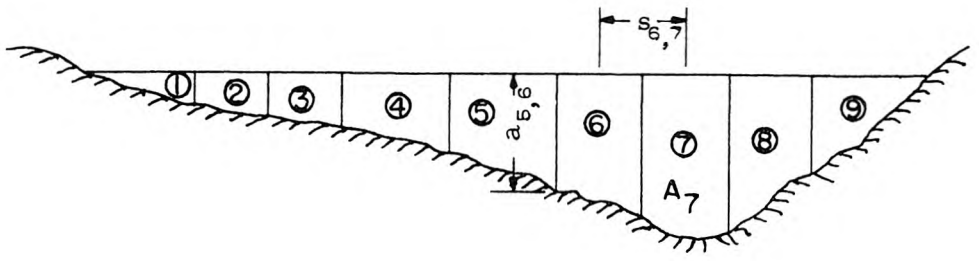

Figure 4 - Division of flow into stream tubes.

Each time step is assumed to consist of two parts: first, the concentration distribution within each stream tube is convected up or downstream according to the velocity of that tube; second, at each cross section transfer is accomplished between adjoining stream tubes according to the predetermined mixing coefficients.

In the convective portion, an entire new set of mesh point values, $d_t(I,J)$ is generated from the values $c_t(I,J)$, where the subscript t indicates the value after t time steps. The convective velocities are converted to units of mesh points per time step by the relation:

$$U_i = u_i' \frac{\Delta t}{\Delta x} . \tag{67}$$

A concentration which is convected part way between two computer mesh points is proportioned between them, inversely as the distance from each. Thus, the d(I,J) are obtained from the relation:

$$d_t(I,J) = c_t(I,J) + H\left[U_J\right] U_J \left[c_t(I-1,J) - c_t(I,J)\right]$$

$$+ H\left[-U_J\right] U_J \left[c_t(I,J) - c_t(I+1,J)\right] . \tag{68}$$

in which H is the Heavyside step function.

For the mixing portion, the following quantities are defined:

$a_{i,i+1}$ = area of surface dividing stream tubes i and i+1, per unit downstream length;

$s_{i,i+1}$ = distance between centroids of stream tubes i and i+1;

$\epsilon_{i,i+1}$ = mixing coefficient between stream tubes i and i+1;

$\Delta c_{i,i+1}$ = difference in concentration between stream tubes i and i+1 (c(I,J+1) - c(I,J)).

The mixing coefficient, $\epsilon_{i,i+1}$, was obtained in this study from equation 23, $\epsilon_z = 0.23\ d\ U^*$, using the depth between stream tubes and the overall shear velocity. Hence

$$\epsilon_{i,i+1} = 0.23\ a_{i,i+1} U^* \tag{69}$$

The mass transport between stream tubes per time step is computed by assuming that for the duration of the step the concentration gradient at the dividing surface equals the difference in convected concentrations at the mesh points divided by the distance between them, i. e.

$$\Delta M_{i,i+1} = a_{i,i+1}\, \epsilon_{i,i+1}\, \frac{\Delta c_{i,i+1}}{s_{i,i+1}}\, \Delta x\, \Delta t \tag{70}$$

Since the mesh point concentration is meant to represent the concentration within the entire stream tube, the change in concentration, $\delta c(I,J)$, at mesh point (I,J) is given by:

$$\delta c(I,J) = \frac{1}{A_J \Delta x}\, (\Delta M_{J,J+1} - \Delta M_{J-1,J}) \tag{71}$$

To facilitate computation, define the transfer coefficient:

$$k_{i,j} = \frac{a_{i,j}\, \epsilon_{i,j}\, \Delta t}{A_i\, s_{i,j}} \tag{72}$$

A new set of c net values for the t+1 time step may be calculated from the d net values of the t step by the relation:

$$c_{t+1}(I,J) = d_t(I,J) + k_{J,J+1} \left[d_t(I,J+1) - d_t(I,J) \right]$$

$$+ k_{J,J-1} \left[d_t(I,J-1) - d_t(I,J) \right] \tag{73}$$

So long as all the $k_{i,j}$ are less than 0.5, negative values cannot be generated; in practice, the criterion for the length of the time step was that the maximum $k_{i,j}$ be approximately 0.2.

This completes the computation for one time step; 300 time steps with 10 stream tubes may be completed using the IBM 7094 computer in approximately three minutes.

For an infinitely wide two-dimensional flow use of the method is similar, the divisions between stream tubes being drawn horizontally. Conceptually, it would be simple to extend the method to a more complicated arrangement of tubes, for instance by drawing a dividing surface half way down the cross section in figure 4; this would increase both the accuracy and complexity, as each stream tube would be able to exchange with three others, rather than two.

Verification and use of the analysis are deferred to chapter VII.

CHAPTER IV

EXPERIMENTAL METHOD

IV-A Design of Experiments

The general procedure for experimentally determining rates of dispersion is to introduce into the flow at some point a tracer material whose concentration may be measured at various times and places downstream. The three kinds of tracers commonly used in water are salt, radioactive isotopes, and florescent dye; standard methods are available for measuring concentrations of all three. Concentration of salt and radioactive isotopes may be measured in place if suitable probes are available; otherwise bottle or tube samples may be extracted.

Methods of introduction of tracer vary widely. Taylor used a plunger arrangement in which one short section of pipe was rapidly replaced by another containing salt solution. In open channels a plane source introduction is generally approximated by dropping the tracer onto the surface in a line; the vertical mixing accomplishes spreading over the cross section. For any flow condition it is very difficult to obtain a true line or point source introduction without affecting the turbulence structure near the insertion. If, however, one is concerned with the asymptotic rate of dispersion, or even with the pattern only a moderate distance from the source, the exact method of insertion is of little consequence.

Since the theory presented in the previous sections has concerned changes of coordinate position with respect to a moving

coordinate system, the ideal experimental data would be tracer concentrations at every point in space at each of a series of times. Elder obtained such data in flows one centimeter deep by inserting dye and taking pictures. Because this procedure is more difficult in larger scale experiments all subsequent workers have set up measuring cross sections downstream from the insertion point. Concentration at various points on each cross section is measured as a continuous function of time, either by inserting probes or taking samples. The result of the experiment is a series of concentration-vs.-time curves at the various measuring stations.

IV-B Methods of Determining the Dispersion Coefficient from Experimental Data

This section presents three methods of calculating a dispersion coefficient from experimental data. The change of moment method, based on a general property of the diffusion equation explained in section III-B, is theoretically exact, and has been used by previous investigators (3), (4), (8), (12), (19). However, in field studies calculation of the required moments is difficult, because of long tails on the measured distributions. For this reason, a routing procedure has been developed which verifies whether the change of moment method has given the correct dispersion coefficient. A third method, based on the diffusive mass transport through a cross section, is presented for use when concentration has been measured simultaneously at a number of points on a cross section. The three methods are discussed below.

1. The Change of Moment Method

The dispersion coefficient for a particular experiment may be most conveniently obtained from equation 37,

$$D = 1/2 \frac{d}{dt} \sigma_\xi^2$$

This equation applies to the tracer distribution during the diffusive period, irrespective of what shape of distribution has been produced in the convective period.

If a uniform, steady flow is maintained throughout the entire channel in which the dispersing cloud is located, it is shown in Appendix I that for any initial distribution of a finite tracer cloud,

$$\Delta\sigma_\xi^2 = \bar{u}^2 \Delta\sigma_t^2 , \tag{74}$$

in which σ_t^2 is the variance of the time-concentration curve measured at a fixed station. Thus when measurements are taken at various fixed points a dispersion coefficient may be calculated from the relation:

$$D = \frac{1}{2} \bar{u}^2 \frac{\sigma_{t_2}^2 - \sigma_{t_1}^2}{\bar{t}_2 - \bar{t}_1} \tag{75}$$

in which the subscripts 1 and 2 refer to two measuring stations, and $\bar{t}$ is the time of passage of the centroid of the cloud at the station.

When the velocity at the measuring stations varies during the passage of the cloud, as during the field experiments, equation 75

does not apply. If the stations are sufficiently close together, it may be possible to reconstruct distance-concentration curves from the time-concentration data, and to apply equation 37. For the reconstruction procedure, let:

T_c = time at which a distance-concentration curve is desired;

q = number of measuring stations in the vicinity of which tracer exists at time T_c;

$X_1, X_2, \ldots X_q$ = location of measuring stations (longitudinal distance upstream from arbitrary datum);

$\bar{u}_i(t)$ = mean velocity measured at the ith measuring station at time t (positive downstream);

$\alpha_1, \alpha_2, \ldots, \alpha_q$ = correction factor to be applied to velocity measured at the ith measuring station, and;

$x_i(T_c, t)$ = actual location at time T_c of the tracer concentration measured at time t at the ith measuring station.

For times differing not too greatly from T_c, an approximate relation, neglecting dispersion, is,

$$c(x_i, T_c) = c(X_i, t), \tag{76}$$

in which

$$x_i(T_c, t) = X_i + \int_{T_c}^{t} \alpha_i \bar{u}_i(\tau)\, d\tau \tag{77}$$

The integration may be performed in steps equal to the time between velocity measurements. The correction factors, $\alpha_1, \ldots, \alpha_q$, are required because flow in natural channels is always locally non-uniform,

so that the mean velocity measured at any one cross section is not exactly that of the adjacent reaches. Equation 77 assumes that changes in mean velocity throughout a local reach are proportional to those at the measuring cross section. Although the proportionality factors, α_i, are not known in advance, a reasonable first guess may be based on the travel time of the mean or peak concentration. The set of first guesses is used with the concentration values obtained at each measuring station to draw q segments of the overall concentration-distance curve. Normally the segments from adjoining stations will not match, but the required changes in the α_i will be evident. The calculation is then repeated with new α_i, and a smooth curve can generally be drawn through all the points. Since dispersion is occurring during the process, results are not expected to be exact.

The accuracy of the method depends on the length of time through which measured values of concentration must be projected, which in turn depends on the distance between measuring stations. In field studies this is usually limited only by available manpower.

2. Routing Procedure

Although the change of moment method is theoretically exact, in practice calculation of moments from experimental data is difficult, because of the long tails on the distributions. Whether or not the correct dispersion coefficient has been obtained may be verified by an integration procedure based on the diffusion theory. If at some time, $t = 0$, an initial distribution of tracer, $c = c_o(\xi)$, is observed, then by

superposition of fundamental solutions the tracer distribution at any later time may be obtained from the relation:

$$c(\xi, t) = \int_{-\infty}^{\infty} c_o(\xi') \frac{e^{-\frac{(\xi-\xi')^2}{4Dt}}}{\sqrt{4\pi D t}} \, d\xi' . \tag{78}$$

The experimental results obtained at time t and position ξ may be plotted against the result of equation 78 to demonstrate the correctness of both theory and dispersion coefficient.

A major problem is that most experimental data are of concentration vs. time, hence not amenable to equation 78. One way this may be overcome is to assume that no dispersion takes place while the cloud passes the measuring probe. Then the concentration-time curve may be converted to a concentration-distance curve by multiplying time differences by the mean velocity, i.e.,

$$c(\xi, \overline{t}_o) = c(X_o, t), \tag{79}$$

in which

$$\xi = \overline{u} (\overline{t}_o - t) \tag{80}$$

and $\overline{t}_o$ is the mean time of passage past a probe located at longitudinal station X_o. To compare a curve measured at station X_1, $c(X_1, t)$, to one measured at X_o, equation 79 is substituted in both sides of equation 78, to yield:

$$c(X_1, t) = \int_{-\infty}^{\infty} c(X_o, \tau) \frac{\exp\left[\frac{-(\bar{u}(\bar{t}_1 - \bar{t}) + \bar{u}(\tau - \bar{t}_o))^2}{4D(\bar{t}_1 - \bar{t}_o)}\right]}{\sqrt{4\pi D(\bar{t}_1 - \bar{t}_o)}} \bar{u}\, d\tau \qquad (81)$$

in which $\bar{t}_1$ is the mean time of passage at X_1.

Conversion from concentration-time to concentration-distance and back to concentration-time is only an approximate procedure, the degree of which is shown by figure 5. Figure 5a shows an imaginary input of a highly skewed curve, assumed to exist at t = 0, which is being convected downstream at a rate of 50 cm./sec. and diffused according to the classical diffusion equation (equation 5) with a dispersion coefficient of 5000 cm.^{2}/sec. (typical values for the experiments described in Chapter V). The cloud is routed downstream according to equation 78; the initial highly-skewed shape is taken as an extreme example, probably more typical of the convective than the diffusive period, but assumed for illustration to be the initial condition for the diffusive period. After 8.14 sec. the input curve has diffused to the shape shown in the figure, with mean position at x = 10 meters; 20 seconds later convection and diffusion have produced a Gaussian curve stretching from x = 5 meters to x = 35 meters, with mean at x = 20 meters.

Figure 5b shows the time-concentration curves which would have been measured by probes located at x = 10 meters and x = 20 meters, due to the process described above. Both curves are highly skewed, because of dispersion during passage of the cloud past the

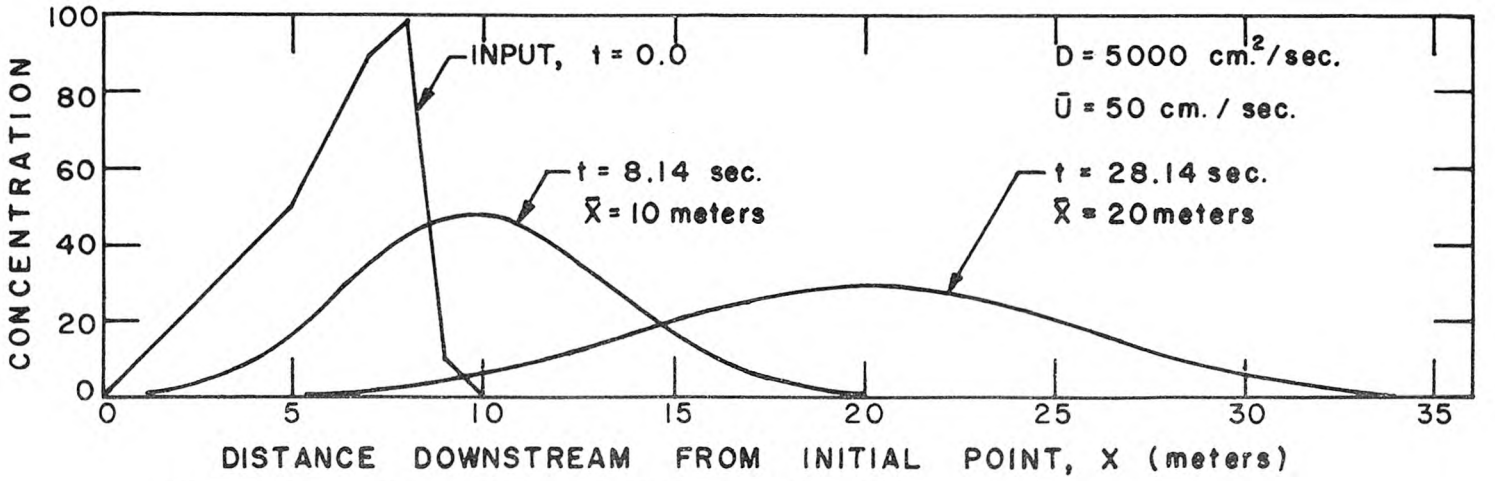

Figure 5a. Convection and diffusion of a skewed input according to Taylor's theory of one-dimensional dispersion.

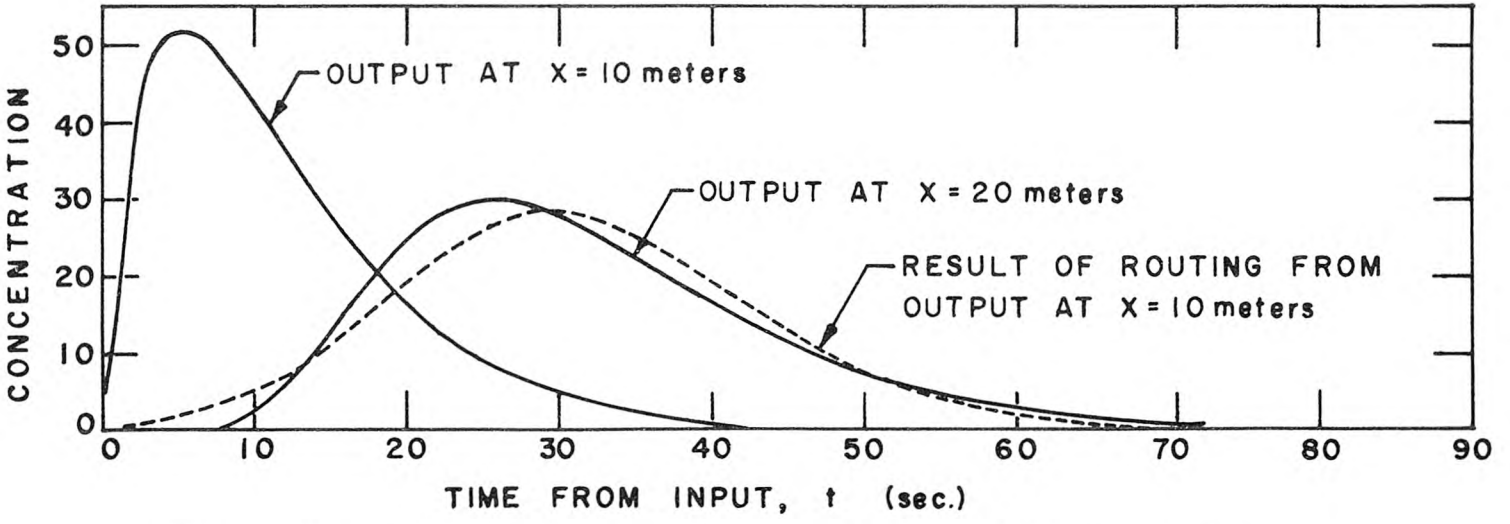

Figure 5b. Concentration-time curves which would be observed at two fixed points during process shown in (a).

probe. The dotted line shows the result of the routing procedure described above, when the time-concentration curve measured at x = 10 meters is used to predict a curve at x = 20 meters. The prediction is by no means exact; however, figure 5 gives a guide to the deviation from the measured curves which one should expect if, in an experiment, the tracer is following the diffusion theory.

A better routing procedure could probably be developed by solving the diffusion equation in the moving coordinate system as a boundary value problem with moving boundary, the boundary conditions being:

$$\begin{aligned} &t = 0, \quad c(\xi, 0) = 0 \text{ for } \xi > X_o \\ &t > 0, \quad c = c(\xi_o, t) \text{ given} \end{aligned} \tag{82}$$

in which: $\xi_o = X_o - \bar{u}\, t$

X_o = position of measuring probe in fixed coordinate system whose origin is at centroid of tracer distribution at t = 0; and

$c(\xi_o, t)$ = concentration measured at probe at X_o.

The solution to such a problem may be obtained by assuming a source of unknown intensity at the boundary, and solving for the source strength as a function of time to satisfy the measured boundary condition. However, such a solution, which would probably have to be obtained numerically, was not used in this study; the curves given in Chapter V were obtained by use of equation 81.

3. The Diffusive Transport Method

In chapter III, a quasi-steady-state concentration profile (quasi- is assumed hereafter) was defined as,

$$f = \frac{c'}{\partial \bar{c}/\partial \xi} , \tag{83}$$

with which a dispersion coefficient may be obtained from equation 11,

$$D = \overline{-u' f} .$$

The function f can be determined numerically or analytically by methods given in chapter III, and also experimentally by maintaining a mean concentration gradient for an extended period of time and measuring concentration simultaneously at a number of points on one cross section.

Let n probes be available to measure tracer concentration at one cross section. The total cross-sectional area is divided into n sub-areas, $A_1, \ldots, A_n$, centered on the probes; each sub-area is assigned a mean velocity, $u'_1, \ldots, u'_n$, based on measurements. Let c_i be the concentration measured by the ith probe; then,

$$\bar{c} = \frac{1}{A} \sum_{i=1}^{n} c_i A_i \tag{84}$$

and

$$c'_i = c_i - \bar{c} . \tag{85}$$

An assumption consistent with Taylor's assumption (3) (page 8) is:

$$\frac{\partial \bar{c}}{\partial \xi} = \frac{1}{\bar{u}} \frac{\partial \bar{c}}{\partial t} \tag{86}$$

(this is exact if $\frac{\partial \bar{c}}{\partial \xi}$ is constant). A dispersion coefficient may be obtained by numerical integration of equation 11 in n steps:

$$D = - \frac{1}{A \frac{\partial \bar{c}}{\partial \xi}} \sum_{i=1}^{n} u'_i A_i c'_i \quad . \tag{87}$$

In equation 87 each element of the sum represents the mass transport within the particular sub-area through a cross-section moving at the overall mean velocity of flow, and the dispersion coefficient, D, is obtained by its definition as the average mass transport through the entire section, divided by the mean concentration gradient. Thus the method is called the diffusive transport method.

IV-C Summary

This chapter has described a typical experiment designed to measure the rate of longitudinal dispersion of a tracer in a channel flow. Three methods have been given for analyzing data to obtain a dispersion coefficient. The easiest, and usually the first which should be applied, is the change of moment method; however, difficulty in calculating moments from experimental curves, particularly from experiments in natural streams, may make the result unreliable. Therefore, in all cases the result of the change of moment method

should be checked by the routing procedure, and if in error should be adjusted until a dispersion coefficient is obtained which gives a correct routing. Although the routing procedure itself does not yield a dispersion coefficient, a coefficient which is used with the procedure which is in error by as little as 10% will usually produce a visually incorrect routing, by which the value of the coefficient can be adjusted. The change of moment method, on the other hand, may produce with field data a result in error as much as 100%, of which the investigator will not be aware unless the routing procedure is used.

Accuracy of the diffusive transport method is limited by three factors: the channel should be uniform; measurements of concentration must be made at enough points on the cross section to adequately define the concentration variation; and the measurements, since they are of small variations from the mean, must be accurate. Non-uniformity of the channel may distort the concentration pattern at any one cross section, because of convection of the pattern from an upstream, different section. However, when the above three conditions are met the diffusive transport method yields both a physical insight into the dispersion mechanism and an accurate dispersion coefficient.

In the next two chapters, the three methods will be applied to experimental data.

CHAPTER V

LABORATORY EXPERIMENTS

V-A Introduction and Objective

Laboratory experiments were conducted in the sub-basement of the W. M. Keck Laboratory of Hydraulics and Water Resources. The experiments had three primary objectives:

(1) to verify Elder's application of Taylor's analysis by studies in flows which approximated the two-dimensional infinitely wide assumption;

(2) to verify, by studies in flows with appreciable lateral velocity variations, the hypothesis that such variations can greatly increase the dispersion coefficient, and that such flows can be treated as two-dimensional in the lateral and flow directions only; and

(3) to observe the time required in both types of flow for elapse of the convective period and beginning of applicability of Taylor's diffusion equation.

Section B of this chapter describes the experimental apparatus. Section C gives a summary of the experiments and major findings, which are described in detail in sections D through G.

V-B Apparatus

1. Flumes

The experiments were conducted in three recirculating flumes, identified as the 40-foot, 60-foot, and 40-meter flumes. Description of each is given below.

a. 40-foot Flume

Three preliminary runs were made in a flume 40 feet long by 10.5 inches wide. This flume is an entirely self-contained, truss-mounted unit, supported by a downstream hinge and upstream jack to allow adjustment of slope; channel, inlet and outlet boxes, variable speed motor and return pipe are all rigidly attached to the truss. Discharge is measured by a 4 inch by 3 inch venturi meter (laboratory number Q-22), and water surface by a point gauge mounted on an instrument carriage which runs on rails above the channel. The runs were made during an experiment on flow resistance of dunes by Hwang (32). The flume condition, sand grain size, measuring procedures, etc. are described in detail in the report of that study.

b. 60-foot Flume

Figure 6 shows an overall view of the 60-foot flume. The channel and inlet box are carried on a truss, which pivots at the downstream end and is supported by a pair of jacks at one point near the inlet box. The upper half of the outlet box moves with the truss; the lower half, connected by a rubber sleave, is rigidly attached to the floor. A variable speed $7\frac{1}{2}$ H.P. motor, 14 inch propellor pump, and 8 inch return pipe are attached to the floor. The return pipe enters the inlet box from above, so that no connection is required between pipe and box. An 8 inch by 5 inch venturi meter (laboratory number Q-21) in the return pipe allows discharge measurement.

The inlet box arrangement is shown in figure 7. The baffle downstream of the return pipe was necessary to prevent flow around

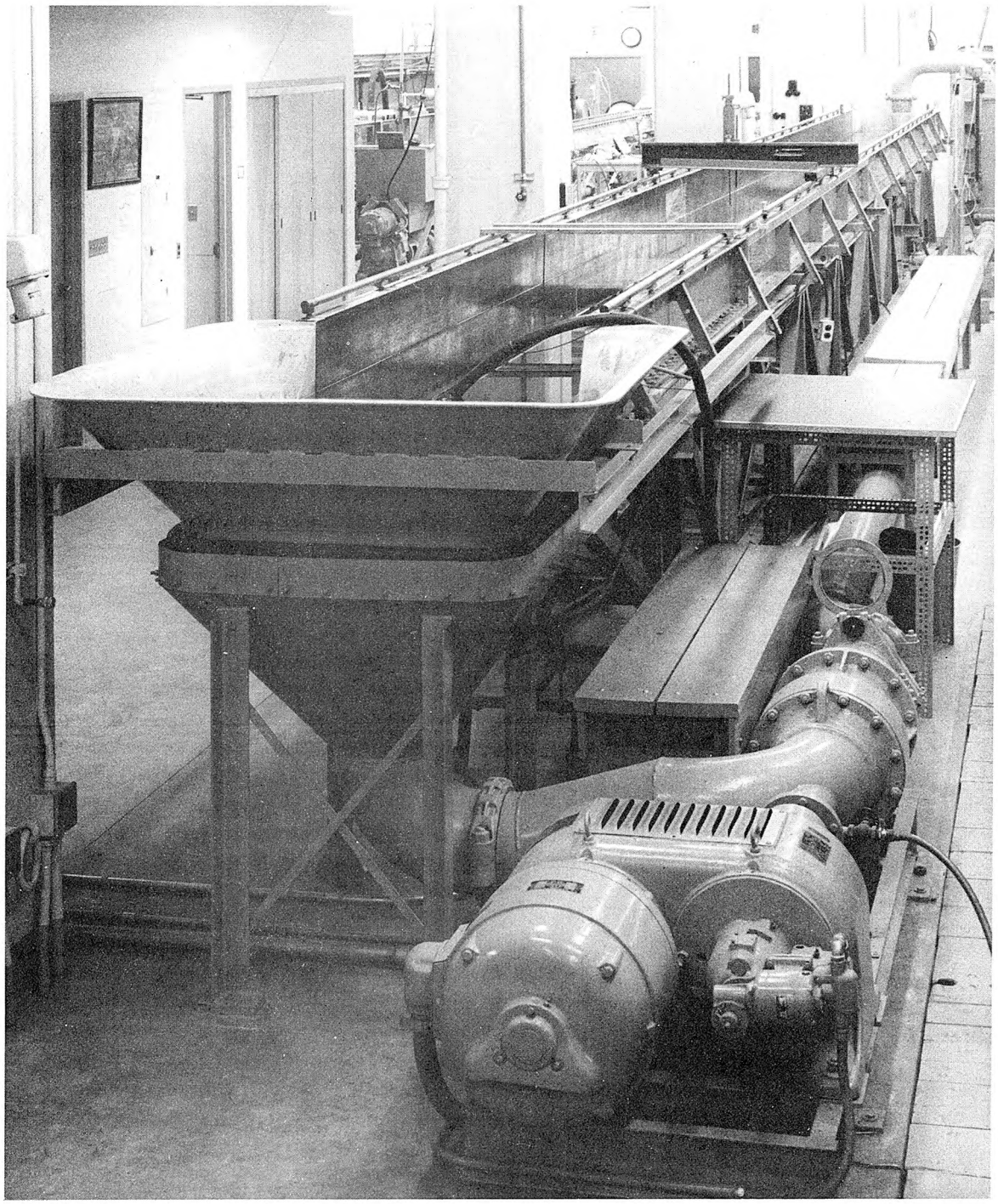

Figure 6. General view of the 60-foot flume, from downstream end.

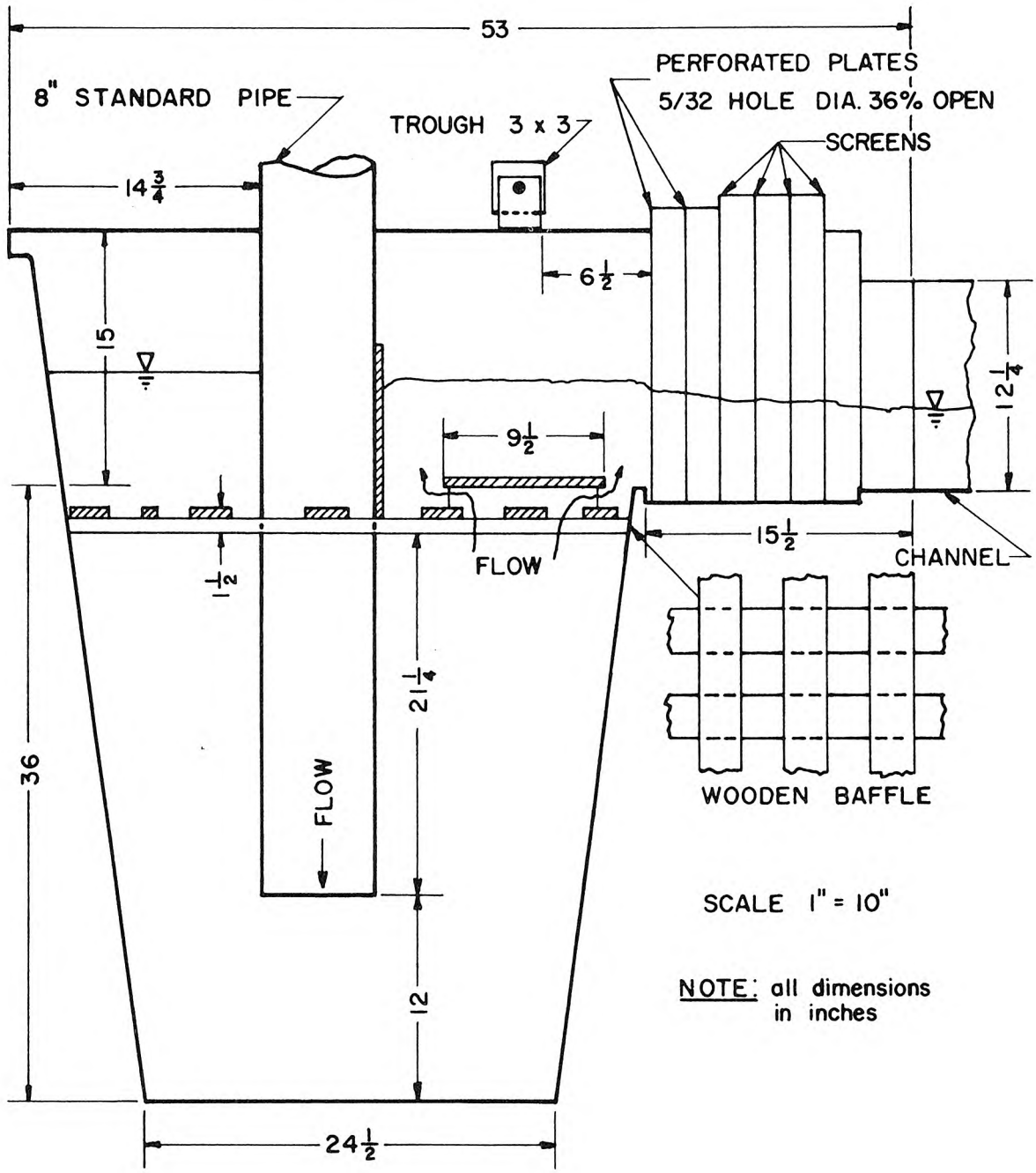

Figure 7. Inlet box to 60-foot flume.

the pipe, which preliminary velocity measurements had indicated might cause three-dimensional effects within the channel. At the discharges used during the experiments a head drop of approximately 1 inch existed across the perforated plate. This eliminated all the residual effects of the baffle arrangement within the inlet box, so that the velocity at the exit from the screens was essentially uniform.

An instrument carriage mounted on rails above the channel carries a point gauge and any other desired equipment. The rails are leveled by reference to still water to within 0.001 foot. The flume sides and bottom are steel plate, painted with two coats of epoxy white paint. The flume is stationed longitudinally by a steel measuring tape, and laterally by a scale on the instrument carriage. The uniform channel section runs from station 0.00 foot to 60.0 feet, south to north. All scales connected with this flume are in the English system of measurement. English units have been used to report quantities directly related to flume geometry, but all results have been converted to the metric system for comparison with results from the 40-meter flume.

c. 40-meter Flume

The 40-meter flume, constructed in 1963, has been described in detail by Hwang (32) and Vanoni (33). A schematic diagram is shown in figure 8; several photographs showing the entire flume are included in the sections describing the experiments.

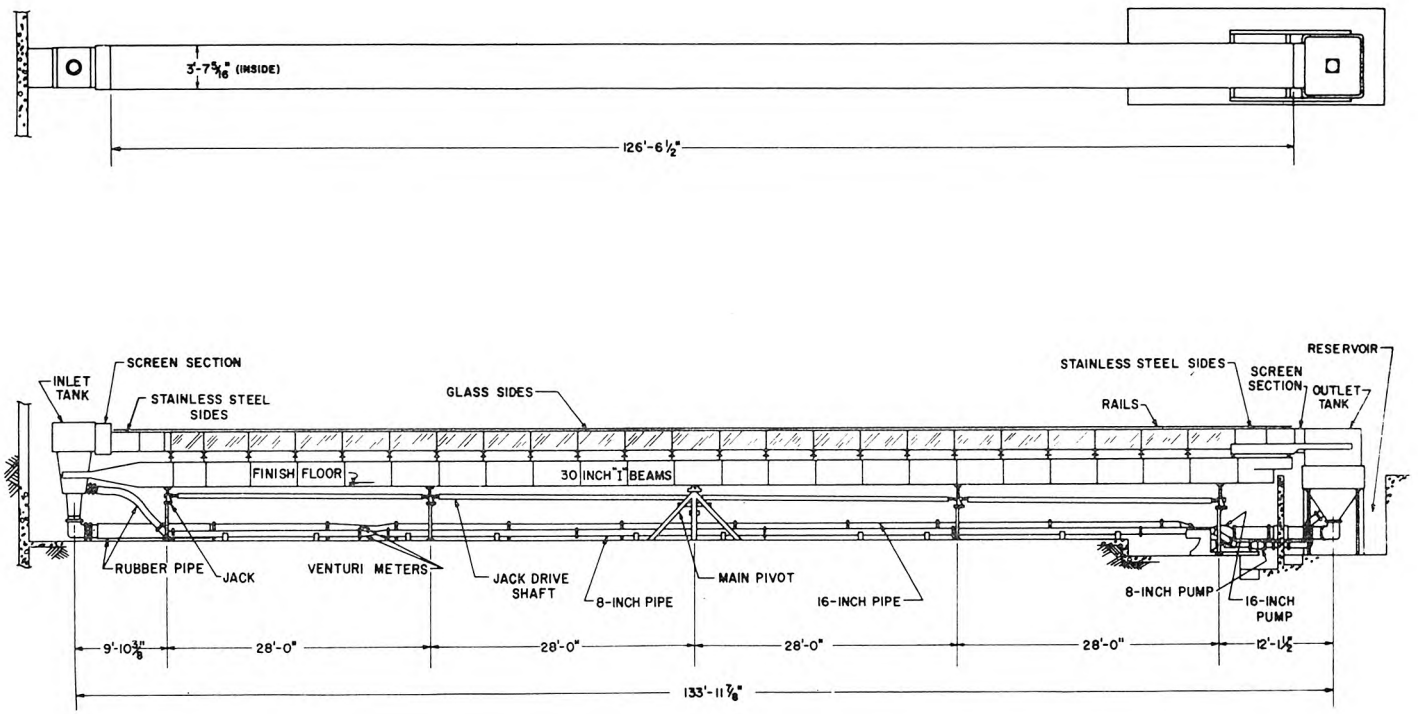

Figure 8. The 40-meter flume.

For these experiments the 16-inch return pipe was disconnected and only the 8-inch pipe used. The line is fitted with a 10-inch mixed flow pump, powered by a 10 H.P. motor with variable speed drive. The line includes an 8-inch by 4-inch venturi meter (laboratory number Q-6) for discharge measurement. However, during the experiments in which a trapezoidal insert was placed in the flume, particularly low discharges were required; for these runs, a section of 8-inch return pipe approximately at mid-flume was replaced by an 8-inch by 4-inch reducer, followed by 12 feet of 4-inch pipe, a 4-inch by 3-inch venturi meter (laboratory number Q-22), another 3-foot section of 4-inch pipe, a 4-inch gate valve, and a 4-inch by 8-inch expansion to rejoin the original line.

Flume slope is measured by a vernier gauge reading within 0.001 inches mounted approximately 15 meters from the rotation point. An instrument carriage mounted on rails above the flume carries a point gauge and other instruments. The rails are leveled with reference to still water at zero slope within a tolerance of 0.01 cm. As a check on slope gauge and rail adjustment, still water depth was read by the point gauge when the indicated slope was 0.001050 and the water depth averaged approximately 8 cm. The point gauge vernier is accurate to 0.01 cm. Of 36 water surface readings, 18 read exactly the value calculated from the measured slope, 17 were in error ± 0.01 cm., and one was in error 0.02 cm.

The flume sides are of glass, and the bottom of stainless steel plate. The bottom elevation was accurate to within ± 0.02 cm. over the adjustment points, and ± 0.05 cm. elsewhere. The flume is

stationed longitudinally by a steel tape reading in meters; the uniform channel section runs from station 0.00 m. to 38.60 m., south to north. A scale mounted on the instrument carriage gives lateral position within one millimeter.

2. Concentration Measuring Equipment

a. Conductivity Probes

The tracer used for quantitative measurements in the laboratory was salt solution, whose density was adjusted to that of the receiving water by addition of methanol. Design requirements for the measuring probes were that (a) they be capable of making in-place measurements in water flowing at up to 80 cm./sec., (b) the measurement be essentially at a point at the instant of recording, (c) the probes be sufficiently sensitive to record accurately changes in concentration of 0.5 parts per million, and (d) in a flow of constant concentration there by no drift or electronic "noise".

Figure 9 shows the design and figures 10 and 11 are photographs of the probes. The main tube, a 12-inch long streamlined cross section, is of Corning 7740 pyrex glass. The bottom is closed using Corning 3320 canary glass, which grades into a tip of Corning 7052 kovar sealing glass. Embedded in the kovar tip are three 0.010-inch diameter pure platinum wires, the upper ends of which have been silver soldered to copper leads. To the lower end of each is spot welded a 99.8% pure platinum plate, 1/8 inch by 1/8 inch by 0.010 inch. The plates are carefully spaced and aligned, and then set rigidly in struts of kovar glass. The center lead is insulated from the outer two, and all three encased in a metallic shield. The upper end of the

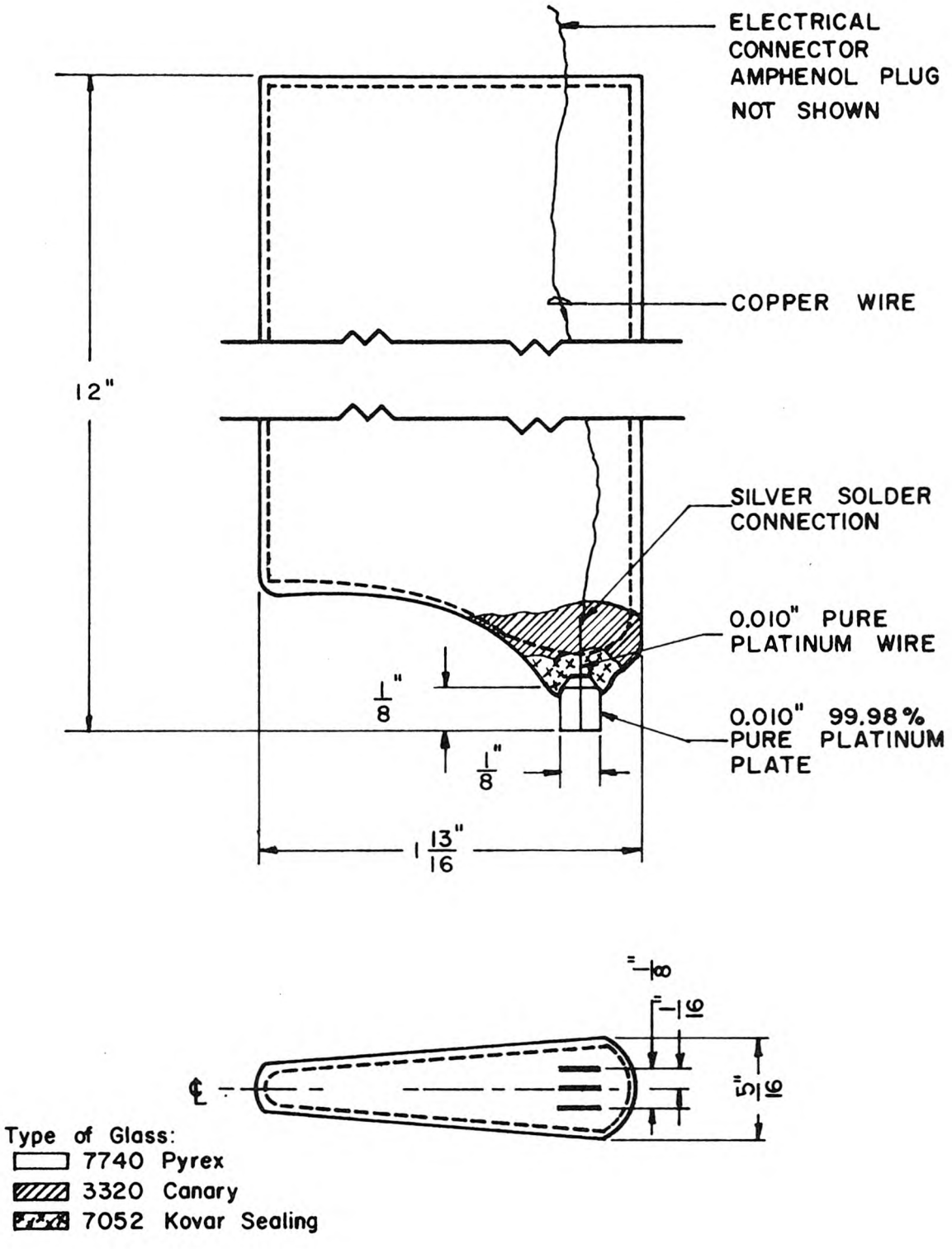

Figure 9. Design of the conductivity probes.

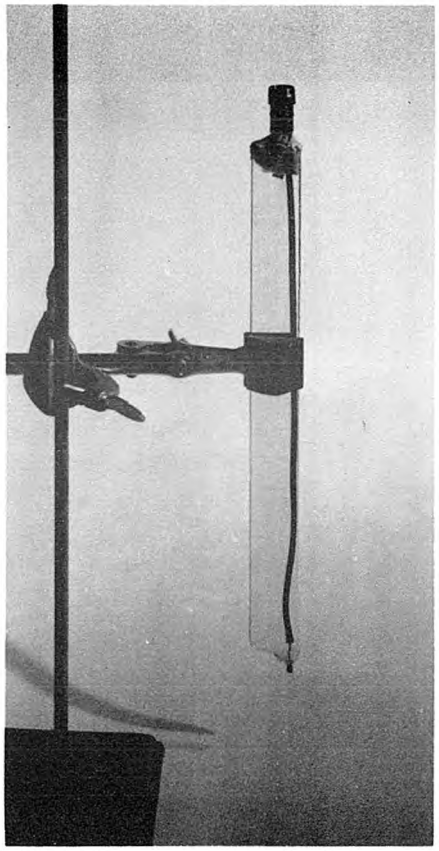

Figure 10. A conductivity probe.

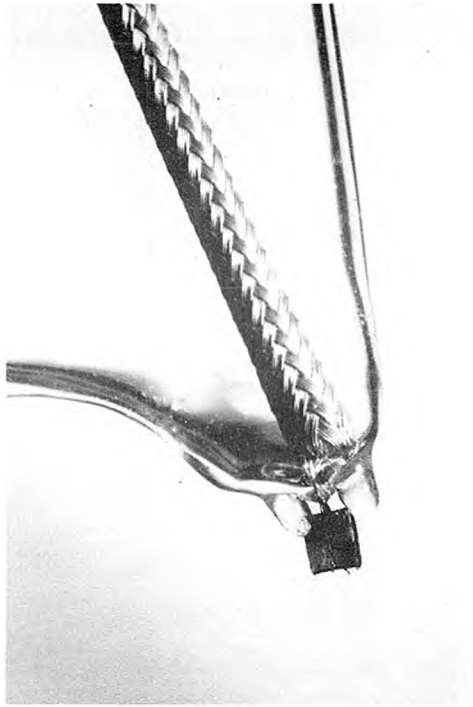

(a)

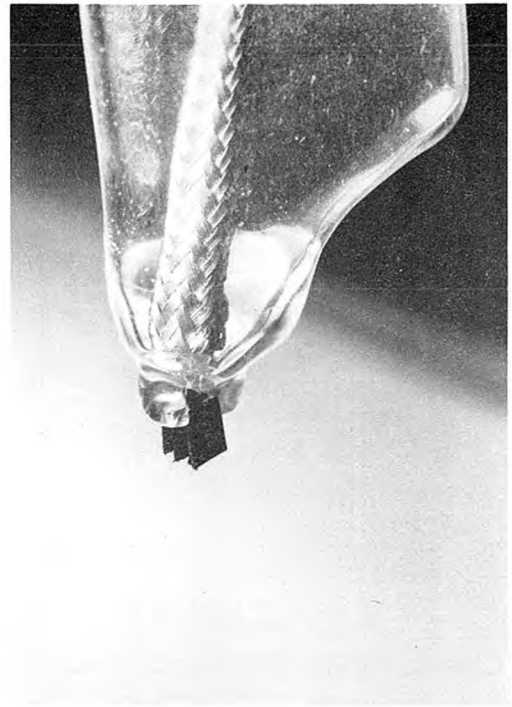

(b)

Figure 11. Close-up of electrodes of a conductivity probe (shown approximately double actual size); (a) side view, (b) oblique front view.

tube is capped with a single connector Amphenol plug and sealed with epoxy resin. The leads are soldered to the Amphenol plug, center lead to center pin and outside leads to outside. A vacuum inside the tube was not required. Since the outside of the mating Amphenol plug is grounded via the shield of the single conductor lead (Belden wire 8411) to the ground side of the Sanborn recorder (see the next section), the outside two plates are grounded. This confines the electric field to the fluid between the three plates, while providing double the response of a conventional two-plate arrangement.

Before first use, and later whenever readings became erratic, each probe was platinized according to a standard chemical method (34). The probes were stored when not in use immersed in distilled water, and were cleaned by electrolysis in 15 normal sulphuric acid before each use.

b. Recording Equipment

The Sanborn recording system series 150 was used for all measurements. In this system an excitation voltage of 4.5 volts alternating at 2400 c.p.s. is impressed onto a wheatstone bridge circuit; half of the bridge, including a balancing arrangement, is built into the recorder. The external half was constructed using IRC WW10J wirewound 1% precision resistors. Figure 12 is a photograph of the equipment with probe connections; a circuit diagram is shown in figure 13.

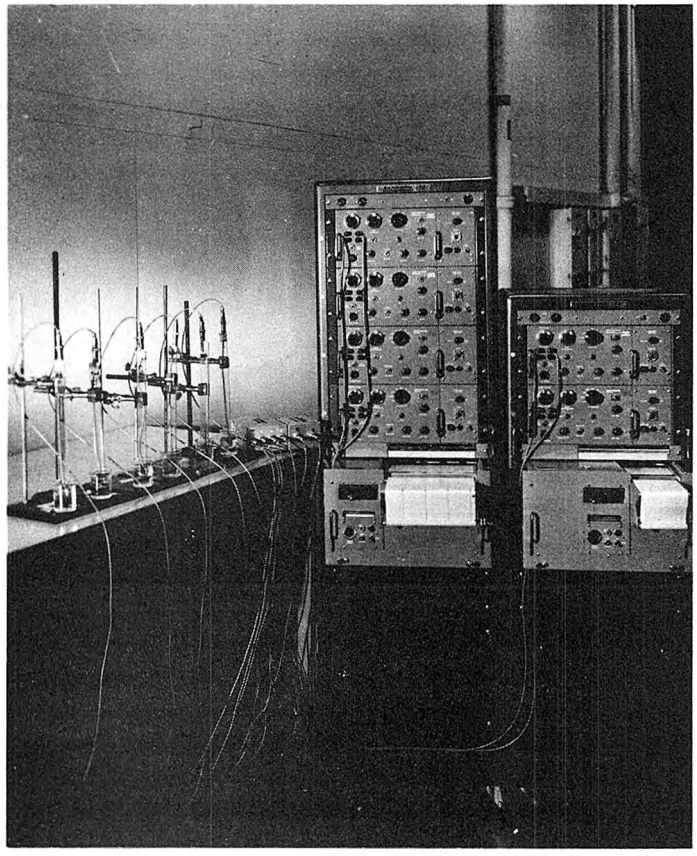

Figure 12. Sanborn recorders, connectors, and probes in storage between runs.

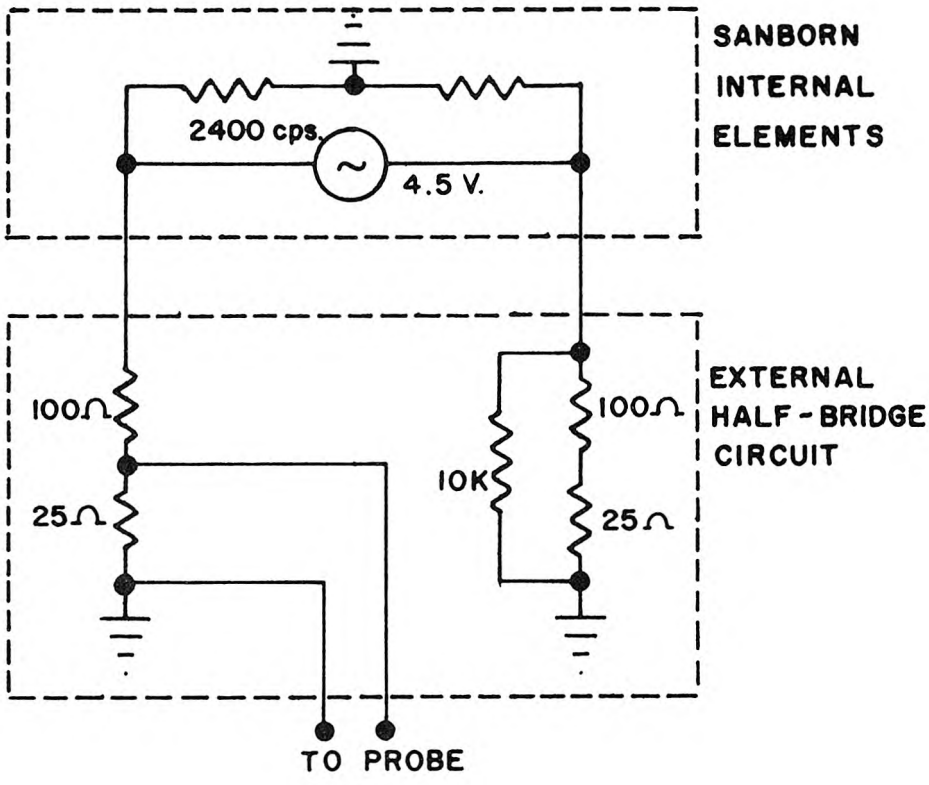

Figure 13. Circuit diagram for conductivity measurements.

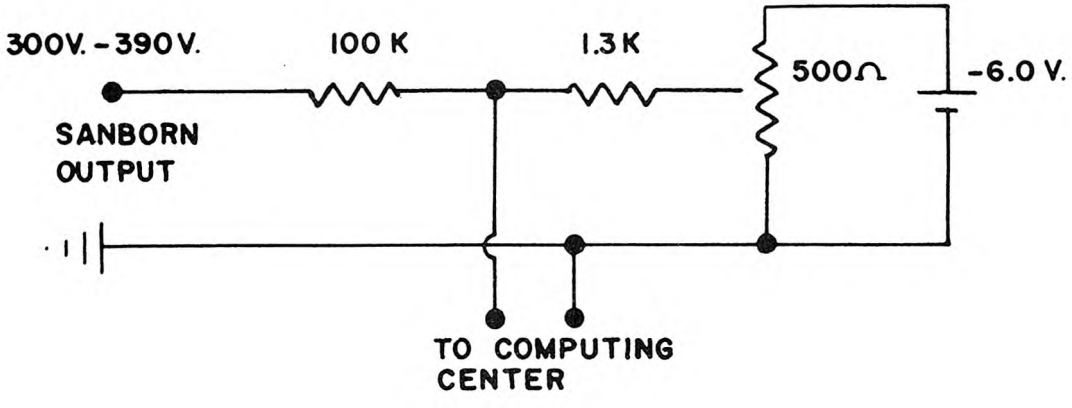

Figure 14. Circuit diagram for digital recording of Sanborn recorder output.

Figure 15 shows a typical set of data obtained simultaneously by six probes during one experiment; the upper four lines are obtained from the four-channel Sanborn strip-chart recorder, and the lower two from the two-channel recorder. One second tick-marks can be seen along the lower edge of each chart; the major chart divisions are 5 mm., and the minor 1 mm., so that the paper speed in this experiment was 2.5 mm./sec. The small arrows drawn in pencil above the time marks point to the insertion mark for each run; by lining up the insertion marks, made simultaneously, the two charts can be synchronized. The charts show the passage of four tracer insertions, between each of which the trace returns to the ambient level prior to any insertion. The steadiness of recording of a constant concentration can be seen by the traces between tracer passages; the violent oscillations during passage indicate that small scale mixing of the tracer and receiving water is not complete.

c. Calibration

The conductivity probes were calibrated either in place in the flume or separately in a beaker, depending on the experimental requirements as described below. Successive measured quantities of salt were added to the beaker or flume, and allowed to dissolve and mix completely. Figure 16 shows a typical set of calibration curves obtained during one series of runs; all measured calibrations were linear within the accuracy of reading of the Sanborn recorder for concentration levels up to 100 parts per million of sodium chloride. Water

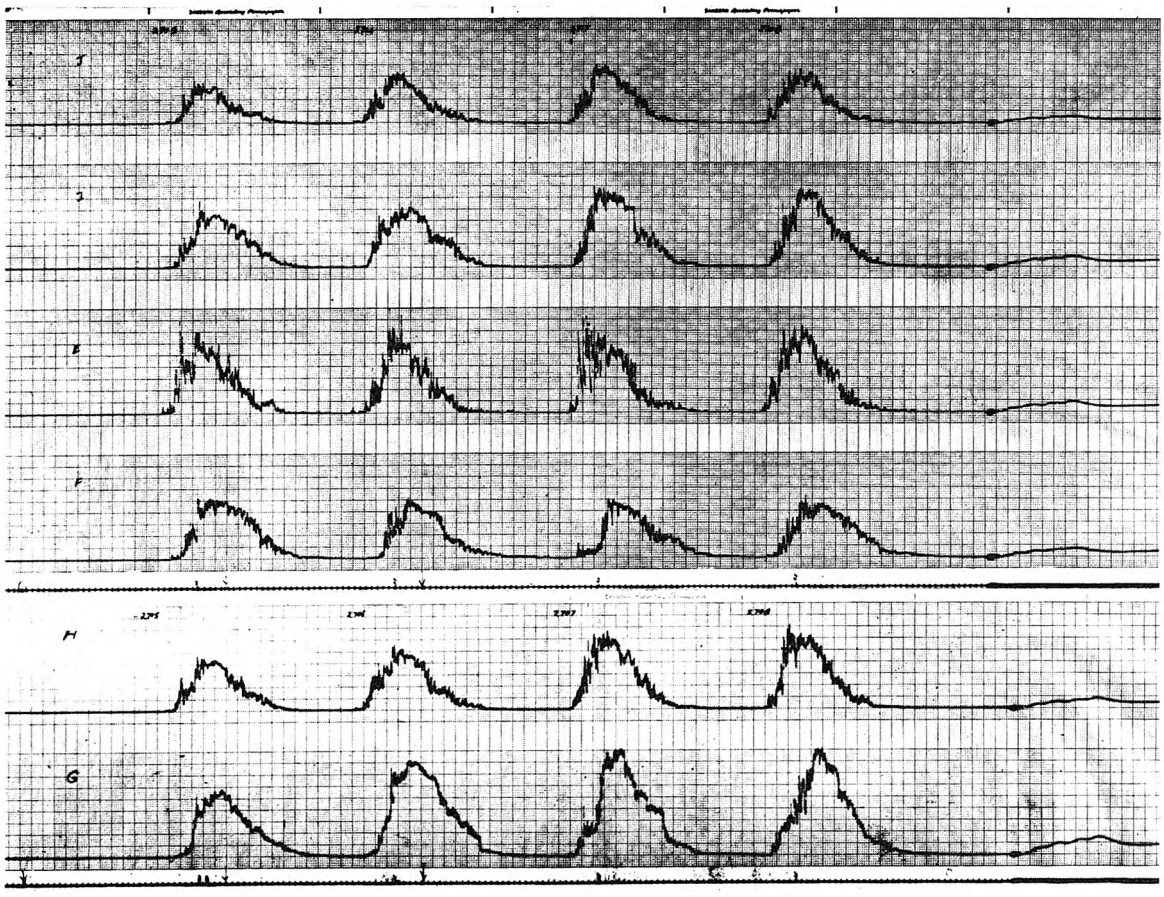

Figure 15. Data obtained during runs 2705-2708 at various places on one cross section.

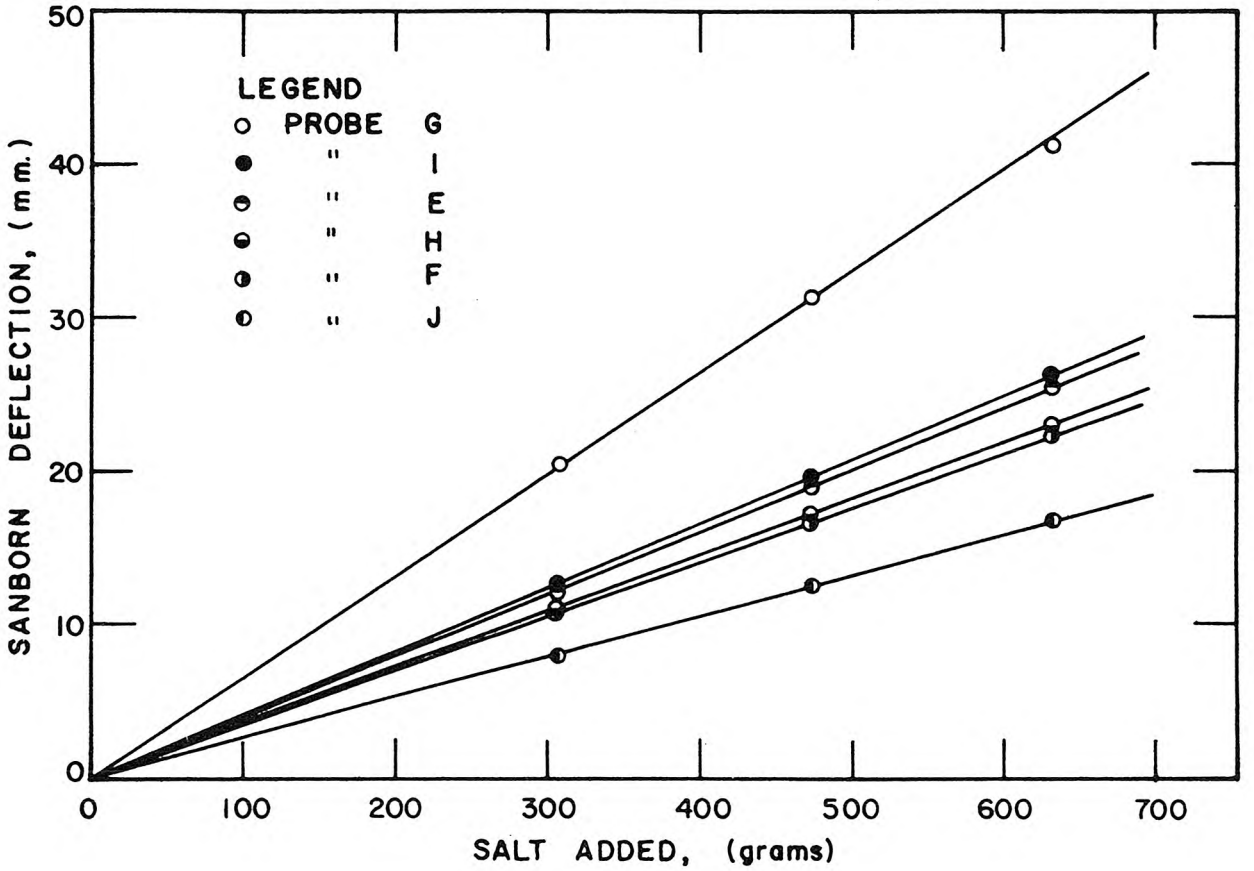

Figure 16. Calibration of probes for series 2900 by successive additions of salt to flow system.

temperature during the experiments was approximately 22° centigrade, and did not vary by more than 1° centigrade during any experiment, so that temperature fluctuations did not affect the calibrations.

d. Data Digitizing Equipment

Equipment located in the Booth Computing center is capable of converting a d.c. voltage signal with range from +1 to -1 volts into digital form recorded on magnetic tape. Sampling rates are available up to 10,000 samples per second, with resolution to ±1 millivolt. A multiplexer allows digitizing several input channels in sequence. During the experiments two cables were available from the laboratory to the Computing Center, allowing direct digital recording of the output of two probes.

The galvanometer pen of the Sanborn recorder is driven by d.c. voltage which varies from +300 volts to +390 volts on one galvanometer terminal and +390 volts to +300 volts on the other during full scale deflection. Both voltages are also available at the output plug located on the face of the power supply unit. Figure 14 shows the circuit by which these variations were reduced to the level required for input to the analog-digital converter. The voltage on one side of the galvanometer was attenuated to a variation of +3.0 to +3.9 volts by a simple resistor circuit. A standard 6 volt dry cell was used to impress a negative bias voltage, which could be varied from 0 to -6 volts by a variable resistor. By adjusting the bias to approximately -3.5 volts the output signal ranged between approximately -0.5 and +0.4 volts.

Digital samples were recorded at intervals of 100 milliseconds. Since the Sanborn output contains considerable high-frequency static (not recorded by the galvanometer pen due to the pen's own inertia), and since only low frequency variations were of interest, the output variations were passed through a D. C. coupled filter eliminating all variations of frequency greater than 30 cps. Correct operation of the system was verified by comparing output recorded on the magnetic tape with that of the Sanborn recorder pen for the same time.

3. Velocity Measuring Equipment

Velocities were measured with a $\frac{1}{8}$-inch diameter Prandtl pitot static tube having a dynamic head opening of 0.042 inches. The pressure difference between the static and dynamic ports was measured by a pressure transducer manufactured by the Pace Manufacturing Co., of Los Angeles, California. In this transducer deflections of a 0.004-inch diaphragm are measured by changes in magnetic reluctance of two magnetic cores, and the resulting voltage is recorded by the same Sanborn recording system as was used to measure concentrations.

The system was calibrated before and after each use by impressing on the pressure transducer differences in head measurable in manometer pots to within 0.001 inch. An exactly linear calibration was always obtained. The variation between calibrations before and after the run was never greater than 1%.

To obtain the velocity at a desired point the Prandtl tube, mounted on a traveler with vernier scale reading to ±0.001 foot, was positioned, and the output of the Sanborn recorder pen observed for a

period of at least two minutes (except in unusual cases of very low turbulence level where the pen output was nearly stationary and a one-minute period was considered sufficient). Normally the galvanometer pen would describe random variations over a range equal to 10 to 20% of the deflection from zero. A reading was obtained by laying a straight edge along the trace and averaging the variations by eye.

V-C Summary of Experiments and Results

All of the laboratory experiments included in this report are listed in numerical order in table 2. Each experiment in a particular flume at a particular set of hydraulic conditions is termed a "series"; each insertion of tracer at those conditions constitutes a "run". Thus all of the runs in a particular series are made at identical hydraulic conditions, although the method and location of tracer insertion and location of measuring probes may vary between runs. The first two digits of a run number indicate the series; the last two a particular run within the series. The missing numbers correspond to preliminary series which did not warrant report.

Details of each experiment are given in the sections which follow, arranged according to objective of the experiment. Sections D and E give all experiments designed to verify Taylor's analysis in two-dimensional flows; section D gives those in which the flume bottom was smooth (series 1200 through 1500, 2600, and 2700), and section E those in which the bottom was rough (series 0100 through 0400, and 2300 through 2500). Section F describes series 1600, in which lateral

Table 2. Summary of Experimental Results

Series	Flume	Channel Configuration			Objective[1]	No. of Runs in Series	No. of Probes in Section	Depth d (cm.)	Characteristic length ℓ (cm.)	Mean Velocity $\bar{u}$ (cm./sec.)	Shear Velocity[2] U^* or U^*_b (cm./sec.)	Friction Factor[3] f_*	Karman Constant κ	Measured Dispersion Coefficient D ($cm.^2/sec.$)			Dimensionless Dispersion Coefficient[4]			Reference for Detailed Results	
		Shape	Bottom	Sides										Change of Moment	Routing Procedure	Diffusive Transport	$\frac{Dx^3}{d\bar{U}^*_b}$	$\frac{D}{d\bar{U}^*_b}$	$\frac{D}{r\bar{U}^*}$	Figure	Table
0100	40-foot	rect.	Sand dunes	Smooth	(1)	2	1	11.6		37.6	4.28	0.10		355				7.1	19		12
0200	"	"	"	"	"	1	1	5.2		19.4	3.94	0.33		106				5.2	8.7		13
0300	40-meter	"	"	"	"	6	1	16.6		36.2	3.86	0.091		456				7.1	10.5		14
0400	"	"	"	"	"	4	1	22.9		48.9	4.52	0.068		742				7.2	12.0		15
1200	60-foot	rect.	Smooth	Smooth	(1)	24	1	4.6		32.3	1.51	0.017	0.37	72			0.52	10.4	11.5		4
1300	"	"	"	"	"	27	1	9.1		29.9	1.29	0.015	0.35	169			0.62	14.5	17.6		5
1400	"	"	"	"	"	18	1	13.7		26.2	1.12	0.015	0.35	191			0.53	12.4	16.4		6
1500	"	"	"	"	"	56	2	6.5		19.4	1.03	0.022	0.36	74			0.52	11.0	12.7		7
1600	60-foot	rect.	Smooth	Constrictions	(2)	29	2	6.4		22.0	1.40	0.032		231					30		22
2300	40-meter	rect.	Stones	Smooth	(1)	12	5	13.9		24.2	2.65	0.096	0.33	578	580		0.56	15.7	21.4	25	19
2400	"	"	"	"	"	11	6	9.4		21.2	3.08	0.166	0.34	427	430		0.58	14.9	18.5	26	20
2500	"	"	"	"	"	10	6	18.4		22.2	2.59	0.109	0.37	626	630		0.67	13.2	21.4	27	21
2600	40-meter	rect.	Smooth	Smooth	(1)	18	5	6.9		26.9	1.36	0.020	0.35	117	120		0.52	12.5	14.1	18	9
2700	"	"	"	"	"	8	6	12.8		36.2	1.62	0.016	0.39	236	240		0.66	11.4	14.0	19	10
2800	40-meter	trap.	Smooth	Rough	(2)	10	6	3.5	20	25.1	2.02	0.052		2220		1230			210	39	23
2900	"	"	"	"	"	10	6	4.7	21.5	45.4	3.59	0.050		3170		2530			190	40	24
3000	"	"	"	"	"	8	6	3.5	20	45.1	3.51	0.049		5590		4150			410	41	25
3100	"	"	"	"	"	8	6	3.5	17	44.4	3.48	0.049		4080	2500	2130			250	42	26
3200	"	"	"	"	"	7	6	2.1	16.5	45.3	3.28	0.042		5650		4000			640	43	27
3300	"	"	"	Smooth	"	10	4	3.4		48.3	2.49	0.021		282	280				39	21	11
3400	"	"	"	Rough	"	9	6	2.1	9.5	46.1	3.88	0.057		2540	2200	1900			330	44	28

Notes:

1. Numbers correspond to objectives listed in section V-A; i.e. (1) verify Taylor's analysis in two-dimensional flow; (2) verify hypothesis on effect of lateral velocity variations.
2. $U^* = \sqrt{grs}$, U^*_b = bed shear velocity, by sidewall correction method. Bed shear velocity given for runs with rough bottoms; otherwise overall shear velocity.
3. Darcy-Weisbach friction factor, $f_* = 8(\bar{u}/U^*)^2$. Bed friction factor given for runs with rough bottoms.
4. Measured value used for dimensionless coefficient is as listed under routing procedure, where available; otherwise under diffusive transport, where available; otherwise under change of moment.
5. Abbreviations: rect., rectangular; trap., trapezoidal.

velocity variations were produced by side channel constrictions. More detailed experiments designed to prove the effect of lateral velocity variations (series 2800 through 3400) are described in section G.

V-D Flume Experiments (Smooth Sides; Smooth Bottom)

This section describes and gives the results of those experiments conducted in flumes with smooth sides and bottoms, in which it was hoped the flow would be essentially two-dimensional. The objective was to test the applicability of Taylor's analysis to two-dimensional open channel flow.

1. Experiments in the 60-foot Flume

Series 1200 through 1500 were conducted in the 60-foot flume with rectangular channel 33.5 inches wide, using the direct data digitizing technique. A salt solution, approximately 5% by weight NaCl, was prepared, the solute being part distilled water and part methanol in proportions to yield a final density equal to that of the water in the flume. A small amount of blue organic dye was added to yield a light blue color. Density of the solution was checked by measurements with a hydrometer graduated to read specific gravity within 0.001, and also by inserting a small amount of solution through a hypodermic needle into a beaker containing flume water, and observing that the solution was neutrally buoyant. A trough,3 inches by 3 inches by thirty-three inches, was attached to the inlet box so that by rotating the trough a line source of solution would drop onto the flow in the flume just upstream from the screen section (see Figure 7).

Probes, supported on wooden struts, were located at two stations, one at approximately the midpoint of the flume and one near the exit section. The output signal from one probe at each of the sections was transmitted to the Computing Center and digitized. (For series 1500 two probes at each station operated in parallel.) Each series consisted of a number of runs, during which the position of the probes on the measuring cross section were changed. Occasionally the measuring stations themselves were also changed.

Velocity measurements were obtained on separate days by obtaining hydraulic conditions similar to those of each series. Velocity profiles were measured at two cross sections, approximately those used for the probes, at the centerline and both quarter points across the channel. All profiles fitted the logarithmic law with reasonable accuracy; the averaged profiles for each series are shown in figure 17, and the complete data are given in table 3.

The shear velocity was obtained from the slopes of the water surface and flume by the formula

$$U^* = \sqrt{g\ r\ S_e} \tag{88}$$

where S_e is the slope of the energy grade line. In most experiments, uniform flow was obtained within the possible accuracy of measurement of the water surface, so that the slopes of the flume and energy grade line are equal; in all the tables which follow, the reported slope is that of the energy grade line. Since the water surface elevation is believed to be measured ± 0.001 feet, and the flume slope ± 0.002 inch, the

Table 3. Velocity Measurements; Flow in 60-Foot Flume 85 Centimeters Wide.

Normalized Depth	Velocity at Station 25 (cm./sec.)				Velocity at Station 50 (cm./sec.)				Average
y/d	30.5 cm. W. of C. L.	21.3 cm. W. of C. L.	on C. L.	21.3 cm. E. of C. L.	30.5 cm. W. of C. L.	21.3 cm. W. of C. L.	on C. L.	21.3 cm. E. of C. L.	
Conditions similar to series 1200; depth = 4.54 cm., U* = 1.57 cm./sec.									
0.872	35.2	36.8	36.8	37.0	34.5	36.0	36.3	36.3	36.1
0.799	34.8	36.0	36.6	36.8	34.2	36.0	36.6	36.3	35.9
0.597	33.2	34.9	34.9	35.2	32.9	35.2	35.2	35.2	34.6
0.396	31.2	32.6	33.2	33.6	31.3	32.9	33.9	33.9	32.8
0.195	28.8	29.1	30.0	30.4	28.5	29.4	30.0	30.0	29.5
0.094	25.9	26.9	27.2	27.9	25.9	27.2	27.2	27.4	27.0
Conditions similar to series 1300; depth = 9.02 cm., U* = 1.34 cm./sec.									
0.916	34.4	35.7	32.9	36.3	34.1	34.6	34.9	35.2	34.8
0.801	34.1	35.2	32.0	35.7	33.5	33.8	34.4	34.6	34.2
0.601	32.9	33.2	30.6	34.6	32.9	32.3	33.5	33.5	32.9
0.402	31.5	31.7	28.8	32.6	31.7	30.6	31.7	31.7	31.3
0.203	28.5	28.5	26.8	30.0	29.1	28.8	29.4	29.1	28.8
0.101	25.9	26.8	24.4	27.1	26.5	26.2	26.8	26.8	26.3
Conditions similar to series 1400; depth = 13.59 cm., U* = 1.12 cm./sec.									
0.944	29.4	29.7	28.5	31.5	27.4	30.0	30.0	31.2	29.7
0.800	29.1	28.5	27.9	30.9	27.4	29.4	29.1	30.6	29.1
0.601	28.5	28.2	27.1	30.0	28.2	28.5	28.5	29.7	28.6
0.402	27.1	26.5	25.9	28.8	26.5	27.1	26.8	28.5	27.2
0.203	25.1	23.6	24.1	26.2	24.4	24.4	25.1	25.9	24.8
0.103	22.6	21.6	22.1	23.3	22.6	22.9	22.9	24.1	22.8

Note: 1. Abbreviations: C. L., centerline; W., West; E., East.
2. Depth and shear velocity measured during velocity measurements; note slight variation from conditions during dispersion experiments.
3. $U^* = \sqrt{g\,r\,S}$.

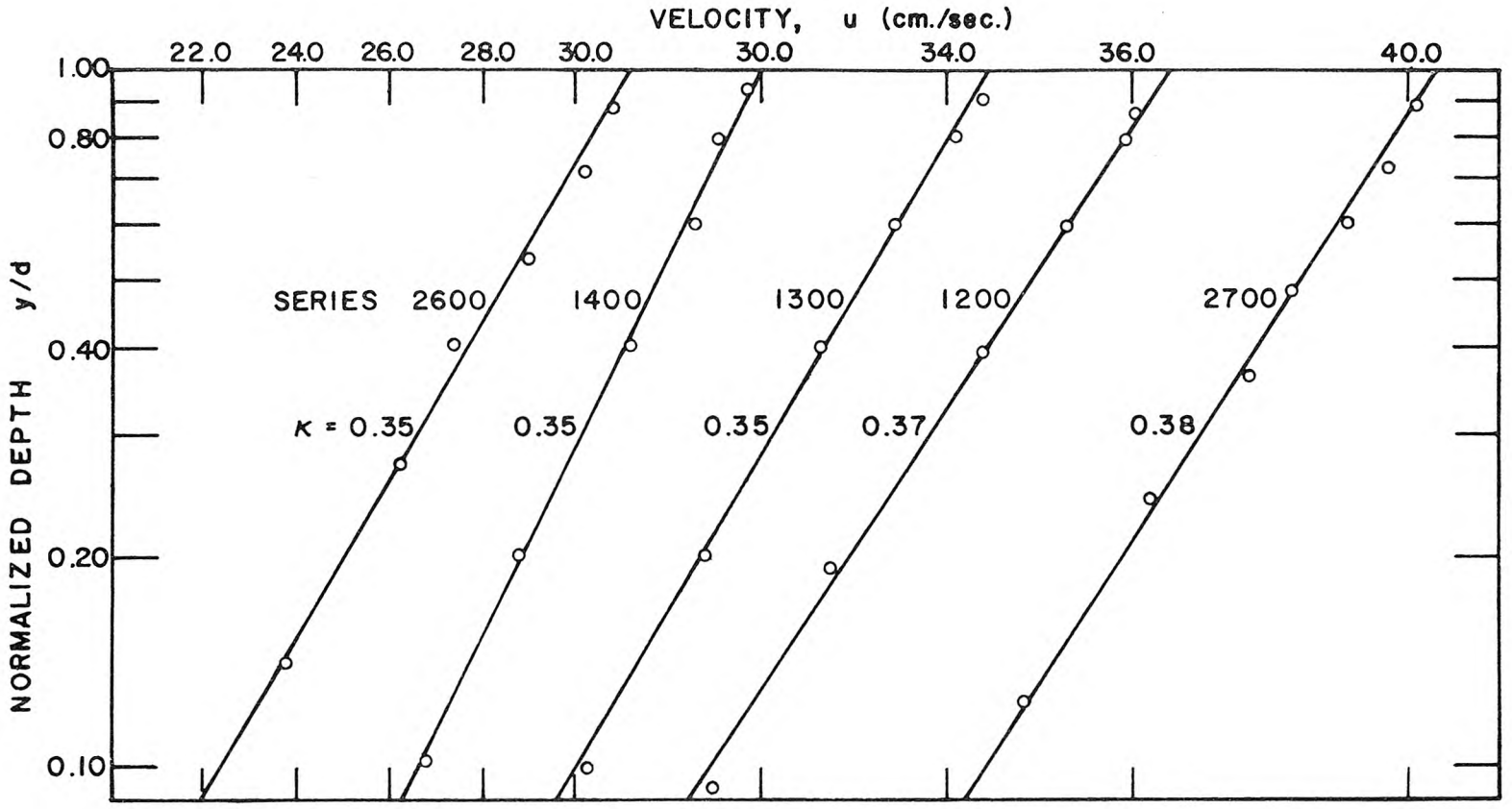

Figure 17. Measured velocity profiles, series 1200, 1300, 1400, 2600, and 2700 (averaged for each series).

accuracy of the slope of the energy grade line is approximately $\pm$ 0.00002.

The conductivity probes were calibrated in a separate calibration tank prior to use. Since all calibrations were linear, it was not necessary to know calibration factors during the experiments in order to calculate the variances. Prior to each run, the background salt concentration was eliminated by balancing the Sanborn recorder to read zero concentration. Enough tracer was inserted for each run so that the concentration at the downstream probe varied over a range of approximately 100 parts per million. The Sanborn recorder was adjusted so that this range would give nearly a full-scale deflection.

The data, stored on magnetic tape, were read into the computer along with the analysis program. The program contained several tests intended to identify when the trace departed significantly from the running mean, and when it returned. The moment calculations were carried out between the start and end points so identified. Drift (originating mainly in the filter system) was accommodated by proportioning a base line linearly from the starting to ending concentration values. The starting and ending values picked by the program were checked against the pen record of the Sanborn recorder; often, because the program tests were fallible, these values would be in error, and the visually established end points would have to be inserted for a repeat calculation.

Tables 4 through 7 show the hydraulic conditions and results of each run in series 1200 through 1500. Mean velocity was calculated by the formula,

Table 4. Results of Series 1200, June 29, 1965.

Depth = 4.6 cm.
Slope = 0.00060

Shear Velocity = 1.51 cm./sec.
$\varkappa$ = 0.37

Run	Probe Positions (all 2.5 cm. above bottom) Up-Stream	Down-Stream	Variances σ_t^2 (sec.^{2}) Up-Stream	Down-Stream	Mean Velocity $\bar{u}$ (cm./sec.)	Dispersion Coefficient D (cm.^{2}/sec.)
1201	Sta. 26.97	Sta. 54.58	8.6	13.1	32.6	94
1202	on C. L.	on C. L.	10.8	13.0	32.6	45
1203	↓	↓	10.9	13.5	32.3	52
1204			8.1	10.6	32.3	52
1205			7.2	9.8	32.6	54
1206			11.9	14.2	32.6	47
1207			16.3	17.1	32.6	17
1208	↓	↓	5.9	9.7	32.3	76
	Average, 1201-1208		10.0	12.6	32.5	54
1209	Sta. 26.97	Sta. 54.58	10.7	13.6	31.7	56
1210	21 cm.	on C. L.	10.2	13.8	32.0	72
1211	east of		9.2	11.6	32.6	50
1212	C. L.		7.8	12.7	32.0	98
1213	↓	↓	12.8	12.4	32.6	- 7
1214			9.5	14.5	31.1	164
1215			7.6	9.6	32.6	42
1216	↓	↓	9.6	13.2	32.3	73
	Average, 1209-1216		9.7	12.7	32.0	69
1217	Sta. 26.97	Sta. 54.58	8.7	15.0	31.7	123
1218	12.2 cm.	on C. L.	12.9	20.0	31.1	128
1219	west of		5.4	8.2	32.3	56
1220	C. L.		5.9	9.8	32.0	78
1221	↓	↓	6.4	9.7	32.6	69
1222			4.5	10.2	32.0	112
1223			4.8	9.0	32.6	87
1224	↓	↓	5.5	10.0	32.0	88
	Average, 1217-1224		6.7	11.5	32.0	92
Average, Series 1200			8.8	12.3	32.3	72

Average Dimensionless Dispersion Coefficients: $D\varkappa^3/dU^* = 0.52$
$D/rU^* = 11.5$

Table 5. Results of Series 1300, June 29, 1965.

Depth = 9.05 cm. Shear Velocity = 1.29 cm./sec.
Slope = 0.00023 κ = 0.35

Run	Probe Positions (all 7.6 cm. above bottom) Up-Stream	Down-Stream	Variances σ_t^2 (sec.^{2}) Up-Stream	Down-Stream	Mean Velocity $\bar{u}$ (cm./sec.)	Dispersion Coefficient D (cm.^{2}/sec.)
1301	Sta. 30.11	Sta. 54.52	10.8	19.8	31.1	182
1302	0.3 cm.	on C.L.	9.9	19.0	31.1	186
1303	west of	↓	7.0	14.8	32.0	172
1304	C.L.		8.2	15.9	31.1	157
1305	↓		9.1	13.5	31.4	92
1306			10.2	14.1	31.7	83
1307			10.4	17.8	31.7	155
1308			10.6	16.0	31.1	108
1309	↓	↓	14.3	18.6	31.7	92
	Average, 1301-1309		10.1	16.6	31.4	137
1313	Sta. 30.11	Sta. 54.52	13.0	23.0	29.0	162
1314	21.0 cm.	20.4 cm.	9.7	18.6	29.6	157
1315	west of	west of	10.8	21.8	28.7	175
1316	C.L.	C.L.	9.4	19.7	29.9	184
1317	↓	↓	12.2	23.3	29.0	181
1318			10.0	20.1	29.0	168
1319			12.2	21.5	29.3	158
1320			12.9	19.7	29.6	118
1321	↓	↓	12.6	23.5	28.7	174
	Average, 1313-1321		11.4	21.2	29.3	164
1322	Sta. 30.11	Sta. 55.27	8.7	22.8	29.3	230
1323	19.8 cm.	20.4 cm.	10.6	20.5	29.9	171
1324	east of	east of	11.1	20.8	30.2	174
1325	C.L.	C.L.	4.7	16.3	29.3	189
1326	↓	↓	6.0	22.4	28.0	234
1327			7.6	18.4	29.6	182
1328			7.0	22.4	29.0	244
1329			8.2	23.5	28.4	228
1330	↓	↓	6.4	19.9	29.6	225
	Average, 1322-1330		7.8	20.8	29.3	208
Average, Series 1300			9.8	19.5	29.9	169

Average Dimensionless Dispersion Coefficient: $D\kappa^3/dU^* = 0.62$

$D/rU^* = 17.6$

Table 6. Results of Series 1400, June 29, 1965.

Depth = 13.7 cm. Shear Velocity = 1.12 cm./sec.
Slope = 0.00012 $\varkappa$ = 0.35

Run	Probe Positions (all 10.2 cm. above bottom) Up-Stream	Down-Stream	Variances σ_t^2 ($sec.^2$) Up-Stream	Down-Stream	Mean Velocity $\bar{u}$ (cm./sec.)	Dispersion Coefficient D ($cm.^2/sec.$)
1401	Sta. 29.98	Sta. 55.27	12.5	33.7	25.0	217
1402	on C. L.	on C. L.	12.9	27.5	26.8	181
1403	↓	↓	12.0	25.2	27.1	171
1404			16.3	29.8	27.7	185
1405			9.2	24.2	27.7	210
1406	↓	↓	10.8	21.6	27.1	139
	Average, 1401-1406		12.3	27.0	26.8	184
1407	Sta. 29.98	Sta. 55.27	7.8	27.8	25.9	222
1408	21 cm.	22 cm.	5.8	25.8	25.3	211
1409	east of	east of	5.9	16.3	26.5	105
1410	C. L.	C. L.	5.3	30.5	26.2	292
1411	↓	↓	7.8	28.8	26.2	243
1412	↓	↓	7.6	20.5	26.5	158
	Average, 1407-1412		6.7	25.0	26.2	205
1413	Sta. 29.98	Sta. 54.34	13.2	32.6	25.0	201
1414	25 cm.	23 cm.	6.6	22.3	26.2	189
1415	west of	west of	7.3	22.9	25.6	178
1416	C. L.	C. L.	9.7	27.2	25.6	196
1417	↓	↓	8.3	23.1	25.6	165
1418	↓	↓	6.0	20.6	25.6	168
	Average, 1413-1418		8.5	24.8	25.6	182
Average, Series 1400			9.2	25.6	26.2	191

Average Dimensionless Dispersion Coefficients: $D\varkappa^3/dU^* = 0.53$
$D/rU^* = 16.4$

Table 7. Results of Series 1500, July 7, 1965.

Depth = 6.5 cm. Shear Velocity = 1.03 cm./sec.
Slope = 0.00019 κ (assumed) = 0.36

Run	Probe Positions		Variances σ_t^2 (sec.^{2})		Mean Velocity $\bar{u}$	Dispersion Coefficient D
	Up-Stream	Down-Stream	Up-Stream	Down-Stream	(cm./sec.)	(cm.^{2}/sec.)
1501	Sta. 14.99	Sta. 55.70	20.3	32.1	19.5	35
1502	on C.L.	on C.L.	11.1	31.3	19.5	60
1503	and	and	10.3	37.2	19.2	78
1504	18 cm.	19 cm.	8.8	33.0	19.2	71
1505	east of	east of	11.8	39.5	19.5	81
1506	C.L.	C.L.	8.3	32.6	19.5	72
1507			8.0	34.9	19.2	77
1508	All 4.3 cm.		9.1	32.3	19.2	67
1509	above bottom		12.2	39.4	19.5	81
1510	↓	↓	7.5	32.4	19.5	73
1511			12.9	32.7	19.2	58
1512			7.2	37.0	19.2	85
1513			8.3	41.4	19.2	95
1514			14.3	38.7	19.5	72
1515			9.3	32.0	19.5	68
1516			11.5	35.1	19.5	70
	Average, 1501-1516		10.7	35.1	19.4	72
1517	Sta. 14.99	Sta. 55.70	15.1	34.7	19.5	58
1518	21 cm.	22 cm.	13.4	45.6	19.2	92
1519	west of	west of	9.6	34.7	19.5	74
1520	C.L.	C.L.	8.7	38.5	19.2	87
1521	and	and	10.3	33.1	19.5	69
1522	18 cm.	19 cm.	8.6	35.2	19.2	77
1523	east of	east of	10.4	37.6	19.5	80
1524	C.L.	C.L.	7.8	30.5	19.2	66
1525			13.8	39.3	19.5	75
1526	All 4.3 cm.		8.8	34.2	19.2	73
1527	above bottom		9.0	35.4	19.2	77
1528			9.7	37.0	19.5	80

(Continued on following page)

Table 7 (Continued)

Run	Probe Positions		Variances σ_t^2 (sec.^{2})		Mean Velocity $\bar{u}$	Dispersion Coefficient D
	Up-Stream	Down-Stream	Up-Stream	Down-Stream	(cm./sec.)	(cm.^{2}/sec.)
1529	Same as 1517-1528		7.2	34.6	19.2	79
1530	↓	↓	12.8	36.8	19.5	72
1531			10.6	34.7	19.5	72
1532			8.2	40.0	19.2	92
1533			10.7	34.3	19.5	70
1534			8.8	33.5	19.2	72
1535			8.9	37.1	19.5	83
1536	↓	↓	13.5	32.0	19.5	56
	Average, 1517-1536		10.3	35.9	19.4	75
1537	Sta. 14.99 on C.L. 2.5 cm. and 4.3 cm. above bottom	Sta. 55.70 on C.L. 2.5 cm. and 4.3 cm. above bottom	10.1	33.9	19.2	69
1538			6.4	33.7	19.2	78
1539			6.3	29.2	19.5	67
1540			6.9	30.8	19.5	71
1541			9.0	30.3	19.5	63
1542			10.5	38.7	19.2	82
1543			10.6	35.9	19.2	74
1544	↓	↓	10.0	34.7	19.5	74
1545			8.1	40.1	19.5	96
1546			9.3	31.5	19.2	64
1547			9.2	32.8	19.5	70
1548			9.1	33.4	19.2	71
1549			8.6	37.0	19.5	83
1550			7.2	31.6	19.5	74
1551			10.0	38.4	19.5	84
1552			8.9	38.3	19.2	85
1553			10.3	35.4	19.5	74
1554			10.3	31.1	19.2	60
1555			8.8	32.1	19.2	68
1556	↓	↓	9.5	38.5	19.5	86
	Average, 1537-1556		9.0	34.4	19.4	74
Average, Series 1500			10.0	35.3	19.4	74

Average Dimensionless Dispersion Coefficients: $D\kappa^3/dU^* = 0.52$

$D/rU^* = 12.7$

$$\bar{u} = \frac{X_2 - X_1}{\bar{t}_2 - \bar{t}_1} , \qquad (89)$$

in which $\bar{t}_1$ and $\bar{t}_2$ are the mean times of passage past the upstream and downstream probes, located at X_1 and X_2 respectively. Dispersion coefficients were obtained from equation 75. As previously mentioned, all station numbers are in feet from the beginning of the uniform channel; all other measurements are in the metric system.

2. Experiments in the 40-meter Flume

Experiments were conducted in the 40-meter flume with rectangular cross section, 110 cm. wide and at various depths. Up to six probes were used; since six Sanborn channels could not be digitized simultaneously, all data were read from the Sanborn strip charts and fed into the computer by punched cards. All probes were located on the same cross section, but at varying depths so that the concentration profile could be observed. Since space did not permit placing all the electrodes in a vertical line, each probe was placed at a desired depth but at a random lateral position. Probe positions were measured after the run by a bent point gauge mounted on the instrument carriage. With this pointer, position could be measured longitudinally within 0.5 cm., laterally within 0.1 cm., and vertically on a vernier gauge reading to 0.001 ft.

Tracer was inserted from a trough, three inches by three inches by forty-three inches, mounted at rail level above the flume. The distance from trough to probes was varied by moving the trough, rather

than the probes, in order not to disturb the calibration of the probes. Several tracer insertions, each identified as a run, were made at each trough position. A set of runs made at one trough position is termed a "group"; the concentration measured at each probe at a particular elapsed time from tracer release was averaged over the runs in a group to obtain a "group-averaged" concentration. Curves of group-averaged concentration-vs.-time were then used in the analysis.

Performance of all the runs in each series was accomplished in about two hours, after which the probes were calibrated by inserting into the flume known quantities of salt. The water was recirculated in the flume until all the salt was dissolved and completely mixed, as indicated by a constant reading of all probes. When mixing was complete another quantity of salt was added, until a complete calibration curve was defined (see figure 16). Since all of the analytical procedures require knowledge only of relative concentrations, the values reported are in entirely arbitrary units; a convenient number of grams of salt added, g, was assigned the value of 100 concentration units. This defined a calibration factor for each probe,

$$f_c = \frac{100}{d_s(g)} , \tag{90}$$

in which $d_s(g)$ is the Sanborn deflection corresponding to addition of g grams. Then

$$c = f_c \, d_s , \tag{91}$$

in which d_s is any Sanborn deflection.

Velocity measurements were obtained on separate days by reproducing the hydraulic conditions of each series. Profiles were taken on centerline at three stations, and off centerline at one. Complete results are shown in table 8, and the plotted averages and resulting von Karman constants are in figure 17.

Tables 9 and 10 show the complete results of series 2600 and 2700. The time scale was calculated from equation 42, the mean velocity from equation 89, and the dispersion coefficient from equation 75 (for series 2600 a single dispersion coefficient was obtained by plotting group-averaged variance vs. time). Calculation of the mean time of passage and variance for each run was made as follows. The time at which the tracer entered the flow was recorded on the Sanborn strip chart by depressing the marker switch. The concentration-time curve at each probe for each run was defined by recording the deflection of each Sanborn pen at each of a sufficient number of times to adequately describe the passage, generally about 25 time values. The same time values were maintained for each run of a group for which the trough was at a constant distance from the probes. For each group, the deflection values were punched onto IBM cards and entered in the computer in a three-dimensional mesh, where the first index corresponded to the time value, the second to the run, and the third to the probe. Each probe was assigned an area of the cross section which included the entire width and half the vertical distance from the lower to the next higher probe (areas assigned the upper and lowermost probes, of course, terminated at the boundaries). The computer was given the calibration factors and assigned percentage areas for each

Table 8. Velocity Measurements; Flow in 40-Meter Flume 110 Centimeters Wide.

Normalized Depth y/d	Measured Velocity (cm./sec.) Sta. 15 on C.L.	Sta. 22 on C.L.	Sta. 30 on C.L.	Sta. 30 27.5 cm. W. of C.L.	Average
Conditions similar to series 2600;			Depth = 6.9 cm. Shear Velocity = 1.36 cm./sec.		
0.894	30.8	30.8	31.1		30.8
0.717	30.2	29.9	30.2		30.2
0.540	29.0	29.0	29.0		29.0
0.407	27.4	27.1	27.7		27.4
0.274	25.9	25.9	26.5		26.2
0.142	23.8	23.5	23.8		23.8
0.0531	21.0	20.7	20.4		20.7
Conditions similar to series 2700:			Depth = 12.8 cm. Shear Velocity = 1.62 cm./sec.		
0.890	39.6	39.9	40.5	40.2	40.2
0.722	39.3	39.6	40.2	39.3	39.6
0.603	38.4	38.4	39.3	38.7	38.7
0.483	37.8	37.2	37.2	37.2	37.5
0.364	36.3	36.9	36.6	36.3	36.6
0.244	34.1	34.4	34.4	34.4	34.4
0.125	31.7	31.7	31.4	32.3	31.7
0.0526	28.3	28.3	28.3	27.7	28.3

Note: Abbreviations: C.L., centerline; W., West.

Table 9. Results of Series 2600, Nov. 31, 1965.

Depth = 6.9 cm.
Slope = 0.000310
κ = 0.35

Shear Velocity = 1.36 cm./sec.
Mean Velocity = 26.9 cm./sec.
Time Scale, T = 5.94 sec.

Probe Locations:

Probe	Longitudinal Sta. (m.)	Lateral cm. from C. L.	Vertical cm. above bottom
E	36.06	8.2 E.	6.2
I	36.06	6.6 W.	4.9
J	36.06	1.9 W.	3.4
F	36.06	19.5 E.	1.6
H	36.06	18.4 W.	0.3

Injection Locations:

Runs	Longitudinal Sta.
2601-05	29.00
2606-10	22.00
2611-14	15.00
2615-18	8.00

Run	$\bar{t}$ (sec.)	Variance (sec.^{2})	Run	$\bar{t}$ (sec.)	Variance (sec.^{2})
2601	24.8	3.36	2611	76.8	19.9
2602	24.6	4.56	2612	76.9	20.4
2603	24.0	3.92	2613	76.8	19.4
2604	24.4	3.59	2614	77.1	18.6
2605	24.8	3.75	Average	76.9	19.6
Average	24.5	3.89			
2606	51.1	11.4	2615	103	29.2
2607	50.6	11.2	2616	103	28.9
2608	51.1	12.2	2617	103	29.1
2609	51.1	12.0	2618	103	29.5
2610	50.4	12.0	Average	103	29.2
Average	50.9	11.8			

Average Dispersion Coefficient = 117 cm.^{2}/sec.

Average Dimensionless Dispersion Coefficients: $D\kappa^3/dU^* = 0.52$
$D/rU^* = 14.1$

Table 10. Results of Series 2700, Dec. 7, 1965.

Depth = 12.8 cm.
Slope = 0.000257
κ = 0.39

Shear Velocity = 1.62 cm./sec.
Mean Velocity = 36.2 cm./sec.
Time Scale, T = 8.30 sec.

Probe Locations:

Probe	Longitudinal Sta. (m.)	Lateral cm. from C.L.	Vertical cm. above bottom
G	36.06	15.7 W.	0.7
F	36.06	19.7 E.	3.1
I	36.06	1.6 E.	5.2
H	36.06	2.8 W.	7.8
J	36.06	8.0 W.	10.2
E	36.07	7.8 E.	12.1

Injection Locations:

Runs	Longitudinal Sta.
2701-04	22.00
2705-08	11.00

Run	$\bar{t}$ (sec.)	Variance (sec.^{2})
2701	38.3	7.77
2702	38.2	9.19
2703	38.7	9.05
2704	38.6	8.17
Average	38.5	8.50
2705	69.3	19.8
2706	68.4	19.6
2707	68.9	18.7
2708	68.7	19.3
Average	68.8	19.4

Average Dispersion Coefficient = 236 cm.^{2}/sec.

Average Dimensionless Dispersion Coefficients: $D\kappa^3/dU^* = 0.66$
$D/rU^* = 14.0$

probe, and computed the mean concentration over the cross section for each time value. These values were then used to compute mean times and variances for each run. The concentration for each time value at each probe was also averaged over the runs in the group, and mean concentrations, times, and variances computed from the group-averaged values. The computer printed out mean concentration and concentration deviation from the mean at each probe, both for each run and for the group average (see Appendix III for group averaged results).

The group-averaged concentrations were used both in the routing procedure to verify the dispersion coefficient (obtained from group-averaged data), and to observe the comparison with the predicted steady state profile. Figure 18 shows the averaged results of each group in Series 2600; the dashed line is the results of runs 2606-10 routed according to equation 81 to compare to runs 2615-18, using the dispersion coefficient obtained by the change of moment method of 117 cm.^{2}/sec. Figure 19 shows the same thing for the groups of Series 2700; the dashed line is the result of runs 2701-04 routed to compare to runs 2705-08, using the dispersion coefficient of 236 cm.^{2}/cm.

The experimental results may be compared with equation 49, the steady state concentration profile, by assuming equation 86,

$$\frac{\partial \bar{c}}{\partial \xi} = \frac{1}{\bar{u}} \frac{\partial \bar{c}}{\partial t} .$$

$\frac{\partial \bar{c}}{\partial t}$ is obtained by measuring slopes on figures 18 and 19. The comparison is shown in figure 20.

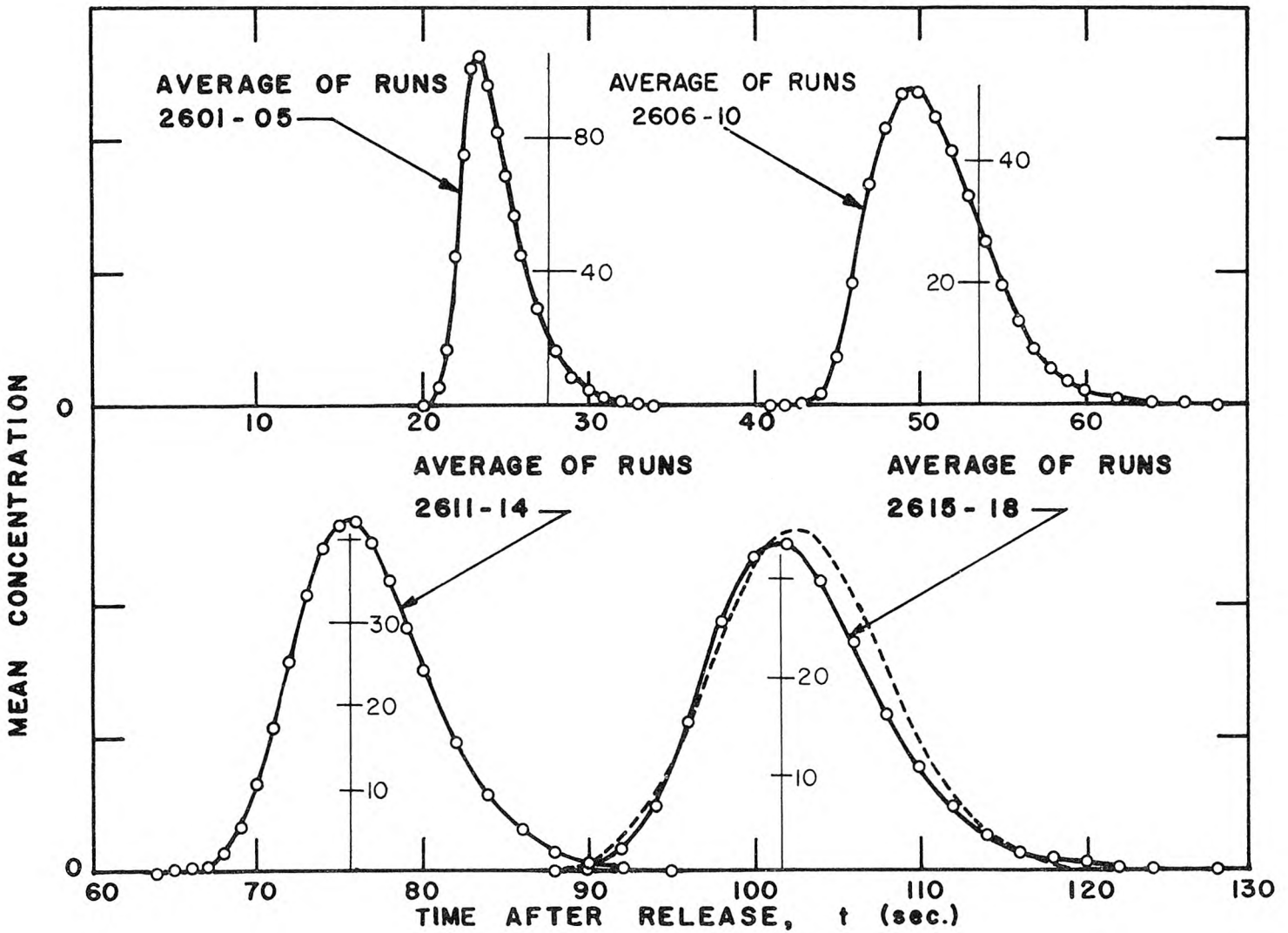

Figure 18. Results of series 2600. ---Result of runs 2606-10 routed to compare with runs 2615-18, D = 117 cm.^{2}/sec. Mean concentration in arbitrary units; note change of scale for each curve.

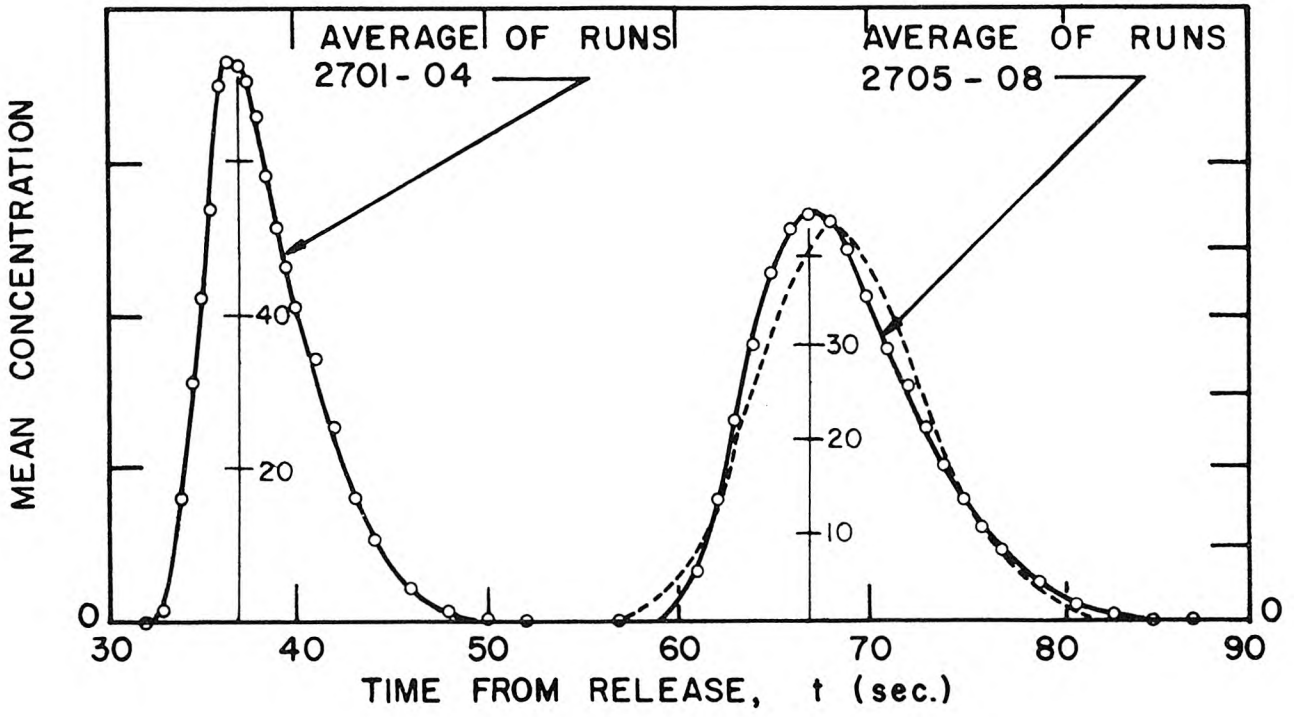

Figure 19. Results of series 2700. ---Result of runs 2701-04 routed to compare with runs 2705-08, D = 236 cm.^{2}/sec. Mean concentration in arbitrary units; note change of scale for each curve.

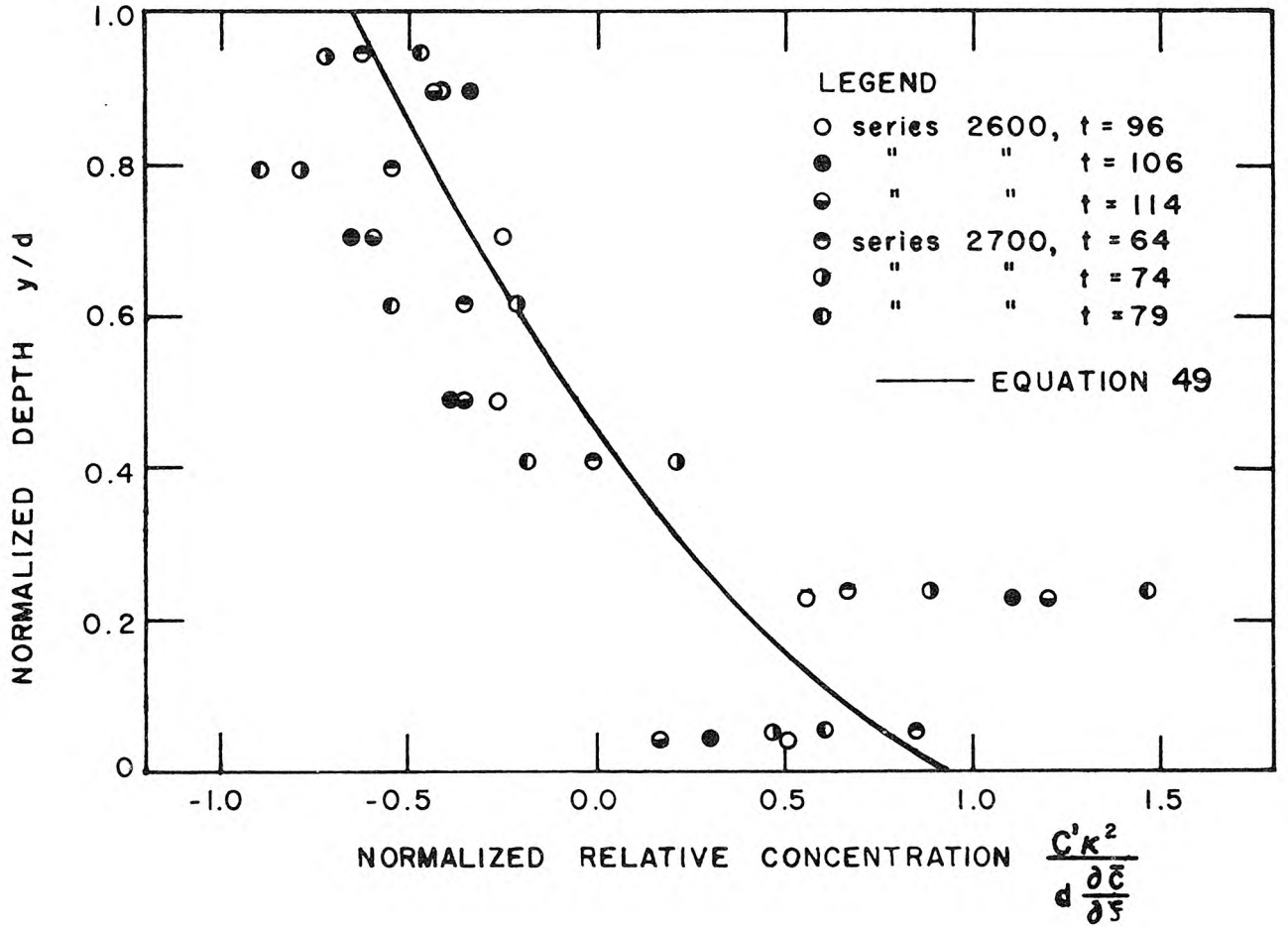

Figure 20. Comparison of measured concentration profiles for series 2600 and 2700 with prediction by Taylor's analysis.

The dispersion coefficients determined in both the 60-foot and 40-meter flumes exceed the predictions of Elder's application of Taylor's analysis by approximately 40%. Some possible explanations will be given in Chapter VIII. Figure 20 shows that concentration profiles measured in the 40-meter flume did tend to assume the form predicted by Taylor's analysis.

3. Experiments in the 40-meter flume with trapezoidal insert.

One experiment (series 3300) was conducted in a trapezoidal channel with smooth sides, to determine whether the shape effect would produce results greatly different from those of the experiments in rectangular channels.

The trapezoidal insert, placed in the 40-meter flume, is completely described in the section on experiments with rough sides, for which it was primarily designed.

A cross section of the channel with measured velocity contours is shown in figure 21a. Lateral stations were measured by positioning the tip of the Prandtl tube and reading the lateral scale on the instrument carriage. Velocity measurements were taken at stations 23.6 and 32.5, and averaged.

The position of each probe is shown in figure 21a. To obtain the cross sectional mean concentration symmetry was assumed about station 12.0W, and each probe assigned the following areas: Probe J, station 12.0W to 16.5W; probe I, station 16.5W to 23.0W; probe G, 23.0W to 27.0W; and probe H, 27.0W to the west wall. Table 11 lists the mean time of passage and variance for each run and group of runs;

Table 11. Results of Series 3300, Feb. 3, 1966.

Depth = 3.4 cm. Mean Velocity = 48.3 cm./sec.
Slope = 0.00218 Shear Velocity = 2.49 cm./sec.

Mean square velocity deviation, $\overline{u'^2}$ = 67.5 cm.^{2}/sec.^{2}.

Probe Locations:

Probe	Longitudinal Sta.	Lateral Sta.	Vertical (cm. above bottom.
J	33.52	12.0 W.	2.0
I	33.52	19.0 W.	2.0
G	33.52	25.0 W.	2.0
H	33.52	28.3 W.	2.0

Injection Locations:

Runs	Longitudinal Sta.
3301-04	23.90
3305-07	14.95
3308-10	4.99

Run	$\overline{t}$ (sec.)	Variance (sec.^{2})
3301	19.9	27.6
3302	19.7	28.3
3303	19.8	26.7
3304	20.1	28.2
Average	19.9	27.8
3305	38.5	71.8
3306	38.8	72.9
3307	39.0	72.2
Average	38.8	72.8
3308	58.9	121
3309	58.7	126
3310	58.9	121
Average	58.8	123

Average Dispersion Coefficient = 282 cm.^{2}/sec.

Average Dimensionless Dispersion Coefficient, $D/rU^* = 39$.

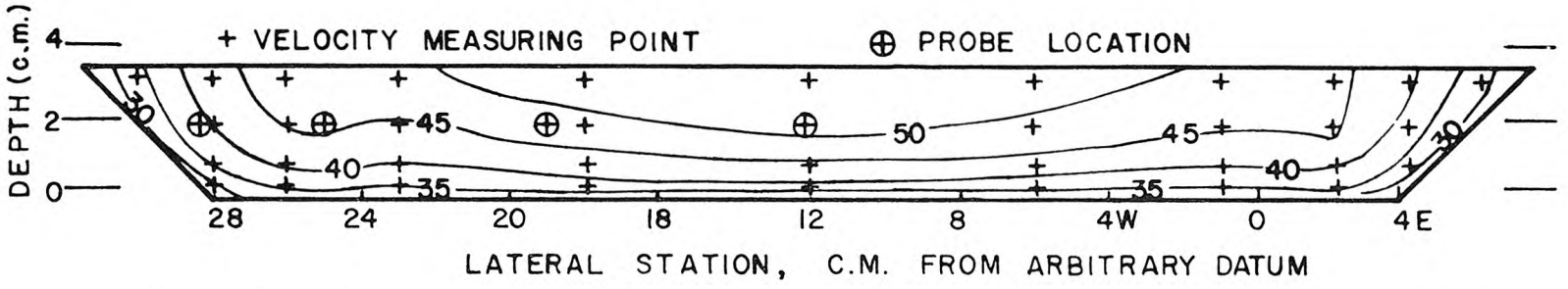

Figure 21a. Cross section of flow, series 3300. Contours are velocity, in cm./sec.

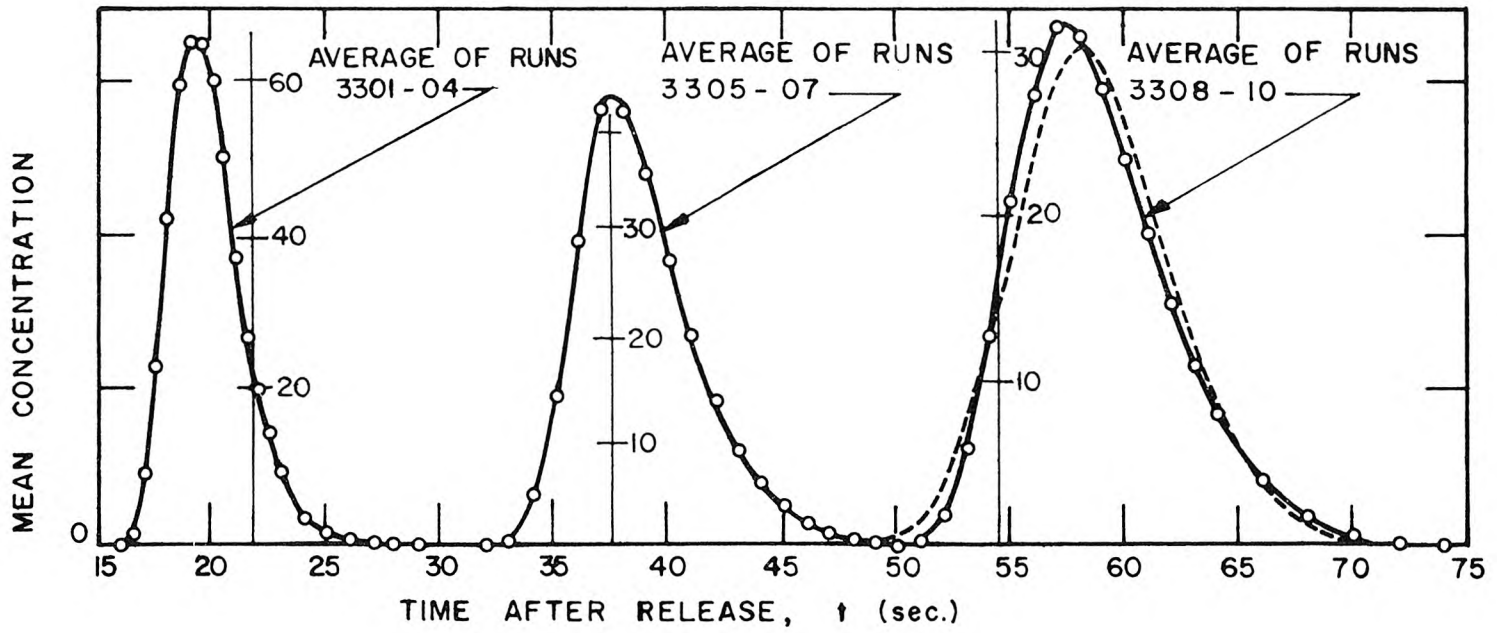

Figure 21b. Results of series 3300. ---Result of runs 3305-07 routed to compare with runs 3308-10, D = 282 cm.^{2}/sec. Concentration in arbitrary units; note change of scale for each curve.

The mean velocity was calculated by equation 89 and the dispersion coefficient by plotting group-averaged variance vs. mean time of passage. Figure 21b shows the group-averaged cross sectional mean concentration as a function of time after release for each group.

The calculated dispersion coefficient of 282 cm.^{2}/sec. was verified by the routing procedure, as shown in figure 21b, by routing the results of runs 3305-07 to coincide with runs 3308-10. The dimensionless coefficient exceeds those measured in rectangular flumes by a factor of three, indicating that the small lateral variations caused by the sloping sides are an important cause of dispersion.

V-E Flume Experiments (Smooth Sides; Rough Bottom)

This section continues the description of experiments designed to test the applicability of Taylor's analysis to two-dimensional flows. By increasing the roughness of the flume bottom relative to the sides, it was hoped that a more truly two-dimensional flow might be produced. Experiments were conducted in flows over established sand dune bottoms and over a bottom roughened by placement of stones.

1. Sand-Dune Bottoms

a. Experiments in the 40-foot flume

Preliminary experiments (series 0100 and 0200) were conducted in the 40-foot flume during experiments by Hwang (32) in which the flume contained a movable bed of sand having a geometric mean size of 0.230 mm. and a geometric standard deviation of 1.43. Uniform

conditions and bed were established by Hwang prior to each run. Tracer was introduced into the downstream hopper from a 2000 ml. beaker, and allowed to recirculate in the flume. Runs 0101 and 0102 are measurements of the same tracer cloud, 0101 after the first passage through the return pipe, and 0102 after the second passage.

Conductivity was recorded by two probes, neither similar to those used in later experiments. The upstream probe, constructed at the Massachusetts Institute of Technology, consisted of two parallel 1/4 inch by 5/16 inch platinum plates, spaced 1/4 inch apart in a glass holder. The downstream probe was made of two platinum 0.040 inch diameter wires, spaced 0.080 inch on centers; the wires were one inch in length bent into a horseshoe shape and fitted into a bakelite rod. Operation of the Sanborn recorder was similar to later experiments.

Results of the three runs are shown in Tables 12 and 13. A result is given for the dispersion coefficient made dimensionless both by the depth times the bed shear velocity U_b^* (assuming an infinitely wide channel), and the hydraulic radius times the overall shear velocity. The former is for comparison with Elder's result, the latter with other channels.

b. Experiments in 40-meter flume

Series 0300 and 0400 also took advantage of experiments by Hwang to utilize an established uniform duned bed. The sand used in these experiments had a geometric mean size of 0.206 mm. and a geometric standard deviation of 1.46. Uniform conditions were established as reported by Hwang. Tracer was introduced at the upstream end of the flume by pouring in an approximately even line across the flow from a 2000 ml. beaker.

Table 12. Results of Series 0100, March 2, 1964
Sand-Dune Bottom in 40-foot Flume

Depth, d = 11.6 cm.
Slope, S = 0.00161

Average Shear Velocity,
$U^* = \sqrt{grS} = 3.09$ cm./sec.
Bed Shear Velocity,
$U^*_b = \sqrt{gdS} = 4.28$ cm./sec.
$\varkappa$ not measured

Bed Form: Dunes, height $\cong$ 2.5 cm.
Wavelength $\cong$ 25 cm.

Probe Positions: on centerline at mid depth
upstream sta. 0.0 ft.
downstream sta. 33.0 ft (5.3 ft downstream from channel entrance)

Run	Variances (sec.^{2})		Mean Velocity (cm./sec.)	Dispersion Coeff. (cm.^{2}/sec.)
	Upstream	Downstream		
101	19.4	30.2	40.3	351
102	50.8	68.2	35.0	358

Average Dimensionless Dispersion Coefficient, $D/dU^*_b = 7.1$
$D/rU^* = 19.0$

Table 13. Summary and Results of Series 0200, March 7, 1964
Sand-Dune Bottom in 40-foot Flume

Depth, d = 5.18 cm.
Slope, S = 0.00305

Average Shear Velocity,
$U^* = \sqrt{grS} = 3.32$ cm./sec.
Bed Shear Velocity,
$U^*_b = \sqrt{gdS} = 3.94$ cm./sec.
$\varkappa$ not measured

Bed form and Probe Positions - same as series 0100.

Run	Variances (sec.^{2})		Mean Velocity (cm./sec.)	Dispersion Coeff. (cm.^{2}/sec.)
	Upstream	Downstream		
201	308	337	19.4	106

Dimensionless Dispersion Coefficient, $D/dU^*_b = 5.2$
$D/rU^* = 8.7$

The two probes used in these experiments were the one previously reported as having been constructed at M. I. T., and one similar to those described above and shown in figure 9. Results of the two series are shown in tables 14 and 15.

Dispersion coefficients obtained in the four experiments over sand-dune bottoms confirmed Elder's result (assuming $\varkappa = 0.41$) with remarkable accuracy, particularly considering the difficulty of measuring depth over the sand dunes. Unfortunately, values of $\varkappa$ were not measured in these preliminary experiments.

2. Stone Bottoms

A large bottom roughness was obtained in the 40-meter flume by covering the bottom with a layer of stones. The stone used was a white crushed limestone, obtained from the Sunburst Decorative Rock Co., of Irwindale, California, and nominally graded 5/8 inch. A sieve analysis yielded the following size distribution:

Sieve mesh size	% passing by weight
1 inch	99.6
3/4 inch	77.1
1/2 inch	28.8
3/8 inch	8.4

Before use the stone was washed in a concrete mixer to remove the dust and fine material. It was then hand placed in the flume bottom in a layer exactly one stone thick. Figure 22 shows a sample of the stone, and figure 23 shows the flume after placement. Measurements with the point gauge after placement indicated an approximate layer

Table 14. Summary and Results of Series 0300, March 3, 1965. Sand-Dune Bottom in 40-Meter Flume.

Depth, d = 16.6 cm.
Slope, S = 0.00091

Average Shear Velocity,
$U^* = \sqrt{grS} = 3.38$ cm./sec.
Bed Shear Velocity,
$U^*_b = \sqrt{gdS} = 3.86$ cm./sec.
κ not measured

Bed Form: Dune approximately 5 cm. high

Probe Positions: On centerline, 7.6 cm. below surface.
Upstream sta. 18.95, Downstream sta. 37.45.

Run	Variances (sec.^{2})		Mean Velocity (cm./sec.)	Dispersion Coeff. (cm.^{2}/sec.)
	Upstream	Downstream		
0302	21.9	62.0	36.4	522
0303	32.4	62.6	36.4	393
0304	27.0	63.8	36.2	472
0305	30.1	68.6	35.7	473
0307	32.7	66.0	37.5	476
0308	32.0	66.4	34.5	398
Average			36.2	456

Average Dimensionless Dispersion Coefficient, $D/dU^*_b = 7.1$
$D/rU^* = 10.5$

Table 15. Summary and Results of Series 0400, March 16, 1965. Sand-Dune Bottom in 40-Meter Flume.

Depth, d = 22.9 cm.
Slope, S = 0.00091

Average Shear Velocity,
$U^* = \sqrt{grS} = 3.81$ cm./sec.
Bed Shear Velocity,
$U^*_b = \sqrt{gdS} = 4.52$ cm./sec.
κ not measured

Bed Form: Dunes approximately 4 cm. high.

Probe Positions: On centerline, 5.0 cm. below surface
Upstream sta. 19.00, Downstream sta. 37.00

Run	Variances (sec.^{2})		Mean Velocity (cm./sec.)	Dispersion Coeff. (cm.^{2}/sec.)
	Upstream	Downstream		
0401	17.2	40.9	48.9	623
0402	14.1	35.7	48.5	682
0403	12.5	37.3	49.1	820
0404	19.8	45.6	49.0	842
Average			48.9	742

Average Dimensionless Dispersion Coefficient, $D/dU^*_b = 7.2$
$D/rU^* = 12.0$

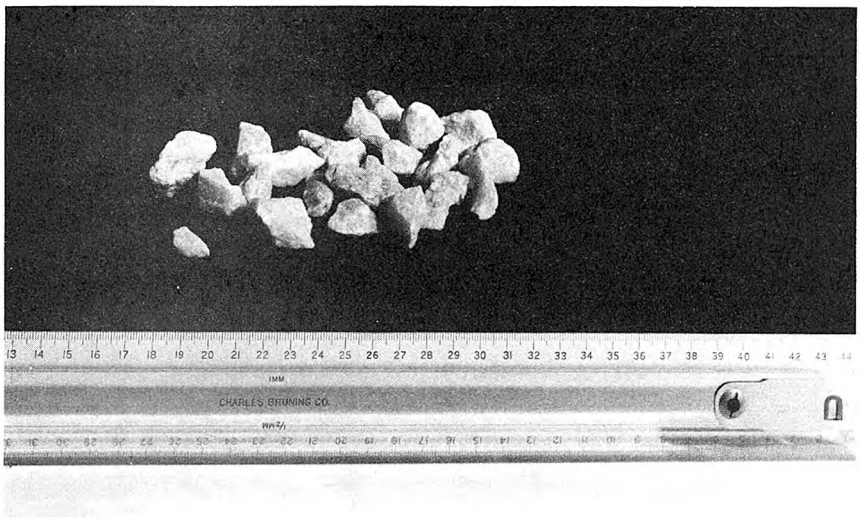

Figure 22. Stone used for bottom roughness in 40-meter flume.

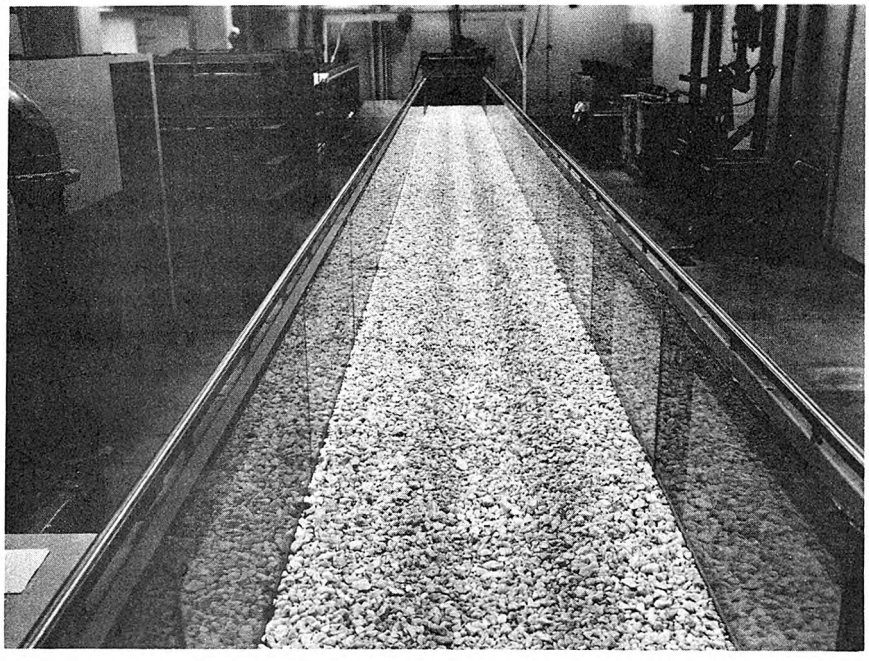

Figure 23. 40-meter flume with stone layer on bottom.

thickness of 1.8 cm. Initial measurements of the surface of a flow indicated that the friction was above average in the vicinity of station 25. A number of the larger stones in this vicinity were interchanged with smaller stones from other positions in the flume, after which a uniform flow was obtained, as shown in Table 16.

As usual, velocities were measured on alternate days from experimental runs. Velocities for series 2300 and 2400 were measured twice, because on the earlier day the water was cloudy, and it was felt that this might affect the von Karman constant. Results of both measurements are presented in table 18; no consistent difference can be observed between the two sets of measurements, and both yield the same von Karman constants. The overall average is plotted in figure 28. Since series 2500 was conducted entirely with clear water, only one set of measurements was taken (table 17).

The experiments (series 2300, 2400, and 2500) were conducted exactly as were those in the 40-meter flume over a smooth bottom, series 2600 and 2700. Figure 24 is a view of the probes during series 2500. The horizontal white line in the center of the picture is the water surface; refraction has distorted the underwater portion. The third probe from the left just penetrates the water surface; its electrodes are visible as a black dot in the center of the picture.

Hydraulic conditions and calculated results of series 2300 through 2500 are given in tables 19 through 21. The bed shear velocity for the stone-covered bed was obtained by application of a side-wall correction procedure given by Vanoni and Brooks (35). Mean velocity and dispersion coefficient were obtained as before. The group-averaged

Table 16. Water Surface Measurements with Stones on Bottom of 40-Meter Flume

Longitudinal Station (meters)	Series 2300	Series 2400	Series 2500
6	25.70 cm.	21.16 cm.	30.16 cm.
8	25.71	21.18	30.18
10	25.68	21.19	30.19
12	25.71	21.19	30.15
14	25.68	21.16	30.15
16	25.71	21.18	30.16
18	25.73	21.19	30.12
20	25.74	21.21	30.14
22	25.73	21.20	30.16
24	25.74	21.20	30.13
26	25.74	21.22	30.16
28	25.78	21.23	30.12
30	25.76	21.21	30.15
32	25.76	21.19	30.17
34	25.75	21.17	30.14
36	25.76	21.17	

Note: Average surface of stone = 11.8 cm.

Table 17. Velocity Measurements; Flow in 40-Meter Flume 40 cm. Wide with Stones on Bottom

Normalized Depth, y/d	Velocity, u(cm./sec.)						
	On Flume C.L.			At West 1/4			Average
	Sta. 14	Sta. 22	Sta. 33	Sta. 14	Sta. 22	Sta. 33	
Conditions similar to series 2500; Depth = 18.4 cm. Bed Shear Velocity = 2.59 cm./sec.							
.985	31.1	30.8	31.1	29.6	29.6	30.5	30.5
.803	30.5	29.6	30.5	26.5	27.1	28.9	28.8
.637	28.9	27.4	28.9	25.0	26.5	28.7	27.6
.472	26.2	25.6	27.1	22.9	24.1	24.1	24.9
.306	23.5	22.3	25.6	19.8	21.3	23.2	22.6
.224	21.0	22.3	23.2	18.6	19.2	21.0	20.1
.141	17.4	19.5	18.9	15.5	16.2	18.6	17.7
.058	7.9	15.5	10.1	13.1	13.1	11.3	11.9

Table 18. Velocity Measurements; Flow in 40-Meter Flume 110 Centimeters Wide With Stones on Bottom.

Normalized Depth, y/d	Velocities measured on Nov. 16 (cm./sec.)						Velocities, Nov. 26 (cm./sec.)				Average
	Sta. 15 E. 1/4	Sta. 15 on C. L.	Sta. 15 W. 1/4	Sta. 30 E. 1/4	Sta. 30 on C. L.	Sta. 30 W. 1/4	Sta. 15 on C. L.	Sta. 22 on C. L.	Sta. 22 W. 1/4	Sta. 30 on C. L.	
Conditions similar to series 2300; Depth = 13.9 cm., Bed Shear Velocity = 2.65 cm./sec.											
.950	31.1	32.2	31.1	31.7	31.7	31.1	32.0	31.7	30.8	32.3	31.7
.840	29.9	30.5	30.2				30.8	31.4	29.6	31.4	30.5
.730	29.0	30.2	29.3	29.3	29.3	28.7	29.9	29.6	28.0	30.5	29.4
.621	29.0	27.7	27.7	27.1	28.7	26.5	28.7	29.3	26.8	28.7	28.0
.511	26.8	25.9	26.8	25.9	25.3	24.1	26.8	26.8	25.9	26.8	26.1
.401	25.3	24.7	24.4	24.4	25.9	23.2	25.6	25.3	23.8	25.0	24.8
.292	22.0	22.6	21.3	22.0	22.0	22.0	21.3	24.1	20.1	23.2	22.1
.182	15.5	19.5	18.3	17.6	18.9	17.1	18.3	20.7	18.3	20.4	18.5
.072	11.6	9.8	12.8	0.0	13.7	9.1	12.5	16.4	13.4	14.3	11.4
Conditions similar to Series 2400; Depth = 9.4 cm., Bed Shear Velocity = 3.08 cm./sec.											
.919		34.1	34.1		33.8	33.8	34.1	33.8	33.8	34.7	34.0
.756		35.4	33.2		32.3	32.6	31.7	32.6	32.6	33.5	33.0
.627		29.9	31.4		30.2	31.7	30.5	31.1	30.8	31.7	30.9
.529		27.4	29.9		28.7	29.0	28.4	29.9	29.6	30.5	29.1
.432		27.1	28.7		27.7	25.9	26.8	27.7	27.4	28.4	27.5
.334		23.5	24.7		24.7	24.1	23.8	26.5	26.2	25.4	24.9
.237		21.3	22.6		22.6	19.8	20.4	24.1	22.9	22.9	22.1
.156		17.7	18.9		19.2	14.6	15.2	21.6	19.8	19.5	18.3
.091		14.6	18.3		13.7	9.1	13.1	18.6	13.7	18.3	14.9

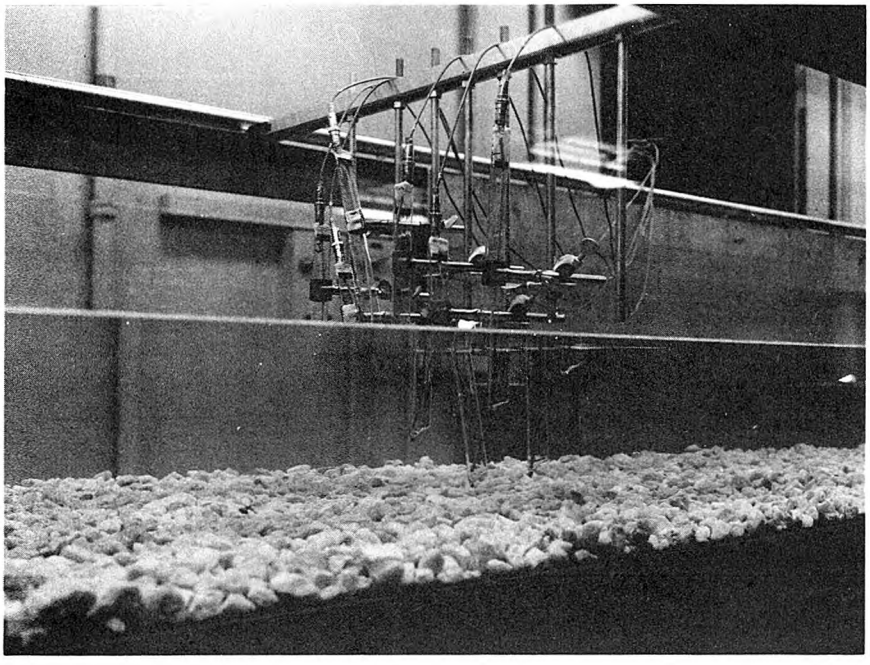

Figure 24. Probe locations during series 2500. View is obliquely from upstream through glass wall.

Table 19. Summary and Results of Series 2300, November 9, 1965
40-Meter Flume with Stones on Bottom.

Depth, d = 13.9 cm.
Slope, S = 0.00054
von Karman Constant, $\kappa = 0.33$

Bed Shear Velocity, U^*_b = 2.65 cm./sec.
Mean Velocity, $\bar{u}$ = 24.2 cm./sec.
Time Scale, T = 6.52 sec.

Probe Locations:

Probe	Long. Sta. m.	Lateral Sta. (cm. from C.L.)	Vertical (cm. above bottom)
F	36.06	11.3 E	1.8
H	36.06	8.4 W	4.2
G	36.06	1.9 E	6.6
E	36.06	13.7 E	9.7
J	36.06	8.7 W	12.3

Injection Locations:

Runs	Long. Sta. (m.)
2301-05	29.0
2306-10	21.0 (poor record - not analyzed)
2311-14	13.0
2315-18	21.0

Run	$\bar{t}$ (sec.)	Variance (sec.^{2})
2301	25.4	22.5
2302	25.6	22.3
2323	24.2	17.7
2304	25.4	19.2
2305	25.7	19.2
Average	25.1	20.5
2311	90.7	148
2312	91.0	153
2313	91.8	153
Average	91.1	151
2315	58.5	101
2316	58.6	96
2317	57.1	93
2318	57.0	88
Average	57.7	94

Dispersion Coefficient, D = 578 cm.^{2}/sec.

Dimensionless Dispersion Coefficient, $D\kappa^3/dU^*_b$ = 0.56

D/rU^* = 21.4

Table 20. Summary and Results of Series 2400, November 12, 1965
40-Meter Flume with Stones on Bottom.

Depth, d = 9.4 cm.
Slope, S = 0.00104
von Karman Constant, κ = 0.34

Bed Shear Velocity, U^*_b = 3.08 cm./sec.
Mean Velocity, $\bar{u}$ = 21.2 cm./sec.
Time Scale, T = 3.68 sec.

Probe Locations: Probe	Long. Sta. (m.)	Lateral Sta. (cm. from C.L.)	Vertical (cm. above bottom)
G	36.07	3.7 W	0.6
H	36.07	10.2 E	2.8
I	36.07	5.7 E	5.5
F	36.07	14.9 W	6.8
E	36.07	0.5 E	8.5

Injection Locations: Runs	Long. Sta. (m.)
2401-04	26.60
2405-08	21.90
2409-11	12.00

Run	$\bar{t}$ (sec.)	Variance (sec.^{2})	Run	$\bar{t}$ (sec.)	Variance (sec.^{2})
2401	37.3	63.0	2405	56.5	95
2402	37.1	58.9	2406	56.6	100
2403	36.6	60.1	2407	57.0	97
2404	37.0	60.4	2408	57.5	98
Average	37.0	60.6	Average	56.9	98
2409	106	191			
2410	106	191			
2411	106	193			
Average	106	192			

Dispersion Coefficient, D = 427 cm.^{2}/sec.

Dimensionless Dispersion Coefficient, $D\kappa^3/dU^*_b$ = 0.58

D/rU^* = 18.5

Table 21. Summary and Results of Series 2500, November 22, 1965
40-Meter Flume with Stones on Bottom.

Depth, d = 18.4 cm.
Slope, S = 0.00033
von Karman Constant, κ = 0.37

Bed Shear Velocity, U^*_b = 2.59 cm./sec.
Mean Velocity, $\bar{u}$ = 22.2 cm./sec.
Time Scale, T = 7.88 sec.

Probe Locations:

Probe	Long. Sta. (m.)	Lateral Sta. (cm.)	Vertical (cm.) above bottom)
G	36.06	5.7 W	0.8
F	36.07	9.5 E	2.9
J	36.06	20.2 W	6.0
I	36.07	0.5 W	10.0
E	36.07	16.8 E	14.6
H	36.07	5.7 W	18.1

Injection Locations:

Runs	Long. Sta. (m.)
2501-04	23.00
2505-10	11.00

Run	$\bar{t}$ (sec.)	Variance (sec.^{2})
2501	53.5	88.6
2502	53.4	91.6
2503	53.4	92.5
2504	52.4	82.6
Average	53.2	88.9
2505	106	218
2506	106	226
2507	108	222
2508	106	214
2509	107	233
2510	107	237
Average	107	226

Dispersion Coefficient D = 626 cm.^{2}/sec.

Dimensionless Dispersion Coefficient, $D\kappa^3/dU^*$ = 0.67

D/rU^* = 21.4

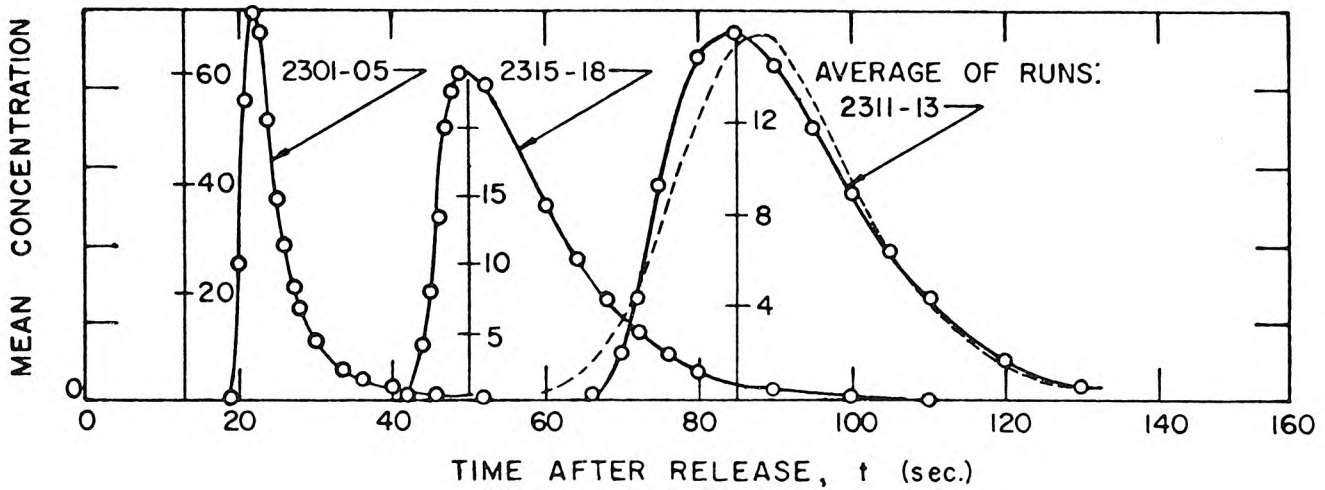

Figure 25. Results of series 2300. ---Result of runs 2315-18 routed to compare with runs 2311-13, D = 580 cm.^{2}/sec. Mean concentration in arbitrary units; note change of scale for each curve.

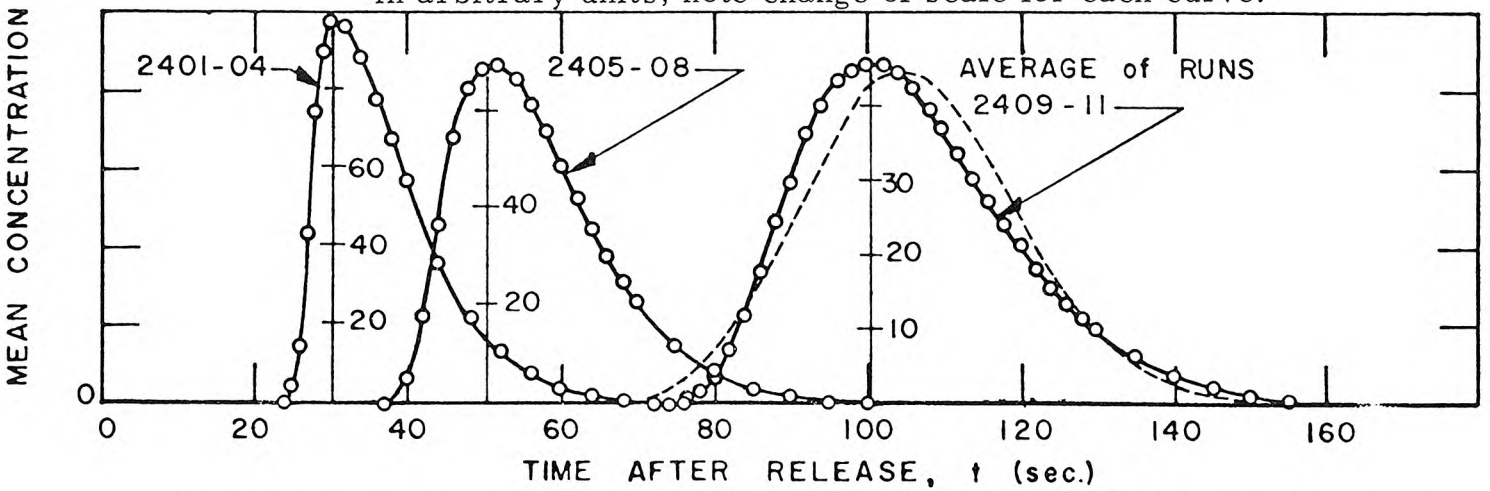

Figure 26. Results of series 2400. ---Result of runs 2401-04 routed to compare with runs 2409-11, D = 427 cm.^{2}/sec. Mean concentration in arbitrary units; note change of scale for each curve.

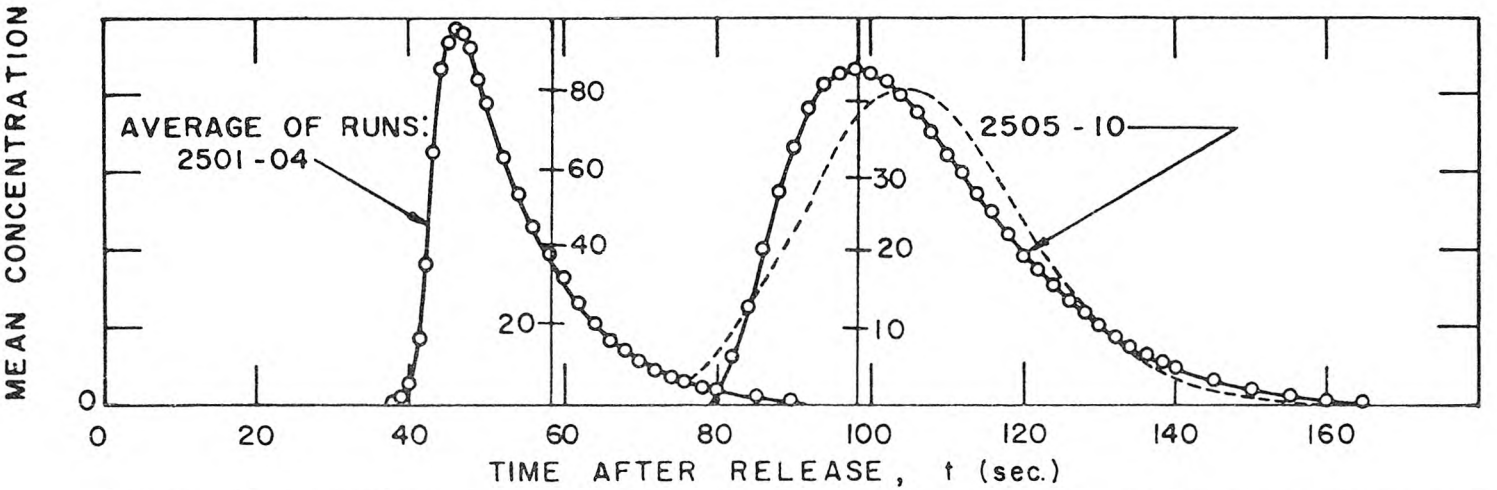

Figure 27. Results of series 2500. ---Result of runs 2501-04 routed to compare with run 2505-10, D = 626 cm.^{2}/sec. Mean concentration in arbitrary units; note change of scale for each curve.

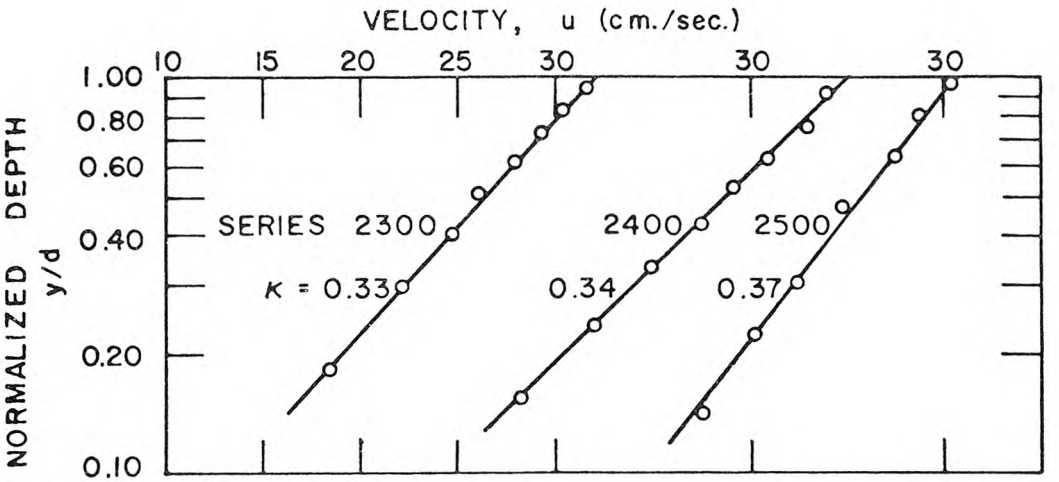

Figure 28. Measured velocity profiles, series 2300, 2400, and 2500 (averaged for each series).

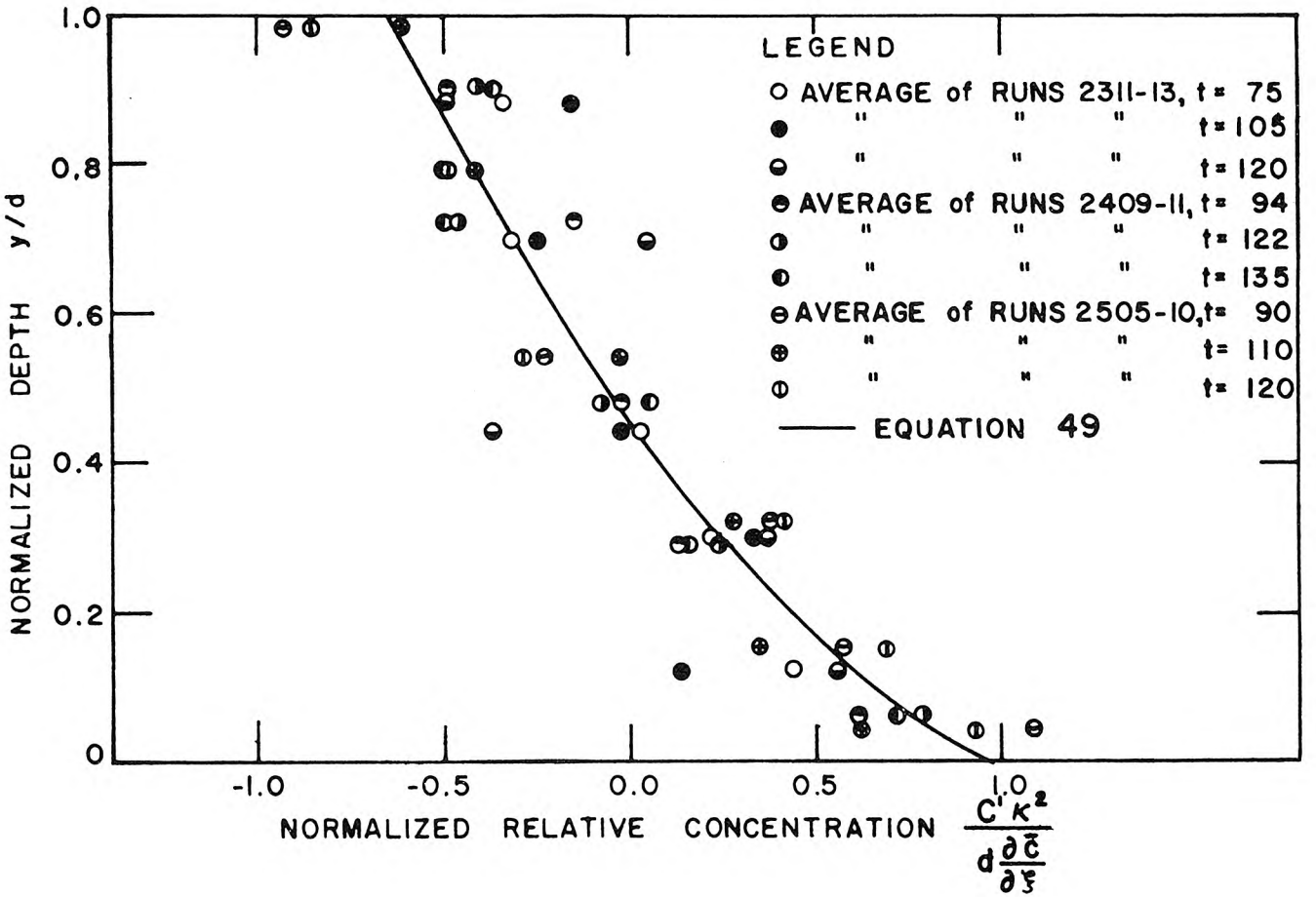

Figure 29. Comparison of measured concentration profiles for series 2300, 2400, and 2500 with prediction by Taylor's analysis.

results of each group of runs are shown in figures 25, 26, and 27; the dashed line, as before, indicates the verification of the dispersion coefficient by the routing procedure. Figure 29 shows comparison of experimental concentration profiles with equation 49, the predicted steady-state profile. The comparison is superior to that of the experiments over a smooth bottom.

The dimensionless dispersion coefficients obtained from the three experiments in flows over stone bottoms are similar to those obtained with smooth bottoms, and exceed the prediction of Elder's analysis by approximately 50%. Possible reasons are given in Chapter VIII.

V-F Flume Experiments (Side Channel Constrictions)

One series of runs (series 1600) was made in the 60-foot flume with the channel modified only by the addition of three side constrictions. The constrictions were made by inserting into the flume cut-outs of 3/4-inch plywood, shaped as shown in figure 30, which blocked the flow in the outer 5 inches on either side. The constrictions were placed at stations 20.0, 22.0, and 24.0 feet, and dispersion rates were obtained by placing two probes above and two below the constricted sections.

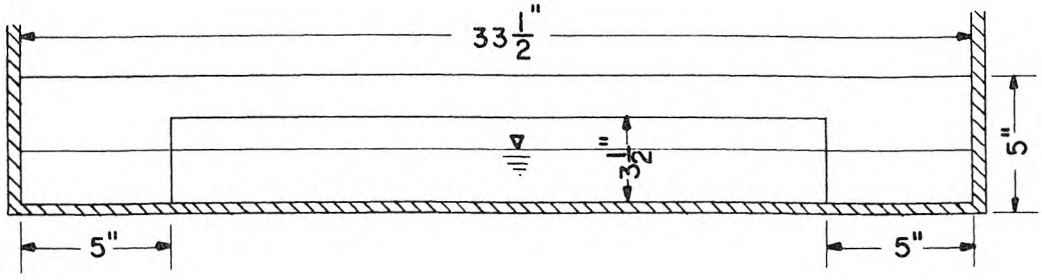

Figure 30 - Flume Constriction (not to scale)

No attempt was made to analyze the complex flow pattern which results from such a channel modification. A nearly uniform flow was obtained (maximum deviation of 0.34 cm. from average depth). Tracer was inserted and conductivity measured in a procedure identical to that of series 1500, in which the flow was similar but not constricted; results are shown in table 22.

The effect of the channel constrictions can be seen by comparing the results of series 1500 and 1600 (tables 7 and 22), in which depth of flow and mean velocity were similar. Addition of the constrictions increased the shear velocity by a factor of 1.4, but the dispersion coefficient by a factor of 3.1, giving an increase in the dimensionless coefficient of a factor of 2.4. This increase may be explained by the presence of lateral velocity variations produced by the constrictions. The next section will describe experiments in which more pronounced lateral velocity variations were produced, leading to much greater values of the dimensionless dispersion coefficient.

V-G Flume Experiments (Rough Sides - Smooth Bottoms)

In section III-E a method was given for extending Taylor's theory to natural flows. Laboratory proof of this method required a flow which contained significant lateral as well as vertical velocity variation. One way to produce it is to greatly roughen the channel sides.

Preliminary experiments to accomplish this were conducted in the 60-foot flume. Sloping embankments were placed on both sides, built by piling the stone which was later used to roughen the bottom of

Table 22. Results of Series 1600, July 7, 1965
Constricted Flow in 60-foot Flume

Depth, d = 6.4 cm. Shear Velocity, $U^* = \sqrt{grS}$ = 1.40 cm./sec.
Slope, S = 0.00036

Run	Probe Positions		Variances σ_t^2 (sec.^{2})		Mean Velocity $\bar{u}$	Dispersion Coefficient D
	Up-stream	Down-stream	Up-stream	Down-stream	(cm./sec.)	(cm.^{2}/sec.)
1601	Sta. 14.99	Sta. 55.70	10.7	49.8	22.3	172
1602	on C.L.	on C.L.	12.6	53.2	22.3	180
1603	2.5 c.m.	2.5 c.m.	10.6	40.9	22.3	137
1604	and	and	10.8	34.4	22.6	111
1605	4.3 c.m.	4.3 c.m.	11.9	52.2	22.6	184
1606	above	above	13.8	67.9	22.0	233
1607	bottom	bottom	12.2	56.3	22.0	191
1608	↓	↓	10.0	42.1	22.3	167
1609			9.9	56.6	22.3	204
1610			10.9	40.9	22.6	138
1611			12.1	31.7	22.6	92
1612			7.6	69.3	21.3	242
1613			12.5	73.6	22.3	266
1614			14.7	35.2	22.9	98
1615			10.0	37.0	22.6	124
1616			8.8	48.7	22.6	185
1617			6.7	85.6	22.0	337
Average, 1601-1617			10.9	51.5	22.3	180
1618	Sta. 14.99	Sta. 55.70	27.4	105.4	21.7	316
1619	4.3 c.m.	4.3 c.m.	21.8	109.4	21.0	332
1620	above	above	18.5	115.7	21.0	365
1621	bottom	bottom	8.9	43.3	22.6	157
1622	20 c.m.	19 c.m.	12.0	85.8	21.0	278
1623	west of	east	11.5	95.0	21.0	319
1624	C.L. and	and	11.1	60.8	22.0	214
1625	20 c.m.	west	12.7	63.8	21.7	210
1626	east of	of	8.9	114.5	20.7	381
1627	C.L.	C.L.	12.7	64.3	22.0	218
1628	↓	↓	10.1	89.4	21.0	302
1629			16.4	99.0	20.7	304
Average, 1618-1629			14.3	87.2	21.3	283
Average, Series 1600			12.6	69.4	22.0	231

Average Dimensionless Dispersion Coefficient, $D/rU^* = 30$

the 40-meter flume (section V-E). As expected from the theory, the resulting dispersion coefficients far exceeded those of the two-dimensional runs; D/r U* varied from 77 to 220. The results are not reported in detail, because (a) the channel was too short to achieve reasonable values of dimensionless time, (b) using only one probe at each cross section may have introduced considerable error, and (c) similar results, but more extensive and reliable, were obtained under similar hydraulic conditions in the 40-meter flume.

The analysis of chapter III implies two experimental requirements: (1) a large length-to-width ratio (since the half-width is the characteristic length of the cross section), in order to attain suitable dimensionless dispersion times; and (2) a width-to-depth ratio of approximately 10, in order for the simplification of the cross section to one dimension (transverse) to be valid. A length-to-width ratio of at least 200 was desired; this required narrowing the channel to approximately 20 cm., and limiting the depth to an approximate maximum of 2 cm. This depth is also nearly a minimum for achievement of a fully turbulent Reynolds number. Thus even with an unusually long flume, the range of experiments was limited.

The narrow channel was obtained inside the 40-meter flume by installing false sides, using the regular flume bottom, inlet and outlet boxes, pump, and all appurtenances. A typical cross section is shown in figure 31. Each side is made of eight foot-long plywood sections, laid in the flume end to end. Upstream and downstream bulkheads were firmly wedged into the upstream and downstream inlet boxes; the adjacent side sections were screwed tightly to the bulkheads, and all

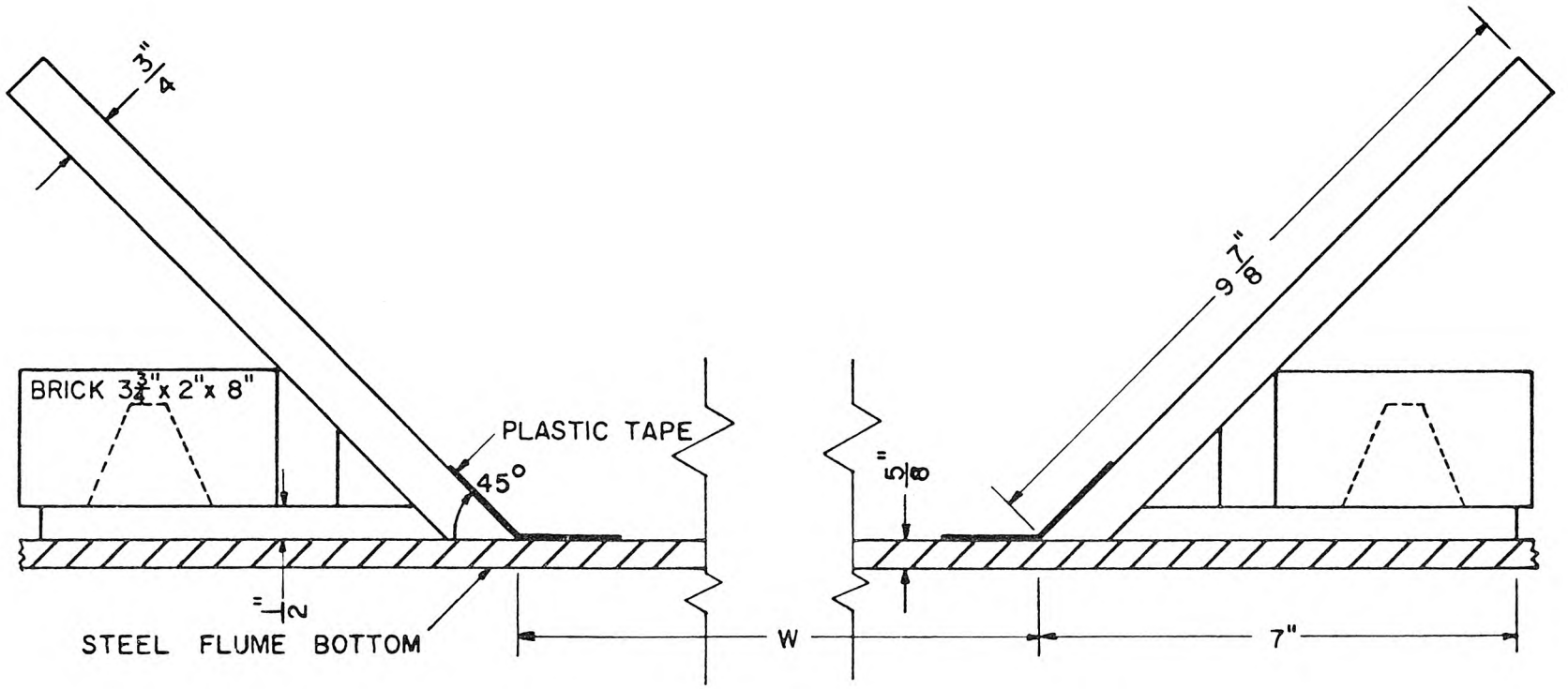

NOTE

SERIES	2800, 2900, 3000	W = 15"
SERIES	3100, 3200, 3300	W = 12½"
SERIES	3400	W = 7½"

Figure 31. Cross section of channel constructed inside 40-meter flume.

other side sections simply placed on the flume floor, weighted by bricks, and taped in place with No. 471 Scotch brand vinyl plastic tape. Joints between sections were taped and occasionally toenailed. The tape formed a watertight seal throughout with negligible leakage.

Side roughness was obtained by hand placing an embankment of white marble stone, one rock thick, of nominal size 1 inch, up the side-walls as far as necessary to be above the maximum water surface. A sample of the stone used gave the following sieve analysis:

Sieve mesh size	% passing, by weight
2 1/2 inches	98.5
2 inches	94.6
1 1/2 inches	59.8
1 inch	12.9
3/4 inch	1.1

The stone was carefully placed to yield a uniform surface and minimum pore space, and was not secured. No motion of any stone was ever observed during a run, and no difficulty was encountered in obtaining uniform flow.

Figures 32 and 33 show the completed channel at two widths, 32 cm. (between bottom edges of wood) for series 3100 and 3200, and 19 cm. for series 3400. In the foreground is the downstream bulkhead, firmly wedged to prevent leakage. Figure 34 shows a typical section of side-wall embankment; the scale reads in centimeters. Figure 35 shows the method for introducing tracer; the trough rotates in brackets clamped to the wooden side-walls.

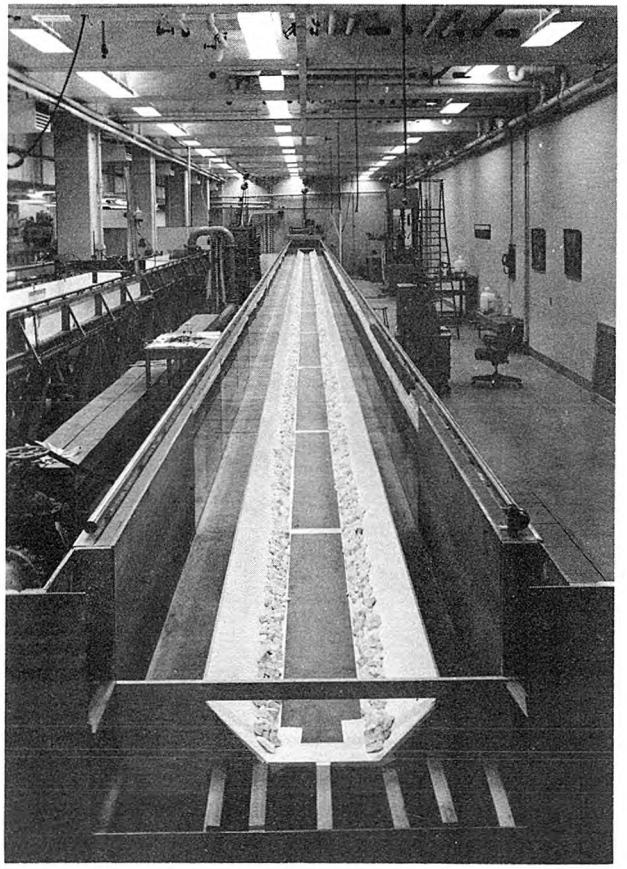

Figure 32. Channel in 40-meter flume for series 3100 and 3200.

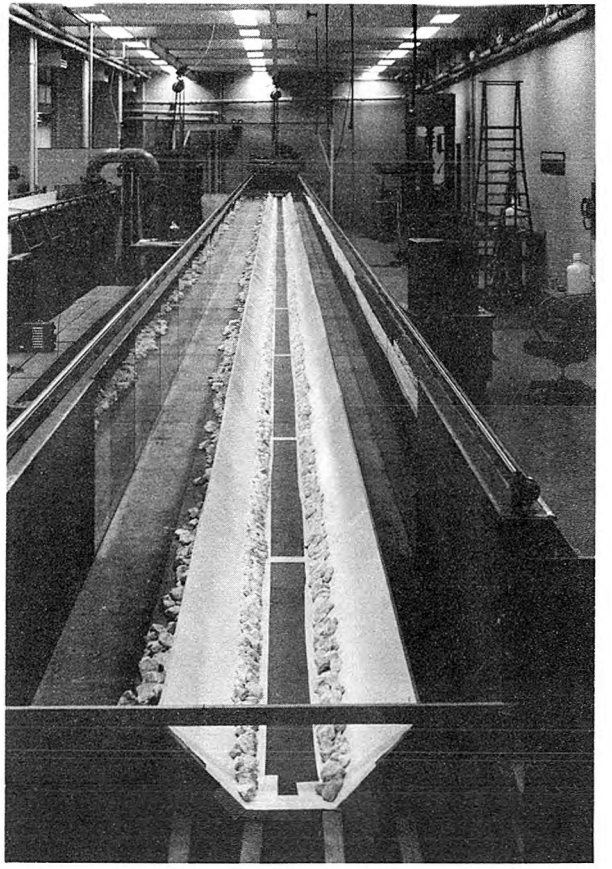

Figure 33. Channel in 40-meter flume for series 3400.

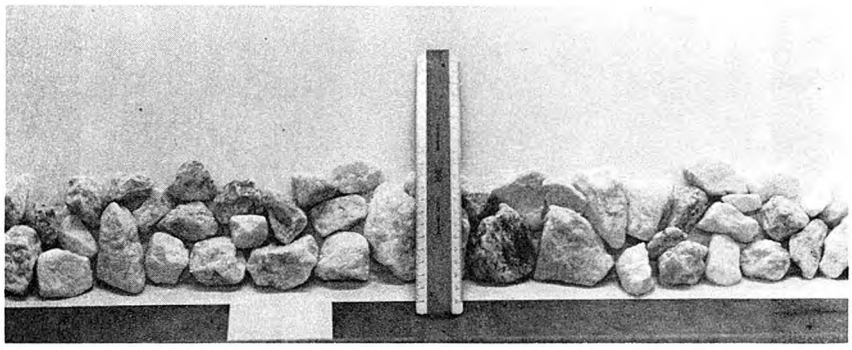

Figure 34. Typical section of side-wall embankment (scale reads in centimeters).

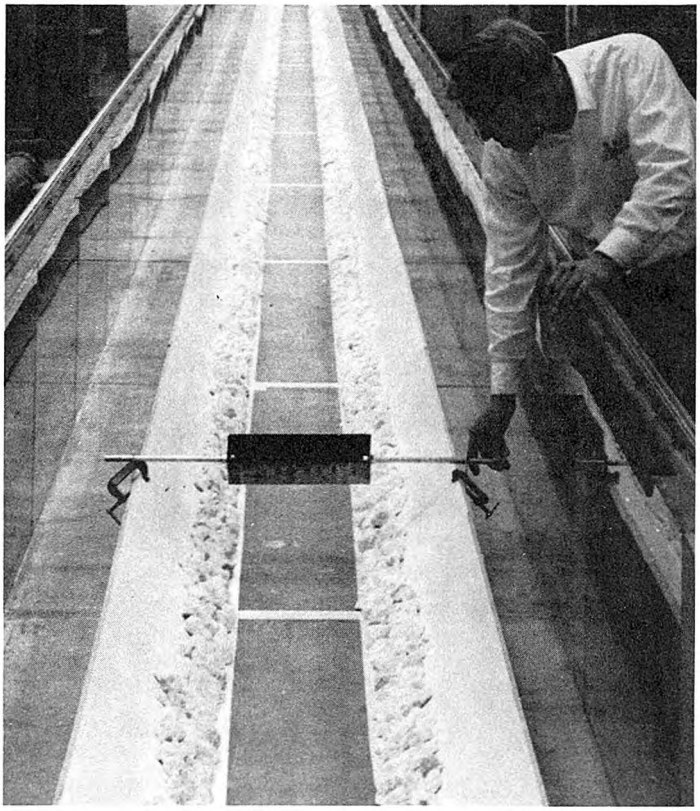

Figure 35. Method of inserting tracer.

The procedure for making runs was similar to that previously described for series 2600 and 2700 (runs with smooth sides and bottom). The probes were always positioned at station 36.06 m. spaced laterally across the flow. Figure 36 shows the probes in position during series 2800. Probe positions were measured by a bent point gauge, the tip of which could be brought almost into contact with the electrodes for reading of vertical, lateral, and longitudinal position. Water surface elevation was measured as usual by the point gauge, and velocity by the Prandtl pitot tube. All three can be seen mounted on the instrument carriage, from left to right respectively, in figure 37.

Visual observations were made by inserting a very highly concentrated blue dye, color No. 179 N, obtained from the Krieger Color and Chemical Co., Hollywood, California. The dispersion pattern can be seen in figures 38a and b, which were taken 5.5 and 8.5 seconds respectively after insertion into the flow conditions of series 3100. Flow is away from the camera; the foreground shows the upstream tail of the distribution, in which high concentrations are found in the low velocity water along the sides, and low concentrations in the center.

Velocity was measured at approximately 40 points on each of three cross sections, and the cross sections averaged to obtain the isovel patterns shown in figures 39a through 44a. The mean square velocity deviations, $\overline{u'^2}$, were found by planimetering areas between isovels on full scale drawings. The water in the pores of the embankment, although small in volume, has the maximum relative velocity and must be included in the calculations. For all series the area shown as stone was assumed to be 20% water, moving at a uniform velocity of 3 cm./sec.

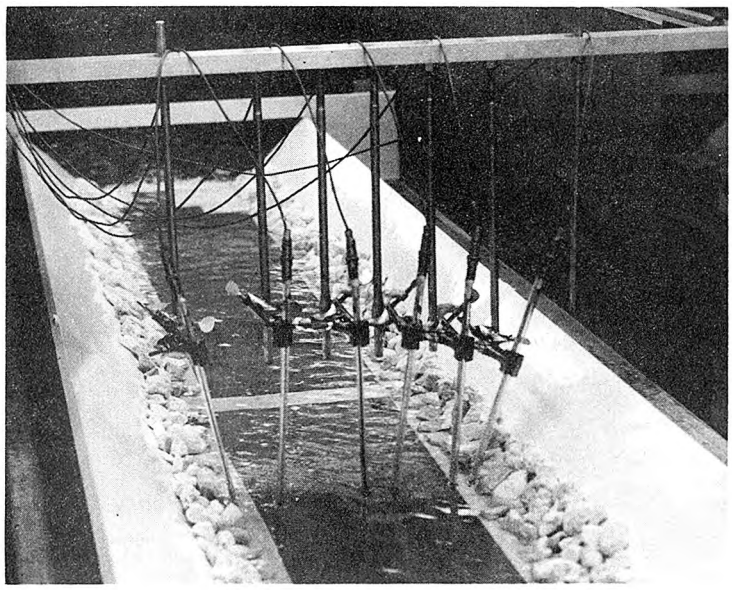

Figure 36. Probes in position during series 2800.

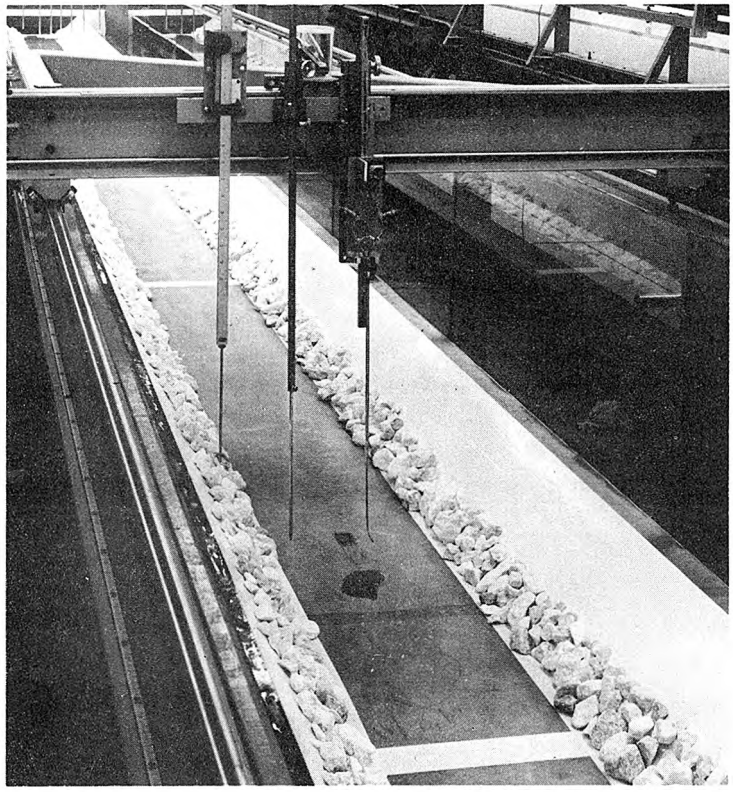

Figure 37. Oblique view of channel for series 2800, 2900, and 3000, showing probe locater pointer, water surface pointer, and Prandtl tube mounted on instrument carriage.

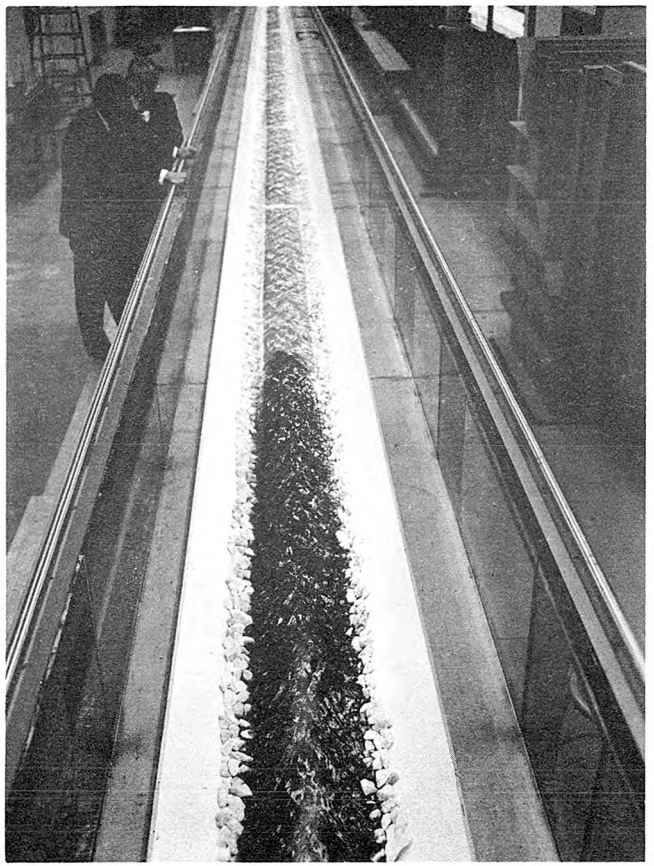

(a)

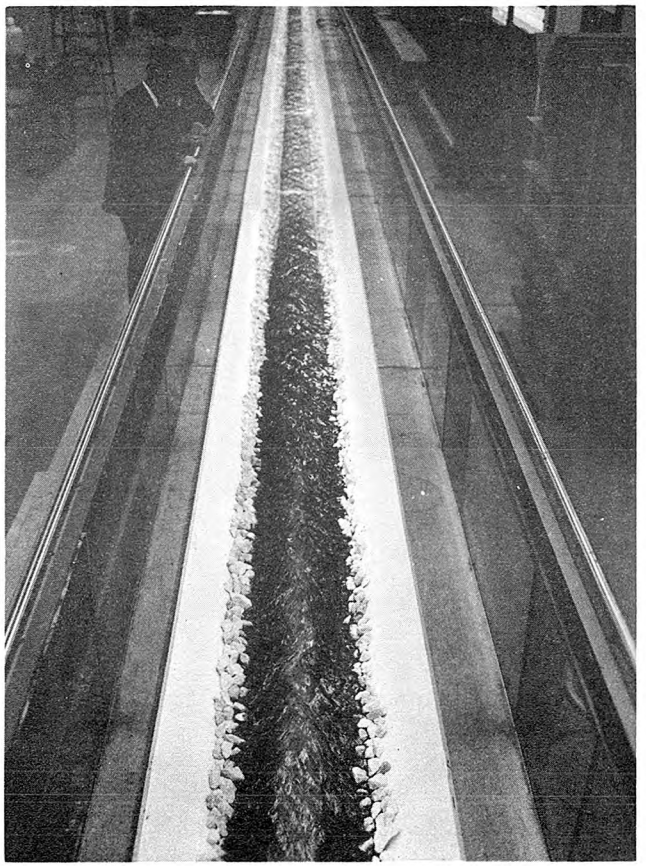

(b)

Figure 38. Dye dispersion in flow conditions of series 3100;
(a) 5.5 sec. after release
(b) 8.5 sec. after release

Hydraulic conditions and results of series 2800, 2900, 3000, 3100, 3200, and 3400 are given in tables 23 through 28. The characteristic length given is the half-width at the water surface, including approximately half of the area shown as stone. The shear velocity is for the entire channel; no attempt was made to calculate a shear velocity for the rough sides. The mean velocity was calculated by equation 89; where available, the velocity obtained from the venturi meter reading agreed within ±5% (for series 3200 and 3400 the reading was below meter calibration).

Curves of group-averaged concentration vs. time for each group of runs are shown in figures 39b through 44b; as before, the dashed line indicates routed results, for various choices of the dispersion coefficient.

A dispersion coefficient for each series was calculated by the procedure given in Chapter IV. First,a value was calculated by the change of moment method. That value was checked by the routing procedure and, for all series, the routing of the group-averaged results of the first group compared poorly with the results of the second group. Various other dispersion coefficients were used in an attempt to improve the routing. For series 3100 and 3400, a good comparison was obtained using the coefficients indicated on figures 42b and 44b; the other series were performed at such low values of dimensionless time that adequate routing comparisons could not be obtained.

A dispersion coefficient for each series was also obtained by the diffusive transport method. The measured steady-state profiles in the cross section were obtained by introducing the salt for calibration

Table 23. Summary and Results of Series 2800, December 20, 1965
Trapezoidal Channel with Rough Sides in 40-Meter Flume

Depth, d	= 3.5 cm.	Shear Velocity, U*	= 2.02 cm./sec.
Hydraulic Radius, r	= 2.9 cm.	Mean Velocity, $\bar{u}$	= 25.1 cm./sec.
Width (bottom of inserts), w	= 38.1 cm.	Mean Square Vel. Deviation, $\overline{u'^2}$	=105 cm.^{2}/sec.^{2}
Characteristic length, $\ell(\cong w/2)$	= 20 cm.	Time Scale, $T = 0.30\ell^2/rU^*$	= 20.5 sec.

Run	$\bar{t}$ (sec.)	Variance (sec.^{2})	Run	$\bar{t}$ (sec.)	Variance (sec.^{2})
2801	61.8	382	2807	102	634
2802	63.4	443	2808	103	703
2803	62.2	353	2809	102	648
2804	61.6	330	2810	104	674
2805	60.3	319	2811	100	581

	Average of Runs 2801-2805	Average of Runs 2807-2811
Distance, Injection to Probes (meters)	16.07	26.11
Mean Time of Passage, $\bar{t}$ (sec.)	61.9	102
Variance, (sec.^{2})	369	651
Dimensionless Mean Time of Passage, $t' = \bar{t}/T$	3.0	5.0

Dispersion Coefficient, D:

Measured Values:	Change of Moment Method	2220 cm.^{2}/sec.
	Diffusive Transport Method	1230
	Best Routing	n.a.
Predicted Values:	Diffusive Transport (eq. 55)	1307 cm.^{2}/sec.
	Estimate by Time Scale (eq. 90)	2150

Dimensionless Dispersion Coefficient, D/rU*
(based on measured value by diffusive transport method) 210

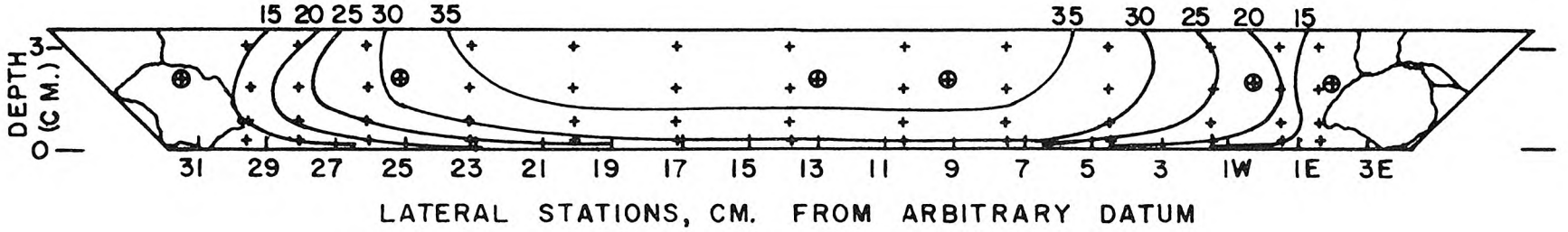

Figure 39a. Cross section of flow for series 2800. Contours are velocity (cm./sec.). + indicates velocity measurement; ⊕ indicates probe location.

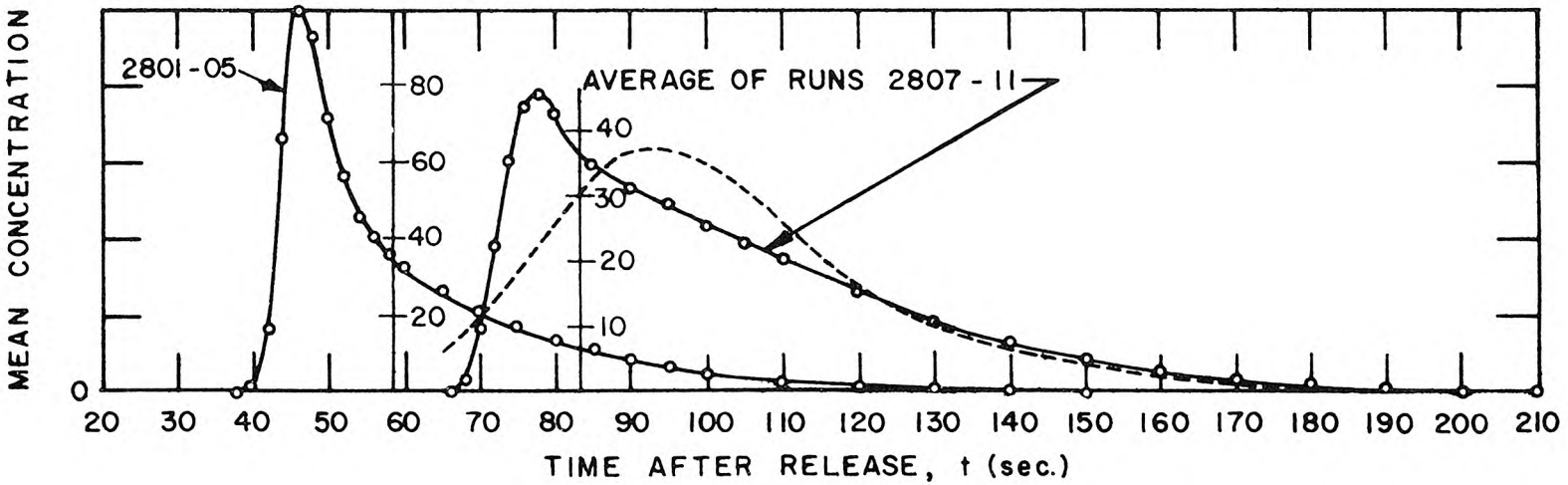

Figure 39b. Results of series 2800. ---Result of runs 2801-05 routed to compare with runs 2807-11, D = 1300 cm.^{2}/sec.
Concentration in arbitrary units; note change of scale for each curve.

Table 24. Summary and Results of Series 2900, January 7, 1966
Trapezoidal Channel with Rough Sides in 40-Meter Flume

Depth, d	= 4.7 cm.	Shear Velocity, U*	= 3.59 cm./sec.
Hydraulic Radius, r	= 3.7 cm.	Mean Velocity, $\bar{u}$	= 45.4 cm./sec.
Width (bottom of inserts), w	= 38.1 cm.	Mean Square Vel. Deviation, $\overline{u'^2}$	= 343 cm.^{2}/sec.^{2}
Characteristic length, ℓ (= w/2)	= 21.5 cm.	Time Scale, $T = 0.30\ \ell^2/rU^*$	= 10.4 sec.

Run	$\bar{t}$ (sec.)	Variance (sec.^{2})	Run	$\bar{t}$ (sec.)	Variance (sec.^{2})
2901	35.7	127	2906	57.1	172
2902	35.2	118	2907	57.5	184
2903	36.0	116	2908	56.5	160
2904	33.9	90	2909	57.2	187
2905	34.5	97	2910	57.7	190

	Average of Runs 2901-2905	Average of Runs 2906-2910
Distance, Injection to Probes (meters)	16.08	26.12
Mean Time of Passage, $\bar{t}$ (sec.)	35.1	57.2
Variance, (sec.^{2})	111	179
Dimensionless Mean Time of Passage, $t' = \bar{t}/T$	3.4	5.5

Dispersion Coefficient, D:

Measured Values;	Change of Moment Method	3170 cm.^{2}/sec.
	Diffusive Transport Method	2530
	Best Routing	n.a.
Predicted Values:	Diffusive Transport (eq. 55)	2513 cm.^{2}/sec.
	Estimate by Time Scale (eq. 90)	3580

Dimensionless Dispersion Coefficient, D/rU* (based on measured value by diffusive transport method) 190

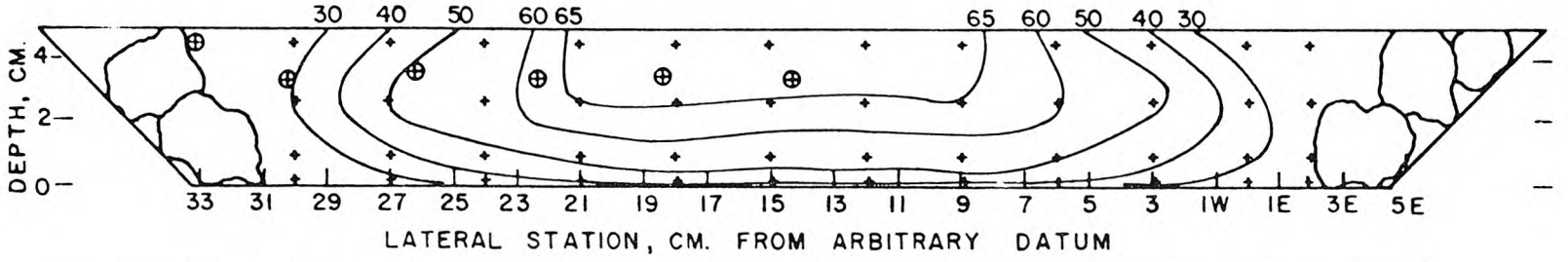

Figure 40a. Cross section of flow for series 2900. Contours are velocity (cm./sec.). + indicates velocity measurement; ⊕ indicates probe location.

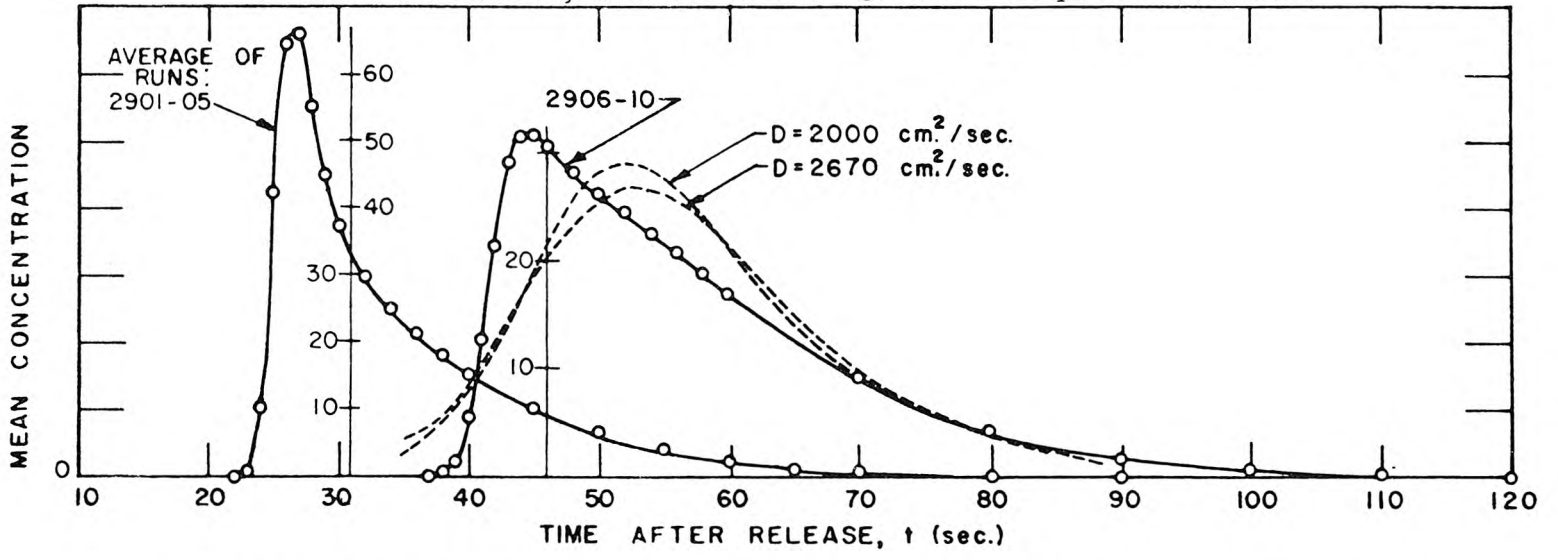

Figure 40b. Results of series 2900. ---Result of runs 2901-05 routed to compare with 2906-10; D as noted. Concentration in arbitrary units; note change of scale for each curve.

Table 25. Summary and Results of Series 3000, January 14, 1966
Trapezoidal Channel with Rough Sides in 40-Meter Flume

Depth, d	= 3.5 cm.	Shear Velocity, U*	= 3.51 cm./sec.
Hydraulic Radius, r	= 2.9 cm.	Mean Velocity, $\bar{u}$	= 45.1 cm./sec.
Width (bottom of inserts), w	= 38.1 cm.	Mean Square Vel. Deviation, $\overline{u'^2}$	=503 cm.^{2}/sec.^{2}
Characteristic length, ℓ ($\cong$ w/2)	= 20 cm.	Time Scale, $T = 0.30\,\ell^2/rU^*$	= 11.8 sec.

Run	$\bar{t}$ (sec.)	Variance (sec.^{2})	Run	$\bar{t}$ (sec.)	Variance (sec.^{2})
3001	36.5	110	3005	60.4	230
3002	35.9	102	3006	61.2	251
3003	36.3	111	3007	60.7	250
3004	36.4	107	3008	59.6	226

	Average of Runs 3001-3004	Average of Runs 3005-3008
Distance, Injection to Probes (meters)	18.10	29.01
Mean Time of Passage, $\bar{t}$ (sec.)	36.3	60.5
Variance, (sec.^{2})	107	240
Dimensionless Mean Time of Passage, $t' = \bar{t}/T$	3.8	5.1

Dispersion Coefficient, D:

Measured Values:	Change of Moment Method	5590 cm.^{2}/sec.
	Diffusive Transport Method	4150
	Best Routing	n.a.
Predicted Values:	Diffusive Transport (eq. 55)	3711 cm.^{2}/sec.
	Estimate by Time Scale (eq. 90)	5930

Dimensionless Dispersion Coefficient, D/rU*
(based on measured value by diffusive transport method) 410

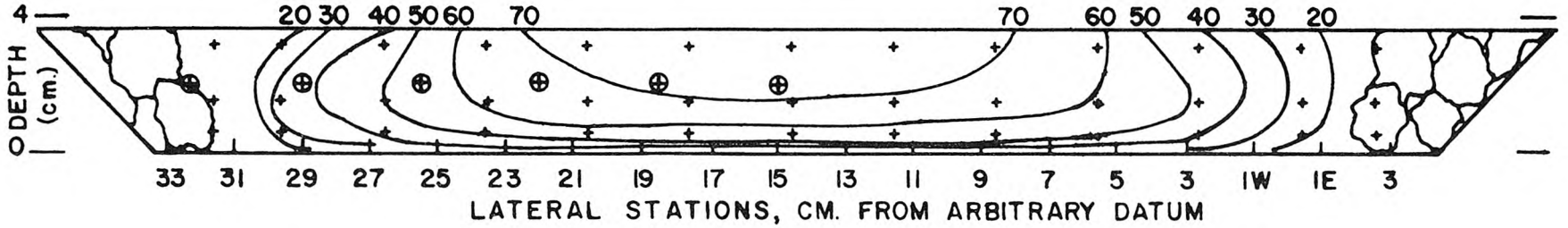

Figure 41a. Cross section of flow for series 3000. Contours are velocity (cm./sec.). + indicates velocity measurement; ⊕ indicates probe location.

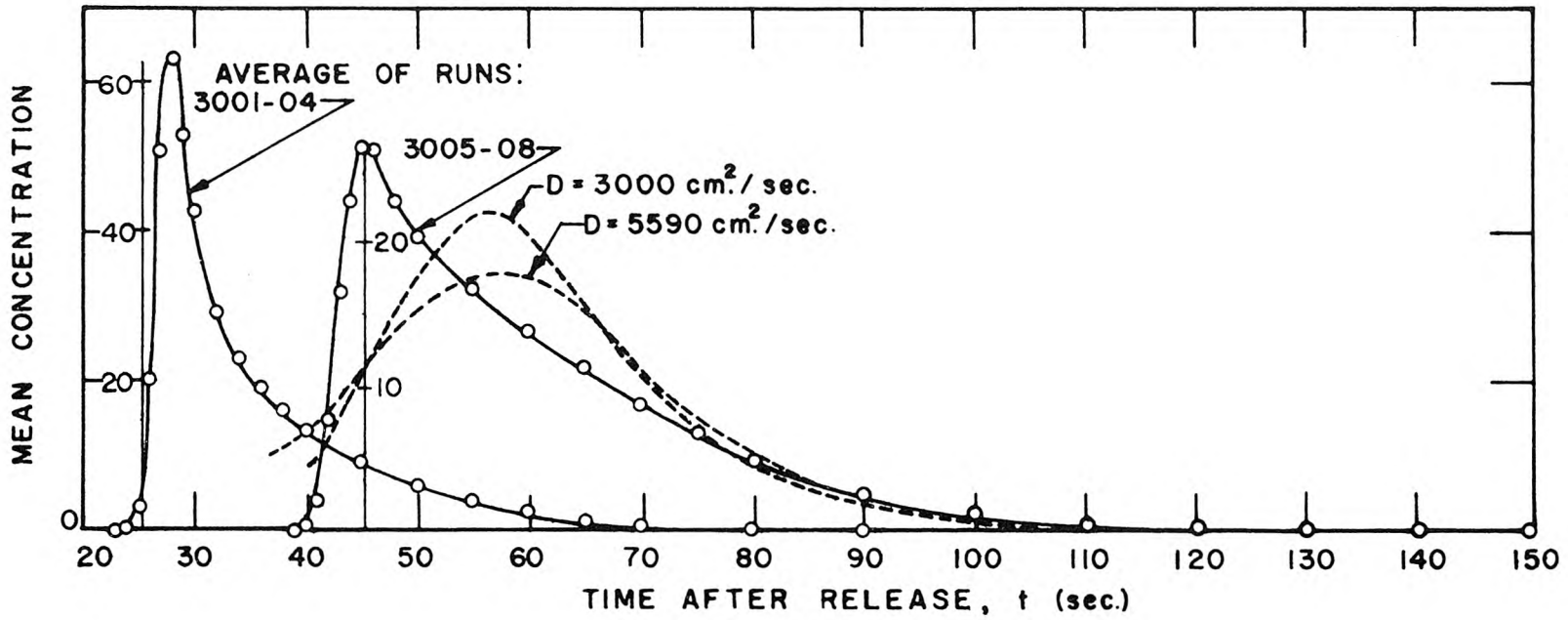

Figure 41b. Results of series 3000. ---Result of runs 3001-04 routed to compare with 3005-08; D as noted. Concentration in arbitrary units; note change of scale for each curve.

Table 26. Summary and Results of Series 3100, January 24, 1966
Trapezoidal Channel with Rough Sides in 40-Meter Flume

Depth, d	= 3.5 cm.	Shear Velocity, U*	= 3.48 cm./sec.
Hydraulic Radius, r	= 2.9 cm.	Mean Velocity, $\bar{u}$	= 44.4 cm./sec.
Width (bottom of inserts), w	= 31.7 cm.	Mean Square Vel. Deviation, $\overline{u'^2}$	= =329 cm.^{2}/sec.^{2}
Characteristic length, ℓ ($\tilde{=}$ w/2)	= 17 cm.	Time Scale, $T = 0.30\ \ell^2/rU^*$	= 8.6 sec.

Run	$\bar{t}$ (sec.)	Variance (sec.^{2})	Run	$\bar{t}$ (sec.)	Variance (sec.^{2})
3103	40.2	132	3107	66.9	239
3104	40.2	134	3108	66.6	242
3105	39.8	131	3109	66.7	240
3106	39.4	123	3110	67.1	244

	Average of Runs 3103-3106	Average of Runs 3107-3110
Distance, Injection to Probes (meters)	17.50	29.45
Mean Time of Passage, $\bar{t}$ (sec.)	39.9	66.8
Variance, (sec.^{2})	130	241
Dimensionless Mean Time of Passage, $t' = \bar{t}/T$	4.6	8.1

Dispersion Coefficient, D:

Measured Values:	Change of Moment Method	4080 cm.^{2}/sec.
	Diffusive Transport Method	2130
	Best Routing	2500
Predicted Values:	Diffusive Transport (eq. 55)	2503 cm.^{2}/sec.
	Estimate by Time Scale (eq. 90)	2820

Dimensionless Dispersion Coefficient, D/rU*
(based on measured value by best routing) 250

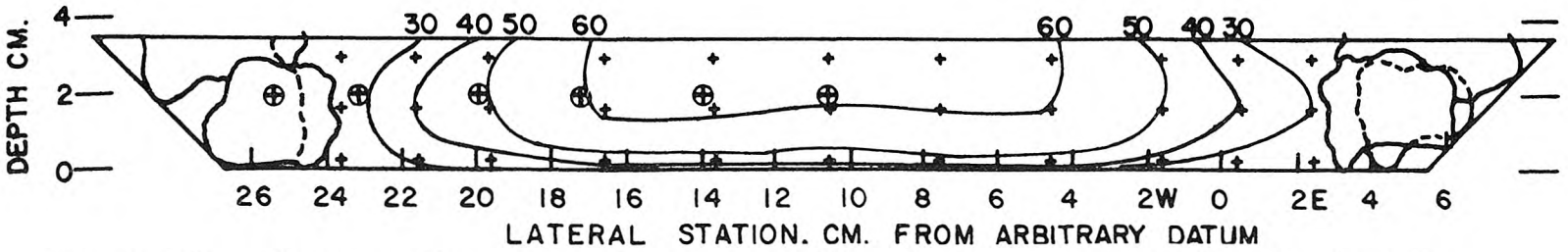

Figure 42a. Cross section of flow for series 3100. Contours are velocity (cm./sec.). + indicates velocity measurement; ⊕ indicates probe location.

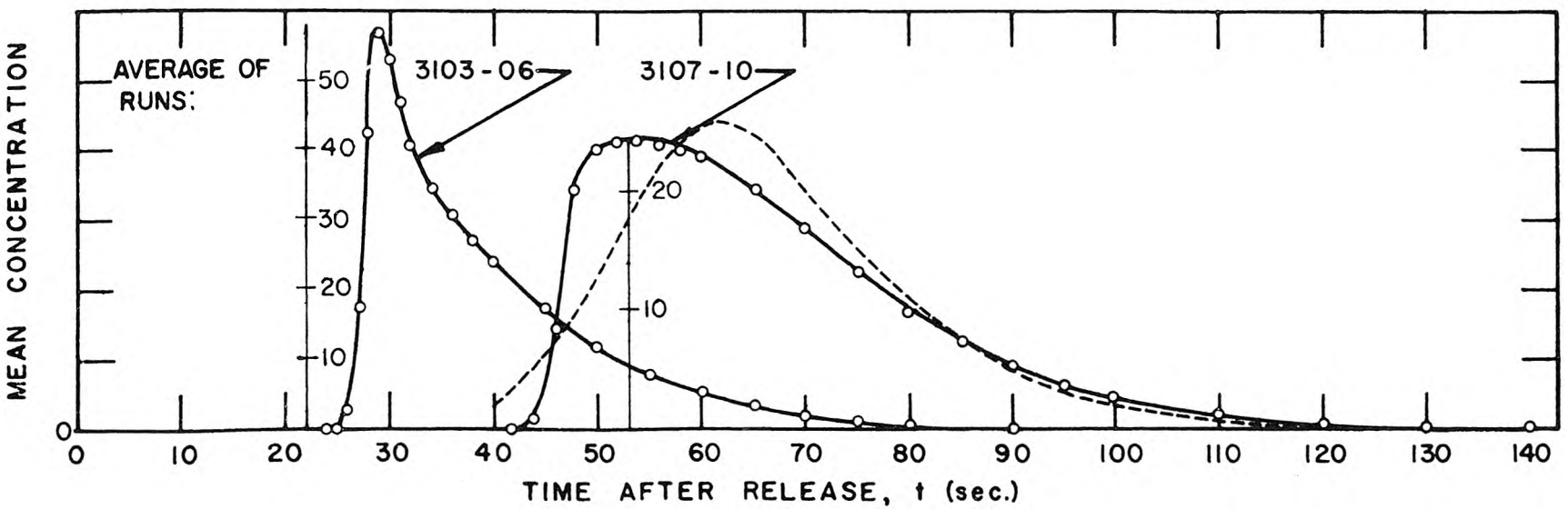

Figure 42b. Results of series 3100. ---Results of runs 3103-06 routed to compare with result of runs 3107-10; D = 2500 cm.^{2}/sec. Concentration in arbitrary units; note change of scale for each curve.

Table 27. Summary and Results of Series 3200, January 28, 1966
Trapezoidal Channel with Rough Sides in 40-Meter Flume

Depth, d	= 2.1 cm.	Shear Velocity, U*	= 3.28 cm./sec.
Hydraulic Radius, r	= 1.9 cm.	Mean Velocity, $\bar{u}$	= 45.3 cm./sec.
Width (bottom of inserts), w	= 31.7 cm.	Mean Square Vel. Deviation, $\overline{u'^2}$	=453 cm.^{2}/sec.^{2}
Characteristic length, ℓ ($\tilde{=}$ w/2)	= 16.5 cm.	Time Scale, T = 0.30 ℓ^2/rU*	= 13.1 sec.

Run	$\bar{t}$ (sec.)	Variance (sec.^{2})	Run	$\bar{t}$ (sec.)	Variance (sec.^{2})
3201	40.0	180	3205	69.1	347
3202	41.0	197	3206	69.2	359
3203	40.3	192	3207	69.6	351
3204	41.3	208			

	Average of Runs 3201-3204	Average of Runs 3205-3207
Distance, Injection to Probes (meters)	17.56	30.57
Mean Time of Passage, $\bar{t}$ (sec.)	40.6	69.3
Variance, (sec.^{2})	194	352
Dimensionless Mean Time of Passage, t' = $\bar{t}$/T	3.1	5.3

Dispersion Coefficient, D:

Measured Values:	Change of Moment Method	5650 cm.^{2}/sec.
	Diffusive Transport Method	4000
	Best Routing	n.a.
Predicted Values:	Diffusive Transport (eq. 55)	4496 cm.^{2}/sec.
	Estimate by Time Scale (eq. 90)	5930

Dimensionless Dispersion Coefficient, D/rU* (based on measured value by diffusive transport method) 640

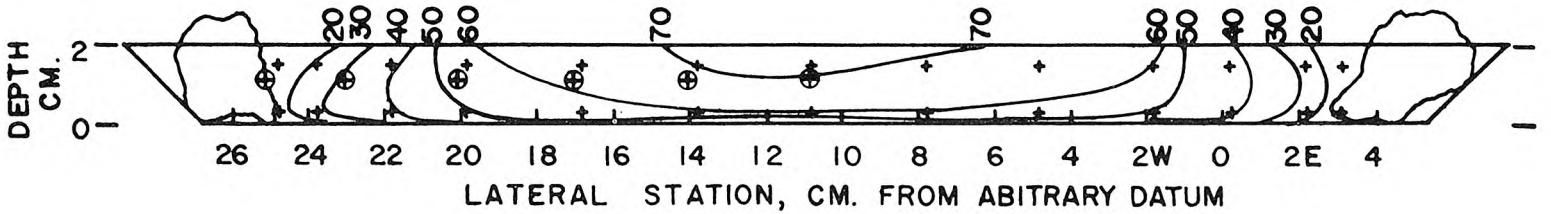

Figure 43a. Cross section for series 3200. Contours are velocity (cm./sec.). + indicates velocity measurement; ⊕ indicates probe location.

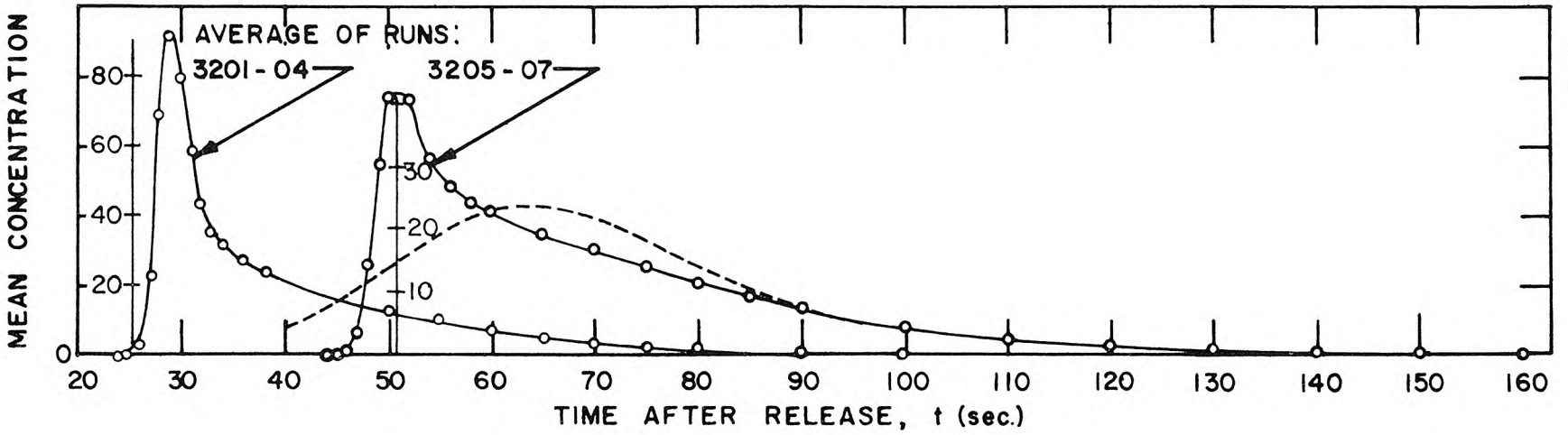

Figure 43b. Results of series 3200. ---Result of series 3201-04 routed to compare with result of runs 3205-07, D = 4500 cm.^{2}/sec. Concentration in arbitrary units; note change of scale for each curve.

Table 28. Summary and Results of Series 3400, February 8, 1966
Trapezoidal Channel with Rough Sides in 40-Meter Flume

Depth, d = 2.1 cm.
Hydraulic Radius, r = 1.7 cm.
Width (bottom of inserts), w = 19.1 cm.
Characteristic length, ℓ ($\cong$ w/2) = 9.5 cm.
Shear Velocity, U* = 3.88 cm./sec.
Mean Velocity, $\bar{u}$ = 46.1 cm./sec.
Mean Square Vel. Deviation, $\overline{u'^2}$ = 469 cm.^{2}/sec.^{2}
Time Scale, $T = 0.30\,\ell^2/rU^*$ = 4.10 sec.

Run	$\bar{t}$ (sec.)	Variance (sec.^{2})	Run	$\bar{t}$ (sec.)	Variance (sec.^{2})
3401	34.6	71.9	3407	69.0	156
3402	34.7	75.3	3408	68.9	155
3403	34.2	71.4	3409	69.2	156
3404	51.3	109			
3405	51.6	115			
3406	51.6	112			

	Average of 3401-3403	Average of 3404-3406	Average of 3407-3410
Distance, Injection to Probes (meters)	16.09	23.98	31.97
Mean Time of Passage, $\bar{t}$ (sec.)	34.5	51.6	69.1
Variance (sec.^{2})	72.9	112	156
Dimensionless Mean Time of Passage, $t' = \bar{t}/T$	8.4	12.6	16.9

Dispersion Coefficient, D:

Measured Values:	Change of Moment Method	2540 cm.^{2}/sec.
	Diffusive Transport Method	1900
	Best Routing	2200
Predicted Values:	Diffusive Transport (eq. 55)	1661 cm.^{2}/sec.
	Estimate by Time Scale (eq. 90)	1920

Dimensionless Dispersion Coefficient, D/rU*
(based on measured value by best routing) 330

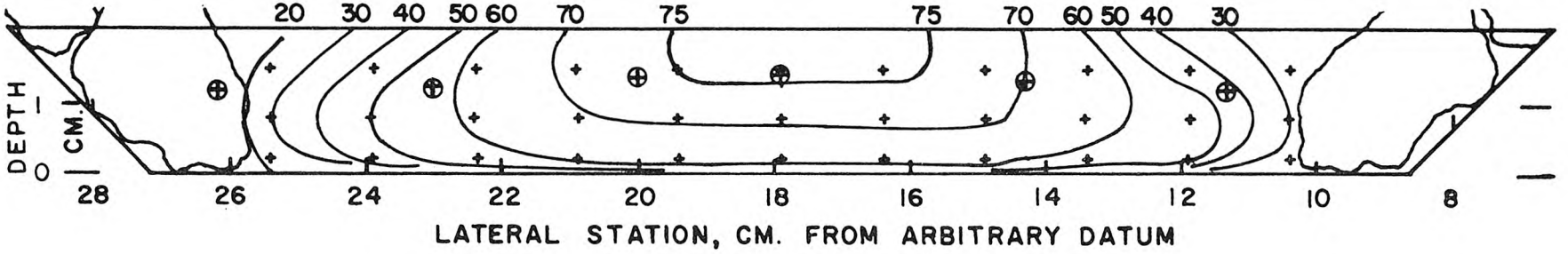

Figure 44a. Cross section of flow for series 3400. Contours are velocity (cm./sec.). + indicates velocity measurement; ⊕ indicates probe location.

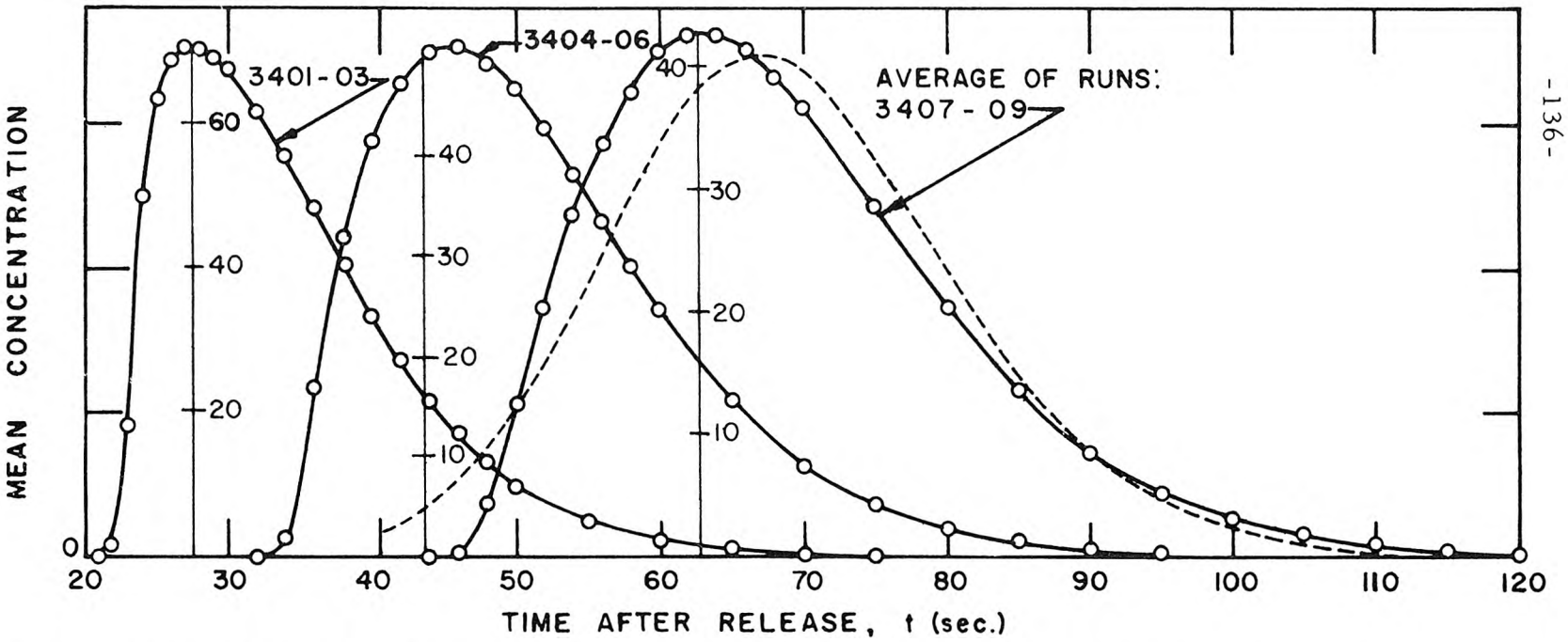

Figure 44b. Results of series 3400. ---Routing of runs 3401-03 to coincide with 3407-09; D = 2200 cm.^{2}/sec. Concentration in arbitrary units; note change of scale for each curve.

into the downstream hopper. This provided time for the slug to dissolve and disperse during circulation through the return pipe, inlet box, and the length of the channel. By varying the rate of dumping of salt, various concentration gradients could be both achieved and maintained at the probes for a considerable time period. Thus the assumed conditions of Taylor's analysis could be achieved within an excellent approximation. The slug was then allowed to recirculate until mixed completely throughout the system, when the calibration readings could be made.

Sub-areas for calculating the dispersion coefficient from the measured steady state profile were obtained by drawing vertical lines midway between the probe positions. Only the half section was used in which the probes were located; for series 2800 and 3400, in which the probes were spread across the entire section, the probes on the east half were reflected about the plane of symmetry into west half image positions. The normalized relative concentration, $c'/\frac{\partial \bar{c}}{\partial \xi}$, at each probe was obtained for three longitudinal concentration gradients, and averaged. In general, the concentration gradient was varied over a factor of approximately three, and the normalized cross-sectional concentration deviations agreed within 10%. The averaged normalized deviation was then used with equation 87 to sum the diffusive transport across the section and obtain the dispersion coefficient.

For each series, a predicted dispersion coefficient was obtained by two methods: estimation of the time scale from bulk channel parameters, and integration of the predicted steady-state profile to obtain

the predicted diffusive transport. Combining equations 57 (for the time scale) and 40 gives a rapid method for estimating a coefficient:

$$D = 0.30 \frac{\ell^2 \overline{u'^2}}{r U^*} \tag{90}$$

A more accurate method is integration of the predicted steady-state profile, which was accomplished by programing equation 55 for the high-speed computer. Each cross section was halved by a plane of symmetry, and one half divided into between 21 and 28 integration elements. The mean velocity of each element, u'(z), relative to the cross-sectional mean was taken from the cross-sectional velocity measurements. The lateral mixing coefficient between elements was based on Elder's result, $\epsilon_z = 0.23\ d\ U^*$, using the local depth and overall shear velocity. Within the section shown as stone the local depth was assumed to be 20% of the total. By thus restricting both the surface area available and coefficient for lateral mixing, quite high relative concentrations were obtained in the pores. However, the pore volume was sufficiently small that the dispersion coefficient was not greatly affected.

The predicted steady-state profiles are shown as solid lines in figures 45 and 46, along with the measured points. For series 2800 through 3200 the prediction is an excellent fit to the measurements; in series 3400 a better fit is obtained (dashed line) by setting, in equation 55, $\epsilon_z = 0.30\ d\ U^*$. The predicted dispersion coefficients, which are an integration in approximately 25 steps of the solid line, were in general slightly higher than the coefficients calculated by integration

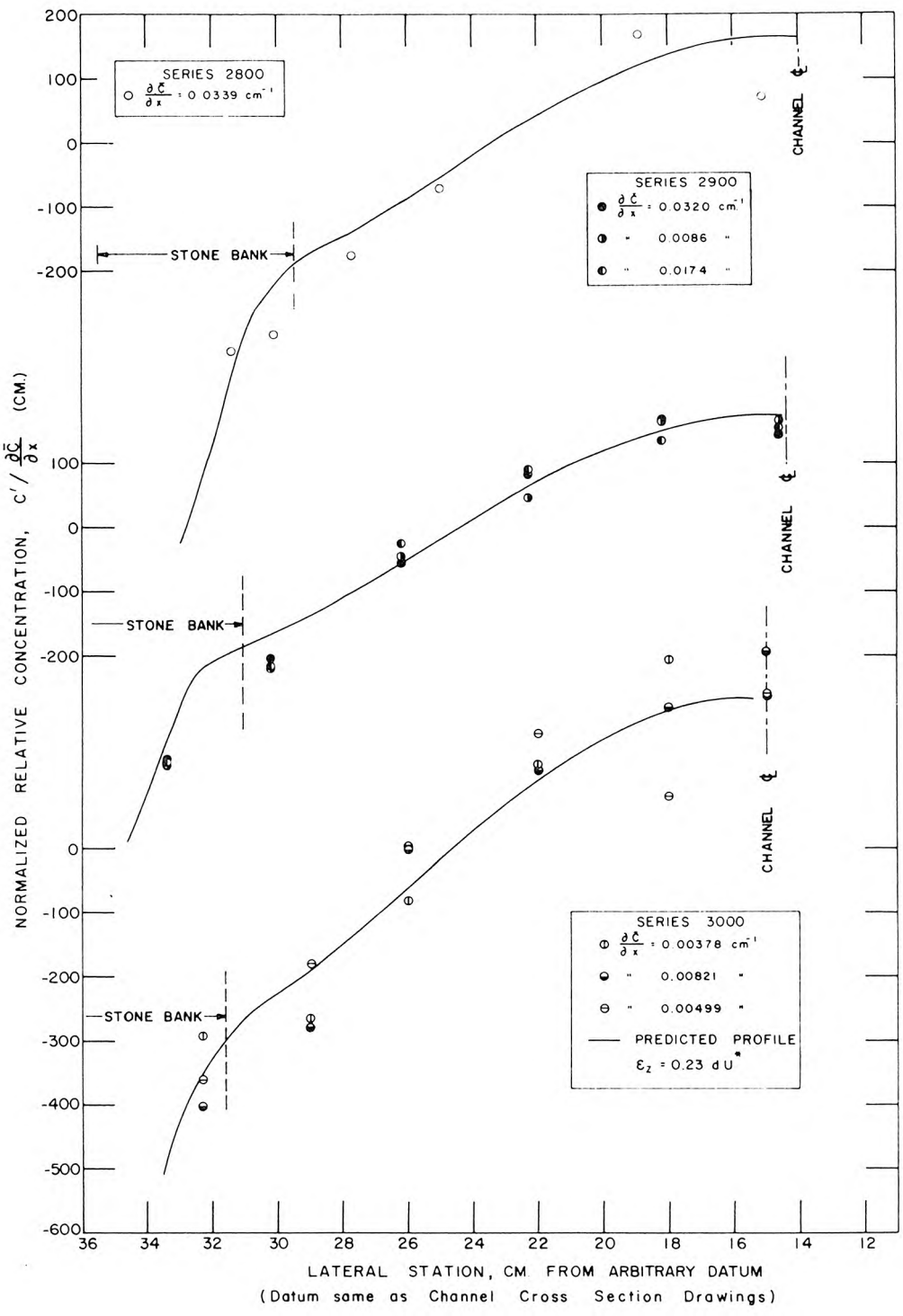

Figure 45. Predicted lateral steady-state profiles (equation 55) and measured points; series 2800, 2900, and 3000.

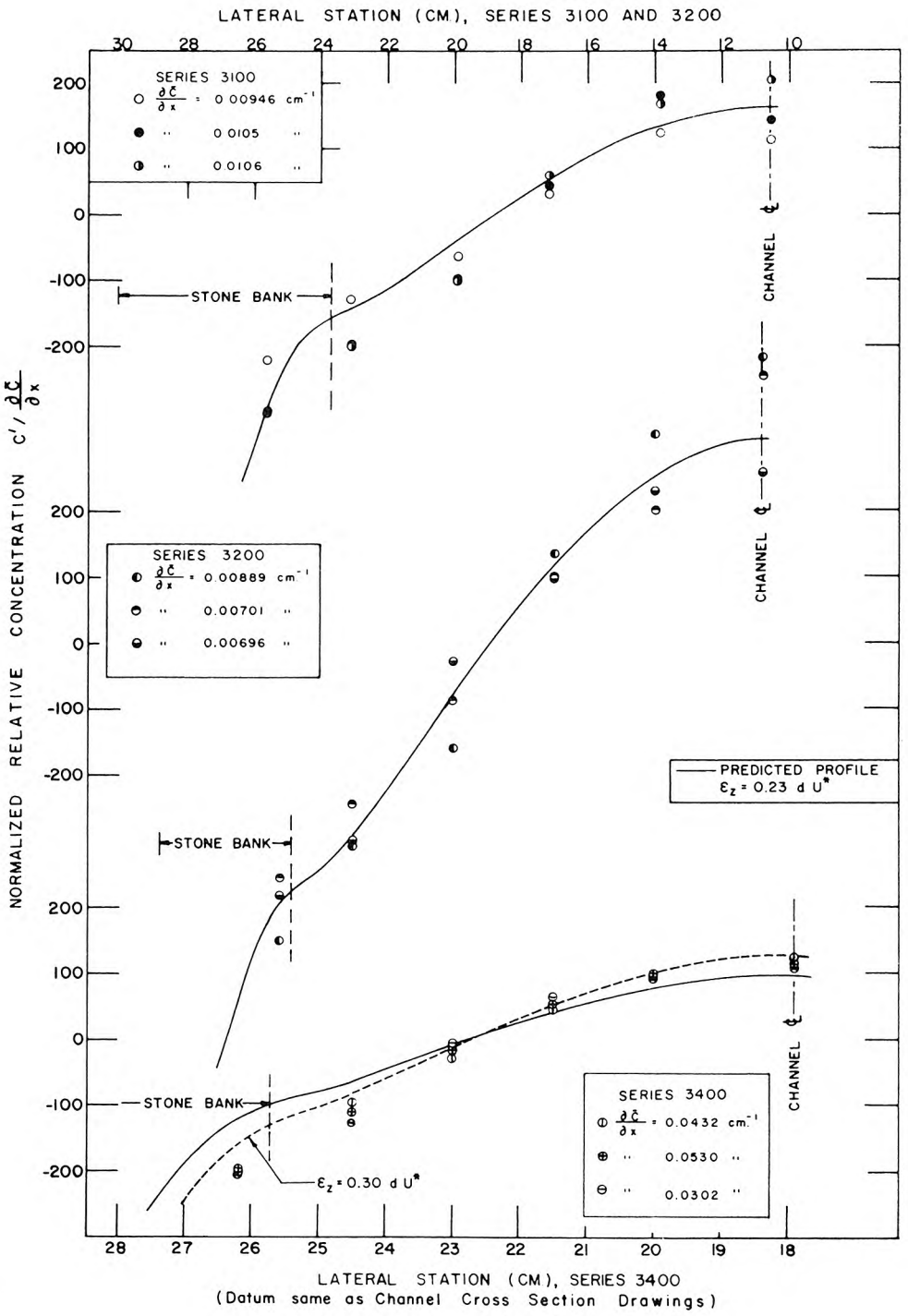

Figure 46. Predicted lateral steady-state profiles (equation 55) and measured points; series 3100, 3200, and 3400.

over the six measured points. However, the agreement in all cases is quite good. For the two series for which a coefficient is available by the routing procedure, series 3100 and 3400, an excellent agreement exists between the result of the predicted diffusive transport and the coefficient which produced the best routing.

In summary, the experiments presented in this section have shown that the dispersion coefficient for a laboratory channel can be vastly increased by addition of side roughness. All of this increase can be explained by the induced lateral variation in velocity. The results will be discussed further in Chapter VIII.

CHAPTER VI

FIELD EXPERIMENTS

VI-A Introduction

In August and September of 1965, a series of experiments was conducted by the U. S. Geological Survey in the Green-Duwamish River, Washington. The author participated in this study as an employee of the Geological Survey, and was involved in all aspects of experimental design and data analysis. The study was part of a broader investigation of the effects of pollution in the Puget Sound area, undertaken with the cooperation of the Municipality of Metropolitan Seattle; choice of the study reach was dictated by the needs of the Municipality, whose Renton Sewage Treatment Plant discharges treated sewage into the river downstream from Renton Junction. A complete report of the study is being prepared by the author for publication as a Geological Survey Professional Paper.

The study consisted of four experiments. The experiments of August 3 and 4 and September 9 measured only one-dimensional longitudinal dispersion; dye was injected upstream from the study reach, and a series of sampling stations established throughout the reach. The experiment of August 17 was similar to that of August 3 and 4, except that only a few stations were sampled, and the dye cloud was photographed from the air at intervals throughout the day. The experiment of August 31 was designed to duplicate the earlier portion of that of August 3 and 4 and to obtain lateral concentration profiles at two cross sections.

VI-B Description of the Study Reach

The Green River rises in the Cascade Mountains just north of Mount Rainier. It flows through the foothill area and emerges onto an alluvial valley at Auburn, Washington. From Auburn to its discharge into Elliott Bay at Seattle, it meanders through a flat alluvial valley. The downstream end, below the confluence of the Black River and comprising mostly the estuary, is known as the Duwamish River. The Black River, once a major tributary, has since 1917 contained hardly any flow; this and other channel realignments and the geology of the area have been described by Mullineaux (36).

The reach of interest (fig. 47) includes the lowest 13 miles of the Green-Duwamish system, commencing at the Renton Junction Bridge and continuing to Elliott Bay. The tidal range at Elliott Bay averages approximately 10 feet, although a maximum of 16 feet has been recorded. In its lowest 6 miles, the estuary is dredged to a depth of 20 feet, varies in width from 400 to 1,000 feet, and may be characterized as a one-dimensional estuary. The upper 7-mile reach, which is the range of primary interest for this study, may be characterized as a meandering, tidally influenced river. At low flows (about 300 cubic feet per second or less), the stage at the uppermost station shows tidal influence for tides that exceed approximately +8 feet at Seattle. Reverse flow occurs at higher tides. Thus, during most high tides the entire study reach is tidally affected. In contrast, much of the reach flows as a normal river at low tide.

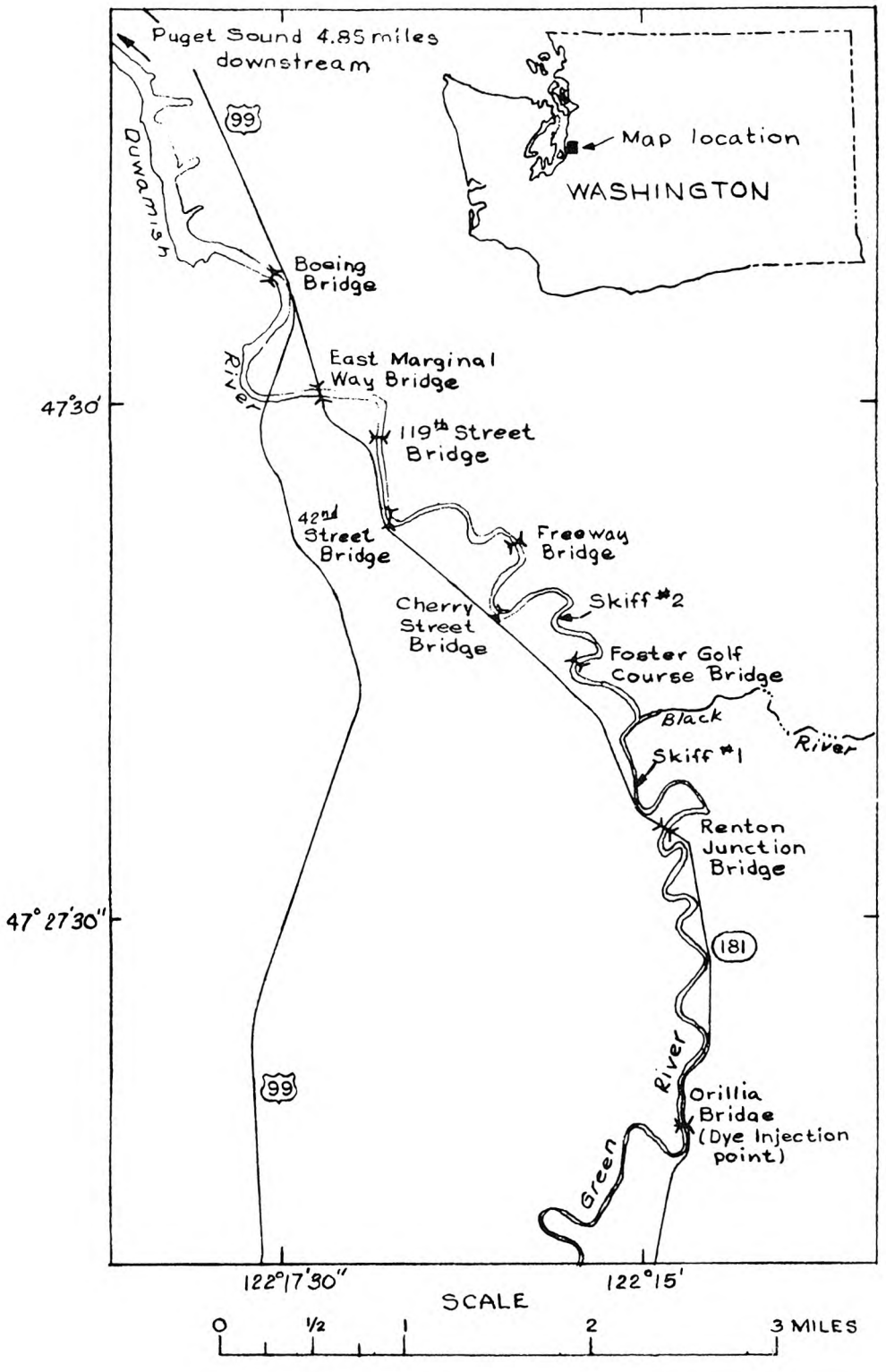

Figure 47. Study reach of the Green-Duwamish River, showing dye-injection point and sampling stations.

Flow in the Green River at Auburn (U. S. Geol. Survey gaging station 12-1130) varies from about 12,000 cfs (cubic feet per second) at flood stage, often recorded during winter floods, to low flows on the order of 200 to 300 cfs. The river is regulated upstream from Auburn by Howard A. Hanson Dam, operated by the U. S. Army Corps of Engineers, which guarantees to maintain a low-flow discharge of at least 80 cfs. From Auburn to the mouth, the river is leveed to a height of 20 feet. Most of the sediment transport and channel degradation takes place during the winter floods, when the river often flows nearly bank full. The present study was conducted during particularly low flows because of the primary interest in pollution. At low stage, the river is confined to the bottom of the levees, where the banks are mud, sand, or occasionally riprap; the upper banks are covered with grass and blackberry vines. The river contains debris of all sorts, including snags, logs, and car bodies, much of which projects above the surface at low stage and adds to the channel roughness.

The slope of the river between Renton Junction and 42nd Street, computed for low tide on August 3, was 0.000224. A mean hydraulic radius for this reach is estimated at 3.6 feet, yielding a shear velocity of 0.161 fps (feet per second), a Darcy-Weisbach friction factor of 0.26, and a Manning n of 0.058. The Manning n value agrees well with a table by Rouse (37).

Table 29 gives a list of all sampling and measuring locations used in the study and the types of information collected at each station. The river stations, in feet upstream from the mouth of the estuary, were established by measuring on the U. S. Geological Survey map

Table 29. Sampling and measuring stations used during the four experiments, and type of information obtained.

Station	Distance upstream from mouth of estuary (feet)	August 3, 4			August 17	August 31	September 9		
		Dye Conc.	Velocity	Stage	Dye Conc.	Dye Conc.	Dye Conc.	Velocity	Stage
Renton Junction	69,270	x	x	x	x	x	x	x	x
Skiff No. 1	63,950						x		
Foster Golf Course	59,240	x	x		x	x	x	x	x
Skiff No. 2	56,640						x		
Cherry Street	53,640	x	x	x	x		x	x	x
Freeway Bridge	50,680						x		
42nd Street	46,240	x	x	x	x		x	x	x
119th Street	43,940						x	x	x
E. Marginal Way	41,450	x	x	x			x	x	x
Boeing Bridge	34,320	x	x	x					

Note: x indicates quantity measured; blank indicates quantity not measured.

titled, Seattle and Vicinity, at a scale of 1:62,500. Figure 48 shows views of three of the sampling stations. Cross sections at several of the stations, shown in figure 49, were measured on August 3.

VI-C Measurement Techniques

The tracer used was Rhodamine B, a commercial dye whose properties have been summarized by Buchanan (38). For the purpose of this study, the primary properties of interest are that: (a) the dye is miscible in water up to concentrations of 2 percent by weight; (b) it does not decay appreciably during the duration of the test; and (c) it is capable of being adsorbed onto river sediments, although in unknown quantities. In this study, the dye, contained in a 40 percent acetic-acid solution, was placed into open buckets and inserted into the river by dumping from a bridge 2 miles upstream from the reach of interest.

Immediately after the dye was inserted and prior to its arrival at any of the sampling stations, samples of river water were collected at several stations for preparation of dye-concentration standards. For the experiment of August 3-4, all of the standards were made from a mixture of river water collected at Renton Junction and East Marginal Way. Standards consisting of 0.5, 1.0, 5.0, 10, 50, and 100 ppb (parts per billion) were prepared. In the later experiments, individual sets of standards were prepared from river water taken at each of the measuring stations, with the exception of the skiffs, the Freeway Bridge, and the 119th Street Bridge. For all stations, standards were prepared consisting of 0.5, 1.0, 2.5, 5.0, 10, 20, 40. 80, 100, 200, and 400 ppb of Rhodamine B. During the dye-cloud passage, samples

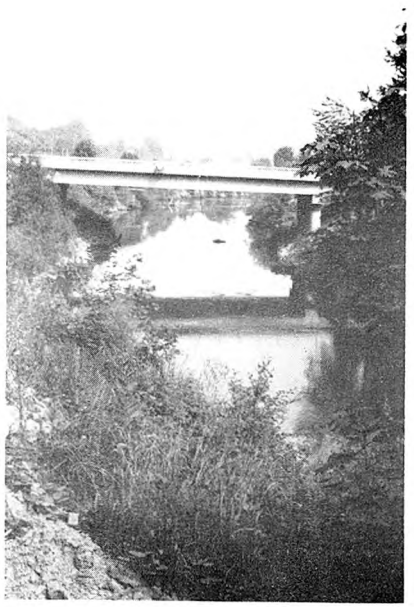

(a)

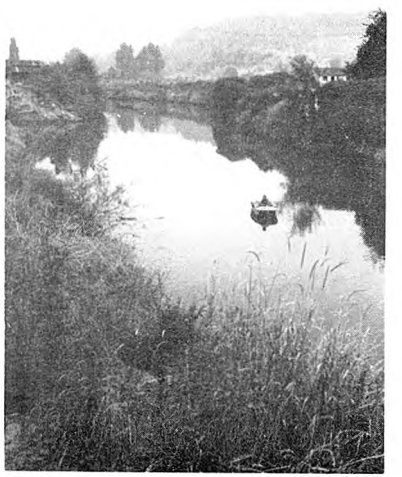

(b)

(c)

Figure 48. Sampling stations along the Green-Duwamish River; (a) Renton Junction, (b) Skiff No. 1, (c) Skiff No. 2; all looking downstream.

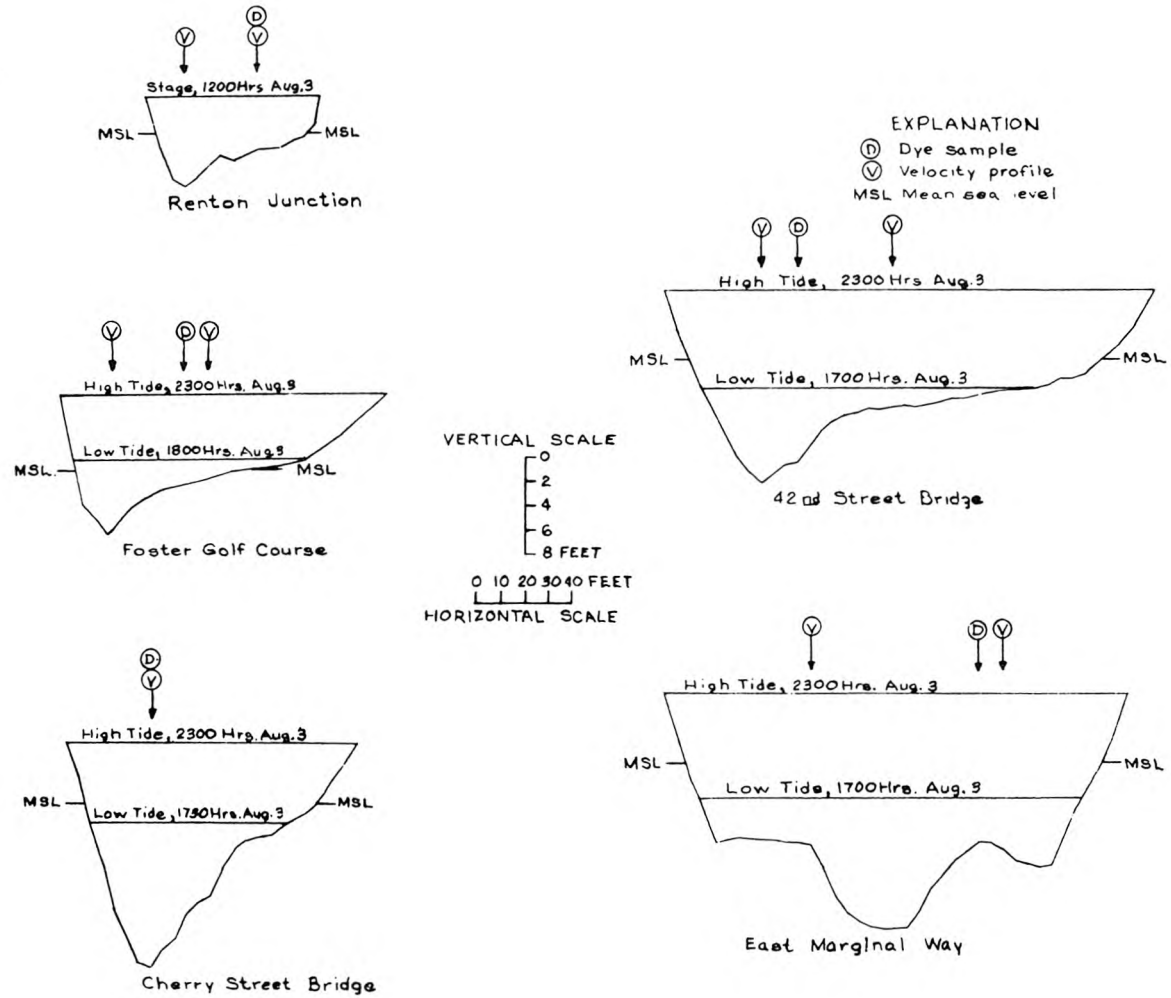

Figure 49. Cross sections looking downstream at selected sampling stations, showing high and low tides on August 3. Symbols denote location of dye and velocity measurements on September 9.

were collected at the various stations by lowering a brass holder with a 16-ounce glass bottle into the water and allowing the bottle to fill by gravity. Samples were taken every 10 minutes, beginning prior to visual arrival of the cloud and extending at least an hour after any dye was visible, after which the samples were taken half-hourly for as long as any dye was believed to remain. Samples were normally taken approximately 1 foot below the water surface. The sampling time recorded was the instant at which the bottle entered the water; approximately 20 seconds were required for the bottle to fill. Upon completion of the experiment, the sample bottles and standards were stored together in a dark location to await reading of fluorescence on the fluorometer. Prior to reading the fluorometer, all bottles were brought to the same temperature. In the first experiment, the standards were analyzed first, followed by all the bottles in sequence. This meant that the last of the bottles was analyzed 4 days after the standards. In the later experiments, the standards for each station were read immediately prior to the analysis of samples from that station. Using this procedure, standards and all bottles for a particular station could be completed during the same day.

At certain stations, the dye cloud was monitored continuously by a recording G. K. Turner fluorometer.

During the passage of the dye cloud, measurements of velocity and stage were also made at most sampling stations (table 29). Velocities were measured with Price current meters, and stage was measured by a wire-weight gage, except at Renton Junction where a continuous stage recorder is in operation.

VI-D Visual and Photographic Observations

Visual observations of the dye cloud, unreliable as they may have been, provided striking qualitative evidence of the effect of lateral velocity variation. Concentration variations could be easily distinguished by eye; by correlating notes on observations with fluorometer readings, the following categories were established:

0 to 10 ppb, not visible;

10 to 25 ppb, very faint;

25 to 75 ppb, dull red (rust color);

more than 75 ppb, bright red.

The observations reported herein come from three sources. Visual observations by all members of the staff, both professional and non-professional, were recorded by the author. Thirty-five-millimeter color slides were taken from both the ground and the air. In addition, a study was made on August 17 during which a Geological Survey De Haviland Beaver aircraft, equipped with an aerial camera, flew over the dye cloud throughout the day, shooting color and black and white film alternately at half-hour intervals. Both tidal conditions and river inflow on this date were identical to those during the study of August 3, and samples analyzed for dye concentration at the various sampling sites showed that almost an exact duplicate of the previous experiment was achieved. The description which follows includes observations from both experiments without differentiation.

Immediately on hitting the water, each pail of dye appeared as a round oily slick, which within 15 seconds developed into a brilliant red disc. The two discs, resulting from the two injections, both began to expand in a triangular pattern, with a broad front and pointed tail. The sides of the two spots met at a point approximately 300 feet downstream from the bridge, where the channel contains a small riffle and a rock projects above the surface at the west one-third point. Downstream from the riffle, the leading edge of the cloud appeared as two fingers, with clear water in the center. The rock at the one-third point forms a shadow of quiet water which did not appear to affect the passage of the front; however, after the cloud had passed, a brilliant tail remained in the shadow, forming a triangle pointing upstream with apex angle of approximately 10^{o}. The tail dissipated very slowly, and was still quite apparent when the main body of the cloud was several hundred feet downstream.

Figure 50 shows all of the characteristic features of the cloud as it appeared when centered approximately 1,600 feet below the injection point. The leading edge is in the form of a point, with clear water along both sides. The picture also shows two clear-water shadows downstream from snags near the leading edge. The leading one-fourth of the cloud, from ground observations, has a distinctly mottled texture, which is repeated in the trailing quarter; the center half is a uniform red color from bank to bank. Apparently in the extremities mixing has occurred between large parcels of fluid, but only in the center has small scale mixing smoothed out the resulting gradients.

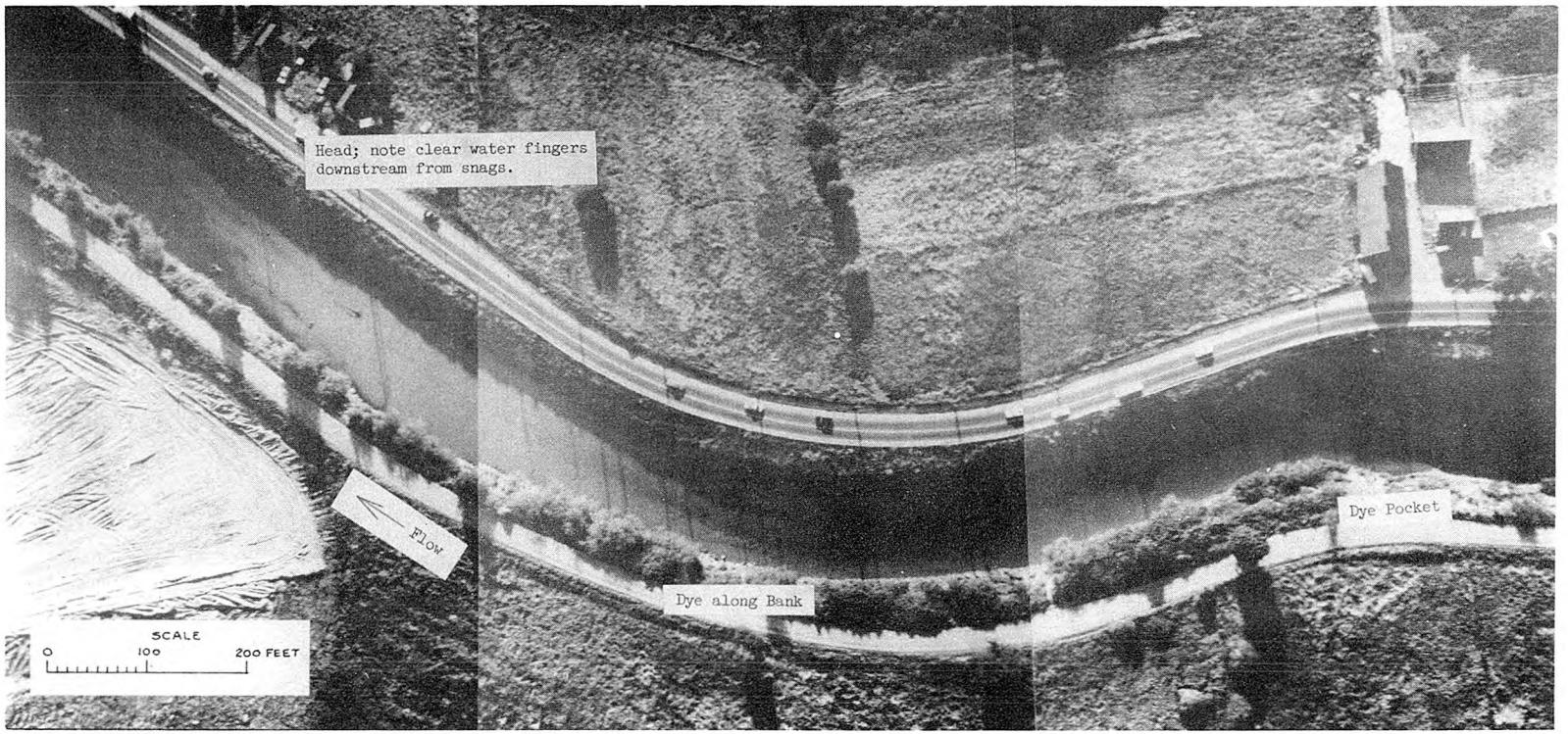

Figure 50. Aerial photograph of dye dispersion, August 17, 0804 hours. Center of cloud approximately 1600 feet downstream from injection point.

In the trailing section of the cloud, clear water penetrates into the cloud in a point much like that of the dye point at the leading edge. Dye that migrated from the center of the cloud towards the side during passage of the main body can be seen lying along the 3 to 5 feet nearest the bank for several hundred feet upstream from the rest of the cloud. The picture also shows a pocket of dye about 500 feet upstream from any other--one of a great many which were observed throughout the day. Such pockets fill quite slowly during passage of the dye cloud; even the smallest indentations, which to the observer appear to be part of the main stream, sometimes contain clear water long after arrival of the cloud, when the rest of the river is running bright red. As the cloud passes, these pockets turn slowly from clear to red; after the cloud has passed and the river appears to have returned to its normal color, the pockets stand out as small patches of bright red. The concentrations contained in these pockets were occasionally verified by bottle samples. For instance, on August 17 at 1120 hours at the Renton Junction Bridge, the concentration in the main flow had dropped to 13 ppb following passage of a peak of 261 ppb, but a pocket of bright red water just upstream contained 130 ppb.

Figure 51, a photograph taken exactly 15 minutes after figure 50, shows many of the same characteristics, although considerable dispersion has obviously taken place. The pattern of flow emerging from the curve, and the slow rate of exchange between the fast and slow moving sections, is particularly evident.

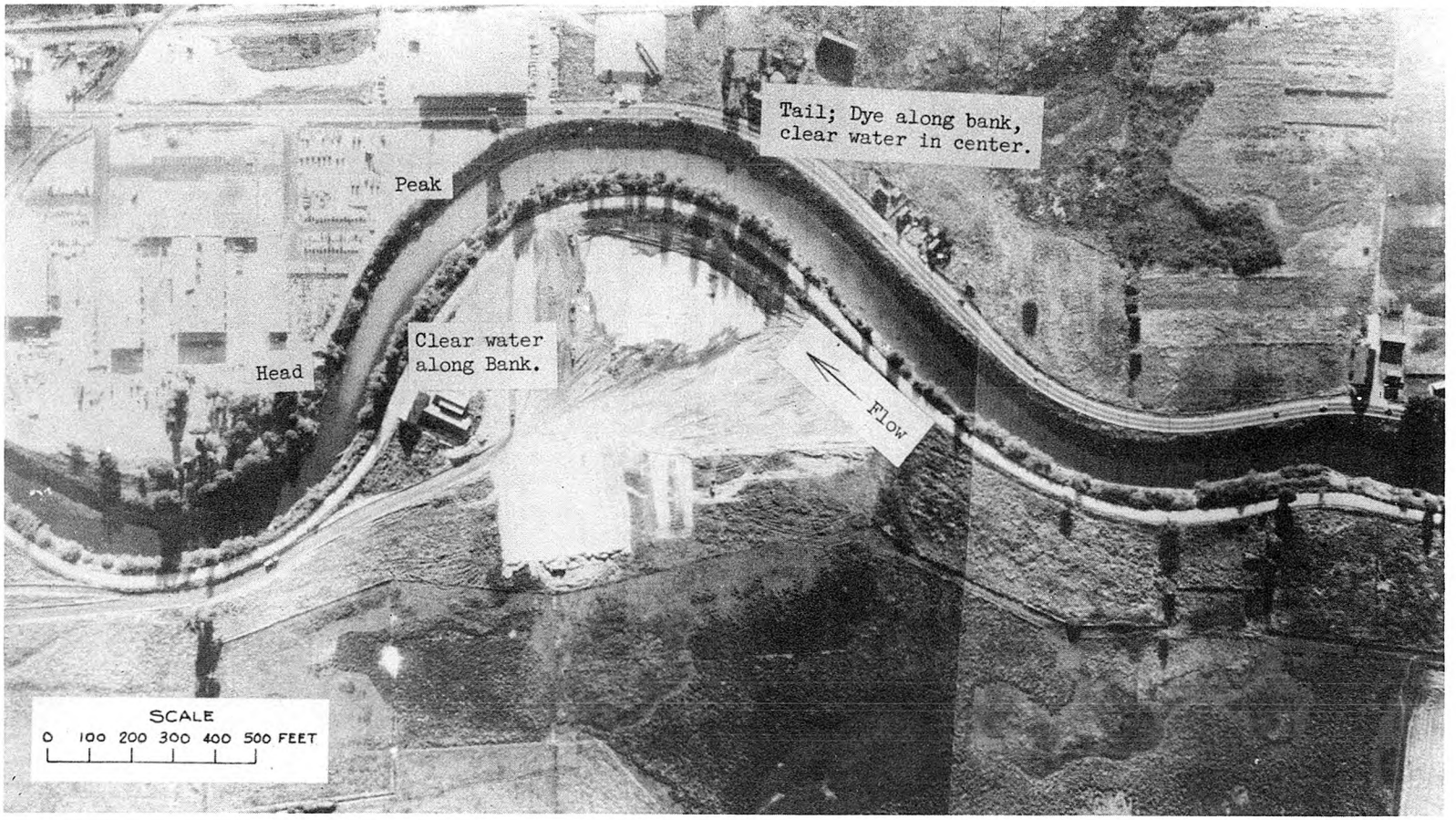

Figure 51. Aerial photograph of dye dispersion, August 17, 0819 hours. Center of cloud approximately 2700 feet downstream from injection point.

In figure 52, taken slightly over an hour after figure 51, the building at the far right center is the same as that at the far left center in the previous photograph. The picture shows that the cloud still displayed all of the characteristics previously mentioned, except that the contrast is not as sharp because of lower concentrations. As the concentration drops, it becomes increasingly difficult to differentiate in the pictures between dye and mudbank; however, careful comparison between the pictures shown, others not included, and the color pictures allowed positive identification at almost all places. For instance, the long, straight reach in figure 52, marked "Tail," exhibits over a distance of about 300 feet a section where lighter zones appear along both banks, with a darker zone in the center. The lighter zones are definitely dye rather than mud or shallow areas, because that section exhibits a uniform color in photographs taken at other times.

The dye arrived at Renton Junction in a reasonably well-defined front 2 hours after release. Elapsed time between colorless water and bright red was less than 5 minutes. However, for the first 10 minutes after bright red color existed in the stream center, the 10 feet of water nearest the right bank appeared completely clear. This area then filled in, and the river ran completely red for more than an hour.

Six hours after release, the front arrived at Cherry Street Bridge. Although the increase in color was at first difficult to distinguish, a pattern was evident within 10 minutes after its first sign.

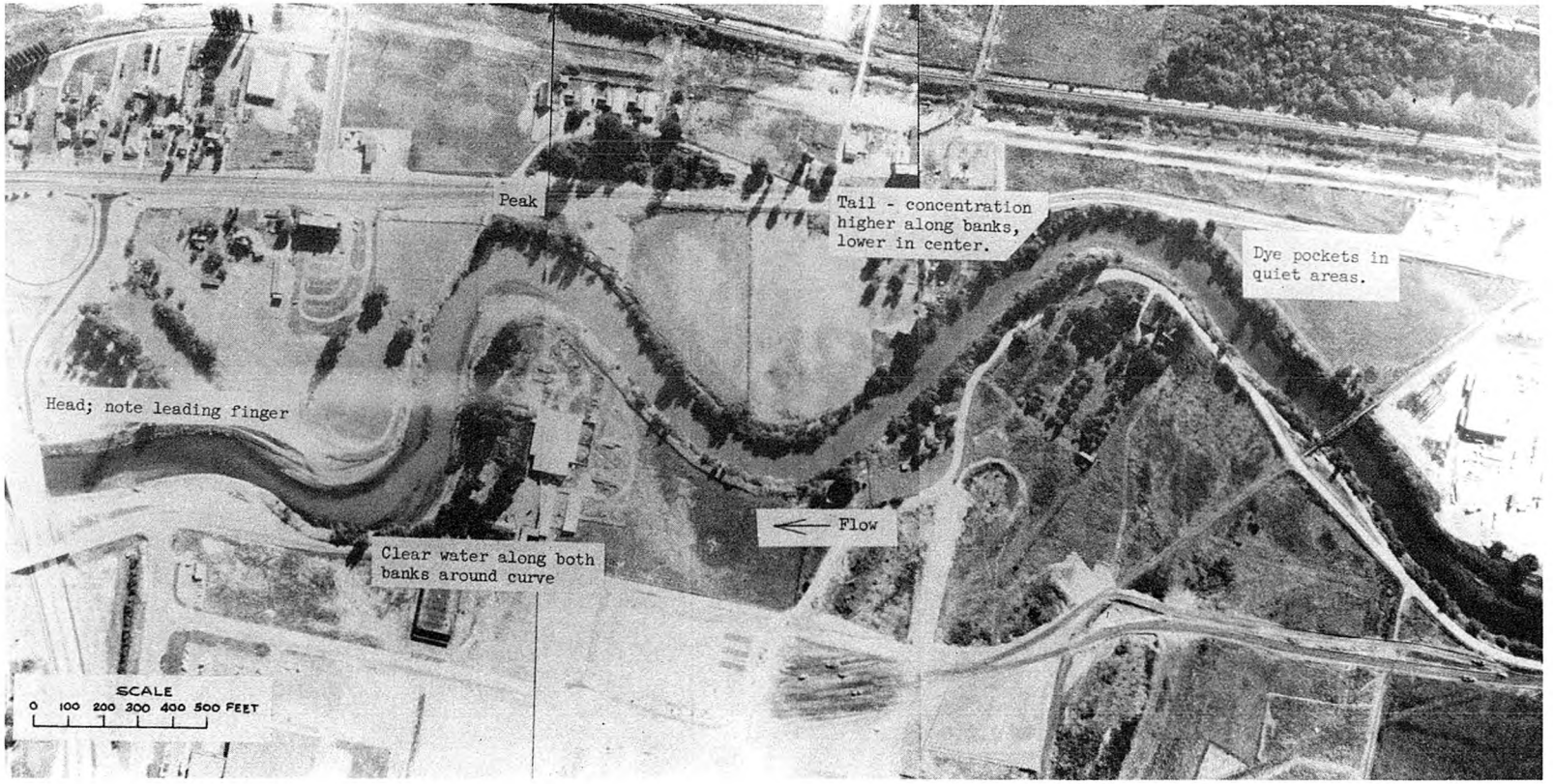

Figure 52. Aerial photograph of dye dispersion, August 17, 0927 hours. Center of cloud approximately 8500 feet downstream from injection point.

Figure 53 shows the pattern after about 20 minutes: the initial color traveled entirely down the west side in the deeper section, until a strong color was evident over the western one-third of the cross section. Color then migrated into the shallow side at a fairly constant slow rate. After 30 minutes, clear water remained in the eastern 10 feet, grading continuously to the highest concentration in the high-

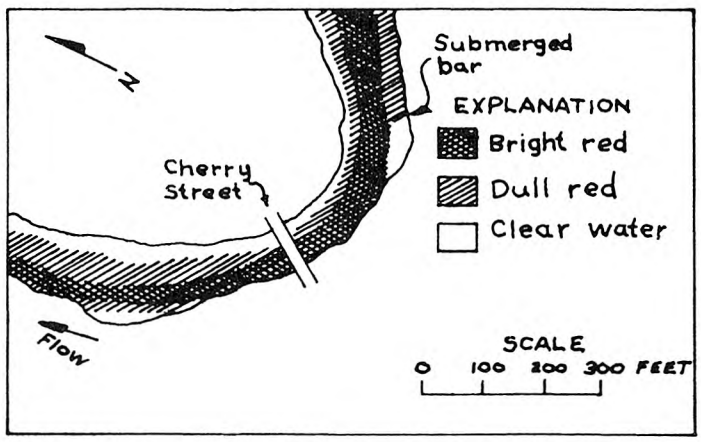

Figure 53. Appearance of dye cloud at Cherry Street, 1550 hours August 3.

velocity area. About 200 feet upstream from the bridge, on the west side, a submerged, hardly apparent bar extends out about 10 feet into the flow. The water below the bar, although the observer would have guessed it to be in the high-velocity area, remained clear for the first 30 minutes. Two and one-half hours later, the bar shadow was a brilliant red, although the river in general was only dully red. The outer edge of the bar-shadow area was absolutely straight, and extended

downstream to intersect the curving bank. The pattern was sufficiently striking to cause unsolicited comments by nontechnical observers during both the experiments of August 3-4 and September 9; it can also be seen in the aerial photographs of August 17.

VI-E Measurement of Longitudinal Dispersion

The experiments of August 3-4 and September 9 were designed to follow for as long as possible the motion of the dye cloud downstream from Renton Junction, to obtain a longitudinal dispersion coefficient, and to observe the effects of the tidal action. No attempt was made to obtain cross-sectional velocity or concentration measurements; samples were taken from only one point on each measuring cross section. Upland river discharge was nearly identical during the two experiments, 266 cubic feet per second on August 3 and 235 cfs on September 9 at the Auburn gaging station. (According to Geological Survey correlation of discharge records, 266 cfs at Auborn corresponds to 310 cfs at the Renton Junction Bridge.) The primary difference between the experiments was the range of forecast tides at Seattle; these are shown in figure 54. Also, during the later experiment greater accuracy was obtained by including more measuring stations.

For each experiment 4 gallons of Rhodamine B dye were injected into the Green River from the Orillia Bridge (river station 80,646 feet). Injection was timed so that the cloud would arrive at the Renton Junction Bridge shortly after high tide, and would travel through the reach of interest during tidal runout. Injection on August 3 was at 0930 hours,

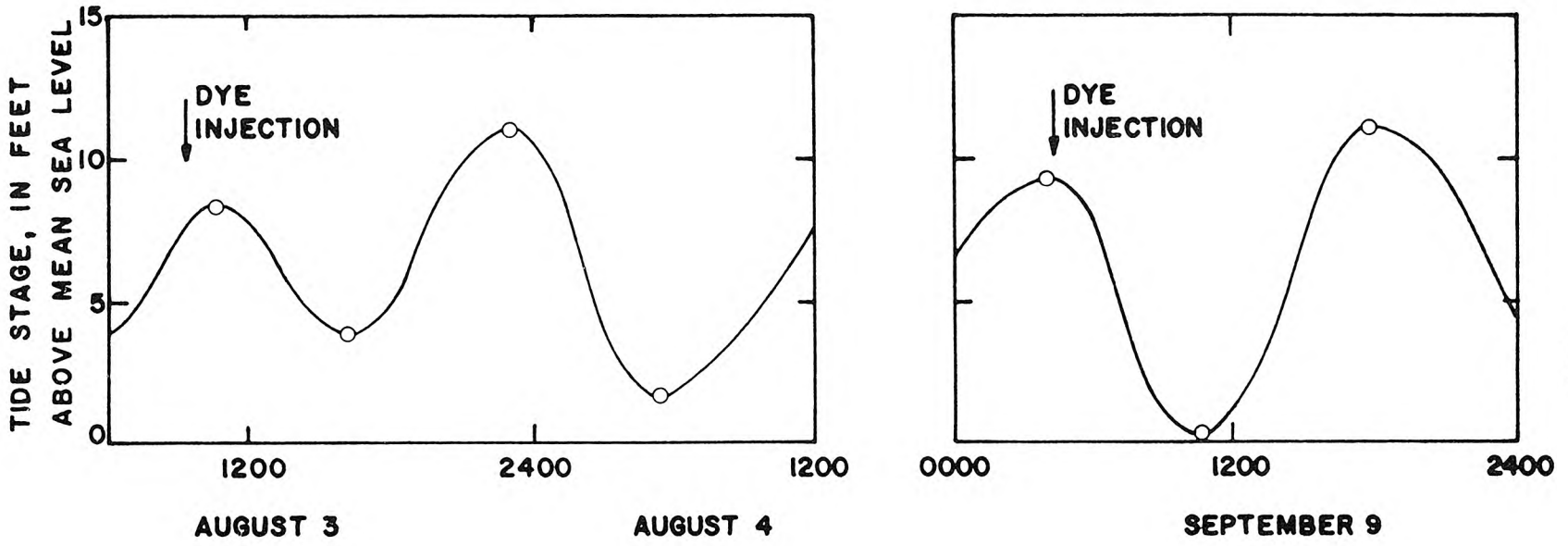

Figure 54. Forecast tides at Seattle, August 3-4 and September 9. Times of dye injection into the Green-Duwamish River are indicated.

and on September 9 at 0430 hours. The data recorded at each measuring station are shown in figures 55 and 56. The velocities indicated at stations where measurements were made at more than one point are the average of both measurements. Where stage was not recorded, depth is shown.

On August 3, the data show that on the first outgoing tide the cloud passed the Renton Junction, Golf Course, and Cherry Street bridges completely, and arrived at the 42nd Street Bridge. The tide changed at 42nd Street at 1810 hours, following which an exact reflection of the dye cloud was observed (fig. 55). On the incoming tide, the cloud returned past Cherry Street completely, and came to a halt between Cherry Street and the Golf Course Bridge. Then, on the subsequent outgoing tide, the cloud passed all measuring stations and continued downstream beyond the Boeing Bridge. At 42nd Street and Boeing Bridge certain erratic breaks in the concentration pattern exist. However, the record of the continuous fluorometer yields a smooth curve at East Marginal Way. The bottle samples for these stations were processed 5 days after the experiment, which was 4 days after processing the standards. For both stations the erratic results occur at a point in which a change in scale was necessary on the fluorometer. The error probably is attributable to a change in the standardization of one or the other of the fluorometer scales during the 4-day period. The preparation of more complete standards during the later experiments eliminated this problem, and provided uniform results.

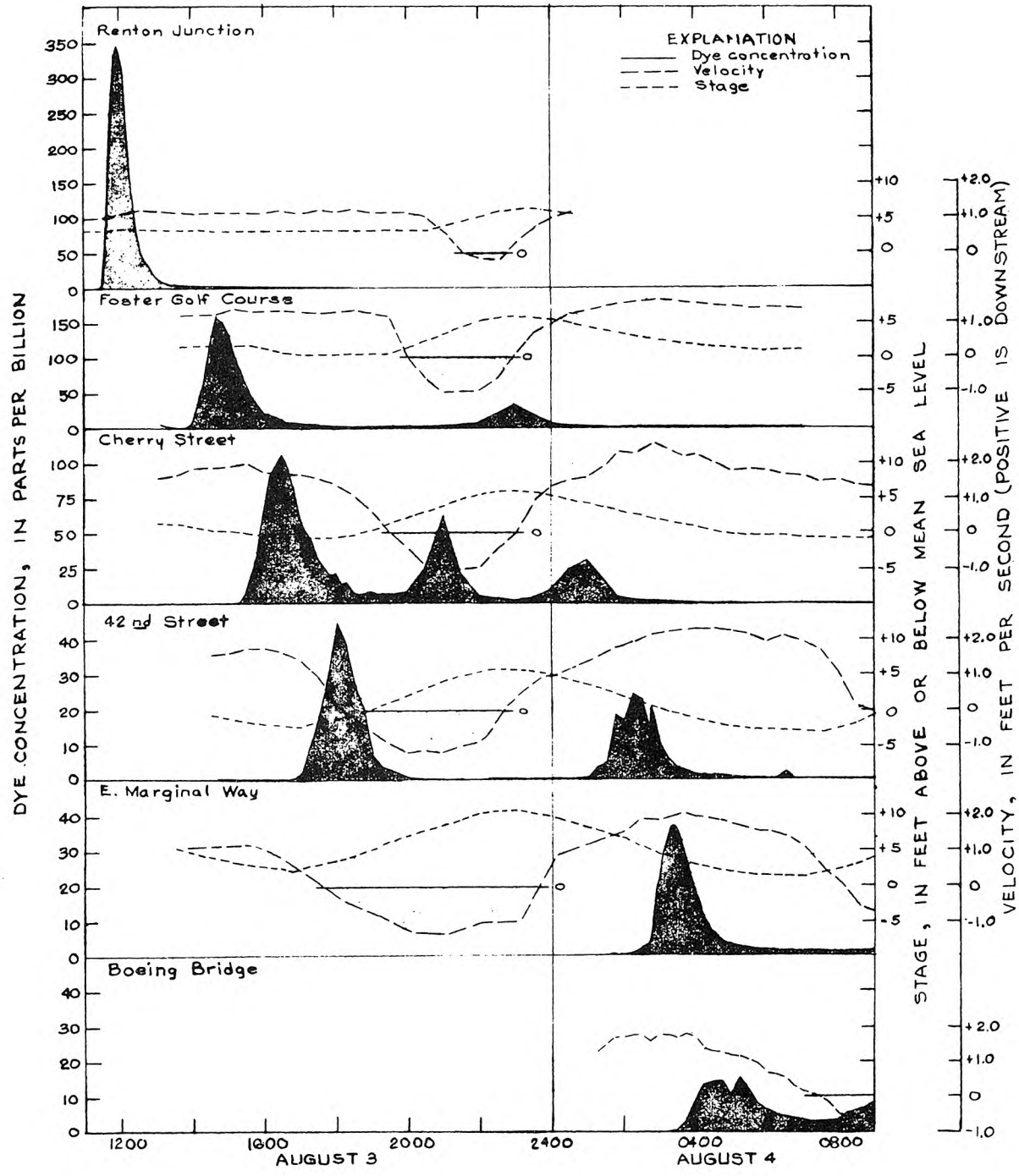

Figure 55. Dye concentration, measured velocity, and stage at sampling stations, August 3-4.

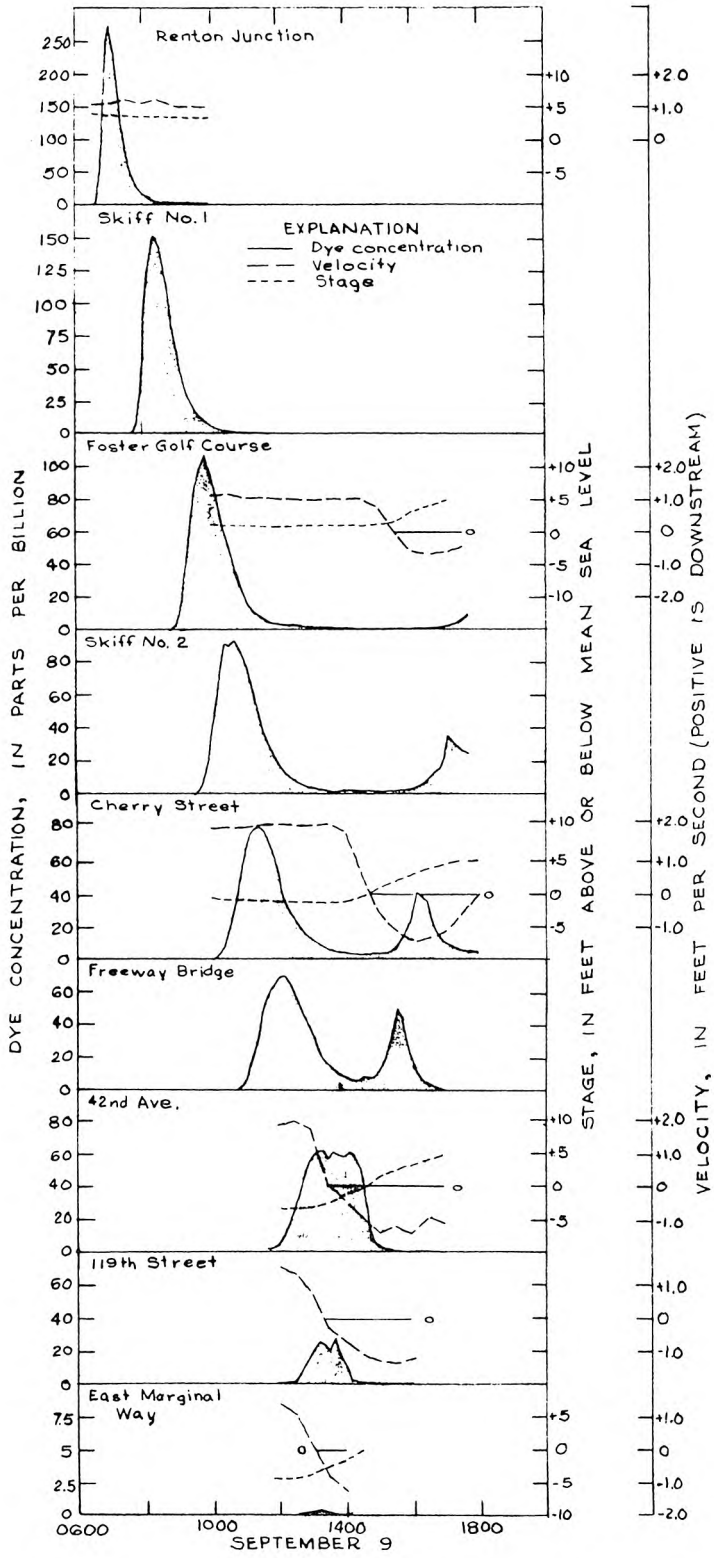

Figure 56. Dye concentration, measured velocity, and stage at sampling stations, September 9.

On September 9, the data show the effect of the increased range of tide. At 1320 hours, the time of tide reversal, the peak concentration had passed the 119th Street Bridge, and a very slight increase in concentration was observed at East Marginal Way (fig. 56). The incoming tide then carried the cloud all the way back up to the Foster Golf Course Bridge, at which time the study was discontinued.

In order to obtain dispersion coefficients by the change of moment method, it was necessary to derive from the data shown in figures 55 and 56 a series of concentration-distance curves for particular times. The method used has been given in section IV-B (equation 76). Figure 57 shows a set of such curves for the experiment of August 3-4. The shapes drawn between measuring stations are, of course, not exact, but no difficulty was found in matching segments extended from adjoining stations. Curves for the experiment of September 9 were easier to draw, because of the additional stations.

Once concentration-distance curves have been obtained, variances may be calculated by numerical integration. The dispersion coefficient may be obtained by the growth rate of the variance (equation 37), and checked by the routing procedure. The check is important, because in field studies measured distributions always exhibit long, low concentration tails upstream of the cloud, which have a strong influence on numerical integration of the second moment. The tails are caused by two mechanisms; adsorbtion, and later re-solution, of tracer onto bed sediments, and detention of small quantities of tracer-bearing fluid in nearly stagnant pools along the banks. Tracer detained in

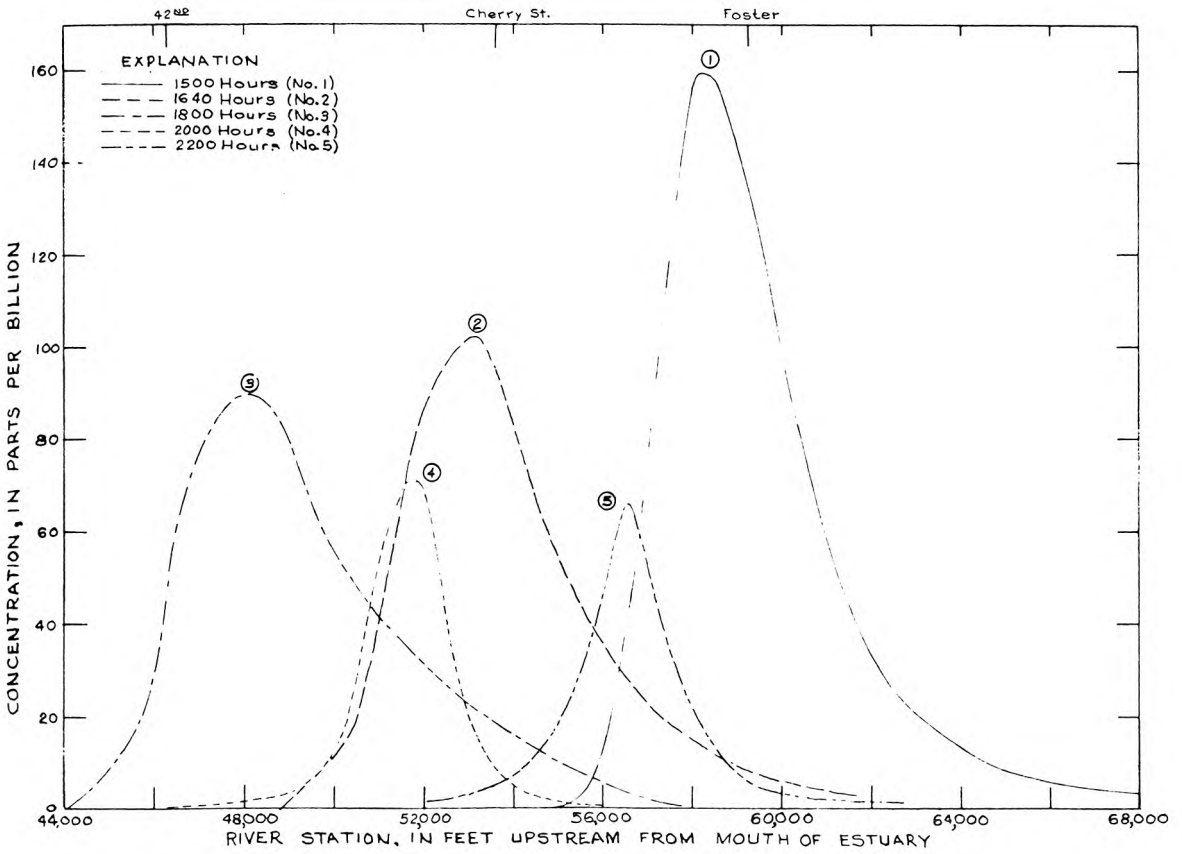

Figure 57. Calculated dye-concentration distribution along the river at selected times, August 3.

either manner should not be included in calculating the variances, but only by the routing procedure may the investigator be sure of having subtracted out the correct amount.

In this study, the subtraction was done as follows. A point on the tail was chosen, entirely by eye, at which the integration was to be terminated. At this point the concentration value was generally about five percent of the peak, and the curve of concentration versus distance was essentially flat. A straight line was then drawn from the termination point to the initial point – a point of zero concentration at the downstream end of the distribution – and this line was used as the base for the integration. By this procedure the value obtained for the variance is insensitive to the exact position of the termination point, and a reasonable dispersion coefficient is obtained for use with the routing procedure.

Figure 58 shows the variances obtained, and the tidal conditions in the reach of the river in which the dye cloud is located at the given time. The first 7 hours of dispersion took place in a reach that behaved essentially as a normal river; that is, the velocity was nearly constant and was controlled by bed friction rather than changes in tide. For this section, a linear increase of variance is observed, corresponding to a dispersion coefficient of 100 square feet per second. A remarkable agreement is obtained between the two experiments.

Tidal changes introduce new and complex factors. As the tidal effect progresses up the estuary, the velocity at the head of the dye cloud is first affected. The head comes to a halt, while the tail is in a section of river still running downstream. The result is a sharp decrease in variance, and a steepening of the slope of the

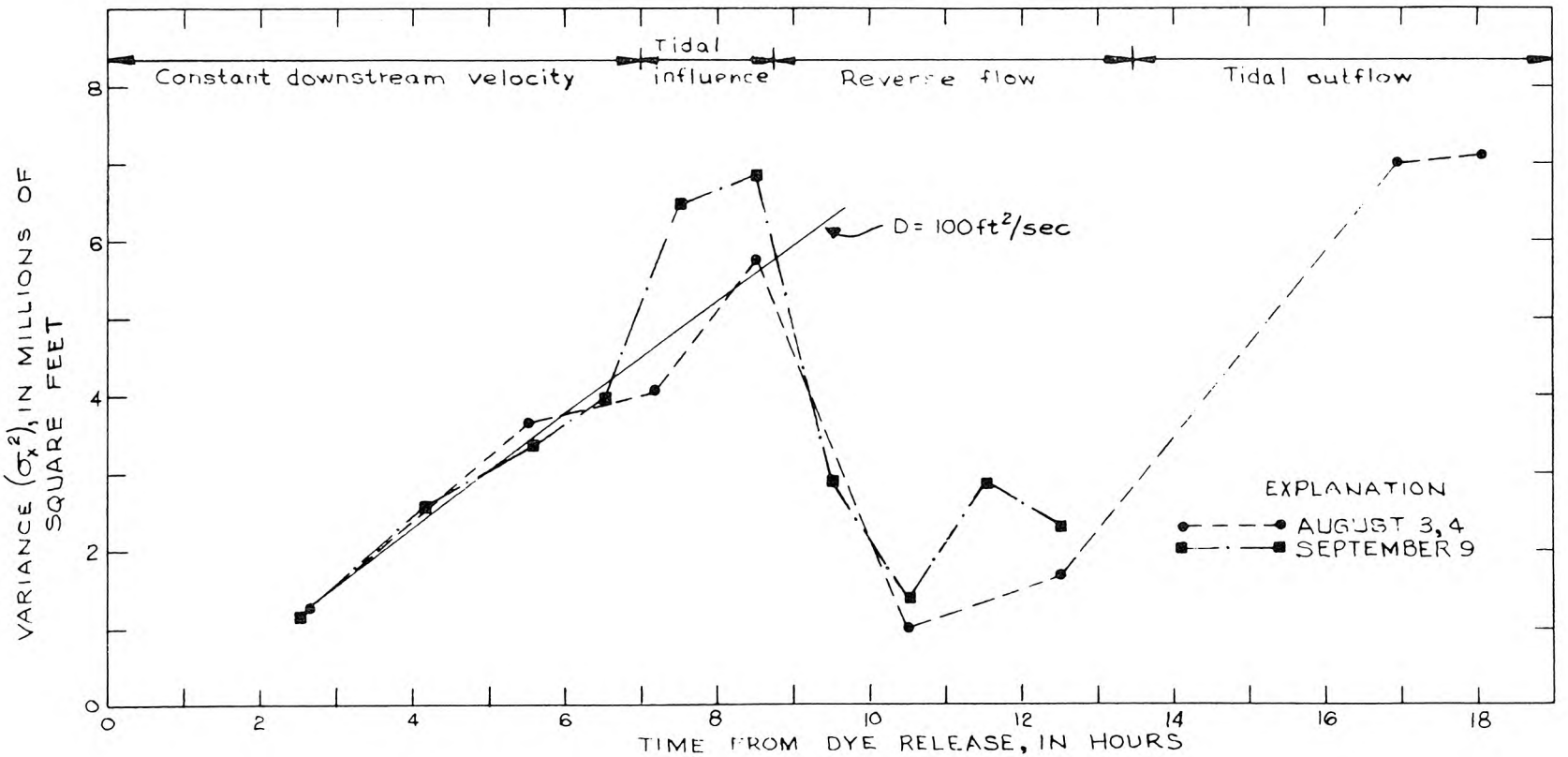

Figure 58. Variance of the dye-concentration distribution, August 3-4 and September 9. Tidal conditions are indicated for that part of the river in which the dye cloud is located.

concentration-distance curve at the head. Further incoming tide causes a stacking phenomenon; all of the dye-containing water, initially spread over several miles of river at low tide, is stacked together into a cloud of greater cross-sectional area but lesser extent. The one-dimensional variance decreases rapidly, although dispersion is still occurring in the sense that dye is constantly diffusing into undyed water.

A complete description of the stacking process during the incoming tide would be extremely difficult. Taylor's analysis may well be correct in the sense that at any local section the transport through a section moving at the mean velocity is proportional to the mean concentration gradient. However, the one-dimensional diffusion equation certainly does not describe the process, because the mean velocity of flow varies along the length of the cloud.

Figures 59 and 60 show application of the routing procedure. For both figures, input is the distribution measured at Renton Junction, and converted to a concentration-distance curve by equation 79. In figure 59, for August 3, the routed curve for 1500 hours is compared to the measured curve at Foster Golf Course Bridge, also converted by equation 79. Both routed curves are adjusted to enclose the same area as the measured curve. The curve for D = 70 ft.^{2}/sec., shifted 285 feet downstream to improve the comparison, is the better fit. In figure 60, for September 9, the input has been routed to 1100 hours, and is compared with the concentration-distance curve derived for that time (the cloud was in the general vicinity of Cherry Street). A dispersion coefficient of 90 ft.^{2}/sec. yields an excellent comparison.

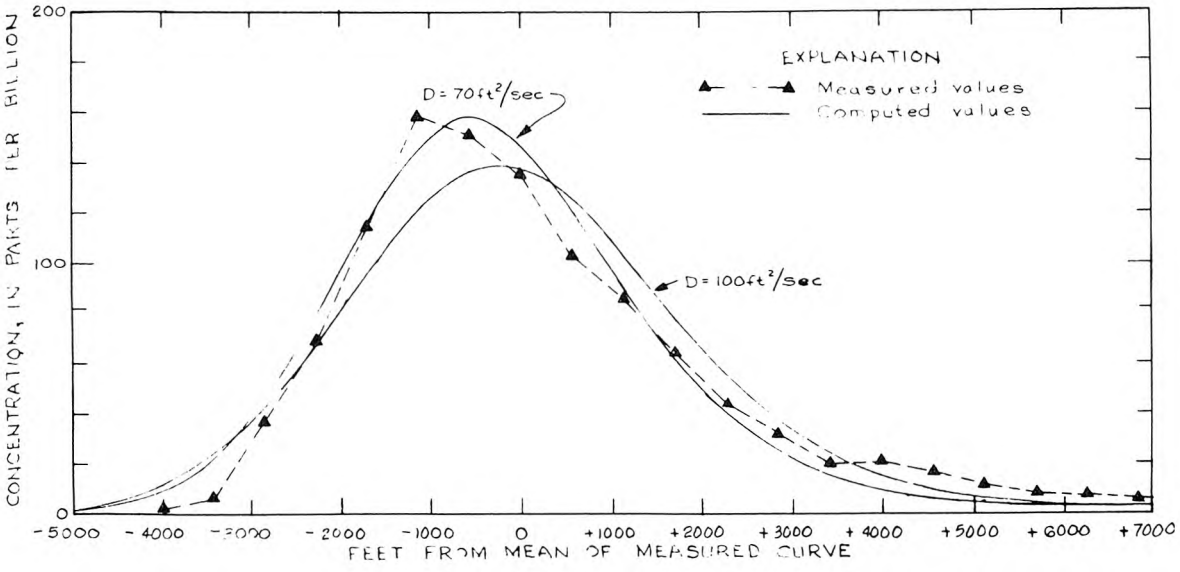

Figure 59. Comparison between calculated concentration-distance curve at 1500 hours, August 3 (curve 1, fig. 57) and prediction for 1500 hours by applying routing procedure to data measured at Renton Junction.

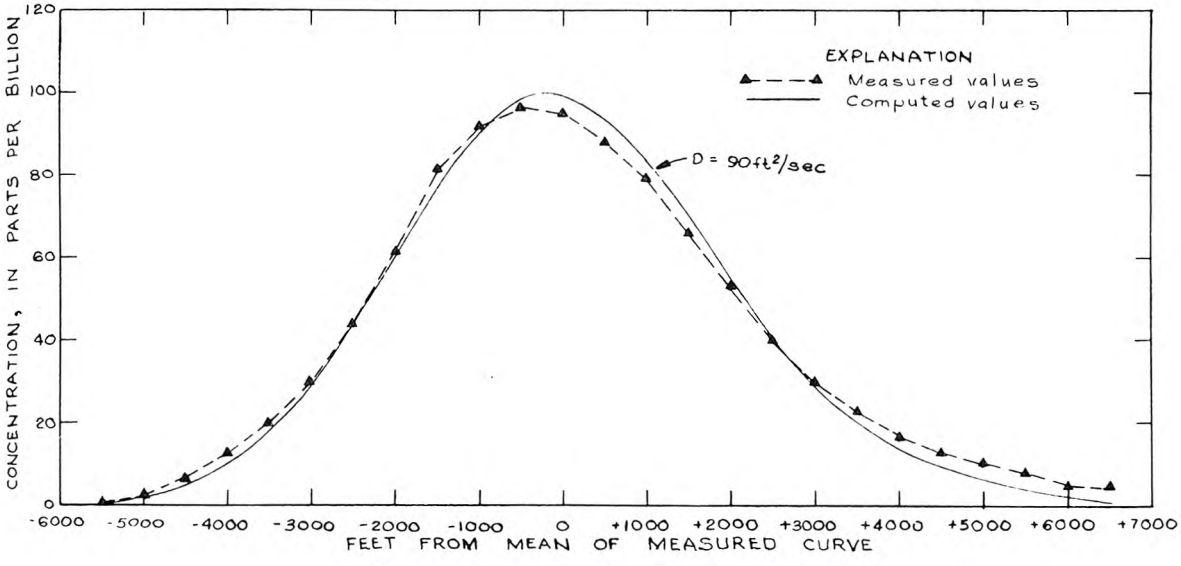

Figure 60. Comparison between calculated concentration-distance curve at 1100 hours, September 9, and prediction for 1100 hours by applying routing procedure to data measured at Renton Junction.

The two figures yield a confident conclusion that the dispersion coefficient for this reach in this flow lies between 70 and 90 ft.^{2}/sec.

VI-F Measurement of Lateral Concentration Variation

The previous section has described two experiments designed to measure longitudinal dispersion in the Green-Duwamish river by observing the passage of a dye cloud at as many stations as possible along the river. In the experiment described in this section only two longitudinal stations were sampled; at these stations concentration and velocity were measured at as many points as possible on each cross section. The purpose was to obtain cross-sectional velocity and concentration profiles, in order to calculate a dispersion coefficient by the diffusive transport method (section IV-B), and to compare measured concentration profiles with those predicted by the application of Taylor's analysis (section III-E).

At 1000 hours on August 31, when river inflow and tidal conditions were nearly identical to those of the study on August 3, two gallons of Rhodamine B dye was injected from the Orillia Bridge. Dye concentration was measured at eight lateral stations at the Renton Junction Bridge and seven at the Foster Golf Course Bridge. Two complete velocity cross sections were measured at each station during passage of the cloud. Conditions at the Foster Golf Course seemed to be atypical of the reach, because the cross section is unusually wide and shallow and the upstream alignment seemed to disturb the velocity distribution; hence the theory was applied only to the cross section at Renton Junction.

Figure 61 shows the cross section at Renton Junction. Lateral stations are from the right end of the bridge. The two velocity measurements at each point, taken approximately one hour apart, were averaged to obtain the isovels; no consistent variation between the two sets of measurements was noted. Concentration samples were taken at ten minute intervals at stations 65, 75, 85, 95, 105, 115, 125, and 135. The three-man crew began at stations 85, 115, and 125, and progressed outward, generally completing the sampling sequence in approximately 2 minutes.

The concentrations measured at each lateral position are shown in figure 62. The pattern already observed visually is quite apparent; concentration rises in the high-velocity part of the stream considerably sooner than near the banks. Conversely, after passage of the peak, concentration near the banks exceeds that in the center. For instance, at 1215 hours the center concentration had reached 110 parts per billion while the banks were at 40, while at 1300 hours the right bank was at 60 and the center at 25.

An "instantaneous" dispersion coefficient can be calculated for any time during passage of the cloud, by calculating the mass transport through a section moving at the mean velocity and the mean concentration gradient, and applying equation 10. To obtain mass transport, the cross section was divided into eight sub-areas by vertical lines midway between the concentration measuring points. Average relative velocities were assigned to each sub-area by counting squares of graph paper on the cross-sectional drawing. Equations 86 and 87 were then applied to determine the mass transport and dispersion coefficient. The

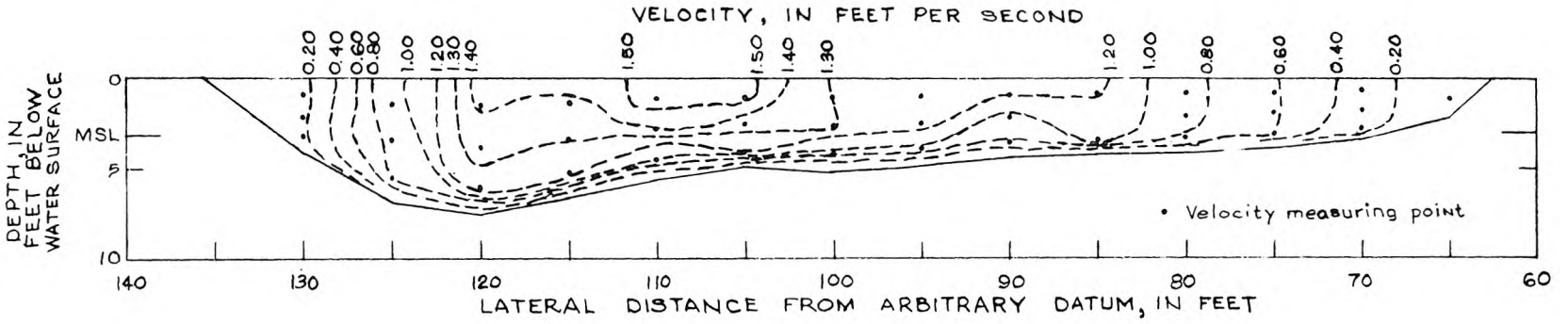

Figure 61. Cross section looking downstream at Renton Junction, showing isovels interpolated from measurements at the indicated points, 1230 hours, August 31.

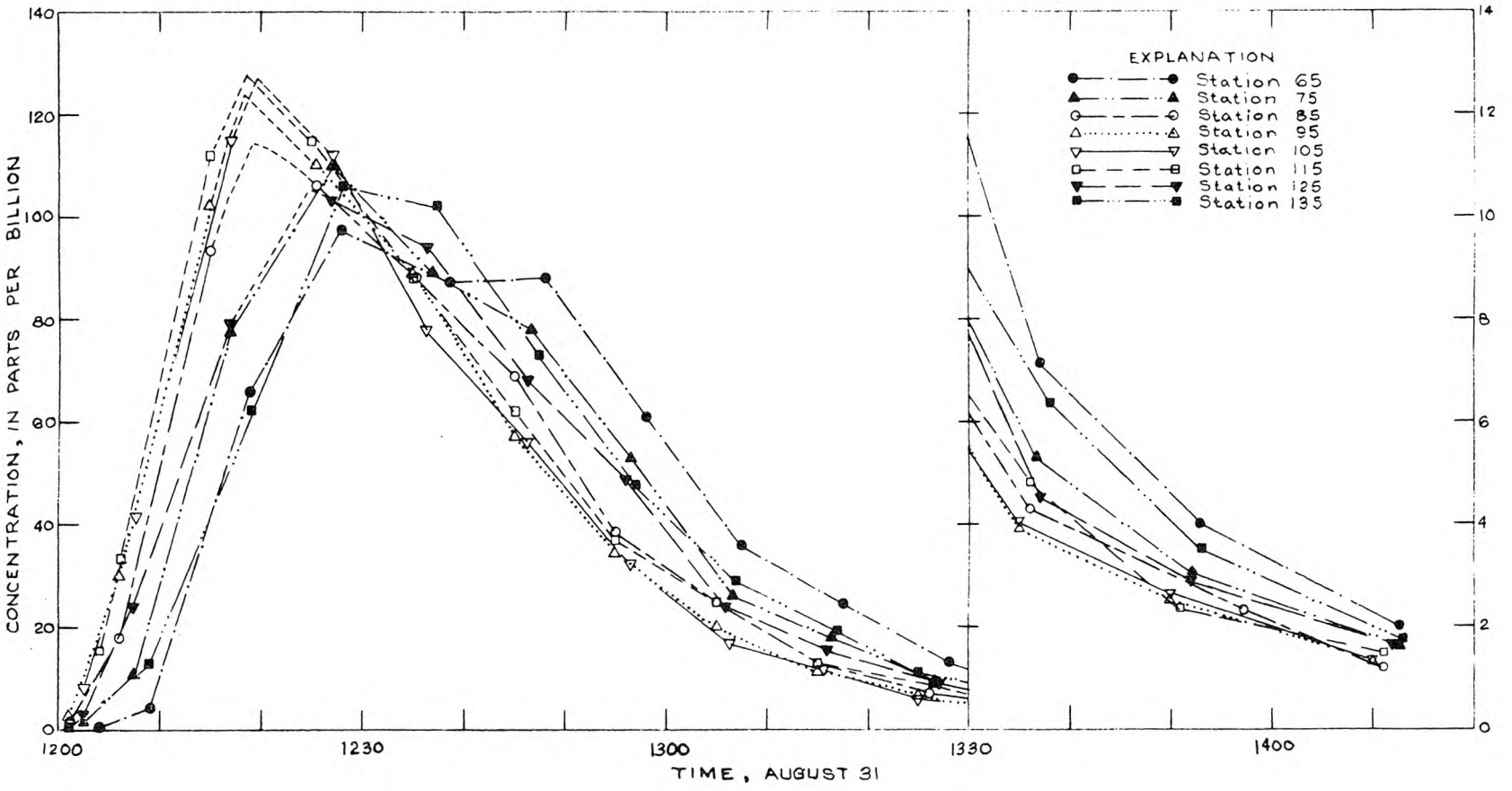

Figure 62. Dye concentration at eight lateral stations at Renton Junction, August 31.

concentration gradient, mass transport, and resulting dispersion coefficient throughout the passage of the cloud are shown in figure 63. Changes in mass transport seem to lag behind changes in mean concentration gradient; in fact, just after passage of the peak both concentration gradient and mass transport are downstream, implying a negative dispersion coefficient. However, once the concentration gradient ceases to vary rapidly, mass transport and concentration gradient maintain a constant ratio through a variation of nearly two log cycles. The ratio gives a dispersion coefficient of approximately 75 ft.^{2}/sec., a good agreement with the 70-90 ft.^{2}/sec. value obtained by the longitudinal dispersion experiments.

VI-G Prediction of the Dispersion Coefficient

A dispersion coefficient for the Green-Duwamish river was predicted using the application of Taylor's analysis given in section III-E and the cross-sectional velocities measured at Renton Junction on August 31 (see previous section). The predicted steady-state profile was obtained by integrating equation 54 in steps of 2 1/2 feet, beginning at station 62.5 and continuing to station 135. The lateral mixing coefficient was taken to be $\epsilon_z = 0.23\ d\ U^*$, in which d is the depth at the center of each integration element, and U* is the overall shear velocity for the reach, 0.161 ft./sec. Further integration of the theoretical profile with the velocity distribution (equation 55) gave a dispersion coefficient of 84 ft.^{2}/sec. (78,000 cm.^{2}/sec.). This

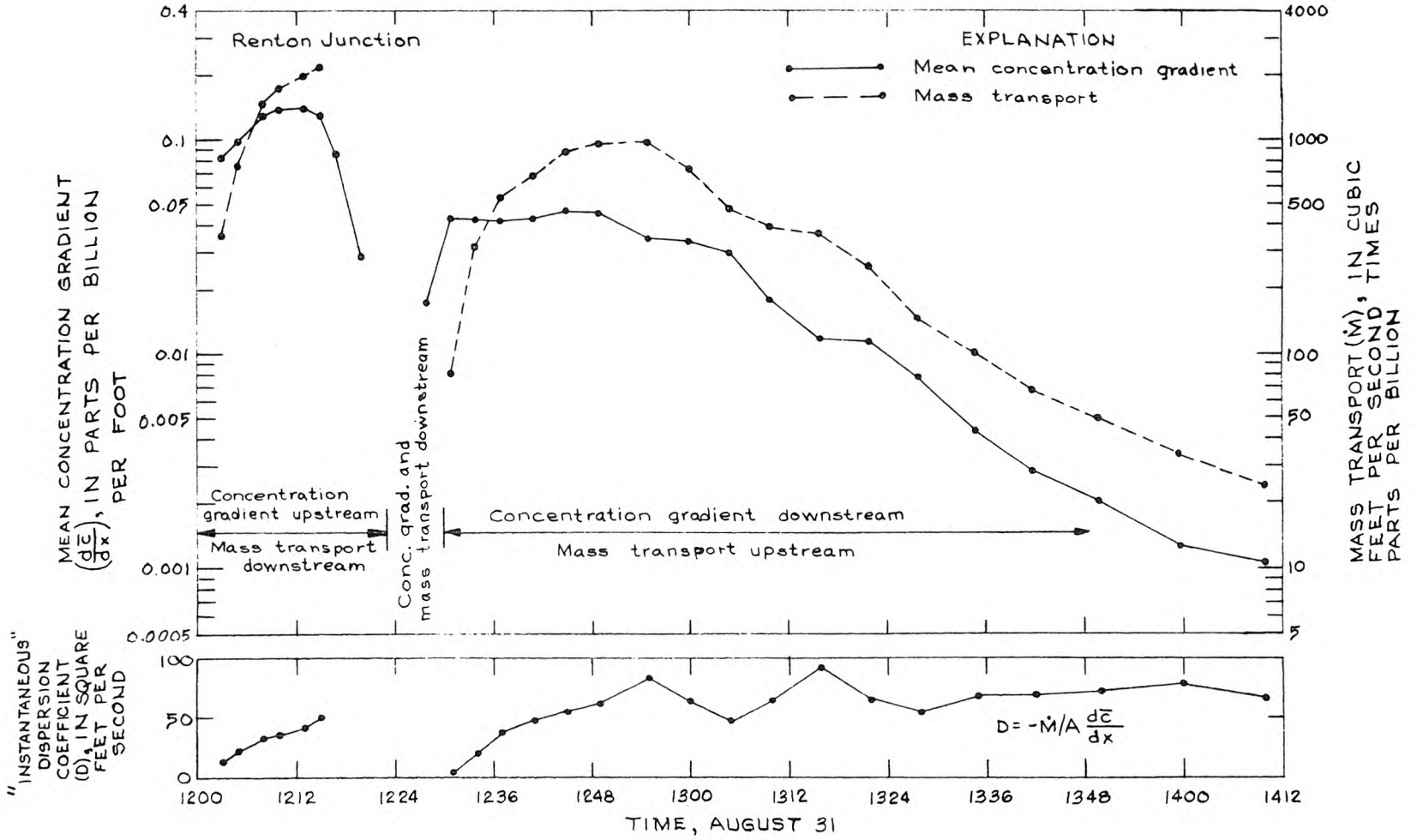

Figure 63. Mean dye-concentration gradient, mass transport through a section moving at the mean velocity, and dispersion coefficient at Renton Junction, August 31.

compares favorably with the coefficients determined from the longitudinal dispersion experiments (August 3 and September 9).

The comparison betweeen predicted steady state profile and actual profiles measured at various times during the passage is shown in figure 64. The agreement in measured points over a wide range of mean concentration gradients is surprisingly good; however, the trend of the points is somewhat different from the theoretical line. This is probably due to a variation in the velocity distribution in the nearby upstream cross sections, rather than to incorrect choice of the lateral mixing coefficient. Reduction of the lateral mixing coefficient would not greatly improve the fit of theory to measured points, but would lower the predicted dispersion coefficient below that which was measured. The conclusion is that the lateral mixing coefficient is reasonably correct, and that the difference between the measured and theoretical lateral profiles stems primarily from the non-uniformity of the river.

VI-H Summary

This chapter has described four dye dispersion experiments in a reach of the Green-Duwamish River, Washington. In two of these the longitudinal growth of the cloud was observed at a number of stations along the river, and the longitudinal dispersion coefficient was established as lying between 70 and 90 ft.^{2}/sec. The third experiment provided aerial photographs which show the shape of lateral concentration variations within the dye cloud. The fourth experiment

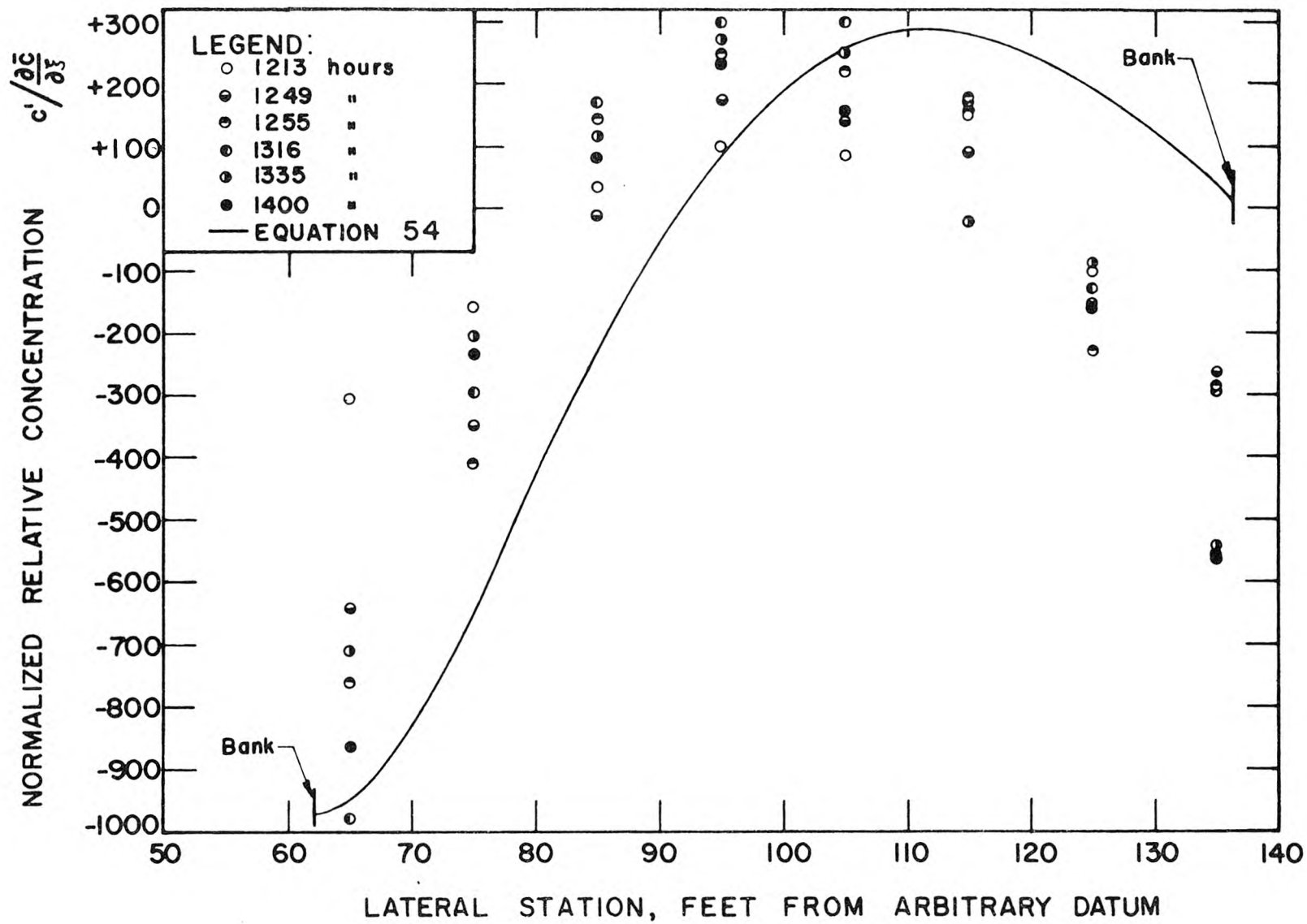

Figure 64. Predicted lateral steady-state profile (equation 54) and measured profiles at various times at Renton Junction, August 31.

measured detailed lateral velocity and concentration variations. The concentration variation predicted by Taylor's analysis was in good agreement with measured values.

The measurements presented in this chapter show that lateral variations in convective velocity were, as hypothesized, the dominant mechanism for dispersion in the study stream. Application of Taylor's analysis, using only lateral velocity variations, gave a dispersion coefficient of 84 ft.^{2}/sec., within the range of experimental measurements. While future experiments in other natural streams will probably not yield such exact agreement, it is believed that in nearly all natural streams dispersion is accomplished almost entirely by lateral variation in the downstream velocity.

CHAPTER VII

NUMERICAL EXPERIMENTS

This chapter describes application of the numerical analysis developed in section III-H. The numerical analysis is useful because it gives the concentration distribution at any time following the introduction of a point or plane source, in both the convective and diffusive periods. In the diffusive period, the analysis gives a dispersion coefficient nearly identical to that obtained by application of Taylor's analysis.

The numerical analysis was applied first to an ideal two-dimensional flow, so that the results could be compared to those by Elder's analysis. Two of the three-dimensional laboratory flows, series 2900 and 3100, and the flow in the Green-Duwamish River were also studied. Detailed comparisons of numerical and experimental results are given below; figure 65 shows the numerically determined variance of the concentration distribution as a function of time for each experiment.

VII-A Numerical Study of Two-Dimensional Flow

Elder's two-dimensional flow was studied entirely in dimensionless variables. Simplifying the convective diffusion equation (equation 3) to two dimensions, and inserting the logarithmic velocity profile and resulting mixing coefficient (equations 14 and 22) yields:

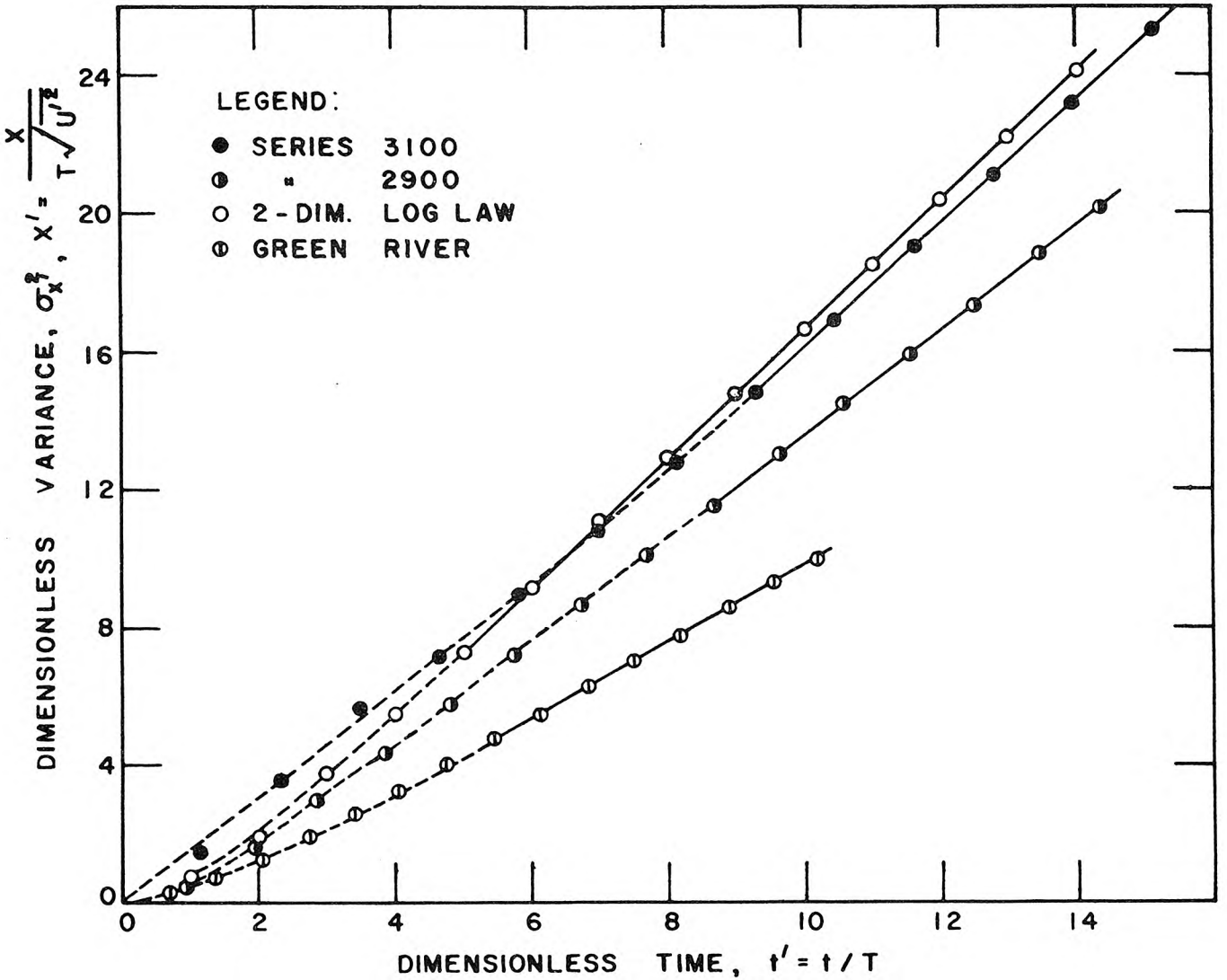

Figure 65. Results of numerical experiments; dimensionless variance vs. dimensionless time.

$$\frac{\partial c}{\partial t} + \frac{U^*}{\kappa}\left(1 + \log_e \frac{y}{d}\right)\frac{\partial c}{\partial \xi} = \frac{\partial}{\partial y}\,\frac{U^*\kappa}{d}\,(d - y)\,y\,\frac{\partial c}{\partial y} \qquad (91)$$

The time and distance scales (equations 42 and 64 with 41) are:

$$T = \frac{0.41}{\kappa}\,\frac{d}{U^*}\,, \qquad (92)$$

and

$$L_2 = \frac{0.41}{\kappa^2}\,d. \qquad (93)$$

Introducing the dimensionless variables,

$$\xi' = \xi/L_2 \qquad (94)$$

$$y' = y/d \qquad (95)$$

and

$$t' = t/T\,. \qquad (96)$$

into equation 91 yields the dimensionless form:

$$\frac{\partial c}{\partial t'} + (1 + \log_e y')\frac{\partial c}{\partial \xi'} = 0.41\,\frac{\partial}{\partial y'}\,y'(1 - y')\frac{\partial c}{\partial y'} \qquad (97)$$

with boundary condition,

$$\frac{\partial c}{\partial y'} = 0 \quad \text{at} \quad y' = 0,\ 1 \qquad (98)$$

Hence all flows satisfying Elder's assumptions will be similar in the dimensionless variables ξ', y', and t'.

The cross section was divided into six stream tubes, separated by planes of $y' = 0.1$, 0.2, 0.4, 0.6, and 0.8. The finer division near the bottom was to obtain accuracy in the region of maximum velocity gradient. The discharge of each tube was obtained by integration of the velocity profile. As initial condition, a plane source was taken; an equal number of concentration units was placed in each computer mesh point, c(300, 1) through c(300, 6). Choice of a time step of 0.05 fixed the distance step at 0.115 and produced a maximum transfer coefficient of 0.219.

Results show that the variance grows linearly for times greater than 5, at a rate which gives a dispersion coefficient (by equation 37),

$$D = 0.39\, d\, U^* / \varkappa^3. \qquad (99)$$

Since Elder's theoretical value is 0.404, the confirmation is very good.

Figure 66 shows that selected concentration profiles in the cross section, at dimensionless times of 5 and 15, match closely the prediction by Elder's analysis (equation 49). Results of the numerical program and the theoretical analysis are in excellent agreement: the numerical analysis appears to be a valid approximation of the physical process, and may be extended with confidence to more complicated flows.

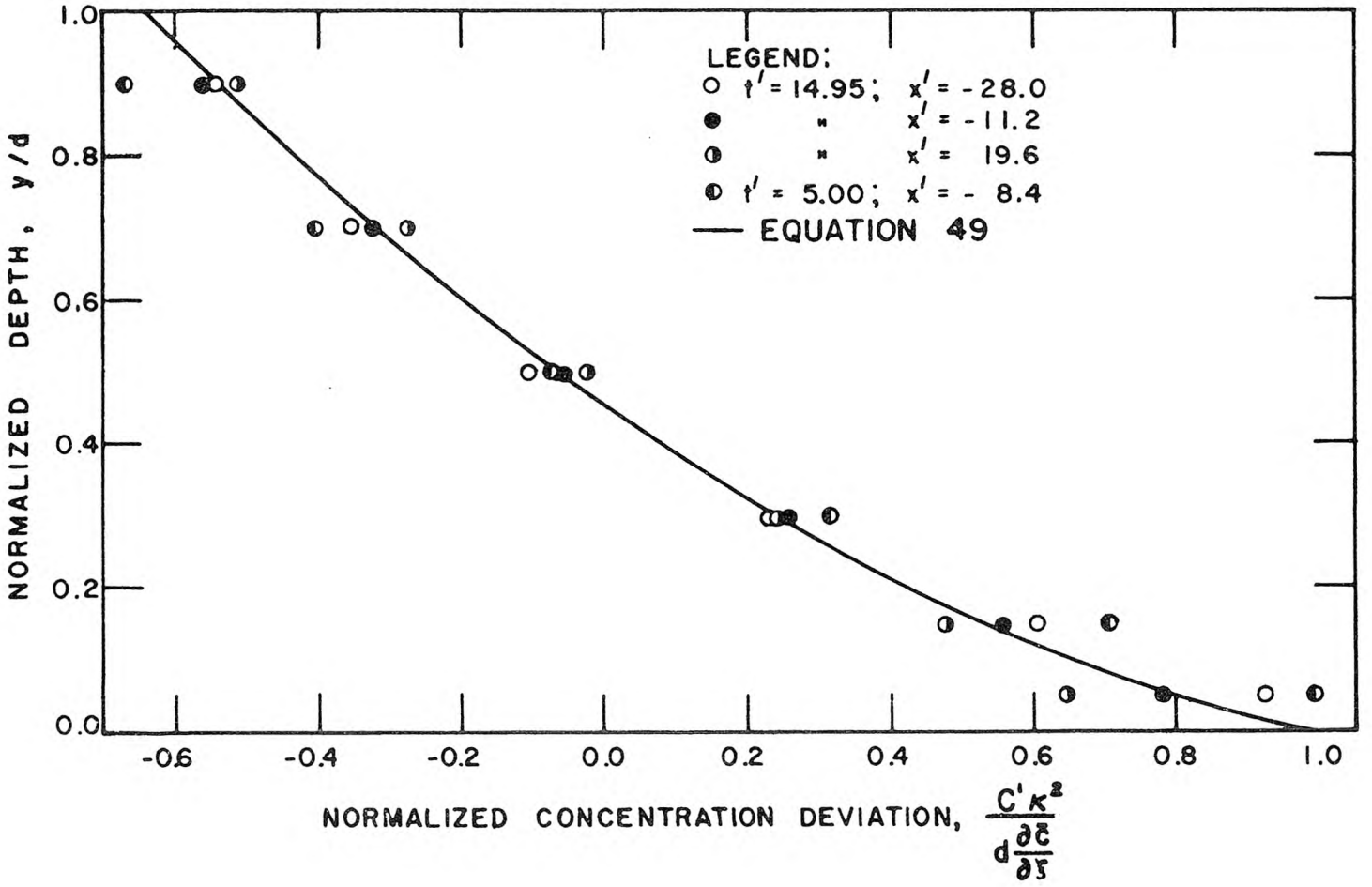

Figure 66. Comparison of numerically obtained concentration profiles with Elder's analysis.

VII-B Numerical Study of the Green-Duwamish River

Numerical study of the Green-Duwamish River was based on the cross sectional measurements of velocity and depth taken at Renton Junction on August 31, 1965. The cross section was divided into eight stream tubes, each centered on a point where samples were taken during the field study. A plane source initial condition was used; as before, equal concentrations were placed in mesh points c(300, 1) through c(300, 8). A constant lateral mixing coefficient was assumed, $\epsilon_z = 0.23\ r\ U^*$. Results show that the variance increased linearly for dimensionless times greater than 5.5 at a rate indicating a dispersion coefficient of 91 ft.^{2}/sec. A comparison between predicted and measured results was obtained by assuming that the time-concentration curve measured at Renton Junction on August 31 could be converted to a distance-concentration curve according to equation 79; figure 67 shows the comparison. Lateral concentration profiles were also compared for two times at Renton Junction; the numerically forecast and measured profiles are shown in figure 68.

VII-C Numerical Study of Laboratory Experiments

Series 2900 was studied using six stream tubes, each corresponding to the area assigned to one probe during the experiment. A constant lateral mixing coefficient, $\epsilon_z = 0.23\ r\ U^*$, was assumed for transfer across each interface except the outermost, where the coefficient was halved to account for the presence of the stone. Figure 65 shows that the variance increased at a linear rate corresponding to a dispersion coefficient of 2670 cm.^{2}/sec. after a dimensionless time

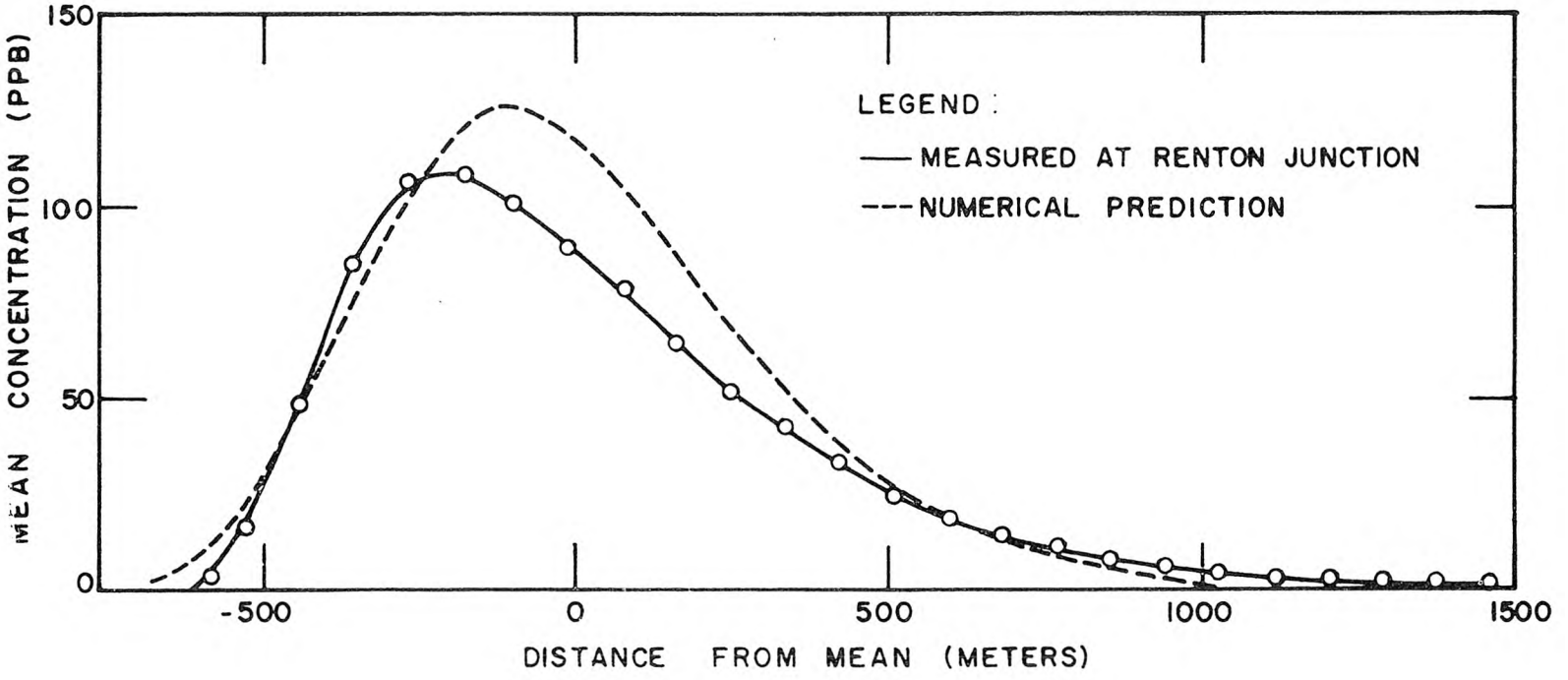

Figure 67. Comparison of numerical prediction and measured concentration distribution at Renton Junction, August 31, 1965. Measured curve converted to a concentration-distance curve by multiplying by the mean velocity (equation 79).

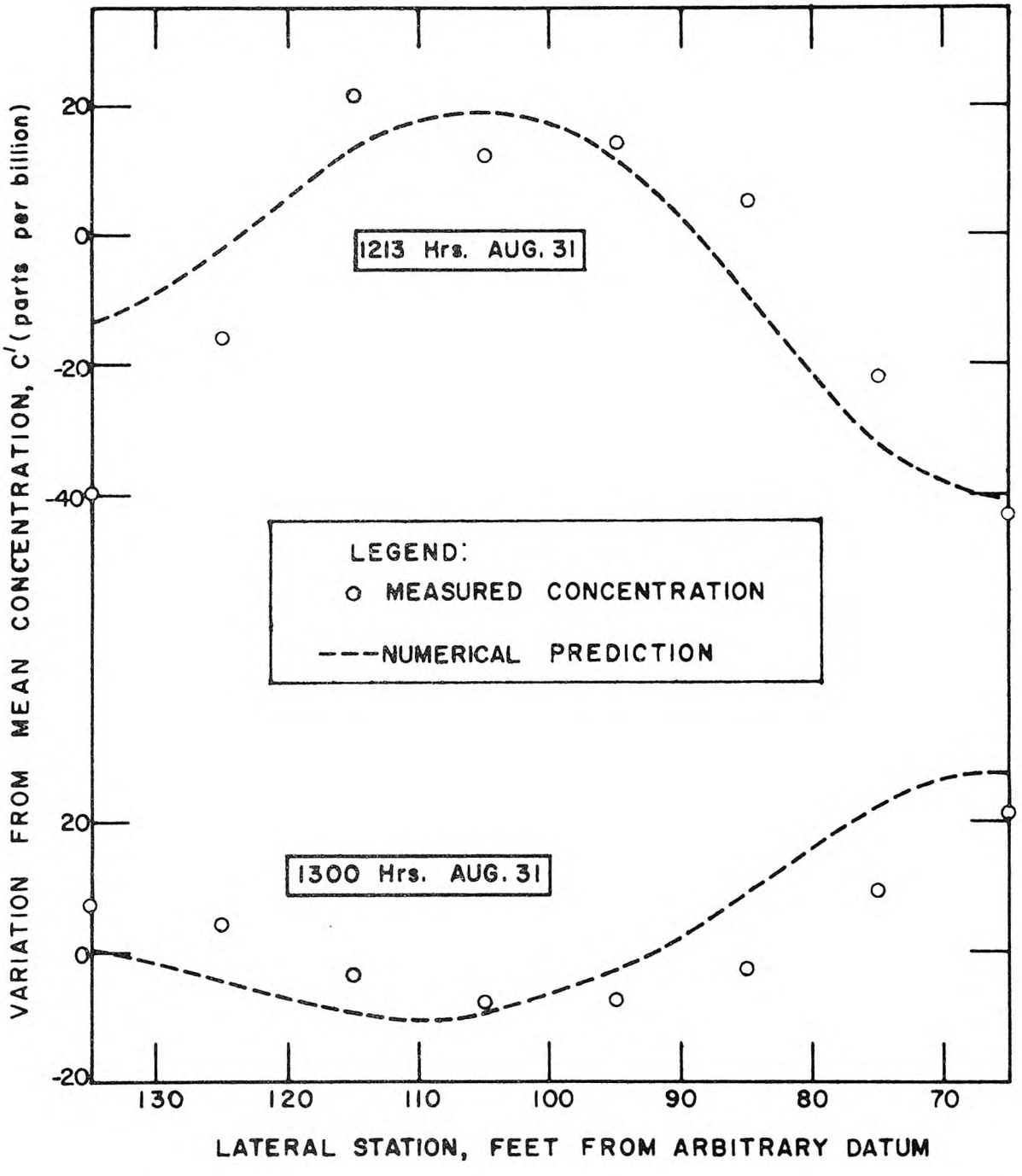

Figure 68. Comparison of numerically predicted and measured lateral concentration profiles at Renton Junction, August 31.

of 8.5. Comparison was made between the numerical output corresponding to a point 26.14 meters downstream from the insertion point and the results of runs 2906-10. To obtain the correct numerical output for the fixed point, the output curve of mean concentration vs. distance was drawn for each time value, and the position of the fixed point with respect to the moving coordinate system was determined from the mean velocity and time from release. The comparison is shown in figure 69.

The same approach was used for Series 3100, except that nine stream tubes were used. Within the stone, depth and area of water were assumed to be 20% of the total (the same assumption used in Chapter V to obtain the steady state profiles; the lateral mixing coefficient was based on local depth and overall shear velocity. This assumption is probably preferable to that used for series 2900, and the results should be more accurate. Figure 65 shows that a linear growth of the variance exists for times greater than 9, at a rate corresponding to a dispersion coefficient of 2570 cm.^{2}/sec. The comparison between numerical and measured outputs for runs 3107-10, obtained as for series 2900, is shown in figure 70.

VII-D Summary

A numerical analysis which simulates the physical process of convective diffusion was verified by application to an ideal two-dimensional flow, for which Taylor's analysis gives an asymptotic theoretical solution. The numerical analysis was then applied to three-

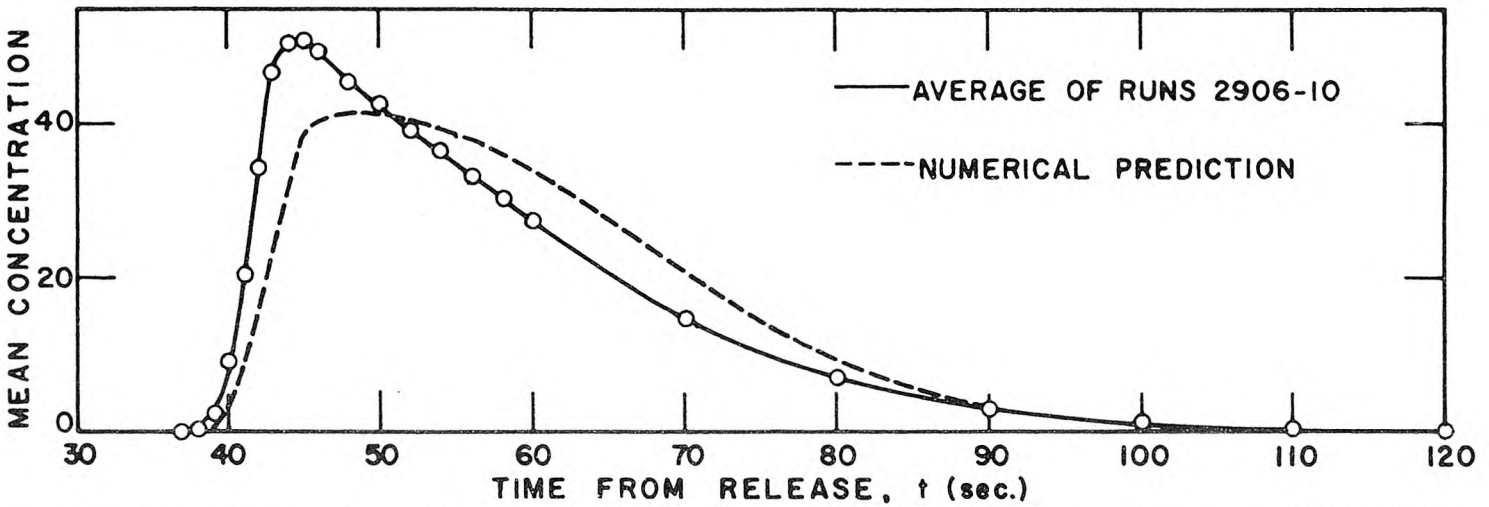

Figure 69. Comparison of numerical prediction with measured results, runs 2906-2910. Conductivity probe and numerical output are 26.14 m. downstream from plane source.

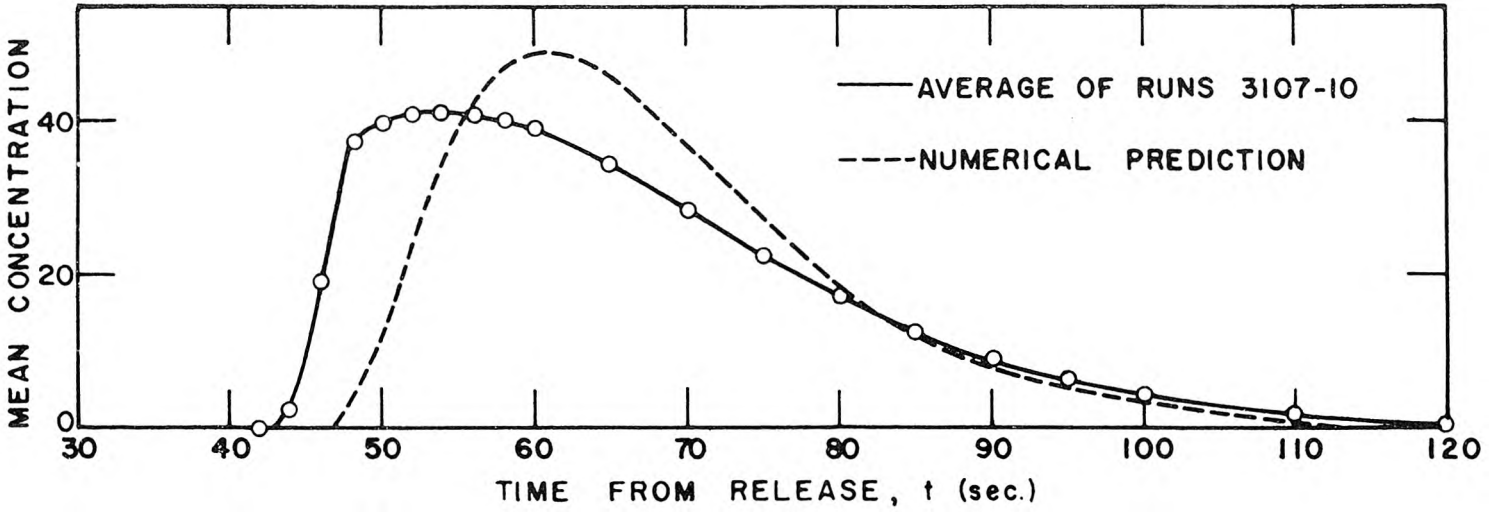

Figure 70. Comparison of numerical prediction with measured results, runs 3107-3110. Conductivity probe and numerical output are 29.45 m. downstream from plane source.

dimensional flows to predict concentration distributions, which were verified by experiment. Table 30 summarizes dispersion coefficients obtained by numerical, analytical, and experimental procedures.

The numerical solution is of value because it predicts the distribution of concentration during the convective period, for which no other solution is available.

Table 30. Comparison of Dispersion Coefficients Obtained by Numerical, Analytical, and Experimental Procedures.

Procedure	Dispersion Coefficient, D (cm.^{2}/sec.)			
	Ideal Two-dimensional Flow	Green-Duwamish River	Series 2900	Series 3100
Numerical Analysis	0.39 dU^*/κ^3	85,000	2670	2570
Application of Taylor's Analysis	0.404 dU^*/κ^3	78,000	2513	2503
Best Experimental Measurement	0.52 - 0.67 dU^*/κ^3	65,000 - 85,000	2530	2500

CHAPTER VIII

DISCUSSION OF RESULTS

VIII-A Range of Dimensionless Dispersion Coefficients

A strict comparison of present and previous experiments and theory can be made only for the two-dimensional studies. The runs over sand dune beds (tables 12 through 15) gave dispersion coefficients which, based on depth and bed shear velocity, are in good agreement with Elder's formula (equation 17). Other runs gave coefficients generally exceeding the formula, even after accounting for the effect of the variable von Karman constants; possible explanations are discussed below (section C).

Taylor's and Elder's results have caused many workers to believe that all dispersion coefficients might be correlated on the basis of r U*; that they can not, as shown in Table 1, was a primary motivation for this study. Previous laboratory results have given values of D/rU* ranging from 6.8 to 25; field results ranged from 13 to 650. In Table 31 the present results are arranged along with the previous results given in Table 1; laboratory values of D/rU* range from 8.7 to 640. This indicates that the effects which produce large coefficients in natural streams have probably been successfully modeled in the laboratory.

Table 31. Comparison of present and previous dimensionless dispersion coefficients. (Results of previous experiments are indented.)

Source	D/rU*
Elder: flume experiment	6.8
Series 0200 (rect. channel, sand-dune bottom)	8.7
Series 0300 (rect. channel, sand-dune bottom)	10.5
Series 1200 (rect. channel, smooth bottom)	11.5
Series 0400 (rect. channel, sand-dune bottom)	12.0
Series 1500 (rect. channel, smooth bottom)	12.7
Schuster: (analysis by Sayre): Yuma Mesa Canal	12
Glover: flume with rough bottom	13
Series 2700 (rect. channel, smooth bottom)	14.0
Series 2600 (rect. channel, smooth bottom)	14.1
Series 1400 (rect. channel, smooth bottom)	16.4
Series 1300 (rect. channel, smooth bottom)	17.6
Glover: triangular flume	18
Series 2400 (rect. channel, stone bottom)	18.5
Series 0100 (rect. channel, sand-dune bottom)	19.0
Series 2300 (rect. channel, stone bottom)	21.4
Series 2500 (rect. channel, stone bottom)	21.4
Glover: flume with smooth bottom	24
Thomas: Chicago ship canal	24.9
Series 1600 (rect. channel, side constrictions)	30
Series 3300 (trap. channel, smooth sides)	39
Godfrey and Frederick: Clinch River	50.5
Godfrey and Frederick: Clinch River	57.5
Sacramento River	77
Godfrey and Frederick: Clinch River	109
Owens, Edwards and Gibbs: River Derwent	131
Green-Duwamish River	160
Series 2900 (trap. channel, stone sides)	190
Series 2800 (trap. channel, stone sides)	210
Godfrey and Frederick: Copper Creek	216
Series 3100 (trap. channel, stone sides)	250
Godfrey and Frederick: Coachella Canal	278
Series 3400 (trap. channel, stone sides)	330
Godfrey and Frederick: Copper Creek	355
Godfrey and Frederick: Copper Creek	408
Series 3000 (trap. channel, stone sides)	410
Godfrey and Frederick: Copper Creek	477
Glover: South Platte River	510
Godfrey and Frederick: Clinch River	535
Series 3200 (trap. channel, stone sides)	640
Godfrey and Frederick: Powell River	654

VIII-B Significance of the Time Scale

In Chapter III the question was raised regarding how much time must elapse before the spread of a tracer cloud can be described by the Taylor diffusion theory. It was suggested that the required period might depend on a time scale based on bulk hydraulic parameters; experiments were to determine the duration of the dimensionless period. Dimensionless time is defined as

$$t' = t/T \ , \tag{62}$$

in which

$$T = \frac{0.404}{\kappa} \frac{d}{U*} \tag{42}$$

for two-dimensional flows, or

$$T = 0.30 \frac{\ell^2}{r\, U*} , \tag{57}$$

for three-dimensional flows in which dispersion is caused primarily by lateral velocity variation.

The dimensionless time span of each of the experiments is listed in Table 32 (for series 1200 through 1500 a line insertion is assumed at station -2.0).

Table 32. Dimensionless Time Span of Experiments.

Series		Span of dimensionless mean time of passage, $\bar{t}'$
Two-dimensional experiments:		
1200	Smooth Bed	8.2 - 15.8
1300	" "	4.0 - 7.0
1400	" "	2.6 - 4.7
1500	" "	4.3 - 13.9
2300	Rough Bed	3.9 - 14.0
2400	" "	10.1 - 28.8
2500	" "	6.8 - 13.6
2600	Smooth Bed	4.1 - 17.3
2700	" "	4.6 - 8.3
Three-dimensional experiments:		
2800		3.0 - 5.0
2900		3.4 - 5.5
3000		3.8 - 5.1
3100		4.6 - 8.1
3200		3.1 - 5.3
3400		8.4 - 16.9
Green-Duwamish River		8.6 - 25.0

If the tracer cloud is following the Taylor diffusion theory, three conditions should be satisfied: (a) the concentration distribution over any cross section should approach the steady-state profile $c'(y, z)/\frac{\partial \bar{c}}{\partial \xi}$; (b) the growth rate of the variance should become linear; and (c) the concentration distribution should decay according to the diffusion equation (equation 5). All three tests can be applied to experimental data, to determine when the Taylor period begins. In practice, all should apply at approximately the same time, and exact satisfaction of each is not required.

Test (a) is the most difficult to apply, as at any given time the degree to which the steady-state profile has been reached varies from cross section to cross section within the cloud. In the moving coordinate system, those cross sections at which the mean concentration gradient changes most slowly, particularly those near the extremities, will approach steady-state long before those experiencing a rapid change of $\frac{\partial \bar{c}}{\partial \xi}$. This is because, as discussed in Chapter III, the steady-state profile changes with changing $\frac{\partial \bar{c}}{\partial \xi}$. Figures 20 and 29 show that for dimensionless times in the vicinity of 7.5 to 10 the approach to steady-state is reasonably complete over a large number of cross sections. The inverted behavior near the bed in figure 20 cannot be explained, although it is consistent for the two series. However, for all experiments it was always possible to find concentration distributions in the cross section which did not approach steady-state; in particular, the steady-state solution requires a uniform distribution at the section where the peak is located; this never occurred. Thus Taylor's theory is never perfectly satisfied for dimensionless times up to 28.8, the maximum value achieved in the laboratory or the field; however, the steady-state profile is established throughout most of the cloud for t' greater than about 10.

Although the laboratory and field experiments were not sufficiently detailed to establish exactly when test (b) is satisfied, the numerical solutions to the complete convective diffusion equation (Chapter VII) do give an indication. The very good agreement between numerically predicted and measured concentration profiles and distributions gives confidence that the numerical variances of the longitudinal

distribution are accurate. Figure 65 shows an exactly linear growth of variance for times greater than the following:

Two-dimensional flow	5.0
Series 2900	8.5
Series 3100	9.0
Green-Duwamish River	5.5

In addition, all curves are very nearly linear for dimensionless times greater than 3.0.

Since all experimental measurements are of concentration vs. time, test (c) cannot be applied exactly. However, the pattern shown in Chapter IV can be compared to the various figures showing experimental and routed results to give a good idea whether the routing procedure is or is not correctly following the measurements. For all of the two-dimensional series, series 3100, 3300, and 3400, and the Green-Duwamish River, the routing procedure adequately follows the measurements. For these series the minimum first measurement and routed measurement times are 4.6 and 8.1. For series 2800, 2900, 3000, and 3200, the routing procedure is clearly not valid; for all of these series the span of first and last measurement times is $t' = 3.0$ to 5.5.

It was never intended to provide a definite dividing line between when Taylor's diffusion theory is exactly applicable, and when it is not; an approach to an asymptote cannot be so defined. It was hoped to provide approximate guidelines for when Taylor's theory should or should not be used; in this, the experiments are unanimous. The following table should apply to any reasonable flow situation:

Dimensionless time, t'	Condition
0 - 3	Convective period; Taylor's theory definitely not applicable.
3 - 6	Transition; nearly linear growth of variance, but one-dimensional diffusion equation not applicable.
> 6	Taylor period; one-dimensional diffusion theory applies.

VIII-C Two-Dimensional Experiments

Since all of the experiments in channels with smooth sides, both with rough and smooth bottoms, were at width to depth ratios of six or greater, the two-dimensional analysis should be a good approximation. The most important characteristics and results are given in Table 33 (the earliest runs over sand beds cannot be included since $\varkappa$ was not measured):

Table 33. Results of Two-Dimensional Experiments.

Series	Depth (cm.) d	Bed Shear Velocity (cm./sec.) U_b^*	$\varkappa$	Dimensionless dispersion coefficient $D\varkappa^3/dU_b^*$
1200	4.6	1.51	0.37	0.52
1300	9.05	1.29	0.35	0.62
1400	13.7	1.12	0.35	0.53
1500	6.5	1.03	0.36	0.52
2300	13.9	2.65	0.33	0.56
2400	9.4	3.08	0.34	0.58
2500	18.4	2.59	0.37	0.67
2600	6.9	1.36	0.35	0.52
2700	12.8	1.62	0.39	0.66
			Average	0.58

The resulting dispersion coefficients show a remarkable uniformity, although about 40% higher than the theoretical value of 0.404 (equation 15).

Replacing κ by the averaged measured value, 0.36, gives an average dimensionless dispersion coefficient, $D/d\,U^*_b$, of 12.5. This is 110% higher than the value of 5.93 (equation 2) given by Elder, using $\kappa = 0.41$. However, Elder's result using $\kappa = 0.36$ becomes $D/d\,U^* = 8.7$. Thus the amount by which the measured values exceed the prediction of equation 2 is due approximately half to the lower value of the von Karman constant, and half to other factors explained below.

In series 1200 through 1500, measurements at one point on the cross section were averaged over many runs, with major variation from run to run; in series 2300 through 2700 five or six measurements were obtained on the cross section during each run, reducing the variation between runs and the number of runs required for an adequate sample. Neither method has much advantage, either with respect to effort required or consistency of results obtained. No consistent difference is evident between runs in the 60-foot and 40-meter flumes.

The consistently high values of the dimensionless dispersion coefficient may be explained in two ways: deviations from the assumed logarithmic velocity profile and mixing coefficient; and deviations from strictly two-dimensional flow. Since a large part of the dispersion is caused by the high relative velocities near the bed, small deviations from the logarithmic profile in the lowest tenth of the flow can indeed have a major effect on the dispersion coefficient. Thomas's power law solution, for instance, yields generally higher dispersion coefficients than Elder's, over the range of Reynolds numbers in the experiments (see Appendix II). However, detailed velocity measurements in the lowest tenth are not available, so this factor must be speculative.

A more speculative but interesting conjecture is the existence of secondary flows which may cause deviations from the assumed two-dimensional flow pattern. The existence of secondary flow in straight non-circular channels was first suggested by Prandtl (39), who termed it "secondary current of the second kind", to distinguish from the spiral flow caused by channel bends. Why current of the second kind exists is not entirely clear; however, numerous recent papers have reported measurement of secondary velocities in square, rectangular, and triangular conduits, both in air and water.

The writer is convinced that secondary flows play an important part in dispersion, but unfortunately his evidence is entirely visual. The spiral flows, which seem to be spaced laterally at distances roughly equal to the depth, convect low-momentum bottom water to the surface, and retard the surface velocity at spacings of roughly two depths. Conversely, at the same spacing, there exist concentrated zones of high momentum water; thus the lateral velocity profile consists of alternating high and low velocity zones, with period of two depths. Attempts to locate these zones by detailed velocity traverses proved fruitless, probably because the zones, not controlled by nearby boundaries, are free to move back and forth. A stationary velocity probe would be sometimes in one zone, sometimes in another. Such a behavior was noticed occasionally; a velocity trace would show a significantly high reading for as much as 20 seconds, and then return to its mean.

Visual evidence was obtained by inserting a small cloud of concentrated blue dye. A 16 mm. color movie was made by mounting the camera, facing straight down, on a motorized trolley 8 feet above the water surface. The movie shows only insertions of a point source;many other, non-photographed, observations were made of insertions from the usual trough. Observations of the dye dumped from the trough are superior to those of a point source, since the full effect of lateral variations acts immediately. In all cases a distinguishing feature of the cloud was the formation of fingers of dye, both fore and aft, usually separated (very approximately) by two depths. Occasionally a localized area of very high velocity would be observed; a finger of dye, resembling the appearance of a jet of dyed water issuing into still water, would race ahead of the main cloud as far as two meters, before losing its excess velocity and dissipating laterally into the adjacent flow.

The following observations were noted immediately after insertion of dye into the 40-meter flume on June 9, 1965; the flow was 6.0 ± 0.1 cm. deep moving at a velocity of approximately 0.4 meters/sec.:

> "Insertion of 100 ml. very concentrated dye + 600 ml. water. Initial shock sent out waves in both directions. Formation of streakiness was immediate. Within 4 meters 3 forward streaks had formed. The two on center and left (looking downstream) were well formed - that on right was broad and poorly formed. Separation was approx. 7" on both sides. Approx. 4 downstream tails formed immediately. After 10 m. of flow approx. 5 heads and numerous tails had formed. Separation of heads roughly 7". After 15 m. and thereafter heads still plainly visible, but broader so that the separating fingers of clear water were narrow (and still sharply defined). Within the body of the dye cloud no cross sectional variations can be seen."

The effect of these unsteady variations can hardly be established from such brief observations, but certainly it exists. The whole concept of two-dimensional flow appears to be a chimera; the internal workings are reflected in the bulk dispersion process, so that the resulting average coefficient, $D \cong 0.58\ d\ U^*/\kappa^3$, appears fairly reasonable.

VIII-D Three-Dimensional Experiments

1. Proof of effect of rough sides

Whether or not lateral velocity variations are the dominant mechanism for dispersion in natural channels was tested both by the field experiments and the laboratory experiments with rough sides. A definitive proof is the comparison of Series 3000 and 3300 (Table 34), in which all geometrical factors except the side roughness and resulting velocity distributions were identical. At constant mean velocity, increasing the side roughness increased the shear velocity by a factor of 1.4, and the dispersion coefficient by 14.2. All other evidence of this dissertation aside, comparison of these two series seems to establish the effect of lateral velocity variations beyond question.

Table 34. Comparison of Experiments with Rough and Smooth Sides.

Series	Banks	Depth of Flow (cm.)	Mean Velocity (cm./sec.)	Width of Open Water (cm.)	Dispersion Coefficient ($cm.^2/sec.$)	Dimensionless Dispersion Coefficient $D/r\ U^*$
3000	rough	3.5	45.1	38	4150	410
3300	smooth	3.4	48.3	39	282	39

2. The lateral mixing coefficient

The lateral mixing coefficient, ϵ_z, has previously been studied only in two-dimensional flows. The steady-state profiles obtained during the three-dimensional experiments may be regarded as a study of lateral mixing, if one accepts the Taylor solution as the correct asymptotic behavior. The experiments yielded extremely self-consistent results; the normalized profiles obtained within each series, for values of mean concentration gradient varying over a factor of roughly four, agree within experimental accuracy. A theoretical steady-state profile based on Elder's lateral mixing coefficient, $\epsilon_z = 0.23\ d\ U^*$, is an excellent fit to the results of all series except 3400; for that experiment the line of best fit requires approximately $\epsilon_z = 0.30\ d\ U^*$.

In the laboratory experiments depth varied from 2.1 to 4.7 cm., and shear velocity from 2.02 to 3.88 cm./sec. The field experiment was at an approximate depth of 120 cm. and shear velocity of 4.92 cm./sec. Over that range of independent variables, Elder's laboratory result in a smooth channel,

$$\epsilon_z = 0.23\ dU^* \tag{23}$$

seems to be an adequate description of the lateral mixing coefficient, even in a channel such as that used in these laboratory experiments in which much of the boundary shear is along the sides.

3. Similarity of results

The validity of the time and distance scales derived in Chapter III may be further tested by observing the similarity of experimental results on a dimensionless time and distance basis. To do this, all experimental results must be brought to the same dimensionless time by using the routing procedure. A time, $t' = 6.0$, was selected, for which results of five experiments were available at slightly earlier times. Each result was routed to a concentration-time curve with mean at $t' = 6.0$, and converted to a distance-concentration curve by assuming equation 79. Distance was made dimensionless by the L_2 scale (equation 64), and the resulting curves plotted together. Good similarity is shown in figure 71.

The same procedure applied to the results of the two-dimensional series would probably produce an even better agreement. However, one would not expect curves from the two-dimensional and three-dimensional series to match exactly, as the degree of skew produced in the convective period is different. True similarity between experiments does not exist unless the geometry and distribution of velocity are similar between cross sections, because otherwise the terms in the basic equation for conservation of mass (equation 3) cannot be made similar. However, when the convective periods are similar, figure 71 shows that the time and distance scales defined in Chapter III do reduce the data to nearly a single curve.

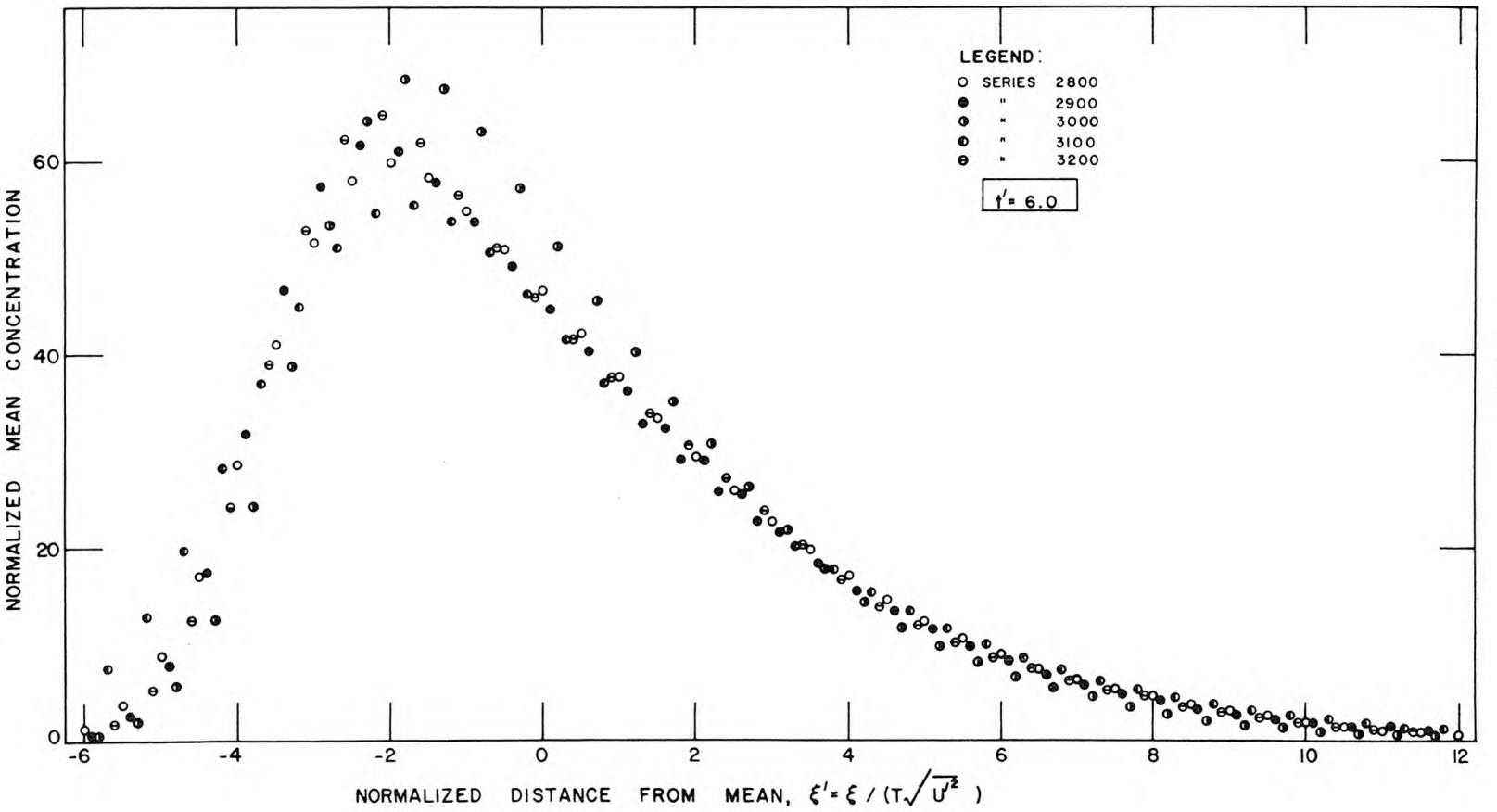

Figure 71. Results of series 2800 through 3200 plotted as concentration vs. dimensionless distance at dimensionless time of t' = 6.0. (Computed approximately from measured time curves.)

4. Prediction of the dispersion coefficient

In Chapter III two methods were given for predicting the dispersion coefficient in a three-dimensional channel without benefit of a dispersion experiment. The first is an application of Taylor's analysis, which predicts the steady-state profile and resultant diffusive transport (equation 55); the second is based on estimating the time scale by bulk channel parameters (equation 57). Measured and predicted dispersion coefficients for each of the three-dimensional series are given in Table 35; the underlined measured value is that which, in the opinion of the investigator, is the most nearly correct.

The table shows that under the experimental conditions, i.e. flows with width to depth ratios greater than six and lateral velocity variations extending an appreciable distance out into the flow, the dispersion coefficient can be predicted reasonably accurately. Application of Taylor's method in the lateral direction (equation 55) yields an accurate coefficient even for series 3300, the flow in the trapezoidal channel with smooth sides in which the lateral velocity differences were not large. Estimation of the time scale, as expected, does not yield such an accurate prediction, but even this easily-applied method is in no case in error by more than 75%.

Table 35. Measured and Predicted Dispersion Coefficients in Three-Dimensional Flows (Field Experiments and Laboratory Experiments in the Trapezoidal Channel).

		Dispersion Coefficient, D (cm.^{2}/sec.)							
		Series							
		2800	2900	3000	3100	3200	3300	3400	Green-Duwamish River
Measured Values	Change of Moment	2220	3170	5590	4080	5650	282	2540	93,000
	Diffusive Transport	1230	2530	4150	2130	4000		1900	70,000
	Best Routing				2500		282	2200	65,000-84,000
Predicted Values	Extension of Taylor method to three-dim. flows (eq. 55)	1307	2513	3711	2503	4496	203	1661	78,000
	Approximation based on estimated time scale (eq. 90)	2150	3580	5930	2820	5930		1920	147,000

Note: Underlined value considered best experimental result.

VIII-E Summary: Experimental Conclusions

The following conclusions may be drawn from the experiments described in Chapters V, VI, and VII.

1. The variety of dimensionless dispersion coefficients observed in natural streams may be explained by variation in downstream convective velocity across the channel. The effect may be modeled successfully in the laboratory.

2. Taylor's analysis may be applied to flow in natural streams or three-dimensional laboratory channels, provided that the width-to-depth ratio is greater than six and that the flow contains appreciable lateral variation in downstream velocity. It is permissible to neglect vertical variation and perform the analysis considering only lateral variation. The formula for the dispersion coefficient is:

$$D = -\frac{1}{A}\int_o^b u'(z)\ d(z)\ dz \int_o^z \frac{1}{\epsilon_z d}\ dz \int_o^z \int_o^{d(z)} u'\ dy\ dz \qquad (55)$$

where the velocity u' and diffusion coefficient ϵ_z are considered as averages over the depth d(z) for each transverse position z.

3. For the lateral mixing coefficient required in equation 55, a satisfactory expression is:

$$\epsilon_z = 0.23\ d\ U^* \qquad (23)$$

4. A satisfactory Langrangian time scale, T, for dispersion in natural streams and three-dimensional laboratory channels can be obtained from the characteristic length for the channel, ℓ (approximately

half the width), the hydraulic radius, r, and the channel shear velocity, U*, by the formula:

$$T = 0.30 \frac{\ell^2}{rU^*} . \tag{57}$$

This scale may be used to predict an approximate dispersion coefficient by the formula,

$$D = \overline{u'^2}\ T , \tag{40}$$

where $\overline{u'^2}$ is the mean square spatial velocity deviation from the cross-sectional mean.

5. On the basis of the time scale given above, time following introduction of a plane source of pollutant into a natural stream may be divided into three dimensionless periods: $t' = t/T = 0$ to 3, convective; $t' = 3$ to 6, transition; $t' > 6$, diffusive. Taylor's theory of one-dimensional dispersion should be applied only in the diffusive period. The concentration distribution in the diffusive period will be originally skewed, because of production of skew in the convective period, but will tend towards a Gaussian distribution with increasing time.

CHAPTER IX

SUMMARY:
DISPERSION IN NATURAL STREAMS

This chapter will summarize what is and what is not known about dispersion in natural streams, what has been contributed by this study, and what requires further research.

IX-A Summary of Prior Knowledge

Prior to the beginning of this study, knowledge of dispersion in natural streams could be summarized as follows. G. I. Taylor had introduced the concept of longitudinal dispersion as a one-dimensional diffusion process, in which the joint effect of convection and diffusion within the cross section of a uniform channel is to give an apparent diffusion in the direction of flow. This he called dispersion, to differentiate from molecular or turbulent diffusion. He limited his analysis specifically to flow in a long, straight pipe, for which he obtained a dispersion coefficient,

$$D = 10.1\, a\, U^* . \qquad (1)$$

Taylor's analysis had been applied to an infinitely wide, two-dimensional open channel by Thomas and Elder; Elder obtained,

$$D = 5.93\, d\, U^* . \qquad (2)$$

Taylor's concept that whatever causes spreading out of a pollutant may be described by the classical diffusion equation, with an apparent diffusion (or dispersion) coefficient, had been accepted in the literature, even for flows in natural streams and estuaries for which it was not specifically derived. However, experiments in these flows had yielded coefficients vastly in excess of the predictions of equations 1 and 2 (see Table 1). Therefore the widespread engineering practice was to assert that a coefficient exists, but to obtain the coefficient by experiment.

A more detailed summary of previous literature has been given in Chapter II.

IX-B Contributions of the Present Study

The major contribution of the present study is to explain why dimensionless dispersion coefficients in natural streams are so much larger than those in two-dimensional laboratory channels, and to give a method of predicting the coefficient in a natural stream.

1. Explanation of large dispersion coefficients

The primary difference between a natural stream and the flows studied by Taylor and Elder is that a natural stream must be described in three dimensions. The concentration in a pipe, assuming a plane source, may be described completely by the radial and downstream position; in an infinitely wide flow, only vertical and downstream position need be specified. In a natural stream, however, even if the

channel is assumed uniform in the downstream direction the local velocity depends on both vertical and horizontal position. Hence the concentration distribution varies in the vertical, horizontal, and streamwise directions. The three-dimensional problem may be formulated in terms of Taylor's analysis, but the added dimension complicates the solution.

In most natural streams, and in any flow which is considerably wider than deep, the presence of lateral (or transverse) variation in the downstream velocity will provide the dominant mechanism for dispersion. This is explained as follows. In natural streams there is considerable variation of velocity between different transverse positions; for instance, there is usually a high velocity zone either in the center or near one bank, and other zones of lower velocity. Since material in the high velocity zone is carried downstream faster than that in the low velocity zone, the effect is a stretching out of the cloud of material. Although inhibited by concurrent crosswise mixing, this convective stretching out is the primary cause of longitudinal dispersion.

The same effect is present at each vertical section; material at the surface is carried downstream faster than material at the bottom. However, lateral convective differences are more important because the separation between the zones of high and low velocity is much greater in the lateral than the vertical direction. Turbulent diffusion within the cross section is always trying to smooth out differences in concentration between high and low velocity zones. In the vertical direction, the distance between zones is small, and turbulent diffusion restricts the possible difference in concentration between top and bottom. In the

lateral direction, however, the distance is large between zones, and much larger differences in concentration can be sustained. This leads to the larger values of the normalized dispersion coefficient D/rU*; in effect the hydraulic radius is no longer the proper characteristic length.

In natural streams, lateral velocity differences are set up primarily by bends and large channel irregularities. A similar flow can be induced in a laboratory flume by artificially adding large roughness to the channel sides. In one set of laboratory experiments, inducing lateral variations by adding side roughness increased the dimensionless dispersion coefficient by a factor of 10 (see Table 34). Experiments conducted in laboratory channels with rough sides produced dimensionless dispersion coefficients, D/rU*, equal to or greater than those recorded in natural streams (see Table 31), proving that the large dimensionless coefficients are not simply a scale effect. In a natural stream, the pattern produced by lateral velocity variation was clearly shown by aerial photographs of a dispersing dye cloud (figures 50, 51, and 52).

2. Prediction of the dispersion coefficient by extension of Taylor's method

Since the dominant mechanism for dispersion in a natural stream is lateral velocity variations, it is possible to neglect vertical variation altogether, and apply Taylor's analysis across the channel rather than over the depth. This procedure is described in section III-E; in effect, prediction of the dispersion coefficient becomes no more difficult than that for the pipe or infinitely wide flow already obtained. One

need only measure downstream velocity, u, as a function of cross-sectional position; then the values over the vertical section at each lateral point are averaged to obtain u(z), and u'(z), the deviation of u(z) from the overall channel average. Finally, one must estimate the lateral mixing coefficient, ϵ_z. Then, making the same assumptions as Taylor did, the dispersion coefficient may be obtained by integration as:

$$D = -\frac{1}{A}\int_o^b u'(z)\ d(z)\ dz \int_o^z \frac{1}{\epsilon_z \bar{d}}\ dz \int_o^z \int_o^{d(z)} u'\ dy\ dz \qquad (55)$$

Although performing this triple integration by hand is tedious, programming for the high-speed computer yields a simple procedure.

An estimate for the lateral mixing coefficient, ϵ_z, which has been found in experiments presented herein to be adequate, is,

$$\epsilon_z = 0.23\ d\ U^* \qquad (23)$$

in which d is the local depth, d(z), and U* is the overall shear velocity.

The big advantage of equation 55 is that a good approximate value of D can be obtained from simple velocity measurements in the field, without recourse to costly dye tracer studies requiring field parties of from 5 to 30 or more men.

3. Prediction of the dispersion coefficient by the time scale

A second method of predicting the dispersion coefficient for a natural channel is more approximate, but more easily applied, than

equation 55. Applying the result of Taylor's analysis of diffusion by continuous movements, it has been shown in section III-B that

$$D = \overline{u'^2}\ T \tag{40}$$

in which u' is the spatial variation of u from the cross-sectional mean, and T is the Lagrangian time scale.

Although one should not expect to be able to correlate the Lagrangian time scale exactly with any set of bulk channel parameters, an adequate expression has been found to be,

$$T = 0.30\ \frac{\ell^2}{rU*} \tag{57}$$

in which ℓ is the characteristic length of the channel, defined approximately as the distance on the surface from the point of maximum velocity to the most distant bank (i.e., for a symmetric channel, the half width). Equation 57 was derived analytically in section III-F, and verified by the experiments.

Thus, to estimate D by this second method one must first measure the hydraulic radius r, energy slope S_e, characteristic length ℓ, and mean square velocity deviation $\overline{u'^2}$ in the field (all but the energy slope may be obtained from a cross-sectional drawing showing measured isovels). Then D is calculated from:

$$D = 0.30\ \frac{\overline{u'^2}\ \ell^2}{r\sqrt{grS_e}} \tag{100}$$

This equation cannot be expected to be exact, because the detailed channel geometry and distribution of roughness elements are not included in the formulation. However, normalizing D as before one obtains:

$$\frac{D}{rU^*} = 0.30 \frac{\overline{u'^2}}{U^{*2}} \frac{\ell^2}{r^2} \qquad (101)$$

Thus the dimensionless dispersion coefficient D/rU^* is seen to become very large for a wide three-dimensional stream because the factor ℓ^2/r^2 becomes very large.

4. Limitation of the dispersion analysis to long time

A secondary contribution of this study is to explain why observed concentration distributions in natural streams are generally skewed, and to caution against using Taylor's one-dimensional diffusion equation to describe the spread of concentration immediately following introduction of a concentrated pollutant source. The skewed distribution arises by convective action immediately after introduction of the source, as explained in Section III-A and shown in figures 1, 2, and 3. Taylor's one-dimensional diffusion equation results in reality from an asymptotic analysis, and does not describe the spread of a source until after elapse of a period whose duration was found by experiment and numerical analysis to be approximately six dimensionless time units. Dimensionless time is defined as $t' = t/T$, where T is the Lagrangian time scale, for which an expression has been given above.

5. Prediction of the dispersion pattern by numerical analysis

The entire concentration pattern at any time after introduction of an instantaneous point or plane source may be calculated by a numerical procedure. Use of the procedure requires the same information as does prediction of the dispersion coefficient by the extension of Taylor's analysis (eq. 55), i.e. the distribution of velocity within a cross section and the lateral mixing coefficient. The numerical procedure is of value because it gives an analytical description of the concentration distribution at times within the convective period. The convective and transitional periods cover approximately the first six dimensionless time units following introduction of the source. The length of this period may be estimated in real time by equation 57; for instance, in a river one mile wide and 25 feet deep, whose shear velocity is 0.1 ft. per sec., the convective period extends through the first 1200 hours, and the numerical analysis is of obvious value. On the other hand, in a small river such as the Green-Duwamish in Washington, Taylor's analysis becomes applicable after approximately 100 minutes, and for greater times the numerical analysis need not be used.

6. Methodology for calculating a dispersion coefficient from observations

A final contribution of this study is to formulate methodology for calculating a dispersion coefficient from measured data. The change of moment method,

$$D = \frac{1}{2} \frac{\partial}{\partial t} \sigma_\xi^2 \qquad (37)$$

in which σ_ξ^2 is the variance of the one-dimensional concentration-distance curve, has been well established for use when concentration-vs.-distance curves are available. However, most experiments measure curves of concentration-vs.-time. In this study it is shown analytically (section IV-B and Appendix I) that in the diffusive period equation 37 may be modified to read,

$$D = \frac{1}{2} \bar{u}^2 \frac{\sigma_{t_2}^2 - \sigma_{t_1}^2}{\bar{t}_2 - \bar{t}_1} \tag{75}$$

in which σ_t^2 is the variance of a concentration-time curve obtained at a fixed point, and $\bar{t}$ is the mean time of passage. This result applies for any finite mass of tracer, and does not presume any particular distribution of tracer in the cloud.

Studies in natural streams always produce time-concentration curves with extremely long, low-concentration tails. Obtaining the variance of such a curve is difficult, because most of the contribution comes from the tail. Hence the dispersion coefficient obtained by equation 75 should always be checked by a routing procedure, described in section IV-B, in which the one-dimensional diffusion equation is assumed and the curve obtained at an upstream station is routed to compare with that at a downstream station. This procedure yields a confident check on the magnitude of whatever coefficient is obtained by any other method, and should always be employed with stream data.

A third method for obtaining the dispersion coefficient, which is based on measuring the diffusive transport across a cross section moving at the mean flow velocity, is presented in section IV-C. This

method can be extremely accurate under uniform flow conditions if sufficient numbers of conductivity probes are available for placement on one cross section. However, it is not generally recommended for use in streams.

IX-C Requirements for Future Research

Throughout this study natural streams have been treated as exactly uniform, so that the data from one cross section would apply to all cross sections. The assumption is obviously fallacious, but seems to yield adequate results. The reason appears to be that in most streams, or at least in the one investigated, it is possible to identify a characteristic cross section which, while not identical to any others, has a typical depth, width, and distribution of velocity. Since the tracer in moving down the stream averages the effects of all cross sections, the data from one typical section seem to suffice. However, further study of the effects of non-uniformity in the channel is clearly warranted.

This study has largely bypassed investigation of the nature of the turbulent mixing tensor. Elder's measured lateral coefficient has been found adequate for this study, and used. However, it has been necessary to divide flows into two classes: those in which vertical variations predominate, a limited class of very wide flows with hardly any lateral variations; and those in which lateral variations predominate, a class which includes most natural streams. Before a flow can be studied in which both horizontal and vertical variations play a significant

role, it will be necessary to have more information on the detailed nature of the turbulent mixing tensor.

Even for the study of flows in which lateral variations clearly predominate, knowledge of the magnitude of the lateral mixing coefficient is at present barely adequate. The lateral mixing coefficient used in this study was obtained by Elder by observing lateral diffusion of dye drops in flow 1 cm. deep down a smooth flume. The result has been found adequate in these experiments, but there is no assurance that it will be correct in other streams or types of laboratory flow. Probably the most important requirement for future study is identification of the factors which control the rate of lateral mixing.

Finally, perhaps the most interesting question is how the present work may be extended to other flow situations, such as the oscillating, often stratified flow in estuaries. Although diffusion in estuaries has received much attention in the past, a more fundamental understanding of the mechanics of estuarine diffusion may possibly be obtained by continuation of the present approach, which has been shown in this study to succeed in rivers.

IX-D Recapitulation

The dominant mechanism for dispersion in natural streams is variation of downstream velocity in the lateral (transverse) direction. Differences in velocity across the stream are primarily responsible for stretching out the pollutant cloud. A dispersion coefficient for most natural streams can be predicted by an extension of Taylor's

analysis; the prediction requires only the geometry of a typical cross section, the distribution of velocity within the cross section, and the channel shear velocity.

Proof of the effect of lateral velocity variation has been given by laboratory experiments. In one experiment the dimensionless dispersion coefficient was increased by a factor of ten by roughening the channel banks. The method for predicting the dispersion coefficient for a natural stream has been verified by numerous laboratory experiments and experiments in one natural stream.

LIST OF SYMBOLS

A	area of cross section of flow
a	radius of pipe
b	width of channel
c	time-averaged concentration
$\bar{c}$	cross-sectional mean concentration
c'	spatial variation of concentration from cross-sectional mean
c''	instantaneous concentration
D	dispersion coefficient
d	depth of flow
d_s	deflection of recording pen of Sanborn recorder
E	rate of energy dissipation per unit mass
f	a function of position on the flow cross section, the normalized solution to the steady-state equation for cross-sectional concentration distribution
f_c	calibration factor for conductivity probes
f_*	Darcy-Weisbach friction factor
g	acceleration of gravity
k_1, k_2	empirical coefficients
L_e	Lagrangian eddy size
L_1	length scale for channel distance from source point ($= \bar{u}\,T$)
L_2	length scale for distance within dispersing cloud. ($= \sqrt{\overline{u'^2}}\;T$)
ℓ	characteristic length of cross section
$\dot{M}$	mass transport per unit time through a cross section moving at the mean velocity

LIST OF SYMBOLS (cont'd.)

n	exponent in power law
P	any point on the flow cross section
p	number of moment of concentration distribution
r	hydraulic radius
S	slope
S_e	slope of the energy grade line
T	Lagrangian time scale
T'	Eulerian time scale
T*	period for time-averaging
t	time
t'	dimensionless time (t/T)
U*	shear velocity = $\sqrt{\tau_o/\rho}$
u, v, w	time averaged velocities in the x, y, and z directions respectively
$\bar{u}$	cross-sectional mean velocity of flow
u'	spatial variation of velocity from cross-sectional mean
u'(z)	depth averaged spatial variation of velocity from cross-sectional mean
u''	instantaneous velocity
X	longitudinal position of a fixed measuring station, referred to a fixed coordinate system
x	cartesian coordinate in direction of flow
x*	dimensionless distance (x/L_1)
y	cartesian coordinate in vertical direction
y'	dimensionless cartesian coordinate in vertical direction (= y/d)

LIST OF SYMBOLS (cont'd.)

z — cartesian coordinate transverse to flow

$\epsilon_x, \epsilon_y, \epsilon_z$ — turbulent mixing coefficients in the x, y, and z directions respectively

κ — von Karman constant

ρ — density

σ^2 — variance of distribution of tracer. Subscript indicates coordinate for integration, i.e.

$$\sigma_\xi^2 = \frac{\int_{-\infty}^{\infty} c\, \xi^2\, d\xi}{\int_{-\infty}^{\infty} c\, d\xi}$$

τ_o — wall shear stress

τ^* — local shear stress

ξ — cartesian coordinate in direction of mean flow in a coordinate system moving at the mean flow velocity

ξ' — dimensionless distance ($= \xi / L_2$)

REFERENCES

1. Faltermayer, E. K., "A Fortune Proposition: We Can Afford Clean Air", Fortune, LXXII, 5 (November, 1965), pp. 159-163, 218-224.

2. Taylor, G. I., "The dispersion of matter in turbulent flow through a pipe," Proc. Royal Society of London 223 (1954), pp. 446-468.

3. Elder, J. W., "The dispersion of marked fluid in turbulent shear flow," J. of Fluid Mech., 5 (1959), pp. 544-560.

4. Holley, E. R., Jr. and Harleman, D. R. F., "Dispersion of Pollutants in Estuary Type Flows," M. I. T., Hydrodynamics Laboratory Report No. 74 (1965), 202 p.

5. Boussinesq, M. J., "Essai sur la Theorie des Eaux Courants," Memoirs, Presente par divers Savents, L'Academie de l'Institut de France, 23 (1877), pp. 1-680.

6. Reynolds, O., "On the extent and action of the heating surface of steam boilers," Proc. Literary and Philosophical Society of Manchester, 14 (1874-1875); reprinted in Reynolds, O., Papers on Mechanical and Physical Subjects, Cambridge University Press 1900 Vol. 1, pp. 81-85.

7. Taylor, G. I., "Diffusion by Continuous Movements," Proc. London Math. Soc., Series 2, 20 (1921), pp. 196-212.

8. Thomas, I. E., "Dispersion in open-channel flow, Ph.D. Thesis, Northwestern University, August 1958, 140 p.

9. Aris, R., "On the dispersion of a solute in a fluid flowing through a tube," Proc. Ser. A, Royal Soc. of London 235 (1956), pp. 67-77.

10. Saffman, P. G., "The effect of wind shear on horizontal spread from an instantaneous ground source," Quart. J. Roy. Meteorol. Soc. 88 (1962), pp. 382-393.

11. Farrell, M. A. and Leonard, E. F., "Dispersion in Laminar Flow by Simultaneous Convection and Diffusion," AIChE Journal 9, (March 1963), p. 190.

12. Yotsukura, Nobuhiro and Fiering, Myron B., "Numerical Solution to a Dispersion Equation," Proc. ASCE, J. Hyd. Div., 90, HY5 (Sept. 1964), pp. 83-104.

REFERENCES (cont'd.)

13. Fischer, H. B., Discussion of reference 12, Proc. ASCE, J. Hyd. Div. 91, HY2, (1965), pp. 402-407.

14. Yotsukura, N. and Fiering, M. B., Closure to reference 12, Proc. ASCE, J. Hyd. Div. (in press).

15. Bugliarello, G. and Jackson, E. D., "Random Walk Study of Convective Diffusion," Proc. ASCE, J. Eng. Mech. Div. 90, EM4 (1964), pp. 49-77.

16. Taylor, G. I., "Dispersion of soluble matter in solvent flowing slowly through a tube," Proc. Roy. Soc. A 219 (1953), pp. 186-203.

17. Patterson, C. C. and Gloyna, E. F., "Dispersion Measurements in Open Channels," Proc. J. San. Eng. Div. ASCE, 91, SA3, (1965), p. 17.

18. Yotsukura, N., personal communication to Patterson and Gloyna.

19. Godfrey, R. G. and Frederick, B. J., "Dispersion in Natural Streams," U.S.G.S. open file report (1963).

20. Schuster, J. C., "Canal discharge measurements with radio-isotopes," Proc. ASCE, J. Hyd. Div. 91, HY2 (1965), pp. 101-124.

21. Glover, R. E., "Dispersion of Dissolved or Suspended Materials in Flowing Streams," U.S.G.S. Prof. Paper 433-B, 32 p.

22. "Sacramento River Water Pollution Survey," Bulletin No. 111, Dept. of Water Resources, State of California, August 1962.

23. Owens, M., Edwards, R. W. and Gibbs, J. W., "Some reaeration studies in streams," Air and Water Pollution Int. J., 8 (1964), pp. 469-486.

24. Sayre, W. W., Discussion of reference 20, Proc. ASCE, J. Hyd. Div. 91, HY6 (1965), pp. 185-192.

25. Kalinske, A. A. and Pien, C. L., "Experiments on eddy-diffusion and suspended-material transportation in open channels," A.G.U. Trans. 1943 Part II, pp. 530-535.

26. Vanoni, V. A., "Transportation of suspended sediment by water," Trans. ASCE 111, (1946), pp. 67-133.

REFERENCES (cont'd.)

27. Al-Saffar, Adnan M., "Eddy Diffusion and Mass Transfer in Open Channel Flow," Ph. D. Thesis, University of California, Berkeley, January 1964.

28. Orlob, G. T., "Eddy diffusion in homogeneous turbulence," Proc. ASCE, J. Hyd. Div. 85, HY9 (1959), pp. 75-101.

29. Sayre, W. W. and Chamberlain, A. R., "Exploratory Laboratory Study of Lateral Turbulent Diffusion at the Surface of An Alluvial Channel," U. S. Geological Survey Circular 484, Washington, D. C. (1964).

30. Hays, J. R., Schnelle, K. B., Jr., and Krenkel, P. A., "A turbulent diffusion study of pipe and stream flow by tracer techniques," presented at the Symposium on Pollution Control in Natural Waters, Fifty-fifth National Meeting AIChE, Houston, Texas, Feb. 7-11, 1965.

31. Batchelor, G. K., "Diffusion from sources in a turbulent boundary layer," Archiwum Mechaniki Stosowanej 16, 3 (1964) pp. 661-670.

32. Hwang, L., "Flow Resistance of Dunes in Alluvial Streams," Ph. D. thesis, Calif. Inst. of Tech., Pasadena, California (1965).

33. Vanoni, V. A., "130-Foot Precision Tilting Flume," Tech. Memo. No. 64-7, W. M. Keck Laboratory of Hydraulics and Water Resources, Calif. Inst. of Tech., Pasadena, California (Jan., 1964).

34. Standard Methods for the Examination of Water and Waste Water. American Public Health Association, New York (1965) p. 282.

35. Vanoni, V. A. and Brooks, N. H., "Laboratory Studies of the Roughness and Suspended Load of Alluvial Streams," report M.R.D. No. 11, Sedimentation Laboratory, California Institute of Technology, Pasadena, California (1957), pp. 100-106.

36. Mullineaux, D. R., "Geology of the Renton, Auburn, and Black Diamond quadrangles, Washington," U. S. Geological Survey open file report (1961), 202 p.

37. Rouse, H., Engineering Hydraulics, Wiley, London, 1950, p. 593.

REFERENCES (cont'd.)

38. Buchanan, T. J., "Time of travel of soluble contaminants in streams," Proc. ASCE, J. San. Eng. Div. 90, SA3 (1964), pp. 1-12.

39. Prandtl, L., Essentials of Fluid Dynamics, Hafner, New York, 1952, p. 149.

APPENDIX I

The purpose of this appendix is to prove equation (74), which shows that in the diffusive period the change of moment method yields an exact solution even when based on time-concentration data, regardless of the input concentration distribution. It is first convenient to obtain the values of certain integrals for the case of a delta function initial condition, for which the solution to the diffusion equation in a fixed coordinate system,

$$\frac{\partial c}{\partial t} + \bar{u}\frac{\partial c}{\partial x} = D\frac{\partial^2 c}{\partial x^2} \quad , \tag{102}$$

is,

$$c = \frac{1}{\sqrt{4\pi D t}}\, e^{\frac{-(x-\bar{u}t)^2}{4Dt}} \tag{103}$$

(in this appendix all concentrations are cross-sectional values, and the overbar has been dropped). Considering a fixed value of x, say $x = x_o$ (corresponding to the measuring position in an experiment), the following integrals can be obtained from tables or by a method given by Glover (21).

$$T_o(x_o) = \int_o^\infty c\,dt = \frac{1}{\bar{u}} \tag{104}$$

$$T_1(x_o) = \int_o^\infty ct\,dt = \frac{1}{\bar{u}^2}\left(x_o + \frac{2D}{\bar{u}}\right) \tag{105}$$

$$T_2(x_o) = \int_o^\infty ct^2 dt = \frac{1}{\bar{u}^3}\left(x_o^2 + 6\frac{Dx_o}{\bar{u}} + 12\frac{D^2}{\bar{u}^2}\right) \quad (106)$$

Now consider the actual case, in which the initial concentration distribution at some time, arbitrarily chosen to be t = 0, is some unknown distribution

$$c(x, 0) = c_o(x) \quad (107)$$

By superposition, the solution to equation (102) with the given initial condition is

$$c(x, t) = \int_{-\infty}^{\infty} c_o(\eta) \frac{\exp\left[-\frac{(x-\eta-\bar{u}t)^2}{4Dt}\right]}{\sqrt{4\pi Dt}} d\eta \quad (108)$$

Maintaining the notation for the moments from a delta function input, and denoting the moments in the general case by primed quantities, we obtain

$$T_o'(x_o) = \int_o^\infty c\,dt = \int_o^\infty dt \int_{-\infty}^{\infty} c_o(\eta) \frac{\exp\left[-\frac{(x_o-\eta-\bar{u}t)^2}{4Dt}\right]}{\sqrt{4\pi Dt}} d\eta$$

$$= \int_{-\infty}^{\infty} c_o(\eta)\, d\eta \int_o^\infty \frac{\exp\left[-\frac{(x_o-\eta-\bar{u}t)^2}{4Dt}\right]}{\sqrt{4\pi Dt}} dt$$

$$= \int_{-\infty}^{\infty} c_o(\eta)\, T_o(x_o-\eta)\, d\eta \quad (109)$$

$$T_1'(x_o) = \int_{-\infty}^{\infty} c_o(\eta)\, T_1(x_o - \eta)\, d\eta \tag{110}$$

$$T_2'(x_o) = \int_{-\infty}^{\infty} c_o(\eta)\, T_2(x_o - \eta)\, d\eta \tag{111}$$

The quantity of interest, $\bar{u}^2 \sigma_t^2$, is obtained from the moments by

$$\bar{u}^2 \sigma_t^2 = \bar{u}^2 \frac{T_2' - \frac{(T_1')^2}{T_o'}}{T_o'} \tag{112}$$

Substituting into equation (112) the results of equations (109), (110), and (111) yields

$$\bar{u}^2 \sigma_t^2 = \frac{1}{\int_{-\infty}^{\infty} c_o(\eta) d\eta} \left\{ \int_{-\infty}^{\infty} c_o(\eta) \left[x_o - \eta)^2 + \frac{6D}{\bar{u}} (x_o - \eta) + \frac{12D^2}{\bar{u}^2} \right] d\eta \right.$$

$$\left. - \frac{\left[\int_{-\infty}^{\infty} c_o(\eta)\, (x_o - \eta + \frac{2D}{\bar{u}})\, d\eta \right]^2}{\int_{-\infty}^{\infty} c_o(\eta)\, d\eta} \right\} \tag{113}$$

Only those terms containing x_o are of interest; the others are constant for any given experiment and will be subtracted out in finding the change of moment. Expanding equation (113) and sorting out those terms containing x_o yields

$$\bar{u}^2 \sigma_t^2 = \frac{2Dx_o}{\bar{u}} + f(D, \bar{u}, c_o) \tag{114}$$

Hence the change in σ_t^2 is directly proportional to the change in time,

$$\bar{u}^2 \Delta\sigma_t^2 = 2D\Delta t \tag{115}$$

and with the help of equation (37), equation (74) is established:

$$\bar{u}^2 \Delta\sigma_t^2 = \Delta\sigma_\xi^2$$

APPENDIX II

Discussion by the writer of "Numerical Solution to a Dispersion Equation", by Nobuhiro Yotsukura and Myron B. Fiering.

Published in the Proceedings of the American Society of Civil Engineers, Journal of the Hydraulics Division, 90, HY2 (March, 1965), pp. 402-407.

NUMERICAL SOLUTION TO A DISPERSION EQUATION[a]

Discussion by Hugo B. Fischer

HUGO B. FISCHER,[18] A. M. ASCE.—The authors have given an interesting numerical solution to the convective diffusion equation that helps to describe the initial mixing phenomena in open channel flow and demonstrates the initial production of skewness. It is regrettable that the solution does not lead

[a] September, 1964, by Nobuhiro Yotsukura and Myron B. Fiering (Proc. Paper 4046).

[18] NDEA Graduate Fellow, California Inst. of Tech., Pasadena, Calif.

asymptotically to the dispersion coefficient derived by Taylor's method[5] as given by Elder.[7] Until this discrepancy is removed the results should be used with some caution; particularly suspect is the conclusion that the dispersion coefficient depends on the friction factor.

The authors create confusion by claiming to find a discrepancy between Eqs. 3, 5, and 6 that only partly exists. Eq. 3 has no place in the discussion; it is derived strictly for pipe flows, and by no stretch of the imagination can be thought to concern open channel flow. Eqs. 5 and 6 are both derived from the integral formula

$$D = -h^2 \int_0^1 dw\, U' \int_0^\omega dw\, \frac{1}{K} \int_0^\omega dw\, U' \quad \ldots\ldots\ldots (27)$$

in which $U' = U - \overline{U}$, $w = 1 - y$, and all other notation is as given by the

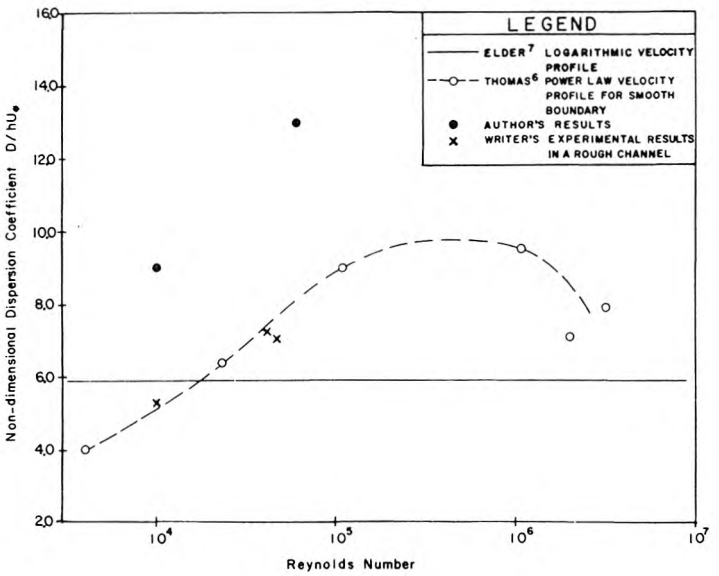

FIG. 11.—COMPARISON OF AUTHORS' RESULTS WITH EQS. 5, 6, AND FISCHER

authors. This integral can be obtained by the method given by Taylor,[5] as was done by both Elder[7] and Thomas,[6] or a moment method given in general form by K. Aris.[19] The writer has shown[20] that Aris's general expressions can be simplified in the two-dimensional case to yield Eq. 27 exactly.

---

[19] Aris, R., "On the Dispersion of a Solute in a Fluid Flowing Through a Tube," Proceedings, Royal Soc. of London, Series A, Vol. 235, pp. 67-77.

[20] Fischer, Hugo B., "Longitudinal Dispersion by Velocity Gradients in Open Channel Flow," Technical Memorandum No. 64-4, W. M. Keck Lab. of Hydraulics and Water Resources, California Inst. of Tech., Pasadena, Calif., May, 1964.

The difference between Eqs. 5 and 6 arises from Elder's use of the universal logarithmic velocity distribution, whereas Thomas confines himself to smooth channels and uses the power law distribution. Thomas's result can be expressed as a single valued function of the Reynolds number by using the well-known experimental relations for smooth pipes between the friction factor, power law exponent, and the Reynolds number, R. Fig. 11 shows the resulting comparison between Eqs. 5, 6, and the authors' results; herein, the friction factor has been calculated from the Blasius formula

$$f = \frac{8\,U^{*2}}{U^2} = 0.316\,R^{-0.25} \quad \ldots\ldots\ldots\ldots (28)$$

for $R \leq 10^5$, and Prandtl's universal law of friction for smooth pipes,

$$\frac{1}{\sqrt{f}} = 2 \log R\sqrt{f} - 0.8 \quad \ldots\ldots\ldots\ldots (29)$$

for $R > 10^5$. The value of the power law exponent, n, as a function of R has been taken as given in Schlichting.[21] The authors' results are shown for

TABLE 2

Mesh point (1)	w (2)	u' (3)	k'_{avg} (4)	I_1 (5)	I_2 (6)	I_3 (7)
i = 0	0	1.000	0.024	0.050	0.0521	0.0009
i = 1	0.1	0.894	0.088	0.139	0.160	0.0134
i = 2	0.2	0.777	0.158	0.217	0.273	0.0506
i = 3	0.3	0.644	0.208	0.281	0.393	0.0718
i = 4	0.4	0.488	0.238	0.330	0.522	0.0880
i = 5	0.5	0.307	0.248	0.361	0.661	0.1094
i = 6	0.6	0.084	0.238	0.369	0.814	0.1156
i = 7	0.7	-0.204	0.208	0.349	0.987	0.0975
i = 8	0.8	-0.609	0.158	0.288	1.190	0.0165
i = 9	0.9	-1.30	0.088	0.158	1.61	-0.155
i = 10	1.00	-3.36	0.024	-0.010		-0.437 (smooth boundary)
		-2.40	0.024	0.038		-0.250 (rough boundary)
		-3.16	0.024	0.000		-0.427 (best choice: $I_1 = 0$)

comparison; for the smooth case, the Reynolds number is determined from Eq. 28 and for the rough case, because no unique Reynolds number relation exists, an arbitrary value is used. Also shown are three experimental results determined by the writer in a pilot study for a research project now in progress; these experiments were conducted in a flume 10 in. wide, using flows 2 in. to 4 in. deep over a movable sand bed whose form was dunes roughly 1 in.

21 Schlichting, H., "Boundary Layer Theory," McGraw-Hill Book Co., Inc., New York, N. Y., 1960.

high. It is worth noting that for large Reynolds numbers, Thomas's result seems to be tending towards Elder's; this is a logical development because, as Schlichting notes, for large Reynolds numbers the power law distribution must tend towards a logarithmic distribution, whereupon Thomas's solution must tend towards Elder's. Unfortunately, Thomas's result loses definition at high Reynolds number, as the value of the exponent n is not experimentally well defined.

Because the authors elect to use a logarithmic velocity profile, their results should tend asymptotically to Eq. 6. That they do not is a clear indication that the numerical method is in error. The writer has made a calculation to determine whether the error arises from the size of the y-direction mesh or the handling of the velocity at the bed, and has found that it does not. The calculation is shown in Table 2, in which the following equations were used:

Col. 2 $$w = 1 = y \quad \ldots\ldots\ldots\ldots\ldots\ldots (30)$$

Col. 3 $$u' = 1 + 1n(1 - w) = \frac{\kappa U'}{U_*} = \kappa \frac{(U - \overline{U})}{U_*} \quad \ldots\ldots\ldots (31)$$

in which κ is the von Karman constant, Col. 4

$$k' = w(1 - w) = \frac{1}{\kappa} k = \frac{K}{\kappa h U_*} \quad \ldots\ldots\ldots\ldots (32)$$

Col. 5 $$I_1 = \int_0^{w_i + 0.05} u' \, dw; \quad I_{1_{10}} = \int_0^{1.00} u' \, dw \quad \ldots\ldots\ldots (33)$$

Col. 6 $$I_2 = \int_0^{w_i + 0.05} \frac{1}{k'} \int_0^{w} u' \, dw \, dw \quad \ldots\ldots\ldots\ldots (34)$$

Col. 7 $$I_3 = \int_0^{w_i + 0.05} u' \, dw \int_0^{w} \frac{1}{k'} \, dw \int_0^{w} u' \, dw \quad \ldots\ldots\ldots (35)$$

$$I_{3_{10}} = \int_0^{1.00} u' \, dw \int_0^{w} \frac{1}{k'} \, dw \int_0^{w} u' \, dw \quad \ldots\ldots\ldots (36)$$

and $$D = \frac{-h U_*}{\kappa^3} I_{3_{10}} \quad \ldots\ldots\ldots\ldots\ldots (37)$$

The numerical calculation is simulated by dividing the velocity profile into 11 segments, as shown in Fig. 12. The value of k for each segment is taken as the average value of k at each end, as has been done in the authors' numerical approach. For simplicity of calculation, the values of both k and u' have been normalized by the von Karman constant, κ, for use in the table, and the final result multiplied by κ^3. It should be noted that the authors use a value for the von Karman constant of 0.40, whereas Elder uses 0.41; the writer has used 0.41 in order that his results be directly comparable with Elder's. The writer obtains the following results:

1. For $u_{10} = 3.36$ (in which u_{10} is the velocity at the bed), which corresponds to the authors' assumptions for a smooth boundary

$$D = 6.33\ h\ U_* \quad \ldots\ldots\ldots\ldots\ldots\ldots (38)$$

2. For $u_{10} = 2.40$, which corresponds to the authors' assumption for a rough boundary,

$$D = 3.62\ h\ U_* \quad \ldots\ldots\ldots\ldots\ldots\ldots (39)$$

3. For $u_{10} = 3.16$, which is the logical value to use, because it is the only one for which the integral of the point velocity over the depth is equal to the mean velocity

$$D = 6.19\ h\ U_* \quad \ldots\ldots\ldots\ldots\ldots\ldots (40)$$

Eq. 40 is an excellent agreement with Elder's result; the other two results are spurious (because the integrated point velocity does not equal the mean

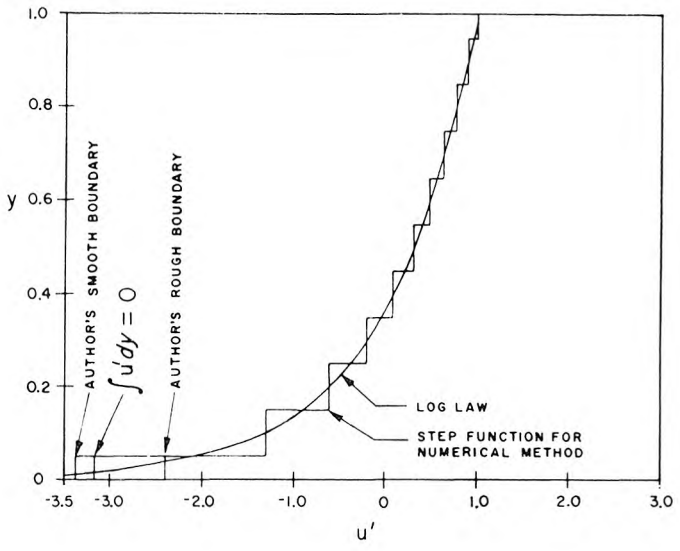

FIG. 12.—VELOCITY PROFILES USED TO SIMULATE NUMERICAL PROCEDURE

velocity), but they show how the authors reached their incorrect conclusion that D depends on the friction factor. The authors' assumption that the bed velocity can be assumed to be the velocity at the top of the roughness projection is not acceptable, as it injects a large error into the result.

The writer's contribution is essentially negative, in that he has only determined what is not the cause of the authors' error; however, when a numerical procedure contradicts a well established analytical result it is certainly the numerical method that must be questioned. The responsibility

remains with the authors to perfect their method to the point where it produces the correct final result; if this can be done the authors will have provided a useful procedure.

Because the authors present Eq. 26 purely as an empirical result, observed from their data, the writer feels it worthwhile to note why this relation must be valid. The proof can be given briefly as follows: Consider any process that satisfies the diffusion equation in a coordinate system moving with velocity, $\overline{U}$. Let $c_o(x)$ be the initial distribution, which is entirely upstream from the fixed observation point located at x_o. Let x' be the moving coordinate, so that

$$x' = x - \overline{U}\,t \quad \ldots\ldots\ldots\ldots\ldots\ldots\ldots (41)$$

and the governing equation is

$$\frac{\partial c}{\partial t} = \frac{\partial^2 c}{\partial x'^2} \quad \ldots\ldots\ldots\ldots\ldots\ldots\ldots (42)$$

Then the well-known fundamental solution to the diffusion equation yields

$$C(x, t) = \int_{-\infty}^{\infty} c_o(\xi)\, \frac{1}{\sqrt{4\pi D t}}\, e^{-\frac{(x-\xi-\overline{u}\,t)^2}{4 D t}}\, d\xi \quad \ldots\ldots\ldots\ldots (43)$$

The variance of the time-concentration curve taken at the fixed point x_o is by definition

$$\sigma_t^2 = \frac{\int_0^{\infty} t^2 C(x_o, t)\, dt}{\int_0^{\infty} C(x_o, t)\, dt} - \left[\frac{\int_0^{\infty} t\, C(x_o, t)\, dt}{\int_0^{\infty} C(x_o, t)\, dt}\right]^2 \quad \ldots\ldots (44)$$

Substituting Eq. 43 in Eq. 44, carrying out the integrations, setting $x = x_o$, and separating out those terms that include a dependence on x_o yields (for details see the writer's memo[22])

$$\overline{U}^2 \sigma_t^2 = 2 D \frac{x_o}{\overline{U}} + f(D, \overline{U}, c_o) \quad \ldots\ldots\ldots\ldots (45)$$

Because D, $\overline{U}$, and c_o are independent of time, the function on the right can be regarded as a constant for any given problem, so that, with $x_o = \overline{U}\,t$ the result is

$$\frac{d}{dt}\left(\overline{U}\,\sigma_t\right)^2 = 2 D \quad \ldots\ldots\ldots\ldots\ldots\ldots (26)$$

---

22 Fischer, Hugo B., "Determination of Dispersion Coefficients by the Change of Moment Method," Technical Memorandum No. 64-6, W. M. Keck Lab. of Hydraulics and Water Resources, California Inst. of Tech., Pasadena, Calif., June, 1964.

APPENDIX III

SUPPLEMENTARY DATA

This Appendix gives all group-averaged concentration measurements obtained during the multiple-probe experiments in the 40-meter flume. The tables give cross-sectional mean concentration, $\bar{c}$, and variation from the mean at each probe, c', at each of the selected times. Probe positions are given in each table. For the two-dimensional series (2300 through 2700) the tables give normalized depth, $y' = y/d$; for the three-dimensional series (2800 through 3400) the tables give lateral position with respect to the same datum as shown in the cross-sectional drawings included in the text (figures 39 through 44).

The concentration units given are those obtained directly from the data according to equation 91. In each series, the area under the concentration-distance curve is given for each group, and increases as the source is moved away from the probes. This is because the amount of tracer injected was increased between groups, so that for each group a nearly full scale Sanborn deflection could be obtained. The figures in the text show measured concentration units for the first group of each series, but for each subsequent group the concentration units are multiplied by a normalization factor so that each curve subtends the same area. The units given in the tables of this Appendix may be converted to those in the text figures by multiplying by the area under the concentration-distance curve of the first group of the series and dividing by the area under the curve of the group under consideration. The original data shown in these tables were used in all detailed calculations, but were normalized for presentation in the text to show the decay of concentration which would occur if a constant amount of tracer had been used.

GROUP AVERAGED RESULTS OF RUNS 2301 THROUGH 2305

DISTANCE FROM SOURCE TO PROBES (METERS) = 7.06
AREA UNDER CURVE (SEC. TIMES CONC. UNITS) = 459.77
MEAN TIME OF PASSAGE (SEC. FROM RELEASE) = 25.06
VARIANCE (SQUARE SECONDS) = 20.47

TIME FROM RELEASE	CONCENTRATION AT PROBE (RELATIVE TO MEAN)						MEAN CONCENTRATION
	PROBE F Y/D=.13	PROBE H Y/D=.30	PROBE G Y/D=.48	PROBE E Y/D=.70	PROBE J Y/D=.89	PROBE Y/D=.	
19.0	-0.6	-0.6	-0.6	1.6	0.3	0.	0.6
20.0	-11.6	-8.8	-18.8	17.3	20.2	0.	25.0
21.0	-31.1	-23.9	-17.0	29.5	38.4	0.	55.0
22.0	-33.9	-31.8	-5.8	15.7	47.3	0.	72.4
23.0	-14.6	-9.0	-0.5	8.4	14.0	0.	67.8
24.0	-2.2	1.8	1.3	2.2	-2.1	0.	51.7
25.0	5.6	3.0	4.8	-5.9	-7.0	0.	36.9
26.0	7.6	0.3	13.8	-8.9	-12.1	0.	29.2
27.0	9.9	1.3	6.2	-6.1	-10.4	0.	21.4
28.0	9.1	1.0	4.9	-6.2	-8.4	0.	17.2
30.0	8.0	1.5	1.4	-4.8	-5.9	0.	11.5
34.0	3.7	1.5	0.8	-2.3	-3.4	0.	5.6
36.0	3.6	1.4	0.4	-1.8	-3.3	0.	3.9
40.0	1.8	1.4	-0.2	-1.3	-1.6	0.	1.8
46.0	1.2	-0.3	-0.4	-0.3	-0.4	0.	0.4
52.0	0.	0.	0.	0.	0.	0.	0.

GROUP AVERAGED RESULTS OF RUNS 2311 THROUGH 2313

DISTANCE FROM SOURCE TO PROBES (METERS) = 23.06
AREA UNDER CURVE (SEC. TIMES CONC. UNITS) = 2795.85
MEAN TIME OF PASSAGE (SEC. FROM RELEASE) = 91.15
VARIANCE (SQUARE SECONDS) = 151.26

TIME FROM RELEASE	CONCENTRATION AT PROBE (RELATIVE TO MEAN)						MEAN CONCENTRATION
	PROBE F Y/D=.13	PROBE H Y/D=.30	PROBE G Y/D=.48	PROBE E Y/D=.70	PROBE J Y/D=.89	PROBE Y/D=.	
66.0	-0.5	0.8	0.9	-0.3	-0.7	0.	1.4
67.0	-1.3	-0.1	1.2	0.3	0.0	0.	2.6
70.0	-8.3	-2.2	4.0	0.3	5.4	0.	11.6
72.0	-16.8	-5.7	4.7	3.9	12.3	0.	26.3
75.0	-27.9	-13.9	-1.6	20.3	21.8	0.	55.7
80.0	-17.2	-13.6	-1.7	7.6	21.3	0.	87.8
85.0	-11.4	-5.8	-3.5	1.7	16.0	0.	94.7
90.0	-5.6	-0.1	-1.9	-4.2	9.5	0.	86.0
95.0	-1.5	3.8	-2.4	-5.6	4.4	0.	70.0
100.0	1.0	5.4	0.7	-4.9	-2.1	0.	53.2
105.0	2.3	5.4	-0.5	-4.2	-2.6	0.	38.4
110.0	2.6	6.3	-1.7	-4.4	-2.6	0.	25.9
120.0	3.5	2.3	-2.3	0.3	-3.1	0.	10.8
130.0	1.3	1.3	-1.0	0.7	-1.8	0.	3.8

GROUP AVERAGED RESULTS OF RUNS 2315 THROUGH 2318

DISTANCE FROM SOURCE TO PROBES (METERS) = 15.06
AREA UNDER CURVE (SEC. TIMES CONC. UNITS) = 1622.13
MEAN TIME OF PASSAGE (SEC. FROM RELEASE) = 57.69
VARIANCE (SQUARE SECONDS) = 94.34

TIME FROM RELEASE	CONCENTRATION AT PROBE (RELATIVE TO MEAN)						MEAN CONCENTRATION
	PROBE F Y/D=.13	PROBE H Y/D=.30	PROBE G Y/D=.48	PROBE E Y/D=.70	PROBE J Y/D=.89	PROBE Y/D=.	
42.0	-0.9	-0.6	-0.6	0.1	1.7	0.	0.9
44.0	-10.2	-9.9	-3.6	7.6	13.9	0.	13.8
45.0	-16.7	-18.4	-6.7	27.9	14.2	0.	27.9
46.0	-21.2	-22.0	-4.7	40.1	10.5	0.	46.9
47.0	-25.6	-30.7	4.8	29.7	20.4	0.	69.5
48.0	-17.2	-32.3	11.0	27.7	10.5	0.	79.9
49.0	-18.5	-26.8	10.2	17.1	15.7	0.	84.5
50.0	-17.8	-18.4	4.2	10.7	18.3	0.	84.9
52.0	-9.9	-10.5	-2.2	4.0	15.6	0.	81.3
54.0	-4.6	-4.6	-4.4	0.7	10.7	0.	76.4
56.0	-0.7	-2.6	-4.6	-2.2	8.0	0.	68.4
60.0	2.7	2.1	-0.4	-1.9	-2.3	0.	50.6
64.0	5.0	2.1	0.5	-3.2	-4.1	0.	36.3
68.0	4.0	4.6	-1.1	-4.4	-2.9	0.	26.3
72.0	3.7	3.6	-0.9	-3.8	-2.5	0.	17.1
76.0	3.4	2.4	-1.4	-1.9	-2.2	0.	11.5
80.0	2.1	1.3	-0.3	-2.5	-0.8	0.	7.5
90.0	0.8	0.3	0.0	-0.9	-0.2	0.	2.1
100.0	0.7	0.2	-0.3	-0.3	-0.3	0.	0.3
110.0	0.	0.	0.	0.	0.	0.	0.

GROUP AVERAGED RESULTS OF RUNS 2401 THROUGH 2404

DISTANCE FROM SOURCE TO PROBES (METERS) = 9.47
AREA UNDER CURVE (SEC. TIMES CONC. UNITS) = 1554.22
MEAN TIME OF PASSAGE (SEC. FROM RELEASE) = 37.00
VARIANCE (SQUARE SECONDS) = 60.62

TIME FROM RELEASE	CONCENTRATION AT PROBE (RELATIVE TO MEAN)						MEAN CONCENTRATION
	PROBE G Y/D=.07	PROBE H Y/D=.29	PROBE I Y/D=.48	PROBE F Y/D=.72	PROBE E Y/D=.90	PROBE Y/D=.	
24.0	-0.5	-0.5	-0.5	0.7	0.8	0.	0.5
25.0	-3.7	-2.8	-1.9	6.6	1.5	0.	3.7
26.0	-13.1	-10.0	-5.6	23.3	4.0	0.	14.6
27.0	-34.2	-18.4	-19.5	42.4	28.2	0.	44.0
28.0	-45.5	-16.0	-17.7	37.5	39.8	0.	75.4
29.0	-43.4	-11.3	-5.1	24.0	33.3	0.	90.3
30.0	-35.9	-2.4	4.9	8.1	22.5	0.	97.5
32.0	-17.5	7.8	2.2	-0.7	6.4	0.	97.4
34.0	-3.3	6.2	1.7	-4.4	-0.7	0.	88.9
36.0	3.8	6.0	1.6	-4.9	-6.7	0.	78.4
38.0	8.1	5.2	1.7	-6.5	-8.2	0.	67.8
40.0	10.4	5.7	1.7	-9.0	-8.1	0.	57.2
44.0	11.5	5.4	0.7	-9.5	-7.2	0.	35.5
48.0	8.8	2.6	-0.8	-4.7	-5.2	0.	21.9
52.0	5.7	1.4	-0.4	-2.6	-3.7	0.	13.2
56.0	1.7	1.3	0.6	-1.7	-1.8	0.	7.6
60.0	2.0	0.6	-0.4	-0.8	-1.3	0.	4.3
64.0	1.3	0.4	-0.7	-0.9	0.0	0.	2.3
68.0	0.4	0.3	-0.2	-0.3	-0.1	0.	0.9
72.0	0.2	0.1	-0.1	-0.0	-0.1	0.	0.1
76.0	0.	0.	0.	0.	0.	0.	0.

GROUP AVERAGED RESULTS OF RUNS 2405 THROUGH 2408

DISTANCE FROM SOURCE TO PROBES (METERS) = 14.17
AREA UNDER CURVE (SEC. TIMES CONC. UNITS) = 1954.39
MEAN TIME OF PASSAGE (SEC. FROM RELEASE) = 56.92
VARIANCE (SQUARE SECONDS) = 97.88

TIME FROM RELEASE	CONCENTRATION AT PROBE (RELATIVE TO MEAN)						MEAN CONCENTRATION
	PROBE G Y/D=.07	PROBE H Y/D=.29	PROBE I Y/D=.48	PROBE F Y/D=.72	PROBE E Y/D=.90	PROBE Y/D=.	
37.0	-0.0	-0.0	-0.0	0.1	0.0	0.	0.0
40.0	-4.9	-2.1	0.4	4.2	1.9	0.	6.2
42.0	-15.8	-1.8	-2.5	10.7	8.0	0.	21.5
44.0	-24.6	-4.1	-4.1	9.8	22.1	0.	46.0
46.0	-24.8	-1.1	0.8	5.4	18.1	0.	67.9
48.0	-22.8	-3.5	3.8	5.9	14.9	0.	80.7
50.0	-13.4	-1.8	2.9	2.5	8.7	0.	85.7
52.0	-6.0	-0.1	2.3	-0.3	3.6	0.	87.1
54.0	-1.5	1.6	2.4	-1.6	-1.4	0.	83.6
56.0	3.1	2.5	1.1	-3.4	-3.2	0.	77.3
58.0	5.8	2.4	1.3	-4.8	-4.3	0.	70.2
60.0	8.4	1.6	0.2	-4.0	-5.6	0.	61.5
62.0	9.3	0.2	1.1	-4.7	-5.1	0.	52.9
64.0	8.4	-1.0	2.6	-4.6	-4.7	0.	45.4
66.0	8.7	0.5	0.8	-4.9	-4.2	0.	37.9
68.0	7.9	0.8	0.4	-4.7	-3.7	0.	30.9
70.0	6.9	-0.1	0.5	-3.8	-2.8	0.	25.7
75.0	5.3	-0.3	0.8	-2.2	-3.2	0.	14.9
80.0	2.5	0.6	0.2	-0.8	-2.4	0.	8.2
85.0	0.9	-0.1	1.1	-0.5	-1.4	0.	4.4
90.0	0.5	-0.1	0.5	0.1	-1.0	0.	2.3
95.0	0.3	0.3	-0.3	-0.0	-0.2	0.	0.6
100.0	0.0	0.2	-0.1	-0.1	0.0	0.	0.1

GROUP AVERAGED RESULTS OF RUNS 2409 THROUGH 2411

DISTANCE FROM SOURCE TO PROBES (METERS) = 24.07
AREA UNDER CURVE (SEC. TIMES CONC. UNITS) = 2928.27
MEAN TIME OF PASSAGE (SEC. FROM RELEASE) = 106.00
VARIANCE (SQUARE SECONDS) = 191.90

TIME FROM RELEASE	CONCENTRATION AT PROBE (RELATIVE TO MEAN)						MEAN CONCENTRATION
	PROBE G Y/D=.07	PROBE H Y/D=.29	PROBE I Y/D=.48	PROBE F Y/D=.72	PROBE E Y/D=.90	PROBE Y/D=.	
74.0	-0.0	-0.0	-0.0	-0.0	0.1	0.	0.0
76.0	-0.7	0.0	0.3	0.2	0.1	0.	0.7
78.0	-1.7	-0.5	-0.5	1.8	0.7	0.	3.8
80.0	-3.1	-1.3	0.4	1.7	2.1	0.	7.5
82.0	-5.3	-2.4	-0.1	2.2	5.5	0.	14.3
84.0	-7.8	-1.3	0.5	1.6	6.5	0.	23.3
86.0	-12.1	-1.5	-0.1	3.2	9.8	0.	34.3
88.0	-13.7	-3.6	-0.2	7.0	9.6	0.	47.0
90.0	-12.6	-4.0	-0.2	7.3	8.6	0.	58.5
92.0	-11.2	-3.8	-0.1	4.0	10.8	0.	68.7
94.0	-10.1	-2.3	0.5	2.7	8.6	0.	77.2
96.0	-7.7	-1.0	1.0	0.3	7.0	0.	82.5
98.0	-4.9	0.1	1.2	-1.5	4.9	0.	86.1
100.0	-3.0	0.1	1.8	-2.5	3.6	0.	87.6
102.0	0.1	1.0	0.9	-3.6	1.9	0.	86.9
104.0	1.2	2.0	0.8	-4.0	0.1	0.	84.8
106.0	4.1	2.1	-0.2	-4.8	-0.6	0.	80.6
108.0	5.7	3.2	-0.7	-6.7	-0.7	0.	75.8
110.0	5.8	2.8	-0.6	-5.5	-1.8	0.	71.0
112.0	7.5	3.4	-0.6	-7.1	-2.3	0.	64.6
114.0	7.4	2.0	-0.6	-5.4	-2.6	0.	57.8
116.0	6.7	2.4	-1.0	-4.4	-3.2	0.	51.8
118.0	7.2	1.4	-1.9	-2.5	-3.5	0.	46.2
120.0	8.0	2.2	-1.2	-3.8	-4.6	0.	40.5
122.0	7.9	2.4	-0.8	-4.7	-4.1	0.	34.7
124.0	7.3	2.1	-0.3	-4.4	-4.0	0.	29.9
126.0	5.8	2.4	-0.2	-3.9	-3.6	0.	25.7
128.0	4.7	2.1	0.4	-4.2	-2.6	0.	21.8
130.0	4.5	1.4	0.4	-3.6	-2.3	0.	19.0
135.0	3.0	0.7	0.2	-2.1	-1.5	0.	12.2
140.0	1.9	-0.0	0.3	-1.4	-0.5	0.	7.2
145.0	1.6	-0.0	-0.0	-0.8	-0.6	0.	4.0
150.0	1.6	0.6	-0.5	-1.2	-0.3	0.	2.3
155.0	1.7	0.2	-0.4	-0.8	-0.4	0.	1.0
160.0	0.6	0.0	-0.2	-0.2	-0.1	0.	0.2

GROUP AVERAGED RESULTS OF RUNS 2501 THROUGH 2504

DISTANCE FROM SOURCE TO PROBES (METERS) = 13.07
AREA UNDER CURVE (SEC. TIMES CONC. UNITS) = 1539.24
MEAN TIME OF PASSAGE (SEC. FROM RELEASE) = 53.18
VARIANCE (SQUARE SECONDS) = 88.86

TIME FROM RELEASE	CONCENTRATION AT PROBE (RELATIVE TO MEAN)						MEAN CONCENTRATION
	PROBE G Y/D=.04	PROBE F Y/D=.16	PROBE J Y/D=.33	PROBE I Y/D=.55	PROBE E Y/D=.79	PROBE H Y/D=.99	
38.0	-0.5	-0.5	-0.5	-0.5	-0.5	3.6	0.5
39.0	-2.3	-2.3	-2.1	-0.3	-1.4	11.9	2.3
40.0	-6.3	-5.6	-5.9	1.8	-1.8	23.3	6.3
41.0	-13.5	-14.1	-13.8	11.2	-3.3	37.6	17.3
42.0	-28.0	-25.5	-24.3	27.0	-8.6	61.1	37.5
43.0	-45.3	-37.3	-41.8	43.3	-4.2	79.8	65.0
44.0	-50.4	-37.0	-53.0	40.2	8.8	84.5	87.2
45.0	-45.1	-25.7	-41.0	38.6	0.4	64.0	94.1
46.0	-29.8	-21.6	-29.4	31.5	1.9	36.5	97.2
47.0	-16.3	-18.4	-9.3	21.2	-1.7	13.4	96.2
48.0	-5.5	-15.4	1.0	11.4	-1.8	2.6	91.6
49.0	2.1	-10.5	3.5	5.9	-3.2	-0.6	83.7
50.0	5.8	-3.8	5.5	1.5	-3.9	-5.3	77.7
52.0	12.2	3.3	12.1	-2.7	-11.5	-8.1	63.8
54.0	14.2	5.8	14.9	-5.5	-11.3	-12.7	54.4
56.0	15.2	7.9	16.1	-8.3	-10.1	-14.8	46.3
58.0	15.4	9.5	15.5	-8.5	-9.7	-16.4	39.3
60.0	13.0	8.5	14.9	-8.4	-8.9	-13.6	33.0
62.0	12.5	4.6	10.6	-5.8	-6.7	-10.4	26.1
64.0	12.3	3.7	7.9	-4.9	-5.5	-8.6	21.1
66.0	11.9	2.9	6.2	-4.3	-4.3	-7.7	17.2
68.0	10.7	2.6	4.8	-3.3	-4.0	-6.5	14.0
70.0	9.1	2.4	4.5	-3.1	-3.5	-5.6	11.4
72.0	7.0	1.9	4.1	-2.1	-3.3	-5.1	9.3
74.0	5.6	2.1	4.0	-2.2	-2.8	-4.6	7.5
76.0	4.1	1.8	3.7	-1.8	-2.3	-4.1	6.4
78.0	4.0	1.9	2.0	-1.2	-2.0	-3.3	5.0
80.0	4.0	1.7	1.2	-0.6	-1.8	-3.1	4.0
85.0	3.1	0.9	0.6	-0.5	-1.0	-2.1	2.3
90.0	1.7	0.7	0.1	-0.2	-0.5	-1.2	1.2
95.0	0.5	0.4	0.1	-0.1	-0.2	-0.5	0.5
100.0	0.2	0.2	-0.1	-0.1	-0.1	-0.1	0.1

GROUP AVERAGED RESULTS OF RUNS 2505 THROUGH 2510

DISTANCE FROM SOURCE TO PROBES (METERS) = 25.07
AREA UNDER CURVE (SEC. TIMES CONC. UNITS) = 2987.06
MEAN TIME OF PASSAGE (SEC. FROM RELEASE) = 106.65
VARIANCE (SQUARE SECONDS) = 226.11

TIME FROM RELEASE	CONCENTRATION AT PROBE (RELATIVE TO MEAN)						MEAN CONCENTRATION
	PROBE G Y/D=.04	PROBE F Y/D=.16	PROBE J Y/D=.33	PROBE I Y/D=.55	PROBE E Y/D=.79	PROBE H Y/D=.99	
80.0	-3.6	-3.4	-2.3	1.8	0.9	6.1	4.1
82.0	-8.8	-9.1	-6.6	4.4	3.2	15.6	12.5
84.0	-14.5	-13.1	-9.1	4.8	9.0	18.0	25.0
86.0	-22.2	-17.4	-8.5	7.3	11.9	18.3	39.8
88.0	-28.4	-20.8	-11.6	9.3	14.6	24.3	54.6
90.0	-29.9	-15.5	-10.3	6.3	13.3	25.4	66.6
92.0	-28.1	-13.6	-9.6	6.0	12.4	22.4	76.7
94.0	-20.9	-11.6	-9.0	6.7	9.0	17.5	82.9
96.0	-13.0	-8.9	-6.7	6.0	5.5	11.3	86.0
98.0	-7.5	-6.9	-4.2	5.0	3.1	6.4	87.0
100.0	-3.7	-3.9	-1.6	4.2	-0.2	2.7	86.4
102.0	-0.3	-0.9	-0.5	2.8	-1.5	-0.5	84.0
104.0	2.7	1.3	0.8	1.9	-3.0	-3.4	80.5
106.0	6.1	2.8	2.7	1.1	-5.2	-5.9	75.7
108.0	7.5	4.3	3.9	-0.0	-5.6	-7.9	70.6
110.0	8.7	4.8	3.9	-0.4	-5.8	-8.5	65.4
112.0	11.1	6.2	3.5	-0.9	-6.2	-9.7	59.8
114.0	12.3	6.8	2.8	-0.5	-6.9	-10.1	54.8
116.0	12.8	6.8	3.3	-0.9	-6.8	-10.8	49.7
118.0	11.8	7.8	4.0	-2.2	-6.3	-10.6	44.3
120.0	10.5	7.8	4.7	-3.4	-5.5	-9.7	39.3
122.0	9.6	6.9	4.9	-3.7	-4.6	-9.3	34.7
124.0	8.3	5.9	4.9	-3.4	-3.8	-9.0	30.7
126.0	8.0	6.2	4.5	-3.3	-3.8	-8.7	27.2
128.0	7.9	6.4	3.5	-3.2	-3.2	-8.5	23.9
130.0	7.5	6.2	3.0	-3.2	-2.9	-7.6	20.8
132.0	7.0	5.4	2.8	-2.6	-2.9	-6.9	17.8
134.0	6.8	5.5	2.3	-2.4	-2.8	-6.6	15.6
136.0	6.6	4.9	1.8	-1.9	-2.7	-5.9	13.3
138.0	6.0	3.8	1.6	-1.6	-2.3	-5.2	11.4
140.0	5.6	3.1	1.1	-1.1	-2.0	-4.6	9.6
145.0	3.8	2.7	1.0	-0.4	-2.5	-2.9	6.5
150.0	2.9	2.1	0.6	-0.8	-1.1	-2.5	4.1
155.0	1.3	1.5	0.7	-0.6	-0.5	-2.0	2.7
160.0	1.6	1.0	0.6	-0.9	-0.2	-1.2	1.4
165.0	0.7	0.8	0.4	-0.5	-0.2	-0.8	0.8

GROUP AVERAGED RESULTS OF RUNS 2601 THROUGH 2605

DISTANCE FROM SOURCE TO PROBES (METERS) = 7.06
AREA UNDER CURVE (SEC. TIMES CONC. UNITS) = 427.80
MEAN TIME OF PASSAGE (SEC. FROM RELEASE) = 24.49
VARIANCE (SQUARE SECONDS) = 3.89

TIME FROM RELEASE	CONCENTRATION AT PROBE (RELATIVE TO MEAN)						MEAN CONCENTRATION
	PROBE H Y/D=.04	PROBE F Y/D=.23	PROBE J Y/D=.49	PROBE I Y/D=.70	PROBE E Y/D=.90	PROBE Y/D=.	
20.0	-0.1	-0.1	-0.0	-0.0	0.1	0.	0.1
21.0	-4.1	-1.9	-0.3	3.2	2.1	0.	5.6
21.5	-15.6	-8.1	4.4	4.3	10.1	0.	18.8
22.0	-38.0	-21.5	14.1	7.0	26.3	0.	44.9
22.5	-60.4	-37.3	20.0	24.0	34.9	0.	75.7
23.0	-44.3	-35.5	14.7	18.4	33.8	0.	102.1
23.5	-33.5	-5.6	7.5	12.6	7.5	0.	105.4
24.0	-16.4	8.7	-0.2	11.1	-9.6	0.	96.3
24.5	4.4	15.4	-5.9	5.5	-18.8	0.	82.0
25.0	17.7	22.5	-9.0	-3.5	-23.1	0.	69.5
25.5	21.1	23.6	-9.9	-7.3	-21.7	0.	57.4
26.0	21.1	22.3	-8.6	-7.6	-21.5	0.	46.0
27.0	23.8	16.9	-9.6	-6.8	-17.0	0.	28.9
28.0	20.7	7.5	-6.0	-4.4	-11.0	0.	16.3
29.0	11.6	2.5	-3.2	-1.9	-5.0	0.	8.3
30.0	5.9	1.7	-1.5	-0.9	-3.2	0.	4.7
31.0	2.7	1.5	-1.0	-0.2	-2.1	0.	2.7
32.0	1.4	1.1	-0.8	-0.1	-1.1	0.	1.4
33.0	0.7	0.3	-0.4	0.1	-0.5	0.	0.5
34.0	0.3	0.0	-0.2	0.1	-0.2	0.	0.2
35.0	0.2	-0.0	-0.0	0.0	-0.0	0.	0.0
36.0	0.0	-0.0	-0.0	-0.0	-0.0	0.	0.0

GROUP AVERAGED RESULTS OF RUNS 2606 THROUGH 2610

DISTANCE FROM SOURCE TO PROBES (METERS) = 14.06
AREA UNDER CURVE (SEC. TIMES CONC. UNITS) = 782.31
MEAN TIME OF PASSAGE (SEC. FROM RELEASE) = 50.87
VARIANCE (SQUARE SECONDS) = 11.83

TIME FROM RELEASE	CONCENTRATION AT PROBE (RELATIVE TO MEAN)						MEAN CONCENTRATION
	PROBE H Y/D=.04	PROBE F Y/D=.23	PROBE J Y/D=.49	PROBE I Y/D=.70	PROBE E Y/D=.90	PROBE Y/D=.	
41.0	-0.0	-0.0	-0.0	-0.0	0.1	0.	0.0
42.0	-0.2	-0.2	-0.0	0.1	0.2	0.	0.2
43.0	-0.8	-0.5	0.0	0.7	0.4	0.	0.8
44.0	-3.7	-3.0	0.6	1.0	4.1	0.	4.0
45.0	-12.6	-9.3	1.4	0.6	16.8	0.	14.8
46.0	-28.7	-16.4	4.6	3.2	29.4	0.	36.9
47.0	-44.3	-22.8	13.8	3.7	35.9	0.	66.3
48.0	-36.0	-16.8	10.0	7.5	24.0	0.	83.9
49.0	-19.3	-7.3	2.7	8.5	9.7	0.	94.0
50.0	-9.3	-1.1	0.1	6.2	1.1	0.	94.4
51.0	-1.0	1.9	-0.5	3.9	-4.9	0.	87.3
52.0	8.7	10.1	-2.1	-0.9	-13.9	0.	76.9
53.0	9.6	14.4	-2.2	-5.7	-14.2	0.	63.4
54.0	7.7	17.2	-4.0	-6.5	-13.2	0.	49.2
55.0	4.8	15.6	-3.3	-6.7	-9.9	0.	36.6
56.0	4.0	11.6	-2.8	-4.5	-7.7	0.	25.0
57.0	3.7	8.6	-2.8	-3.4	-5.4	0.	16.9
58.0	4.7	5.4	-2.1	-2.7	-4.1	0.	11.0
59.0	4.0	3.6	-1.5	-2.0	-2.9	0.	7.1
60.0	2.5	2.2	-1.3	-1.1	-1.6	0.	4.4
62.0	0.4	0.9	0.1	-0.0	-1.4	0.	2.0
64.0	-0.3	0.4	-0.2	0.4	-0.4	0.	0.9
66.0	-0.3	0.1	-0.1	0.3	-0.2	0.	0.4
68.0	-0.2	0.0	-0.1	0.3	-0.1	0.	0.2
72.0	-0.0	-0.0	-0.0	0.1	-0.0	0.	0.0

GROUP AVERAGED RESULTS OF RUNS 2611 THROUGH 2614

DISTANCE FROM SOURCE TO PROBES (METERS) = 21.06
AREA UNDER CURVE (SEC. TIMES CONC. UNITS) = 1074.63
MEAN TIME OF PASSAGE (SEC. FROM RELEASE) = 76.91
VARIANCE (SQUARE SECONDS) = 19.62

TIME FROM RELEASE	CONCENTRATION AT PROBE (RELATIVE TO MEAN)						MEAN CONCENTRATION
	PROBE H Y/D=.04	PROBE F Y/D=.23	PROBE J Y/D=.49	PROBE I Y/D=.70	PROBE E Y/D=.90	PROBE Y/D=.	
64.0	-0.0	-0.0	-0.0	-0.0	0.1	0.	0.0
65.0	-0.3	-0.3	-0.2	0.1	0.7	0.	0.3
66.0	-0.9	-0.8	-0.1	-0.1	1.7	0.	1.0
67.0	-1.4	-1.5	-0.2	0.7	2.0	0.	2.1
68.0	-2.9	-4.5	1.1	3.6	2.0	0.	5.6
69.0	-6.8	-10.0	5.0	4.2	5.6	0.	13.2
70.0	-14.6	-17.8	8.9	5.9	13.3	0.	26.9
71.0	-22.0	-19.5	11.2	9.3	14.1	0.	43.5
72.0	-30.2	-19.0	12.8	7.3	19.3	0.	63.5
73.0	-29.2	-14.3	10.7	6.4	16.8	0.	83.7
74.0	-22.0	-12.5	6.4	8.2	13.2	0.	97.0
75.0	-12.9	-7.5	3.7	5.5	7.3	0.	104.2
76.0	-5.3	-1.9	1.5	0.6	3.4	0.	104.9
77.0	5.1	4.6	-1.5	-7.3	0.7	0.	99.2
78.0	13.0	11.2	-4.6	-10.1	-5.6	0.	87.9
79.0	17.7	15.9	-7.3	-13.2	-7.8	0.	73.4
80.0	18.5	17.0	-5.8	-14.4	-10.2	0.	60.6
82.0	21.7	16.2	-6.0	-12.3	-13.4	0.	39.2
84.0	14.2	13.9	-7.3	-8.1	-8.4	0.	23.6
86.0	7.7	8.3	-4.1	-5.1	-4.5	0.	13.0
88.0	3.8	4.0	-1.7	-2.9	-2.1	0.	6.1
90.0	2.1	1.7	-0.6	-1.4	-1.2	0.	3.2
92.0	0.8	1.3	-0.5	-0.7	-0.8	0.	1.5
95.0	0.6	0.5	-0.3	-0.2	-0.4	0.	0.7
100.0	0.1	0.2	-0.1	-0.1	-0.1	0.	0.1
105.0	0.	0.	0.	0.	0.	0.	0.

GROUP AVERAGED RESULTS OF RUNS 2615 THROUGH 2618

DISTANCE FROM SOURCE TO PROBES (METERS) = 28.06
AREA UNDER CURVE (SEC. TIMES CONC. UNITS) = 1245.17
MEAN TIME OF PASSAGE (SEC. FROM RELEASE) = 102.89
VARIANCE (SQUARE SECONDS) = 29.23

TIME FROM RELEASE	CONCENTRATION AT PROBE (RELATIVE TO MEAN)						MEAN CONCENTRATION
	PROBE H Y/D=.04	PROBE F Y/D=.23	PROBE J Y/D=.49	PROBE I Y/D=.70	PROBE E Y/D=.90	PROBE Y/D=.	
88.0	-0.2	-0.1	0.0	-0.2	0.4	0.	0.2
90.0	-1.2	-1.1	0.6	0.6	0.6	0.	1.7
92.0	-3.7	-3.2	1.2	1.8	2.7	0.	6.6
94.0	-9.7	-11.7	4.9	4.7	9.2	0.	20.3
96.0	-16.9	-18.7	8.7	8.2	13.8	0.	45.5
98.0	-13.7	-17.5	9.4	6.0	11.6	0.	74.8
100.0	-10.1	-9.4	5.5	2.7	8.2	0.	95.0
102.0	-4.9	4.8	-1.1	-1.4	0.7	0.	98.4
104.0	0.0	15.6	-5.3	-4.4	-6.7	0.	87.2
106.0	6.2	22.3	-6.5	-13.1	-8.0	0.	68.7
108.0	6.1	22.5	-7.8	-13.1	-6.7	0.	48.0
110.0	5.3	19.1	-6.7	-11.6	-5.2	0.	31.6
112.0	2.5	13.3	-4.1	-7.4	-4.2	0.	19.0
114.0	1.1	8.3	-2.4	-4.0	-3.0	0.	10.5
116.0	1.3	4.8	-1.8	-2.3	-1.7	0.	5.7
118.0	1.2	3.2	-1.1	-1.9	-1.2	0.	3.7
120.0	0.6	2.4	-0.7	-1.2	-1.0	0.	2.3
122.0	0.7	1.3	-0.4	-0.9	-0.6	0.	1.3
124.0	0.4	1.3	-0.3	-0.8	-0.6	0.	1.0
128.0	0.2	0.4	-0.0	-0.3	-0.2	0.	0.3
132.0	0.1	0.2	-0.0	-0.2	-0.2	0.	0.2

GROUP AVERAGED RESULTS OF RUNS 2701 THROUGH 2704

DISTANCE FROM SOURCE TO PROBES (METERS) = 14.06
AREA UNDER CURVE (SEC. TIMES CONC. UNITS) = 469.07
MEAN TIME OF PASSAGE (SEC. FROM RELEASE) = 38.48
VARIANCE (SQUARE SECONDS) = 8.50

TIME FROM RELEASE	CONCENTRATION AT PROBE (RELATIVE TO MEAN)						MEAN CONCENTRATION
	PROBE G Y/D=.06	PROBE F Y/D=.24	PROBE I Y/D=.41	PROBE H Y/D=.61	PROBE J Y/D=.80	PROBE E Y/D=.95	
32.0	-0.0	-0.0	-0.0	-0.0	0.1	-0.0	0.0
33.0	-1.5	-1.5	-0.5	0.3	-0.8	5.1	1.5
34.0	-14.4	-15.2	-2.5	10.4	16.8	3.6	16.2
34.5	-25.7	-26.3	1.0	22.9	20.8	2.9	31.2
35.0	-24.8	-32.9	-0.9	21.0	23.2	13.1	42.4
35.5	-28.9	-38.2	-6.9	19.1	28.0	30.4	54.0
36.0	-36.8	-38.2	-11.0	24.9	40.3	20.6	70.0
36.5	-30.3	-18.4	-4.6	17.7	21.6	12.1	73.3
37.0	-19.8	-0.2	-3.9	9.9	6.7	4.9	72.9
37.5	-8.0	5.4	-1.4	3.5	-3.7	3.1	70.6
38.0	3.0	10.1	0.8	-1.2	-12.2	-0.8	66.0
38.5	13.4	17.6	4.4	-8.0	-15.7	-13.4	58.4
39.0	18.6	23.1	0.6	-9.7	-15.0	-19.9	51.7
39.5	20.0	27.3	-4.8	-11.8	-11.7	-20.6	46.3
40.0	21.8	29.6	-10.7	-13.3	-8.1	-20.0	41.0
41.0	24.6	24.9	-11.4	-10.3	-10.2	-17.1	34.3
42.0	19.8	21.5	-7.3	-7.6	-12.9	-13.6	25.6
43.0	11.3	15.6	-2.6	-8.0	-8.8	-7.0	16.1
44.0	7.9	13.5	-2.7	-6.5	-6.7	-5.3	10.9
46.0	6.2	5.7	-0.9	-3.8	-3.6	-3.2	4.7
48.0	2.3	2.6	-0.4	-1.5	-1.6	-1.4	1.7
50.0	0.4	1.1	0.0	-0.5	-0.5	-0.5	0.5
52.0	0.1	0.5	-0.0	-0.2	-0.2	-0.2	0.2

GROUP AVERAGED RESULTS OF RUNS 2705 THROUGH 2708

DISTANCE FROM SOURCE TO PROBES (METERS) = 25.06
AREA UNDER CURVE (SEC. TIMES CONC. UNITS) = 1111.89
MEAN TIME OF PASSAGE (SEC. FROM RELEASE) = 68.80
VARIANCE (SQUARE SECONDS) = 19.42

TIME FROM RELEASE	CONCENTRATION AT PROBE (RELATIVE TO MEAN)						MEAN CONCENTRATION
	PROBE G Y/D=.06	PROBE F Y/D=.24	PROBE I Y/D=.41	PROBE H Y/D=.61	PROBE J Y/D=.80	PROBE E Y/D=.95	
57.0	0.	0.	0.	0.	0.	0.	0.
59.0	-0.7	-0.7	-0.3	0.7	0.6	0.4	0.7
61.0	-11.1	-11.6	-2.4	5.6	10.7	9.8	13.4
62.0	-21.8	-24.3	-2.1	6.4	12.3	35.8	31.4
63.0	-31.3	-34.1	-2.8	17.9	16.2	38.8	52.4
64.0	-41.5	-33.5	0.3	17.7	27.2	31.1	72.5
65.0	-37.5	-36.2	1.8	17.9	26.6	28.8	91.5
66.0	-29.1	-23.7	3.9	13.9	16.3	18.4	102.1
67.0	-23.1	-5.9	0.9	10.4	6.7	8.9	106.6
68.0	-10.7	0.6	2.5	9.2	-3.5	-1.4	105.3
69.0	0.9	7.1	2.9	6.2	-11.9	-8.7	97.1
70.0	4.8	15.6	2.9	2.9	-19.3	-10.4	84.8
71.0	8.5	23.3	-1.4	-1.2	-19.3	-12.8	71.6
72.0	14.7	24.9	-3.4	-6.1	-16.6	-15.7	61.4
73.0	7.9	24.2	1.8	-5.2	-16.7	-15.4	50.6
74.0	10.2	19.2	4.5	-4.6	-17.0	-15.5	41.1
75.0	10.9	17.7	3.4	-5.9	-14.8	-13.6	32.1
76.0	11.4	17.4	0.4	-6.8	-11.8	-11.9	25.0
77.0	5.9	15.8	0.3	-5.7	-9.8	-7.7	18.4
79.0	5.1	12.3	-1.5	-4.6	-7.5	-3.9	10.3
81.0	1.9	6.9	-0.5	-2.0	-3.8	-3.0	4.9
83.0	0.7	4.0	-0.7	-1.2	-1.8	-1.2	2.0
85.0	0.5	2.3	-0.4	-0.8	-1.0	-0.7	1.0
87.0	0.1	1.5	-0.2	-0.4	-0.5	-0.5	0.5
89.0	0.0	0.6	-0.1	-0.2	-0.2	-0.2	0.2

GROUP AVERAGED RESULTS OF RUNS 2801 THROUGH 2805

DISTANCE FROM SOURCE TO PROBES (METERS) = 16.07
AREA UNDER CURVE (SEC. TIMES CONC. UNITS) = 1828.83
MEAN TIME OF PASSAGE (SEC. FROM RELEASE) = 61.89
VARIANCE (SQUARE SECONDS) = 368.72

TIME FROM RELEASE	CONCENTRATION AT PROBE (RELATIVE TO MEAN)						MEAN CONCENTRATION
	PROBE G 31.4W	PROBE J 25.0W	PROBE I 12.9W	PROBE E 9.1W	PROBE F 0.3W	PROBE H 2.1E	
38.0	0.	0.	0.	0.	0.	0.	0.
40.0	-1.4	-1.2	1.0	0.8	-1.4	-1.4	1.4
42.0	-17.0	-8.3	11.2	6.2	-16.2	-17.1	17.1
44.0	-64.2	-9.8	30.4	20.9	-56.9	-64.3	67.0
46.0	-91.7	-16.6	34.0	37.1	-65.4	-87.6	100.4
48.0	-66.7	-10.4	23.8	22.2	-32.4	-65.4	92.5
50.0	-36.0	-6.0	6.4	15.6	-6.8	-30.5	71.8
52.0	-16.7	-3.4	1.3	6.8	3.6	-10.4	57.3
54.0	-4.0	0.6	-4.5	3.0	8.9	2.3	46.3
56.0	2.0	1.6	-6.3	0.9	10.9	7.8	40.6
58.0	5.5	2.0	-7.3	-0.1	12.0	10.5	36.5
60.0	7.9	3.0	-8.0	-1.2	12.2	12.5	33.0
65.0	11.7	2.9	-7.8	-2.7	11.7	14.4	26.8
70.0	12.5	2.4	-6.7	-3.7	10.7	14.6	21.8
75.0	12.2	2.6	-6.8	-2.9	9.3	13.4	17.5
80.0	11.8	2.6	-5.1	-3.9	7.3	11.4	14.3
85.0	10.8	2.3	-5.2	-2.7	6.3	10.3	11.0
90.0	8.8	1.7	-3.9	-2.3	4.9	8.3	8.6
95.0	7.1	0.7	-2.8	-1.9	3.7	6.7	6.9
100.0	5.6	0.8	-2.5	-1.3	3.0	5.6	5.4
110.0	4.5	0.3	-1.2	-1.3	1.7	3.4	3.3
120.0	2.9	0.5	-0.9	-0.9	0.9	2.1	2.1
130.0	1.8	0.9	-0.7	-0.7	0.5	1.3	1.3
140.0	1.0	0.3	-0.4	-0.5	0.8	1.4	0.5
150.0	0.6	-0.0	-0.3	-0.3	0.7	1.1	0.3
160.0	0.5	-0.1	-0.1	-0.1	0.4	0.5	0.1
170.0	0.3	-0.1	-0.1	-0.1	0.2	0.2	0.1
180.0	0.	0.	0.	0.	0.	0.	0.

GROUP AVERAGED RESULTS OF RUNS 2807 THROUGH 2811

DISTANCE FROM SOURCE TO PROBES (METERS) = 26.11
AREA UNDER CURVE (SEC. TIMES CONC. UNITS) = 3100.63
MEAN TIME OF PASSAGE (SEC. FROM RELEASE) = 102.23
VARIANCE (SQUARE SECONDS) = 651.49

TIME FROM RELEASE	CONCENTRATION AT PROBE (RELATIVE TO MEAN)						MEAN CONCENTRATION
	PROBE G 31.4W	PROBE J 25.0W	PROBE I 12.9W	PROBE E 9.1W	PROBE F 0.3W	PROBE H 2.1E	
66.0	-0.1	-0.1	0.2	-0.1	-0.1	-0.1	0.1
68.0	-3.4	-1.7	2.1	1.5	-3.4	-3.4	3.4
70.0	-16.9	-8.8	10.3	7.5	-15.5	-17.0	17.3
72.0	-36.4	-15.1	19.1	15.9	-30.6	-35.8	38.3
74.0	-54.3	-14.7	27.5	18.3	-43.2	-53.3	61.1
76.0	-61.6	-9.2	24.7	20.0	-39.9	-59.2	75.0
78.0	-56.1	-5.8	17.9	19.7	-28.6	-56.1	78.6
80.0	-42.4	-4.6	12.2	15.2	-19.1	-38.3	73.6
85.0	-17.5	-3.6	1.5	9.7	-3.0	-13.1	60.2
90.0	-8.2	-3.6	-1.8	6.9	2.8	-1.5	53.8
95.0	-3.1	-3.8	-4.4	6.0	6.8	4.9	48.9
100.0	0.8	-3.8	-5.2	3.6	10.6	9.6	43.8
105.0	2.7	-3.8	-5.7	2.4	12.5	13.5	39.0
110.0	3.7	-3.5	-6.1	1.5	13.9	15.6	34.4
120.0	3.1	-4.8	-4.2	0.7	12.5	15.9	26.6
130.0	3.8	-3.4	-4.7	0.3	12.2	15.9	18.5
140.0	2.5	-2.3	-3.9	0.4	9.1	13.0	13.0
150.0	2.4	-1.6	-2.9	-0.1	7.1	10.5	8.4
160.0	1.4	-1.4	-1.7	-0.2	4.7	7.6	5.7
170.0	0.7	-1.0	-1.2	0.4	2.6	4.5	4.0
180.0	0.6	-0.7	-0.9	0.2	1.7	3.7	2.4
190.0	0.5	-0.5	-0.5	-0.1	1.3	2.2	1.2
200.0	0.7	-0.4	-0.4	-0.1	0.9	1.5	0.6
210.0	0.5	-0.3	-0.2	-0.2	0.7	1.1	0.3
220.0	0.2	-0.1	-0.1	-0.1	0.3	0.6	0.1
230.0	0.0	-0.0	-0.0	-0.0	0.0	0.2	0.0
240.0	0.	0.	0.	0.	0.	0.	0.
250.0	0.	0.	0.	0.	0.	0.	0.

GROUP AVERAGED RESULTS OF RUNS 2901 THROUGH 2905

DISTANCE FROM SOURCE TO PROBES (METERS) = 16.08
AREA UNDER CURVE (SEC. TIMES CONC. UNITS) = 724.17
MEAN TIME OF PASSAGE (SEC. FROM RELEASE) = 35.14
VARIANCE (SQUARE SECONDS) = 111.25

TIME FROM RELEASE	CONCENTRATION AT PROBE (RELATIVE TO MEAN)						MEAN CONCENTRATION
	PROBE H 33.2W	PROBE G 30.2W	PROBE J 26.2W	PROBE F 22.3W	PROBE E 18.4W	PROBE I 14.3W	
22.0	0.	0.	0.	0.	0.	0.	0.
23.0	-1.1	-1.1	-0.7	0.9	1.0	-0.0	1.1
24.0	-10.5	-9.8	-6.6	5.0	9.5	5.9	10.6
25.0	-41.9	-36.0	-21.7	17.8	34.3	20.8	42.3
26.0	-63.1	-49.4	-8.2	17.6	31.4	33.9	64.5
27.0	-58.7	-37.4	-5.3	13.4	24.1	28.7	65.9
28.0	-43.1	-22.3	-1.0	8.7	13.2	18.0	55.1
29.0	-27.7	-10.3	1.9	4.3	5.9	7.8	44.9
30.0	-16.9	-2.4	3.1	1.8	0.3	2.8	37.6
32.0	-4.0	3.0	3.3	-1.0	-2.4	-2.7	29.8
34.0	3.4	4.5	2.7	-1.0	-4.1	-4.3	25.1
36.0	7.4	6.0	2.2	-2.3	-4.3	-4.8	21.5
38.0	9.8	5.9	2.5	-2.8	-4.6	-5.1	18.1
40.0	10.9	6.0	2.1	-2.9	-4.7	-4.8	15.6
45.0	10.6	5.8	0.8	-2.6	-3.8	-4.1	10.3
50.0	8.2	4.2	0.8	-2.0	-2.9	-3.0	6.8
55.0	6.5	3.0	0.4	-1.5	-2.0	-2.3	4.2
60.0	5.1	2.1	0.0	-1.2	-1.3	-1.2	2.6
65.0	3.1	1.4	-0.1	-0.7	-0.9	-0.7	1.5
70.0	2.1	0.7	0.2	-0.4	-0.6	-0.6	0.9
80.0	0.9	0.4	0.1	-0.3	-0.2	-0.2	0.4
90.0	0.3	0.1	0.1	-0.1	-0.1	-0.0	0.1
100.0	0.2	0.0	-0.0	-0.0	-0.0	-0.0	0.0
110.0	0.	0.	0.	0.	0.	0.	0.

GROUP AVERAGED RESULTS OF RUNS 2906 THROUGH 2910

DISTANCE FROM SOURCE TO PROBES (METERS) = 26.12
AREA UNDER CURVE (SEC. TIMES CONC. UNITS) = 1181.59
MEAN TIME OF PASSAGE (SEC. FROM RELEASE) = 57.21
VARIANCE (SQUARE SECONDS) = 178.97

TIME FROM RELEASE	CONCENTRATION AT PROBE (RELATIVE TO MEAN)						MEAN CONCENTRATION
	PROBE H 33.2W	PROBE G 30.2W	PROBE J 26.2W	PROBE F 22.3W	PROBE E 18.4W	PROBE I 14.3W	
37.0	0.	0.	0.	0.	0.	0.	0.
38.0	-0.3	-0.3	-0.2	0.2	0.4	0.1	0.3
39.0	-2.3	-2.3	-1.2	0.4	2.4	1.8	2.3
40.0	-8.9	-8.0	-4.0	2.4	7.6	5.8	9.0
41.0	-20.3	-17.3	-8.3	4.0	16.9	13.8	20.6
42.0	-33.1	-26.1	-11.6	8.2	24.0	19.2	34.5
43.0	-44.5	-31.4	-7.1	10.6	22.4	23.7	47.0
44.0	-45.5	-31.7	-5.2	12.7	19.1	23.4	50.8
45.0	-42.9	-26.8	-2.7	10.4	16.3	19.5	51.1
46.0	-36.6	-19.7	-1.1	7.2	12.6	14.9	49.5
48.0	-25.2	-11.4	0.9	4.5	6.8	8.0	45.3
50.0	-14.9	-5.6	1.2	1.9	3.5	4.1	42.4
52.0	-7.5	-2.0	1.6	0.2	1.3	1.1	39.4
54.0	-2.0	0.5	1.8	-0.5	-0.8	-0.5	36.5
56.0	1.8	2.4	1.9	-1.7	-1.8	-1.8	33.6
58.0	5.2	4.0	2.2	-2.0	-3.6	-2.6	30.5
60.0	7.8	5.1	2.7	-3.8	-4.0	-2.5	27.4
70.0	11.5	5.9	2.1	-3.6	-4.3	-4.3	14.9
80.0	8.1	3.7	0.8	-2.2	-2.6	-2.6	7.0
90.0	4.5	2.1	0.4	-1.2	-1.4	-1.4	3.2
100.0	2.6	1.0	0.0	-0.7	-0.7	-0.5	1.3
110.0	1.0	0.5	-0.0	-0.3	-0.3	-0.2	0.5
120.0	0.5	0.1	-0.0	-0.1	-0.1	-0.1	0.2
130.0	0.2	0.1	0.0	-0.1	-0.1	-0.1	0.1
140.0	0.1	-0.0	-0.0	-0.0	-0.0	-0.0	0.0
150.0	0.0	-0.0	-0.0	-0.0	-0.0	-0.0	0.0

GROUP AVERAGED RESULTS OF RUNS 3001 THROUGH 3004

DISTANCE FROM SOURCE TO PROBES (METERS) = 18.10
AREA UNDER CURVE (SEC. TIMES CONC. UNITS) = 605.42
MEAN TIME OF PASSAGE (SEC. FROM RELEASE) = 36.25
VARIANCE (SQUARE SECONDS) = 107.39

TIME FROM RELEASE	CONCENTRATION AT PROBE (RELATIVE TO MEAN)						MEAN CONCENTRATION
	PROBE F 32.3W	PROBE E 29.0W	PROBE J 25.5W	PROBE I 22.0W	PROBE G 18.5W	PROBE H 15.0W	
23.0	0.	0.	0.	0.	0.	0.	0.
24.0	-0.1	-0.1	-0.1	0.0	0.2	0.2	0.1
25.0	-3.4	-3.3	-1.5	2.1	1.6	5.8	3.4
26.0	-20.3	-17.1	-5.4	15.1	11.6	13.4	20.4
27.0	-49.4	-36.1	-15.4	21.9	34.7	43.2	51.0
28.0	-54.5	-37.7	-8.8	18.5	34.8	45.2	62.9
29.0	-35.2	-21.4	-11.9	10.8	23.9	35.3	53.2
30.0	-19.3	-10.0	-3.7	3.6	12.1	16.9	43.0
32.0	-0.8	-0.1	0.2	-0.9	-0.4	3.1	28.6
34.0	4.2	1.9	0.2	-2.5	-2.3	0.6	22.7
36.0	5.2	2.8	0.2	-2.2	-3.0	-1.2	19.0
38.0	5.8	3.1	0.3	-2.8	-3.0	-1.3	16.3
40.0	5.9	3.3	0.4	-2.8	-3.2	-1.9	13.9
45.0	5.2	3.2	-0.1	-2.3	-2.5	-1.9	9.2
50.0	4.2	2.3	0.3	-1.7	-2.4	-1.6	6.2
55.0	3.3	1.7	0.1	-1.5	-1.3	-1.5	4.0
60.0	2.5	1.3	-0.2	-0.9	-1.2	-0.7	2.6
65.0	1.6	1.0	-0.0	-0.9	-0.7	-0.5	1.6
70.0	1.1	0.6	-0.1	-0.7	-0.2	-0.5	0.9
80.0	0.6	0.5	-0.3	-0.3	-0.1	-0.2	0.3
90.0	0.2	0.1	-0.1	-0.1	-0.1	0.0	0.1
100.0	0.	0.	0.	0.	0.	0.	0.

GROUP AVERAGED RESULTS OF RUNS 3005 THROUGH 3008

DISTANCE FROM SOURCE TO PROBES (METERS) = 29.01
AREA UNDER CURVE (SEC. TIMES CONC. UNITS) = 1170.82
MEAN TIME OF PASSAGE (SEC. FROM RELEASE) = 60.50
VARIANCE (SQUARE SECONDS) = 240.18

TIME FROM RELEASE	CONCENTRATION AT PROBE (RELATIVE TO MEAN)						MEAN CONCENTRATION
	PROBE F 32.3W	PROBE E 29.0W	PROBE J 25.5W	PROBE I 22.0W	PROBE G 18.5W	PROBE H 15.0W	
39.0	0.	0.	0.	0.	0.	0.	0.
40.0	-0.5	-0.5	-0.4	0.9	0.2	0.1	0.5
41.0	-4.3	-3.6	-1.2	3.5	1.8	3.7	4.3
42.0	-15.0	-12.5	-6.1	11.2	9.3	12.2	15.1
43.0	-29.8	-24.2	-10.1	16.4	20.3	27.5	31.7
44.0	-38.8	-29.3	-9.6	17.3	26.5	32.4	44.1
45.0	-42.2	-26.6	-6.9	15.6	25.2	31.0	51.3
46.0	-34.1	-20.4	-5.2	10.7	21.5	23.7	51.5
48.0	-17.9	-9.8	-0.4	4.6	9.8	10.9	44.1
50.0	-8.5	-4.6	0.0	2.1	4.5	5.1	39.5
55.0	0.8	0.5	0.6	-0.4	-0.6	-0.8	32.5
60.0	4.2	2.9	1.0	-2.3	-2.3	-3.0	27.0
65.0	5.7	3.3	1.7	-2.7	-3.4	-3.9	21.8
70.0	6.1	3.6	1.3	-2.6	-3.6	-4.0	17.1
75.0	5.6	3.0	0.7	-1.7	-3.3	-3.4	12.9
80.0	5.2	2.6	0.4	-1.6	-2.8	-2.9	9.4
90.0	3.1	1.8	0.3	-1.0	-1.9	-1.9	5.0
100.0	1.7	0.8	0.1	-0.5	-0.8	-1.1	2.6
110.0	0.9	0.4	0.2	-0.4	-0.5	-0.6	1.0
120.0	0.3	0.2	0.1	-0.1	-0.2	-0.4	0.5
130.0	0.2	0.0	0.0	0.1	-0.1	-0.2	0.2
140.0	0.1	0.0	0.0	0.0	-0.1	-0.1	0.1
150.0	0.	0.	0.	0.	0.	0.	0.

GROUP AVERAGED RESULTS OF RUNS 3103 THROUGH 3106

DISTANCE FROM SOURCE TO PROBES (METERS) = 17.50
AREA UNDER CURVE (SEC. TIMES CONC. UNITS) = 810.95
MEAN TIME OF PASSAGE (SEC. FROM RELEASE) = 39.87
VARIANCE (SQUARE SECONDS) = 130.27

TIME FROM RELEASE	CONCENTRATION AT PROBE (RELATIVE TO MEAN)						MEAN CONCENTRATION
	PROBE J 25.4W	PROBE I 23.1W	PROBE G 19.9W	PROBE H 17.2W	PROBE F 13.9W	PROBE E 10.6W	
24.0	0.	0.	0.	0.	0.	0.	0.
25.0	-0.2	-0.2	-0.2	-0.1	0.2	0.5	0.2
26.0	-3.1	-3.0	-1.6	-0.3	2.4	5.0	3.1
27.0	-16.8	-15.5	-6.6	2.7	12.2	15.9	17.7
28.0	-39.5	-31.8	-15.3	9.1	26.8	28.5	42.7
29.0	-48.5	-32.8	-8.4	10.4	23.9	26.6	57.0
30.0	-35.3	-23.0	-5.6	7.5	16.3	19.1	53.1
31.0	-23.4	-13.9	-2.9	4.3	10.3	11.6	46.9
32.0	-13.4	-7.4	-0.9	1.7	5.4	6.7	41.0
34.0	-4.6	-1.6	0.2	0.2	1.4	1.6	34.5
36.0	-0.2	0.8	0.5	-0.6	-0.5	0.1	30.6
38.0	2.4	2.1	0.8	-1.2	-1.3	-1.3	27.2
40.0	4.1	2.8	0.9	-1.4	-2.2	-1.5	24.3
45.0	6.4	4.3	1.3	-1.7	-3.2	-3.2	17.5
50.0	6.3	4.1	0.8	-1.6	-2.9	-2.6	12.3
55.0	5.4	3.2	0.4	-1.0	-2.3	-2.4	8.3
60.0	4.4	2.6	0.5	-1.1	-1.9	-1.6	5.4
65.0	2.7	1.8	0.3	-0.5	-1.5	-1.0	3.4
70.0	2.1	1.3	0.3	-0.8	-0.8	-0.7	2.1
75.0	1.4	1.0	0.2	-0.4	-0.6	-0.5	1.2
80.0	0.9	0.5	0.3	-0.3	-0.5	-0.3	0.7
90.0	0.4	0.3	0.1	-0.1	-0.2	-0.2	0.2
100.0	0.1	0.1	0.1	-0.1	-0.1	-0.1	0.1
110.0	0.0	-0.0	-0.0	-0.0	-0.0	-0.0	0.0

GROUP AVERAGED RESULTS OF RUNS 3107 THROUGH 3110

DISTANCE FROM SOURCE TO PROBES (METERS) = 29.45
AREA UNDER CURVE (SEC. TIMES CONC. UNITS) = 1366.95
MEAN TIME OF PASSAGE (SEC. FROM RELEASE) = 66.81
VARIANCE (SQUARE SECONDS) = 241.26

TIME FROM RELEASE	CONCENTRATION AT PROBE (RELATIVE TO MEAN)						MEAN CONCENTRATION
	PROBE J 25.4W	PROBE I 23.1W	PROBE G 19.9W	PROBE H 17.2W	PROBE F 13.9W	PROBE E 10.6W	
42.0	0.	0.	0.	0.	0.	0.	0.
44.0	-1.4	-1.4	-1.0	0.3	1.2	1.7	1.4
46.0	-13.9	-13.0	-6.8	3.0	11.6	11.5	14.6
48.0	-28.8	-22.8	-6.6	5.9	17.3	18.4	33.7
50.0	-25.9	-17.3	-4.0	4.5	13.0	14.3	39.9
52.0	-18.9	-12.5	-2.5	3.8	9.3	9.1	41.1
54.0	-13.4	-9.0	-1.7	3.2	6.3	6.2	41.3
56.0	-9.7	-6.1	-0.9	2.2	4.4	3.8	40.9
58.0	-6.3	-4.0	-0.6	1.6	2.7	2.5	40.3
60.0	-3.4	-1.8	0.2	0.7	1.2	0.8	39.1
65.0	1.9	1.7	0.6	-0.3	-1.2	-1.9	34.6
70.0	5.2	3.5	1.2	-1.3	-2.4	-3.2	28.7
75.0	7.0	4.6	1.0	-1.3	-3.3	-4.0	22.7
80.0	6.8	4.5	1.2	-1.7	-3.2	-3.4	17.3
85.0	6.3	4.1	0.7	-1.3	-2.9	-3.1	12.6
90.0	5.3	3.7	0.6	-1.5	-2.2	-2.7	9.0
95.0	4.5	2.8	0.6	-1.2	-1.9	-1.9	6.3
100.0	3.2	2.0	0.5	-0.7	-1.4	-1.6	4.5
110.0	1.4	0.9	0.3	-0.3	-0.6	-0.9	2.1
120.0	0.8	0.4	0.4	-0.3	-0.4	-0.4	0.9
130.0	0.3	0.2	0.2	-0.1	-0.2	-0.4	0.4
140.0	0.1	0.1	0.1	-0.1	-0.1	-0.1	0.1
150.0	0.0	0.0	0.0	-0.0	-0.0	-0.0	0.0
160.0	0.	0.	0.	0.	0.	0.	0.

GROUP AVERAGED RESULTS OF RUNS 3201 THROUGH 3204

DISTANCE FROM SOURCE TO PROBES (METERS) = 17.56
AREA UNDER CURVE (SEC. TIMES CONC. UNITS) = 944.92
MEAN TIME OF PASSAGE (SEC. FROM RELEASE) = 40.62
VARIANCE (SQUARE SECONDS) = 193.98

TIME FROM RELEASE	CONCENTRATION AT PROBE (RELATIVE TO MEAN)						MEAN CONCENTRATION
	PROBE E 25.2W	PROBE H 23.0W	PROBE F 20.0W	PROBE G 17.0W	PROBE I 14.0W	PROBE J 10.8W	
24.0	0.	0.	0.	0.	0.	0.	0.
25.0	-0.2	-0.2	-0.2	-0.2	0.3	0.5	0.2
26.0	-2.7	-2.6	-1.6	0.3	2.3	4.6	2.7
27.0	-22.7	-22.0	-17.2	3.1	24.6	34.8	22.8
28.0	-67.9	-62.6	-42.8	24.6	58.1	84.4	69.4
29.0	-84.7	-73.0	-30.6	29.1	62.0	78.6	91.5
30.0	-65.3	-49.4	-12.5	20.5	41.4	45.2	80.5
31.0	-36.3	-20.9	-1.3	10.7	17.1	16.6	58.8
32.0	-16.5	-6.0	2.9	4.5	3.9	3.7	43.8
33.0	-6.1	0.3	3.7	1.4	-1.3	-1.8	36.3
34.0	-0.2	3.1	3.9	0.2	-3.7	-5.4	31.8
36.0	5.0	5.2	3.6	-1.8	-5.2	-6.3	26.6
38.0	6.8	5.9	3.2	-1.9	-5.9	-6.8	23.8
40.0	7.8	6.3	3.1	-2.1	-6.1	-7.3	21.5
45.0	8.5	6.5	2.9	-2.6	-6.0	-7.3	16.9
50.0	8.2	5.9	2.3	-2.2	-5.6	-6.5	13.0
55.0	7.4	5.5	2.0	-2.1	-5.0	-5.9	9.6
60.0	6.0	4.5	1.6	-2.0	-4.0	-4.3	7.3
65.0	4.8	3.4	1.2	-1.8	-2.9	-3.3	5.1
70.0	3.7	2.4	0.9	-1.1	-2.2	-2.6	3.7
75.0	2.8	1.9	0.6	-0.7	-1.9	-2.0	2.6
80.0	2.3	1.5	0.4	-0.7	-1.3	-1.3	1.6
90.0	1.1	0.7	0.3	-0.4	-0.6	-0.7	0.7
100.0	0.5	0.4	0.1	-0.2	-0.3	-0.3	0.3
110.0	0.3	0.1	0.0	-0.1	-0.1	-0.1	0.1
120.0	0.2	0.0	0.0	-0.0	-0.0	-0.0	0.0

GROUP AVERAGED RESULTS OF RUNS 3205 THROUGH 3207

DISTANCE FROM SOURCE TO PROBES (METERS) = 30.57
AREA UNDER CURVE (SEC. TIMES CONC. UNITS) = 1707.78
MEAN TIME OF PASSAGE (SEC. FROM RELEASE) = 69.29
VARIANCE (SQUARE SECONDS) = 352.04

TIME FROM RELEASE	CONCENTRATION AT PROBE (RELATIVE TO MEAN)						MEAN CONCENTRATION
	PROBE E 25.2W	PROBE H 23.0W	PROBE F 20.0W	PROBE G 17.0W	PROBE I 14.0W	PROBE J 10.8W	
44.0	0.	0.	0.	0.	0.	0.	0.
45.0	-0.1	-0.1	-0.0	0.0	-0.1	0.4	0.1
46.0	-1.2	-1.2	-0.4	0.2	0.9	1.6	1.2
47.0	-6.9	-6.7	-4.2	3.4	6.0	7.0	7.2
48.0	-24.8	-22.6	-12.6	14.7	21.4	14.7	25.6
49.0	-52.7	-47.6	-20.7	23.9	40.3	41.9	55.0
50.0	-66.4	-56.8	-22.9	20.4	49.0	62.7	73.8
52.0	-52.3	-37.8	-13.1	14.3	34.4	40.5	73.3
54.0	-25.5	-17.3	-2.1	7.1	12.5	17.6	56.5
56.0	-11.4	-7.4	-0.3	3.7	4.8	6.8	47.9
58.0	-5.0	-2.6	0.3	1.3	1.6	2.5	43.4
60.0	-1.7	-0.5	0.9	0.6	-0.3	0.1	40.7
65.0	3.3	2.7	2.0	-1.3	-2.9	-3.3	35.5
70.0	6.4	4.8	2.6	-2.0	-4.9	-5.3	30.3
75.0	7.7	5.8	2.5	-2.4	-5.3	-6.3	25.7
80.0	8.2	6.0	2.8	-2.7	-5.7	-6.4	21.3
85.0	8.0	6.2	2.4	-2.7	-5.2	-6.6	17.1
90.0	7.3	5.2	2.0	-2.0	-5.0	-5.5	13.4
100.0	5.5	3.8	1.7	-1.7	-3.7	-3.9	7.9
110.0	3.5	2.2	0.6	-1.0	-1.9	-2.5	4.6
120.0	2.1	1.3	0.7	-0.2	-1.6	-1.7	2.5
130.0	1.4	0.7	0.4	-0.4	-0.8	-0.8	1.3
140.0	0.7	0.4	0.5	-0.3	-0.6	-0.6	0.6
150.0	0.5	0.3	0.2	-0.2	-0.3	-0.3	0.3
160.0	0.2	0.1	0.1	-0.1	-0.1	-0.1	0.1
170.0	0.1	0.0	0.0	-0.0	-0.0	-0.0	0.0
180.0	0.1	-0.0	-0.0	-0.0	-0.0	-0.0	0.0

GROUP AVERAGED RESULTS OF RUNS 3401 THROUGH 3403

DISTANCE FROM SOURCE TO PROBES (METERS) = 16.09
AREA UNDER CURVE (SEC. TIMES CONC. UNITS) = 1235.41
MEAN TIME OF PASSAGE (SEC. FROM RELEASE) = 34.48
VARIANCE (SQUARE SECONDS) = 72.93

TIME FROM RELEASE	CONCENTRATION AT PROBE (RELATIVE TO MEAN)						MEAN CONCENTRATION
	PROBE F 26.2W	PROBE J 11.3W	PROBE E 23.0W	PROBE I 14.3W	PROBE G 20.0W	PROBE H 17.9W	
21.0	0.	0.	0.	0.	0.	0.	0.
22.0	-1.8	-1.7	-1.2	0.7	1.9	1.7	2.0
23.0	-16.6	-11.8	-9.3	6.0	13.4	14.1	18.2
24.0	-39.5	-21.5	-14.7	9.6	24.3	32.4	50.2
25.0	-40.4	-20.0	-8.6	9.7	20.4	28.5	83.7
26.0	-35.0	-13.1	-3.9	5.7	15.0	21.5	69.1
27.0	-25.7	-9.9	-2.0	3.4	11.9	14.6	70.5
28.0	-17.7	-6.7	-0.3	1.6	8.4	9.1	70.4
29.0	-11.3	-3.9	1.0	-0.5	5.3	5.8	69.1
30.0	-6.5	-2.4	2.2	-1.5	3.1	2.9	67.4
32.0	1.2	0.5	3.2	-3.0	-0.6	-1.0	61.9
34.0	6.5	2.1	4.6	-4.6	-2.4	-4.6	55.1
36.0	10.0	2.7	4.5	-5.5	-3.2	-5.7	48.0
38.0	11.3	3.1	4.8	-5.8	-3.4	-7.0	40.6
40.0	11.5	3.6	4.6	-5.2	-4.4	-7.1	33.7
42.0	11.5	3.9	4.0	-5.0	-4.4	-6.9	27.3
44.0	11.1	3.6	3.1	-4.5	-3.9	-6.3	21.7
46.0	9.5	2.8	2.3	-3.8	-3.0	-5.0	17.1
48.0	8.5	2.7	0.9	-3.3	-2.3	-4.1	13.3
50.0	6.2	2.7	0.2	-2.1	-2.0	-3.4	9.9
55.0	3.8	1.6	0.7	-1.6	-1.6	-1.9	5.1
60.0	2.0	1.0	0.2	-0.7	-1.0	-0.8	2.7
65.0	1.4	0.6	0.3	-0.5	-0.7	-0.5	1.2
70.0	0.7	0.2	0.3	-0.2	-0.5	-0.3	0.6
75.0	0.5	0.0	0.1	-0.0	-0.2	-0.2	0.2
80.0	0.2	-0.0	0.1	-0.0	-0.1	-0.1	0.1
85.0	0.1	-0.0	-0.0	-0.0	-0.0	-0.0	0.0
90.0	0.	0.	0.	0.	0.	0.	0.

GROUP AVERAGED RESULTS OF RUNS 3404 THROUGH 3406

DISTANCE FROM SOURCE TO PROBES (METERS) = 23.98
AREA UNDER CURVE (SEC. TIMES CONC. UNITS) = 1709.57
MEAN TIME OF PASSAGE (SEC. FROM RELEASE) = 51.52
VARIANCE (SQUARE SECONDS) = 111.89

TIME FROM RELEASE	CONCENTRATION AT PROBE (RELATIVE TO MEAN)						MEAN CONCENTRATION
	PROBE F 26.2W	PROBE J 11.3W	PROBE E 23.0W	PROBE I 14.3W	PROBE G 20.0W	PROBE H 17.9W	
32.0	0.	0.	0.	0.	0.	0.	0.
34.0	-2.6	-2.3	-1.4	0.6	2.1	3.3	2.6
36.0	-20.4	-11.8	-7.2	5.9	11.8	17.1	23.7
38.0	-29.4	-12.6	-6.7	6.1	15.2	19.3	44.3
40.0	-27.9	-9.6	-3.8	4.8	11.9	16.6	57.8
42.0	-20.4	-8.2	-2.1	3.8	8.6	12.7	65.9
44.0	-12.6	-5.7	-0.7	1.2	6.0	8.4	70.1
46.0	-7.5	-2.9	0.8	-0.8	3.7	4.5	70.8
48.0	-2.1	-0.4	1.4	-1.4	0.8	1.0	68.8
50.0	2.7	1.4	2.6	-2.1	-1.9	-1.8	65.0
52.0	6.8	2.6	2.5	-2.7	-3.2	-3.9	59.4
54.0	8.9	4.0	2.8	-4.0	-4.1	-5.1	53.3
56.0	10.9	3.7	2.4	-3.5	-4.1	-6.3	46.7
58.0	11.8	4.4	2.2	-4.0	-4.6	-6.3	40.5
60.0	12.1	4.3	1.7	-3.4	-4.8	-6.4	34.5
65.0	10.2	3.9	1.2	-3.0	-4.4	-4.5	22.0
70.0	7.2	2.8	0.2	-1.9	-2.6	-3.6	12.8
75.0	4.5	1.4	0.2	-1.1	-1.6	-2.0	7.4
80.0	2.6	0.8	-0.0	-0.5	-0.9	-1.2	4.0
85.0	1.4	0.4	-0.1	-0.1	-0.5	-0.6	2.2
90.0	0.6	0.5	0.3	-0.2	-0.7	-0.2	1.2
95.0	0.9	0.0	-0.1	-0.2	-0.3	0.1	0.5
100.0	0.4	-0.1	-0.0	-0.1	-0.1	0.1	0.1
105.0	0.1	-0.0	-0.0	-0.0	-0.0	0.2	0.0
110.0	0.	0.	0.	0.	0.	0.	0.

GROUP AVERAGED RESULTS OF RUNS 3407 THROUGH 3409

DISTANCE FROM SOURCE TO PROBES (METERS) = 31.97
AREA UNDER CURVE (SEC. TIMES CONC. UNITS) = 2101.45
MEAN TIME OF PASSAGE (SEC. FROM RELEASE) = 69.06
VARIANCE (SQUARE SECONDS) = 155.83

TIME FROM RELEASE	CONCENTRATION AT PROBE (RELATIVE TO MEAN)						MEAN CONCENTRATION
	PROBE F 26.2W	PROBE J 11.3W	PROBE E 23.0W	PROBE I 14.3W	PROBE G 20.0W	PROBE H 17.9W	
44.0	0.	0.	0.	0.	0.	0.	0.
46.0	-0.5	-0.2	-0.5	0.0	0.3	1.0	0.6
48.0	-5.9	-2.9	-3.3	1.0	3.9	5.9	7.5
50.0	-15.0	-7.1	-4.8	3.0	8.4	11.9	21.3
52.0	-19.4	-7.4	-7.2	2.5	11.2	15.2	34.4
54.0	-22.2	-7.8	-3.7	3.4	9.9	14.3	47.5
56.0	-19.2	-6.9	-2.7	1.8	9.3	12.3	57.6
58.0	-14.8	-5.8	-1.2	-0.4	8.4	9.5	64.7
60.0	-11.0	-3.6	-0.8	-0.8	5.8	7.2	70.3
62.0	-7.1	-2.4	-0.4	-0.2	3.6	4.5	72.4
64.0	-3.7	-0.7	0.2	-0.6	1.8	1.8	72.3
66.0	-0.2	0.7	0.8	-0.2	-0.7	-0.7	70.2
68.0	2.5	1.6	1.2	0.3	-2.2	-2.8	66.9
70.0	5.1	3.1	1.1	0.5	-4.0	-4.5	62.3
75.0	8.7	4.4	0.2	2.0	-6.3	-6.5	48.5
80.0	8.2	4.5	-0.7	4.6	-7.0	-7.6	34.9
85.0	7.3	2.7	-0.6	3.9	-5.3	-6.1	23.3
90.0	4.9	2.5	-0.7	2.7	-3.8	-4.2	14.8
95.0	3.4	1.9	-0.8	1.7	-2.5	-2.9	9.0
100.0	2.4	1.3	-0.3	1.2	-2.0	-1.8	5.3
105.0	1.2	0.7	-0.7	0.5	-0.7	-0.7	3.3
110.0	1.0	0.4	-0.1	0.3	-0.8	-0.3	1.8
115.0	0.7	0.6	-0.2	0.2	-0.6	-0.3	0.9
120.0	0.8	0.3	-0.3	0.0	-0.4	-0.1	0.4
125.0	0.5	0.2	-0.2	-0.1	-0.2	-0.1	0.2
130.0	0.3	0.1	-0.1	-0.1	-0.1	0.0	0.1
135.0	0.1	-0.0	-0.0	-0.0	-0.0	-0.0	0.0
140.0	0.	0.	0.	0.	0.	0.	0.